Aalborg Universitet

AALBORG UNIVERSITY
DENMARK

Multidimensional HAM-conditions

Measurements on full-scale wall elements in the large climate simulator at SBi

Hansen, Ernst Jan de Place

Publication date:
2010

Document Version
Publisher's PDF, also known as Version of record

Link to publication from Aalborg University

Citation for published version (APA):
Hansen, E. J. D. P. (2010). *Multidimensional HAM-conditions: Measurements on full-scale wall elements in the large climate simulator at SBi*. (1. udgave ed.) SBI forlag. SBi-anvisning 2010 No. 6 http://www.sbi.dk/byggeteknik/bygningsfysik/fugt/multidimentional-ham-conditions/http://www.sbi.dk/byggeteknik/bygningsfysik/fugt/multidimentional-ham-conditions/multidimensional-ham-conditions

General rights
Copyright and moral rights for the publications made accessible in the public portal are retained by the authors and/or other copyright owners and it is a condition of accessing publications that users recognise and abide by the legal requirements associated with these rights.

? Users may download and print one copy of any publication from the public portal for the purpose of private study or research.
? You may not further distribute the material or use it for any profit-making activity or commercial gain
? You may freely distribute the URL identifying the publication in the public portal ?

Take down policy
If you believe that this document breaches copyright please contact us at vbn@aub.aau.dk providing details, and we will remove access to the work immediately and investigate your claim.

Downloaded from vbn.aau.dk on: November 29, 2020

SBi 2010:06

Multidimensional HAM conditions

Measurements on full-scale wall elements in the large climate simulator at SBi

Statens Byggeforskningsinstitut
AALBORG UNIVERSITET

Multidimensional HAM conditions

Measurements on full-scale wall elements in the large climate simulator at SBi

Ernst Jan de Place Hansen

SBi 2010:06
Danish Building Research Institute, Aalborg University · 2010

Title	Multidimensional HAM conditions
Subtitle	Measurements on full-scale wall elements in the large climate simulator at SBi
Serial title	SBi 2010:06
Edition	1 edition
Year	2010
Author	Ernst Jan de Place Hansen
Language	English
Pages	125
References	50
Key words	Wall elements, climate simulator, indoor environment, multidimensional HAMM conditions.
ISBN	978-87-563-1413-8
Cover	Photo: Ernst Jan de Place Hansen
Publisher	SBi, Statens Byggeforskningsinstitut Danish Building Research Institute Dr. Neergaards Vej 15, DK-2970 Hørsholm E-mail sbi@sbi.dk www.sbi.dk

Extracts may be reproduced but only with reference to source: *SBi 2010:06: Multidimensional HAM conditions. Measurements on full-scale wall elements in the large climate simulator at SBi. (2010)*

Content

Content 3
Foreword 4
Introduction 5
Test design 6
  Test elements 7
  Elements and sensors 10
  Test series 13
Results and discussion 16
  Steady-state without vapour barrier (test M1) 16
  Steady-state with vapour barrier (test M2) 20
  April without cladding (test M3A) 23
  September without cladding (test M3S) 26
  April with cladding (test M4A) 28
  September with cladding (test M4S) 30
  Comparison of elements 33
  Experimental results vs modelled cycles 44
Conclusion 49
References 50
Appendix A. Test set-up 51
Appendix B. Test series 63
Appendix C. Materials 65
Appendix D. Sensor mapping 66
Appendix E. Temperature cycles 68
Appendix F. Steady-state without vapour barrier (M1) 72
Appendix G. Steady-state with vapour barrier (M2) 83
Appendix H. April without cladding (M3A) 91
Appendix I. September without cladding (M3S) 101
Appendix J. April with cladding (M4A) 109
Appendix K. September with cladding (M4S) 118

Foreword

This SBi report describes the test design and results of a series of full-scale tests carried out as part of the project 'Model for Multidimensional Heat, Air and Moisture Conditions in Building Envelope Components'. The project is a joint project between DTU BYG and SBi with DTU BYG as project leader. Its purpose was to obtain a better prediction of the interaction between the indoor environment and the building components used in computational models for multidimensional Heat, Air and Moisture (HAM) conditions. This was mainly done as a PhD project at DTU BYG by PhD fellow Paul Steskens with Carsten Rode and Hans Janssen, both DTU BYG as supervisors.

Experimental data are needed in order to validate such a model. The provision of such data was the main task of the part of the project carried out at SBi. Such data will of course also give knowledge about the conditions in building components in general, which can form the basis for further research at SBi in this field.

Thanks to Carsten Rode, Hans Janssen and Paul Steskens at DTU BYG. Also thanks to Lasse B. Eriksen at SBi and former employees at SBi, Morten Hjorslev Hansen and Birgitte Dela Stang who made the test set-up and all the wiring of sensors etc. They also chose the test design and the boundary conditions. The experiments were carried out and monitored by Ernst Jan de Place Hansen and Lasse B. Eriksen at SBi and the impact of the results of the PhD project was discussed with DTU BYG. These discussions showed that not all the output from the tests could possibly be explained without carrying out further tests beyond the scope of this project.

The overall project was financed by The Danish Research Council for Technology and Production Sciences. The support is gratefully acknowledged.

Danish Building Research Institute, Aalborg University
Construction and health
Marts 2010

Niels-Jørgen Aagaard
Research director

Introduction

Background

Moisture and temperature levels and variations in time and space play a crucial role in degradation processes of building materials, such as silicate materials, metals and polymeric materials where also UV radiation is a very important factor. An exterior wall can consist of more than 10 layers of different materials. Furthermore, a wall element is often inhomogeneous in a plane because of counteracting structural and insulating properties. The moisture and temperature conditions inside such a wall are highly dependent on the material combinations and the climate conditions on both sides of the wall.

Most damages that happen to building components occur in places with a complex geometry that cannot be handled correctly by today's design tools. This could for instance be where different materials meet in joints and where conditions most often are multidimensional by nature. Also apparently regular construction elements have multidimensional parts and features whose hygrothermal conditions should be considered more carefully in the design of buildings, e.g. near beams and columns in common building elements. These loci often represent thermal bridges in the constructions, and they involve the assembly of different components and materials, so there is an increased risk of unintentional airflow or accumulation of moisture. The combination of these factors too often leads to the degradation of materials.

Purpose and content of the project

The purpose of the project 'Model for Multidimensional Heat, Air and Moisture Conditions in Building Envelope Components' was carried out in cooperation between DTU BYG and SBi to get a better prediction of the interaction between the indoor environment and the building component used in computational models for multidimensional (2D) Heat, Air and Moisture (HAM) conditions. This was mainly performed in a PhD project at DTU BYG by PhD fellow Paul Steskens and starts from an existing one-dimensional model MATCH, developed at DTU. A new 2D calculation model would be a valuable tool, which would for instance have a large impact on the possibilities for predicting and diagnosing problems related to (lack of) durability, for instance moisture problems followed by attack by moulds etc.

SBi prepares and performs full-scale tests in a large climate simulator of multi-layer wall elements to generate validation data. The tests results in time series of temperatures and relative humidity in cross sections of the wall elements in addition to time series of the boundary conditions. The design of the tests, i.e. the type of elements and the boundary conditions, is based on numerical investigations and parameter studies (not published). The test design was prepared and carried out in 2006-2007, pre-tests were made in 2008 and the main tests in 2008-2009.

It was the aim to compare the results of these tests with results obtained in other projects, either experimental or in-situ. However, it was rather time demanding to get the test set-up to perform in such a way that it was possible to obtain some relevant results. Therefore, this report focuses on presenting the output from these specific tests including comprehensive appendices. Further studies on how they comply with results from other projects could be the task for a future project.

Test design

Four wall elements were tested in SBi's large climate simulator which has a 3010 x 3200 mm test area (w × h). Figure 1 shows a cross section of the climate simulator.

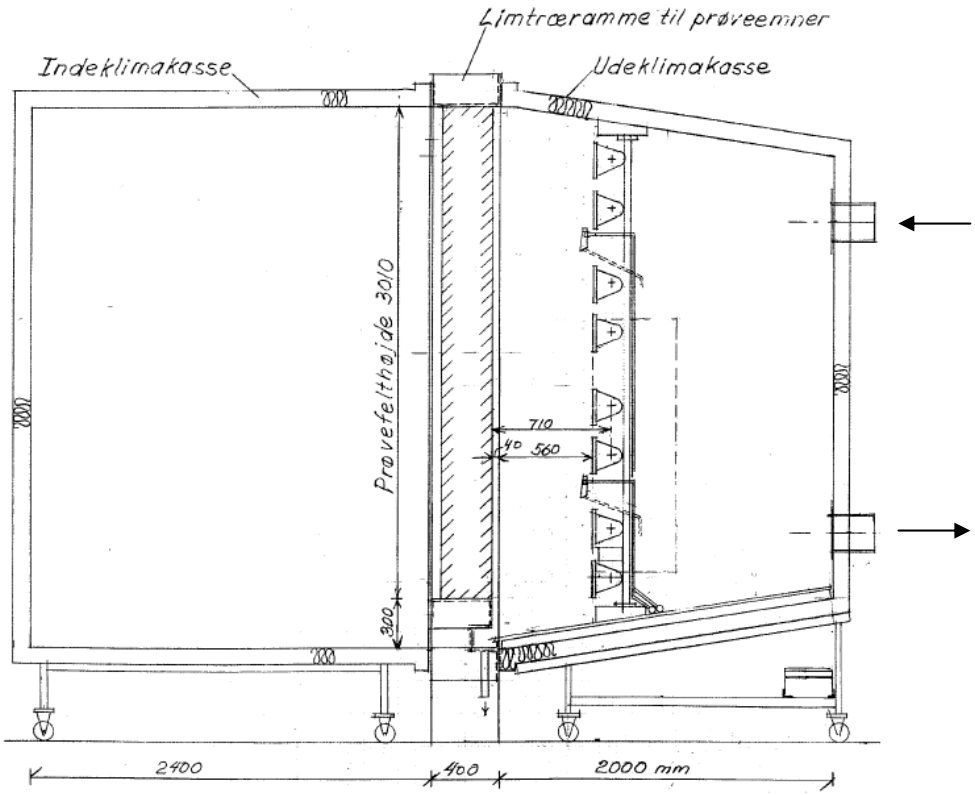

Figure 1. Cross section of large climate simulator at SBi. Indoor climate box ("Indeklimakasse") at the left, outdoor climate box ("Udeklimakasse") at the right, equipped with UV lamps (not used in this project). Maximum height of test elements ("Prøvefelthøjde") is 3010 mm. Openings for inlet (top) and outlet (bottom) of air at the outdoor climate box are shown (see arrows). The indoor climate box is shielded from the laboratory hall by 100 mm of mineral wool thermal insulation, while the outdoor climate box is shielded by 100 mm of foam-based thermal insulation normally used for freezers, refrigerating plants, etc.

The climate simulator can be controlled with a Programmable Logic Controller (PLC), making it possible to design cycles at the outdoor side consisting of x minutes of heat and UV exposure (UV lamps), y minutes of rain (spraying of water), z minutes of cooling, w minutes of ventilation and v minutes with no exposure in a specified order. A further description of this configuration can be found in (Kaaris, 2003).

Neither UV lamps nor spraying with water was used in this project. Spraying with water would destroy the wind barrier and the cladding since these were installed without surface treatment. The use of UV lamps without spraying with water would result in very low RH at the outdoor side.

A description of the boundary conditions used in the test series in this project is given in chapter 'Test series'.

Test elements

The test set-up consisted of four wall elements w × h = 0.65 m x 2.72 m (including top rail and bottom rail). The walls were supported by vertical 45 × 195 mm timber studs wrapped in blue 0.375 mm PE to eliminate moisture exchange (buffering). The two central elements were separated by a 50 mm duct with thermal insulation. A buffer zone was placed along each outer boundary of the testing field, to reduce 3D effects, cf. Figure 5. See Appendix A for details.

Focus in the tests was on timber framed constructions. Full-scale elements were designed in order to analyse the effect of a vapour barrier and the effect of an air flow inside (and outside) an element. As a variant an element with a cellular concrete back wall was chosen, as it is a typical Danish outer wall construction. The test design should enable multidimensional and cyclic conditions and the tests should represent different seasons. The elements consisted of the following layers starting at the outdoor side.

Timber frame, vapour barrier (reference) – Element 1

– 15 mm plywood (cladding)
– 25 mm cavity
– 9 mm gypsum board (wind barrier)
– 195 mm glass wool (thermal insulation)
– 13 mm gypsum board
– 0.20 mm vapour barrier

Timber frame, no vapour barrier – Element 2

– 15 mm plywood (cladding)
– 25 mm cavity
– 9 mm gypsum board (wind barrier)
– 195 mm glass wool (thermal insulation)
– 13 mm gypsum board

Timber frame, slits in vapour barrier and wind barrier – Element 3

– 15 mm plywood (cladding)
– 25 mm cavity
– 9 mm gypsum board (wind barrier) with horizontal slit at the top (3 mm)
– 195 mm glass wool (thermal insulation)
– 13 mm gypsum board with horizontal slit at the bottom (3 mm)
– 0.20 mm vapour barrier with horizontal slit at the bottom (3 mm)

Cellular concrete, no vapour barrier – Element 4

– 15 mm plywood (cladding)
– 25 mm cavity
– 9 mm gypsum board (wind barrier)
– 145 mm glass wool (thermal insulation)
– 50 mm cellular concrete

The plywood cladding was mounted after the third of the four main tests (M3), cf. Table 2, chapter 'Test series'. Elements 1 and 3 were without vapour barrier in the first of four main tests (M1), cf. Table 2, chapter 'Test series'.

The buffer zone consisted of a 9 mm gypsum board, 195 mm glass wool and a 13 mm gypsum board. The width of the buffer zone was 75 mm along the vertical boundaries and 100 mm along the horizontal boundaries of the test area, cf. Appendix A, Figure A2.

U values without vented cavity and cladding:
Elements 1, 2 and 3 and the buffer zone: $U = 0.195\ W/m^2\ K$
Element 4: $U = 0.238\ W/m^2\ K$

Figures 2, 3 and 4 show the test set-up. Additional photos are placed in Appendix A. Data for the different materials are given in Appendix C.

Figure 2. The test rig with the four elements seen from the outdoor side before (left) and after (right) mounting the thermal insulation. Element 4 at right.

Figure 3. The test rig with the four test elements seen from the indoor side with gypsum board as inner cladding at three of the four elements. The wires coming from the sensors inside the elements are seen at the bottom of each element.

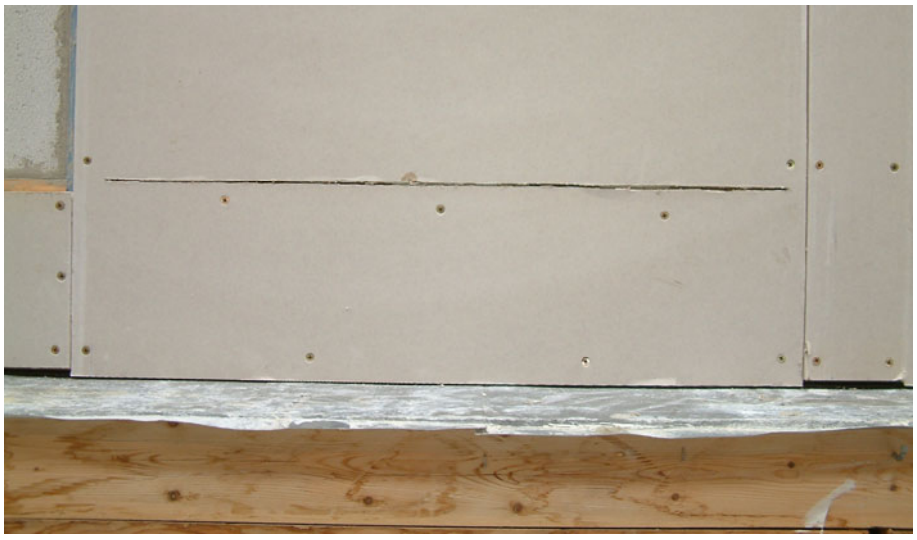

Figure 4. Slit at the bottom of the gypsum board at Element 3 at the indoor side. A similar slit is made at the top of in the wind barrier at the outdoor side. Condition before mounting the vapour barrier.

Elements and sensors

Figure 5 shows the positions of the sensors, seen from the outdoor (cold) side.

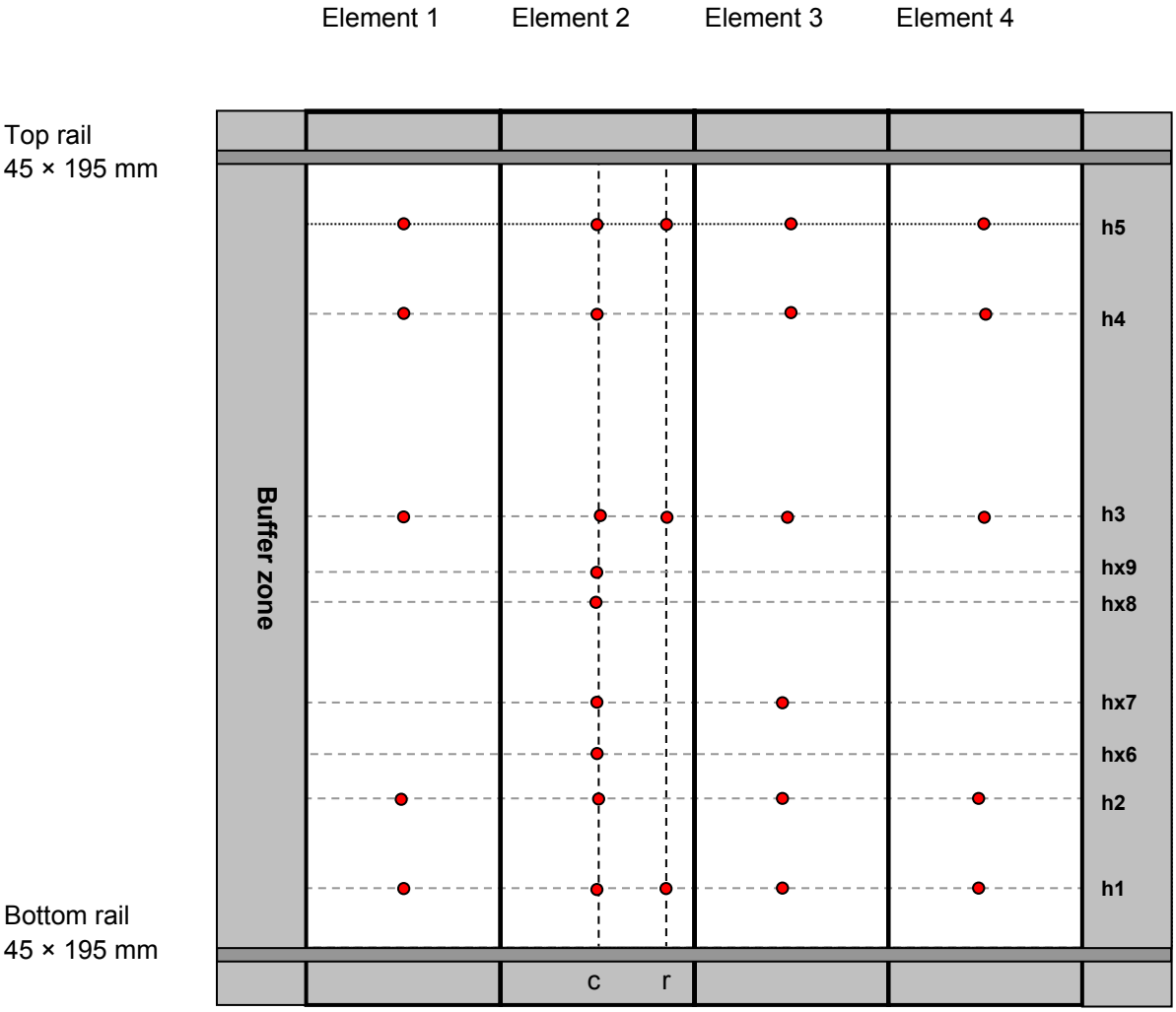

Figure 5. Position and numbering of sensors in the four elements seen from the outdoor side.

Dots show sensor position (moisture and temperature) in the elements. Approximate heights of sensors measured from the top side of the bottom rail:

h1:	h=200 mm	hx6:	h=650 mm
h2:	h=500 mm	hx7:	h=825 mm
h3:	h=1450 mm	hx8:	h=1160 mm
h4:	h=2130 mm	hx9:	h=1260 mm
h5:	h=2430 mm		

Index 'c' means centre line, 325 mm from left side of element seen from the outdoor side. Index 'r' means right side, 100 mm from right side of element seen from the outdoor side.

Elements 2 and 3 were separated by a duct leading the wires from the different sensors, see Figure 6. Wires from sensors in Elements 1 and 4 were led along the buffer zone between the elements and the test frame.

Sensors were placed at hx6, hx7, hx8 and hx9 to study local conditions at the indoor side when adding a shelf and a radiator, cf. Figure A2 – A6, Appendix A. Because of several delays in the test schedule the shelf and the radiator was not added. Therefore, results from the positions hx6 – hx9 are not included in this report since they are not relevant without the shelf and the radiator.

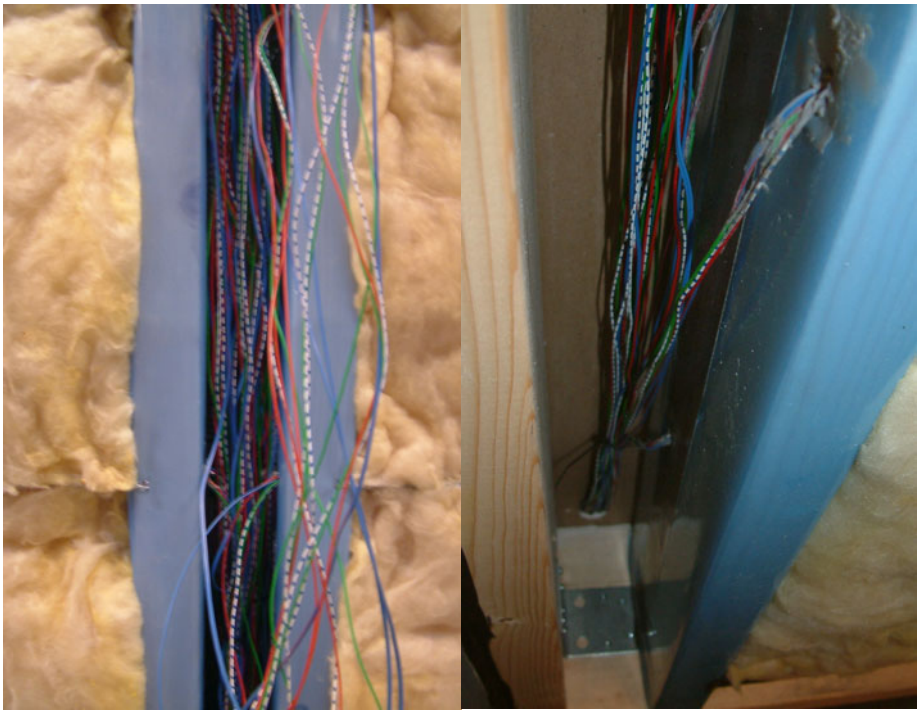

Figure 6. Duct for cables between Elements 2 and 3 (left) and next to Element 1 (right) seen from the outdoor side. The timber studs framing the elements are wrapped in a (blue) vapour barrier in order to ensure that they do not affect the moisture transport through the elements.

Figure 7 shows how the sensors placed in the thermal insulation are fixed by means of wires stretched between the two timber studs on each side of an element. Figure 8 shows how sensors are fixed on the gypsum boards, in this case the wind barrier. All the holes made in the frames for leading the wires are sealed afterwards.

Figure 7. Placement of moisture sensors in fixed positions in the insulation layer.

Figure 8. Fixing of sensors at the outdoor side of the wind barrier.

Figure 9 and Table 1 describes the position of the sensors at different depths in the elements from the indoor to the outdoor side, and what the different depths are designated. Not all combinations of elements and positions are used, cf. Appendix D.

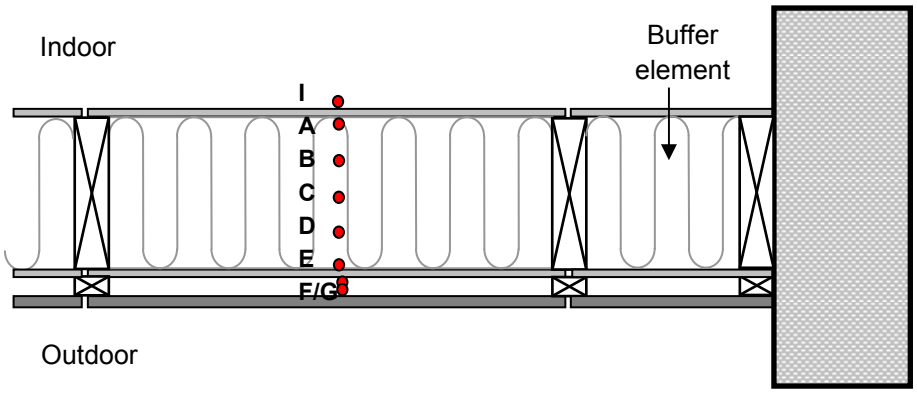

Figure 9. Horizontal cross section of the test-set-up with position of sensors.

Table 1. Position of sensors through the element.

Depth	Depth from indoor side[1]	Position
Indoor	- 500 mm	500 mm in front of the elements, at the indoor side
I	0 mm	Indoor conditions – at the indoor gypsum cladding[2]
A	13 mm	In the insulation, at the indoor gypsum cladding[3]
B	61.5 mm	In the insulation, 48.75 mm insulation (1/4) on the indoor side
C	110.5 mm	In the insulation, 97.5 mm insulation (1/2) on the indoor side
D	159.25 mm	In the insulation, 146.25 mm insulation (3/4) on the indoor side
E	208 mm	In the insulation, at the wind barrier, 195 mm insulation on the indoor side
F	217 mm	In the vented cavity, at the wind barrier
G	242 mm	In the vented cavity, at the cladding
Outdoor	1057 mm	800 mm in front of the elements, at the outdoor side

1: Element 4 contained no gypsum board. Depth B is at the outdoor side of the cellular concrete, Depth C was 48 mm inside the thermal insulation, corresponding to 97 mm from the indoor side of the element etc.
2: See also Appendix B, Table B1, note 1.
3: No sensors in Element 4 at Depth A; cf. no gypsum board

Sensors at Depth I were removed when the vapour barrier was added. Later these sensors were used at Depth G when the cladding was added.

A grid with relative humidity (RH) sensors and thermocouples was added at the indoor side at 500 mm from the surface and at the outdoor side at 800 mm from the surface. At the indoor side nine pairs of sensors were placed in a 3×3 grid of 700 × 750 mm. At the outdoor side four pairs of sensors were placed in a 2×2 grid of 900 × 1000 mm.

Before the test all the sensors were calibrated and checked for any misleading readings. Names, numbers and placement of sensors are described in Appendix D. A description of the sensors is given in Appendix A. It was assumed that all the work with preparing and adjusting the test set-up would be made in such a way that it did not affect the results.

Test series

The test series consisted of four main tests (named M1, M2, M3 and M4). Previously a few pre-tests with anemometers were carried out at steady-state conditions, in order to get data concerning the surface transfer coefficients at the indoor side before a vapour barrier was mounted at Element 1 and 3 (table B1). These data were necessary for tuning the calculation model at DTU BYG (Steskens, in press). All measurements in the pre-tests were made manually and they are not reported here.

The main tests are presented in Table 2. Refer to Appendix B for a further description.

Table 2. Main tests.

Test	Description
M1	Steady-state without vapour barriers at Elements 1 and 3
M2	Steady-state with vapour barriers at Elements 1 and 3. At Element 3, a horizontal slit at the top at the outdoor side and at the bottom at the indoor side is unsealed
M3	Varying climate without cladding. April (M3A) and September (M3S) are simulated
M4	Varying climate with cladding and vented cavity at the outdoor side. April (M4A) and September (M4S) are simulated

In order to ensure that Elements 1, 2 and 3 behaved identically, test M1 was performed. Test M2 was performed in order to study the effect of a vapour barrier and/or an air flow inside the element. Both these tests were performed at steady-state which made it easier to control whether the test setup and the test elements behaved as expected. Tests M3 and M4 were chosen in order to study cyclic conditions at different seasons without and with an outer cladding.

The test design included mounting of a shelf and a radiator in the indoor side in order to study local 2D phenomena around these, but several delays in the test programme made it impossible to carry out these within the limits of this project.

Before each of the tests involving varying climate, the elements were exposed to a period of constant boundary conditions in order to establish steady-state. As the results showed the conditions for performing M3 and especially M4 were not optimal. Several delays in the preparation of the test set-up, not least due to problems with the cooling machine, which in the end had to be replaced, resulted in a very narrow time schedule for delivering the results needed for the PhD project (Steskens, in press) included in the overall project. Therefore there was insufficient time to reach steady-state in all cases.

Boundary conditions – steady-state

The following boundary conditions were used in the pre-tests and in tests M1 and M2.

Indoor climate (indoor side of the set-up)

– Temp.: 23-24 °C (optimum) *
– RH: 40-45 % **

*: The indoor climate chamber is insulated with 100 mm of mineral wool thermal insulation. The temperature and RH in the laboratory hall was free floating, i.e. it was relatively cold in the winter and hot in the summer. At days with sunshine during the daytime and a clear sky during the night, especially in the spring and summer, it was not possible to keep a constant temperature at the indoor side.

**: A vaporiser ensured a stable RH level, provided that RH in the laboratory hall was within specific limits. On a yearly basis the conditions in the laboratory hall changed from rather dry to rather humid. The present set-up was not able to compensate for this.

Outdoor climate (outdoor side of the set-up)

– Temp: +2 °C (to avoid frequent need for defrosting) *
– RH: 55 % **

*: In order to stabilise the temperature at steady-state, 100 kg of bricks were installed at the outdoor side (see photo A11 in Appendix A)

**: In practice the RH was free floating because it was decided not to spray water as a way to change the RH, cf. the introduction to chapter 'Test design'.

Air pressure across element, ΔP: 0.

Climatic cycles

For tests performed at varying conditions (M3 and M4), it was not possible to program an hourly set point for temperature and RH at the outdoor side of the climate chamber, which would be optimal in order to simulate the climate in Denmark in specific months of the year. As previously described the UV lamps at the outdoor side were not used.

Instead 24-hour temperature cycles representing specific months of the year in the Danish climate were simulated by manually changing the inlet temperature of the air from the cooling machine twice a day, while the air velocity was kept constant to ensure a good circulation of the air.

Two climatic cycles were selected based on the average hourly air temperature per month as part of weather data presented by the U.S: Department of Energy (U.S. Department of Energy, 2009). The restrictions for the maximum cooling load which could be supplied by the cooling machine were taken into account. Table E1, Appendix E, presents the average hourly air temperature. The relative humidity was free floating.

Both climatic cycles were modified in order to make them operational in the laboratory as the set points of the cooling machine had to be switched manually. Therefore, the April cycle consisted of an 8 hour period at 9 ºC and a 16 hour period at 4 ºC, measured in front of the test elements, at the outdoor side. The September cycle consisted of an 8 hour period at 15 ºC and a 16 hour period at 11 ºC. These set points had to be translated to set points for the temperature of the air provided by the cooling machine. Details can be found in Appendix E.

Numerical investigations of the walls without cladding were carried out to estimate the time it would take to reach steady-state. This should be after

approximately 1 month. Because of a tight test schedule, this was reduced to 14 days if the set-up was close enough to steady-state.

Results and discussion

A typical 24-hour cycle in one of the four elements was chosen from each of the main test, M1-M4. Both temperature and RH profiles – and in some cases vapour pressure profiles – from the indoor side to the outdoor side at a specific height were made. In some cases this chapter also includes figures where the conditions in different heights at a specific depth are compared. For each test these results are discussed.

The number of elements, sensors and tests made the potential comparisons of test results enormous and this report only displays some of them. In general, results shown in this chapter were based on data from Element 1 (reference). Results for all elements are shown in Appendices F to K. If not otherwise indicated, the comments in this chapter are relevant for all four elements.

This chapter also shows whether it was possible to follow the modelled temperature cycles, and figures show the repeatability of the cycles. Finally, a comparison was made between the experimental results and the computed results based on the work in (Steskens, in press).

General remarks

The different sensors were designated by their position in at a specific element, a specific height, and a specific depth according to Appendix D. If not otherwise indicated, the presented results were based on measurements at height 'h3c', 1450 mm from the top side of the bottom rail. Total height of an element was 2630 mm excl. the top rail and the bottom rail (Figure 5).

The presentation of results does not include the sensors placed at hx6, hx7, hx8 and hx9, since they are not relevant in the present context, cf. section 'Elements and sensors' of the chapter 'Test design'.

The results showed that the sensor placed at position 'h3c' in Elements 2 and 3 was not representative of RH at Depth C (in the middle of the thermal insulation). Instead the sensor at position 'h4c', 2130 mm from the top side of the bottom rail, represented RH at Depth C in these elements. It is not considered likely that the sensors in position 'h3c' and 'h4c' by accident were exchanged. A great effort was done at the preparation of the test setup in order to ensure that the sensors were placed in accordance with their designation.

Please note that there were only four temperature and RH sensors at the outdoor side, placed in front of Elements 2 or 3, i.e. no sensors in front of Element 1 or Element 4, cf. Appendix D. Since the difference between them was less than 0.3 – 0.5 $^{\circ}$C (temperature) or 2 % (RH) it was of no importance which of them were used to represent the outdoor conditions. At the indoor side sensors were placed in front of all four elements.

Steady-state without vapour barrier (test M1)

As expected, the temperature and the RH at Depth A – just behind the indoor gypsum cladding – was very close to the temperature and the RH at the indoor side since none of the elements contained a vapour barrier at this stage (Figures 10 and 11). It was also expected that the temperature decreased and the RH increased from the indoor to the outdoor side, also when data from Depths B and D inside the thermal insulation (see Table 1) were included (Elements 2, 3 and 4, cf. Figures F4 – F10, Appendix F). The

two deviations from a stable condition in the temperature and RH at the outdoor side showed the frequency of the defrosting of the cooling machine.

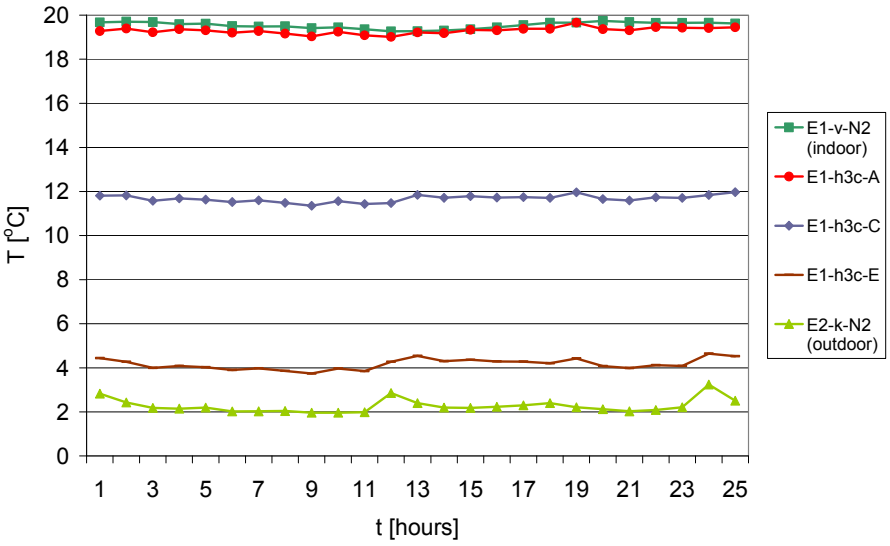

Figure 10. Temperature, Element 1. Steady-state without vapour barrier. Temperature at the indoor side, behind the indoor gypsum cladding (A), in the centre of the thermal insulation (C), in the thermal insulation, at the wind barrier (E) and at the outdoor side. 24-hour cycle starting at midnight with defrosting periods at noon and midnight. 'E2-k-N2' placed in front of Element 2 represents the temperature at the outdoor side.

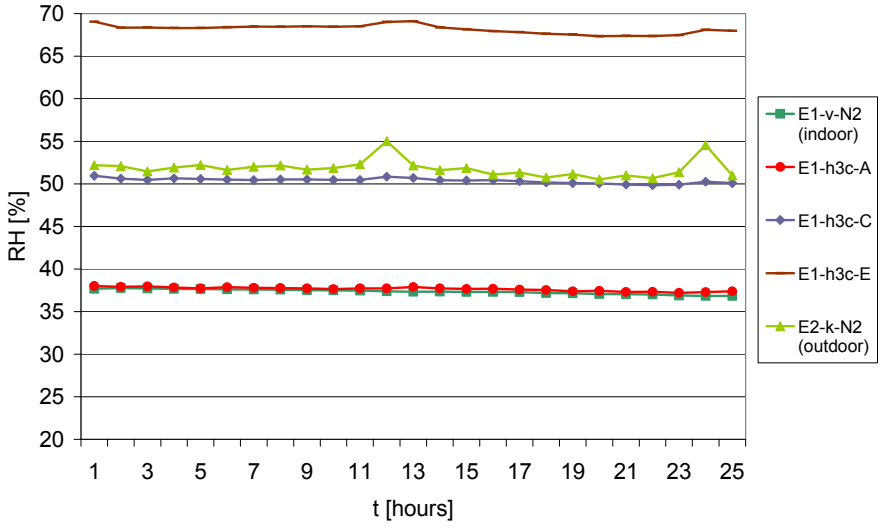

Figure 11. RH, Element 1. Steady-state without vapour barrier. Indoor, Depths A, C and E, and Outdoor. 24-hour cycle starting at midnight with defrosting periods at noon and midnight. See also Figure 10.

Another way to show the output of the test was by displaying the vapour pressure at the different depths. In Figure 12 this was done in Element 1. As for the temperature and the RH, it was expected that the vapour pressure at the indoor side and at Depth A was the same. Figure 12 shows that this was the case and also that the vapour pressure as expected descended through the element from the indoor side to the outdoor side.

In Figure F6, Appendix F, the vapour pressure is displayed for Element 2, which as expected showed to be very similar to Element 1. On the other hand, Figure F6 shows a surprisingly high vapour pressure at Depth B (1/4 inside the thermal insulation) in Element 2. Vapour pressure is related to the temperature which in this case was scattered. Maybe the sensor was not placed at the optimal position. A similar observation regarding the temperature could be found in Element 4. Here the sensor at Depth B was placed at

the outdoor side of the cellular concrete, i.e. between two different materials, which could to some extent explain the behaviour of the temperature curve (Figure F10). The high vapour pressures at Depth B was also found in the following tests, cf. Figures G6, H6, I6, J6 and K6.

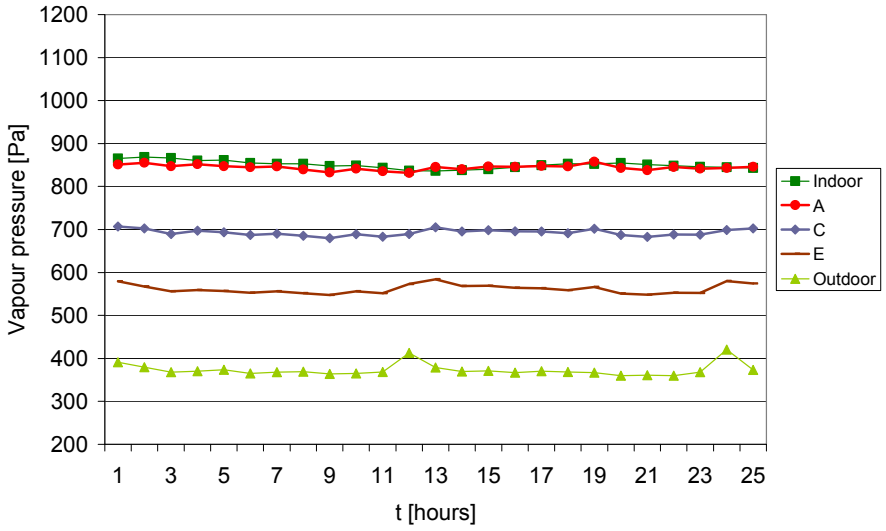

Figure 12. Vapour pressure, Element 1. Indoor, Depths A, C and E, and Outdoor. Steady-state without vapour barrier. Designations, see also Figure 10.

In Element 4 the temperature at Depth E in height 'h3c' was not constant at all; it fluctuated between 5 ºC and 8 ºC. Figure 13 shows that the temperature measurements at different heights at Depth C did not correspond very well. Similar observations were made in tests M2 and M3A, except that the differences between 'h2c', 'h3c' and 'h4c' diminished, see for instance Figure H15. Therefore 'h4c' and not 'h3c' represented Element 4 at Depth E in these cases. None of these sensors were placed closer than 100 mm to a joint, i.e. closeness to a joint can not explain the rather irregular curves.

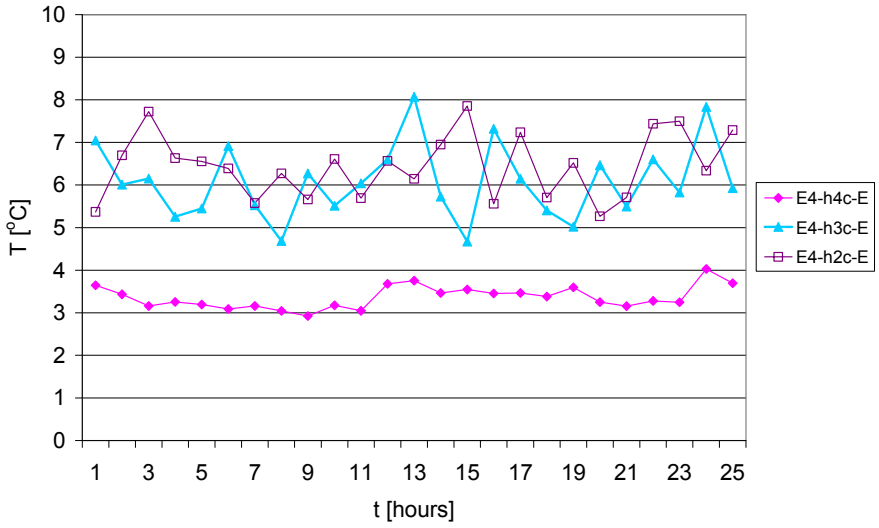

Figure 13. Temperature, Depth E (in the thermal insulation, behind the wind barrier). Element 4. Steady-state without wind barrier.

In the middle of the thermal insulation (Depth C) large differences in RH at different heights were observed, e.g. Figure 14, while the differences were much smaller at other depths, e.g. Figure F14 and F16. No explanation was found but it indicated that the results at this depth in Element 3 were not totally reliable, at least at 'h3c' and 'h5c'. Similar observations were made for Element 2 (not displayed), and also in test M2, M3 and M4, e.g. Figure G11.

Therefore, 'h4c' was chosen to represent Depth C in Elements 2 and 3 instead of 'h3c'.

Although the temperature was the same in the different heights at Depth C, cf. Figure 15 and Appendix F, Figure F12, 'h3c' was replaced by 'h4c' both for RH and temperature, in order to use RH and temperature data from the same position at Depth C.

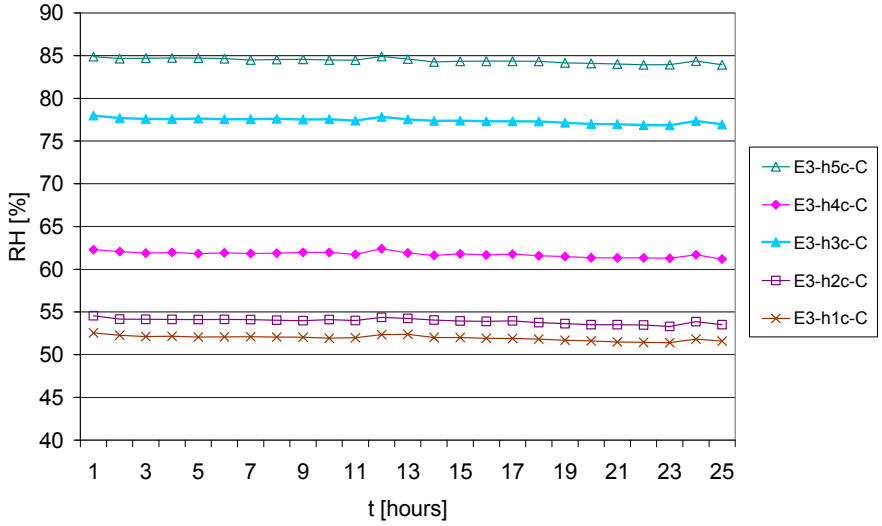

Figure 14. RH, Depth C (in the middle of the thermal insulation). Element 3. 2430 mm from the bottom of the element (h5c), 2130 mm from the bottom of the element (h4c), 1450 mm from the bottom of the element (h3c), 500 mm from the bottom of the element (h2c) and 200 mm from the bottom of the element (h1c). Height of element 2630 mm (excl. top rail and bottom rail). 24-hour cycle starting at midnight with defrosting periods at noon and midnight.

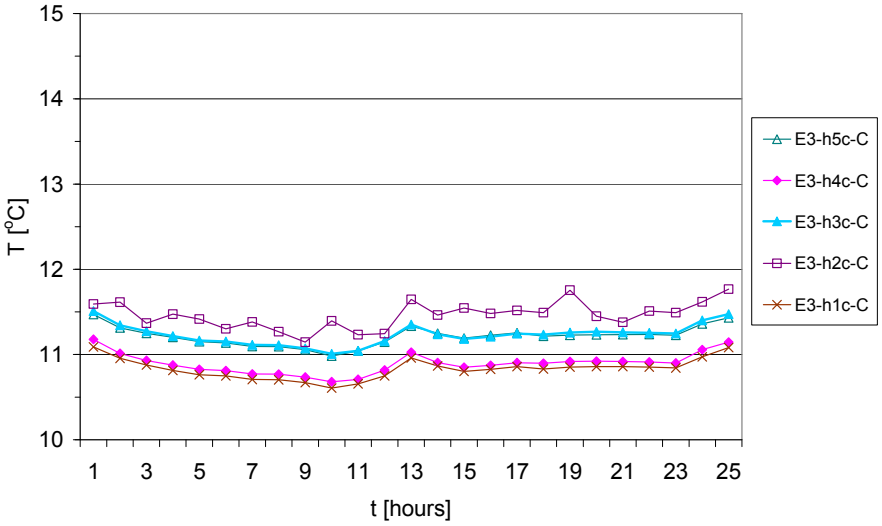

Figure 15. Temperature, Depth C. Element 3. Steady-state without vapour barrier. 24-hour cycle starting at midnight with defrosting periods at noon and midnight. See also Figure 14.

Figure 16 shows the RH at the different depths in Element 3 when 'h3c' was replaced by 'h4c' at Depth C. Apart from a very small difference in RH at Depths C and D this result was as expected.

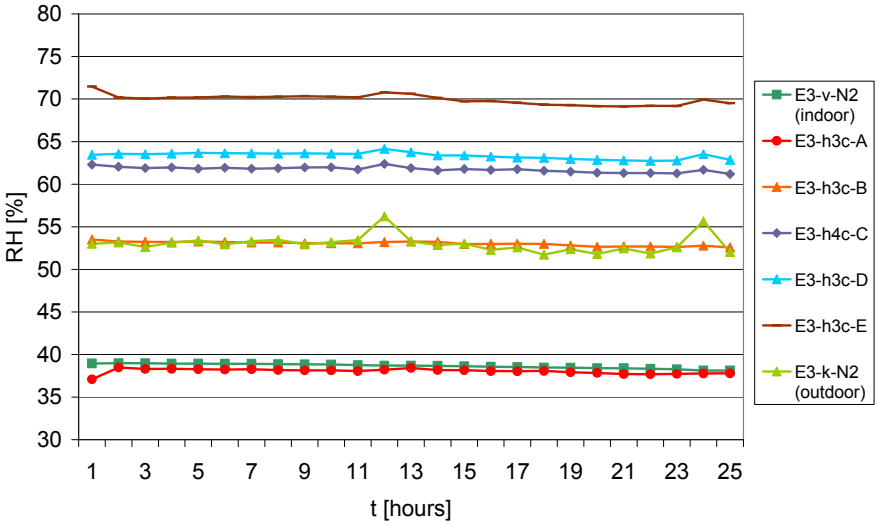

Figure 16. RH, Element 3. Steady-state without vapour barrier. RH at the indoor side, at the inner gypsum board (A), ¼ inside the thermal insulation (B), ½ inside the thermal insulation (C), ¾ inside the thermal insulation (D), at the wind barrier (E) and at the outdoor side. 24-hour cycle starting at midnight with defrosting periods at noon and midnight.

In the steady-state test without vapour barrier, the temperature is a little higher in the upper fifth of an element (position 'h5c' and 'h4c') than in the lower fifth (position 'h2c' and 'h1c'). In Appendix F this is shown for Element 2 at Depths A, C and E. At Depth E the difference was about 1 ºC, while at Depths A and C the difference was even smaller, about 0.4 – 0.6 ºC.

Apart from the cases where a sensor seemed to be unreliable, comparison of RH at different heights showed that RH was higher at the upper part in the elements than in the lower parts, in accordance with the difference in temperature. See for instance Figures F14 and F16 in Appendix F.

Steady-state with vapour barrier (test M2)

Elements 1 and 3 included a vapour barrier, while Elements 2 and 4 were the same as in test M1 (steady-state without vapour barrier).

Temperature and RH from a 24-hour period about three weeks after mounting vapour barriers at Elements 1 and 3 is shown in Figures 17 and 18. RH at Depth A (right behind the gypsum board inner cladding) was much lower than at the indoor side, as opposed to the condition before mounting the vapour barrier (Figure 11); i.e. the vapour barrier worked. With a vapour barrier RH was 22 % at Depth A, without a vapour barrier it was 38 %. The effect of the vapour barrier was even larger, since RH_{indoor} was higher in test M2 than in M1.

The effect of the vapour barrier was also seen at Depth C (in the middle of the thermal insulation) and at Depth E behind the wind barrier. At Depth C the RH was reduced from about 50 % RH to about 35 % RH. At Depth E it was reduced from about 70 % RH to about 60 % RH. Similar changes was seen in Element 3, cf. Appendix F.

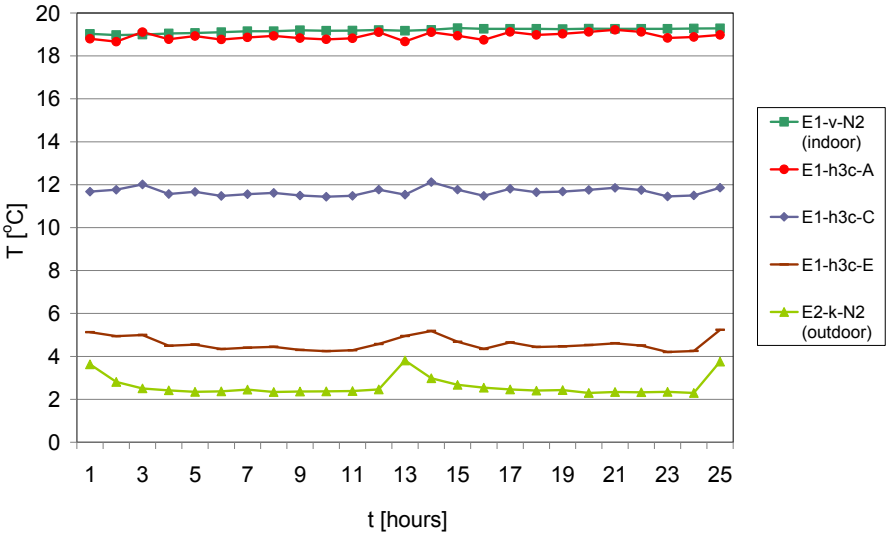

Figure 17. Temperature, Element 1. Steady-state with vapour barrier. Indoor, Depths A, C and E, and Outdoor. 24-hour cycle starting at midnight with defrosting periods at noon and midnight. For designations, see also Appendix D.

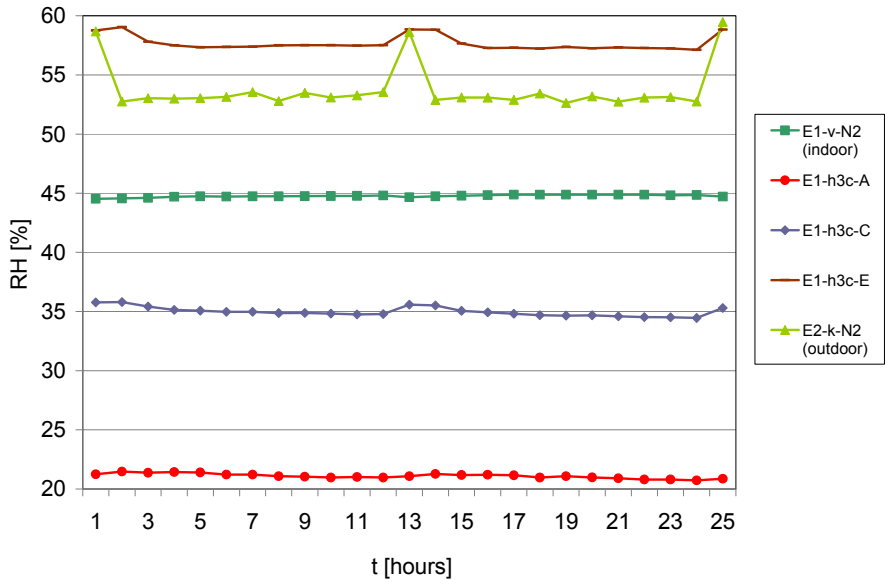

Figure 18. RH, Element 1. Steady-state with vapour barrier. Indoor, Depths A, C and E, and Outdoor. 24-hour cycle starting at midnight with defrosting periods at noon and midnight. For designations, see also Appendix D.

Figure 19 shows the vapour pressure for the same period as used in Figure 17 and 18. It shows the effect of the vapour barrier at Element 1 since the vapour pressure was almost the same at all depths on the outdoor side of the vapour barrier and much lower than on the indoor side, as opposed to the output of the previous test (Figure 12).

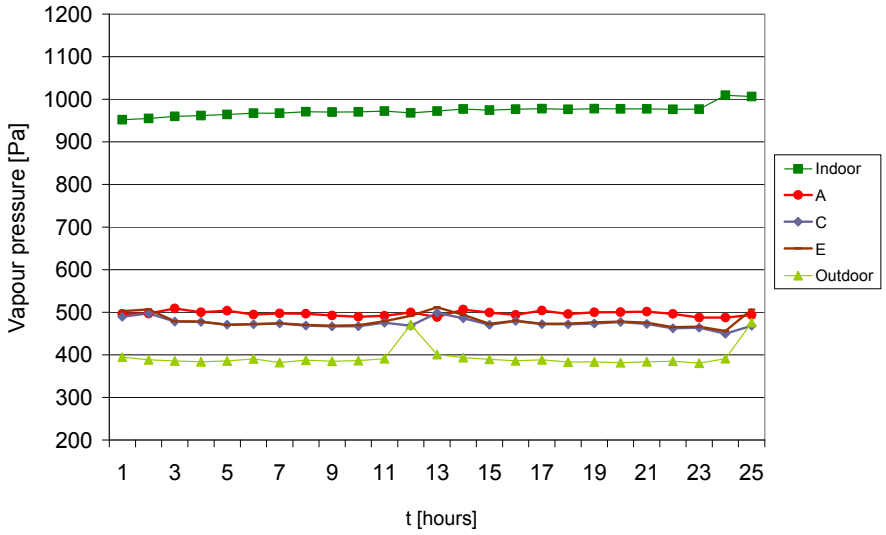

Figure 19. Vapour pressure, Element 1. Steady-state with vapour barrier. Indoor, Depths A, C and E, and Outdoor. 24-hour cycle starting at midnight with defrosting periods at noon and midnight. For designations, see also Appendix D.

Figure 20 shows the vapour pressure at the different depths in Element 2. Because this element contained no vapour barrier the vapour pressure was the same at Depth A as at the indoor side. As in test M1 (Figure F6, Appendix F), Figure 20 shows that the vapour pressure at Depth B was higher than at the indoor side which of course makes no sense, i.e. indicating that the sensors at this depth were unreliable. Apart from this, Figure 20 shows a descending vapour pressure from the indoor side to the outdoor side.

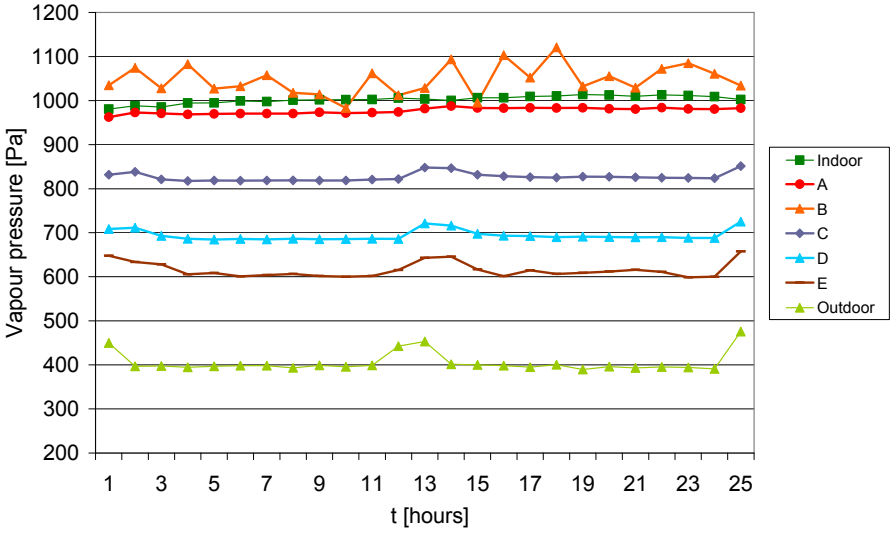

Figure 20. Vapour pressure, Element 2. Steady-state with vapour barrier. Indoor, Depths A – E, and Outdoor. 24-hour cycle starting at midnight with defrosting periods at noon and midnight. For designations, see also Appendix D.

As expected, there were no changes in Elements 2 and 4 concerning RH, when the results were adjusted for the higher RH_{indoor} in test M2 compared with test M1. See Figures G5 and G10, Appendix G.

In all four elements the temperature in the different layers was the same as in test M1. This was not surprising since the only change was the addition of vapour barriers in Elements 1 and 3.

April without cladding (test M3A)

As the next step the elements were exposed to a number of 24-hour temperature cycles, representing April, cf. chapter 'Test series'. For Element 1 this gave the results shown in Figure 21 (temperature), Figure 22 (RH) and Figure 23 (vapour pressure).

While the RH was kept constant at the indoor side by means of a vaporiser, Figure 22 shows the result of not trying to simulate the outdoor RH in April: the $RH_{outdoor}$ was much lower than if a moisture load had been introduced. In Denmark it is normal with 70 – 80 % RH in April. Note also the delay in the peak of the RH cycle through the different layers of the element, which expressed how fast a change in the $RH_{outdoor}$ was distributed through the element.

Compared with test M2 (steady-state with vapour barrier) RH was higher in the different layers, which was caused by a higher RH at the outdoor side.

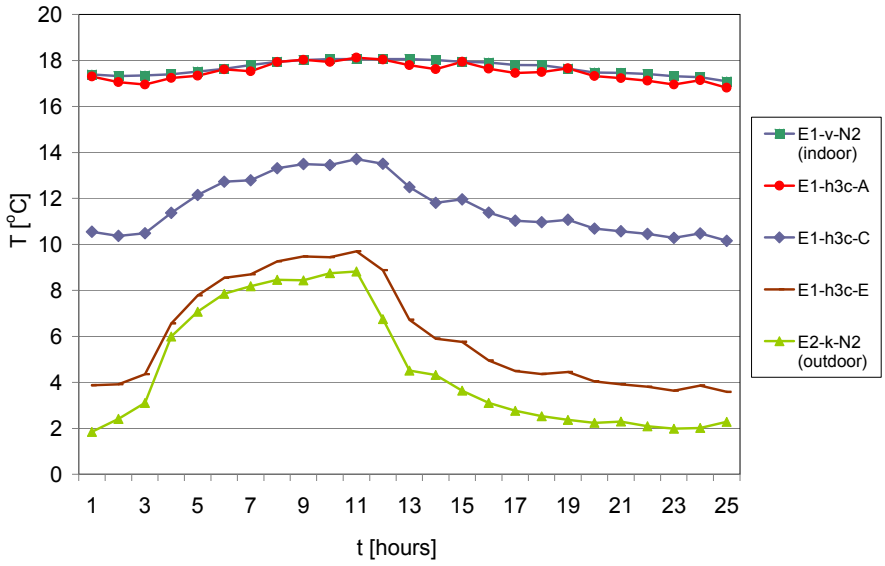

Figure 21. Temperature, Element 1. April without cladding. Indoor, Depths A, C and E, and Outdoor. Example of 24-hour cycle starting at 9 AM. For designations, see also Appendix D.

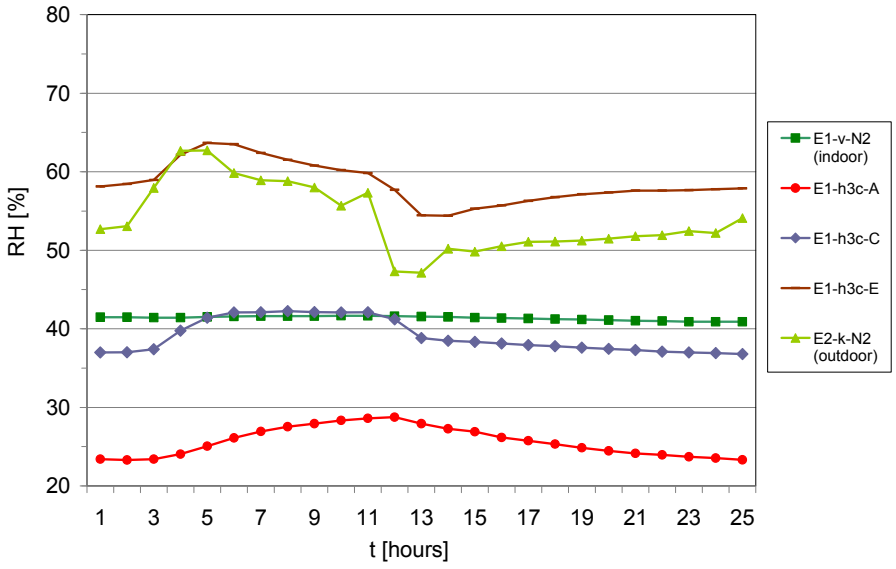

Figure 22. RH, Element 1. April without cladding. Indoor, Depths A, C and E, and Outdoor. Example of a 24-hour cycle starting at 9 AM. For designations, see also Appendix D.

Figure 23 shows that the changes in vapour pressure in Element 1 were determined by the outdoor conditions, because of the vapour barrier at the indoor side. The changes in the outdoor vapour pressure as a result of the stipulated 24-hour cycle, were more or less reflected in the pattern of the vapour pressure inside the element, and of course most distinct at Depth E (just behind the wind barrier). The high vapour pressure at the outdoor side in this phase gave rise to an inward transport of moisture, cf. a higher vapour pressure at the outdoor side than in Depth A (behind the inner cladding) and Depth C (in the middle of the thermal insulation). When the temperature stabilised at the end of the 24-hour period (Figure 21) the pattern of the vapour pressure was the same as in the case with a steady-state exposure (Figure 19).

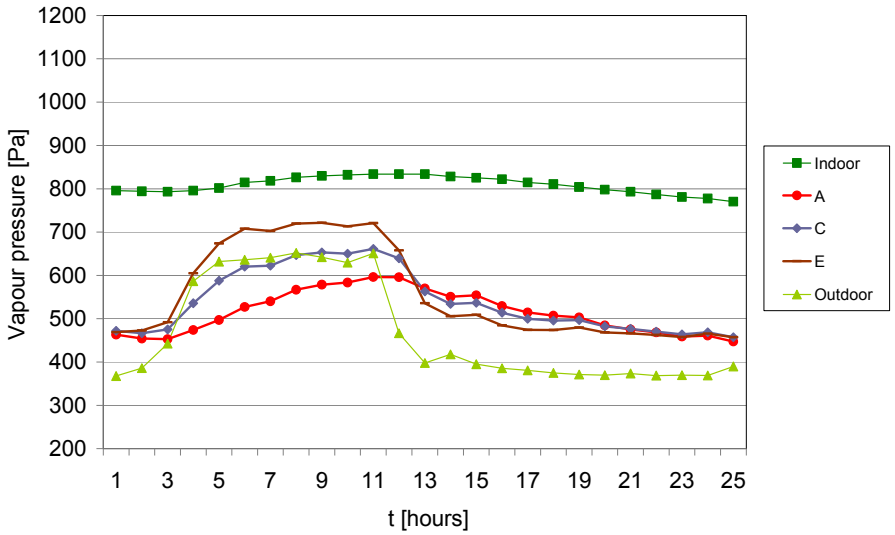

Figure 23. Vapour pressure, Element 1. April without cladding. Indoor, Depths A, C and E, and Outdoor. Example of a 24-hour cycle starting at 9 AM. For designations, see also Appendix D.

In Figure 24, showing the vapour pressure in Element 2 exposed to an April cycle, a descending vapour pressure from the indoor side to the outdoor side was still visible. Because of this the internal order of the curves representing the different depths inside the element did not change as in the case with Element 1. Instead, due to the relatively higher vapour pressure at Depths A and C in Element 2, the vapour pressure at these depths became higher than at the indoor side when the outdoor vapour pressure rose.

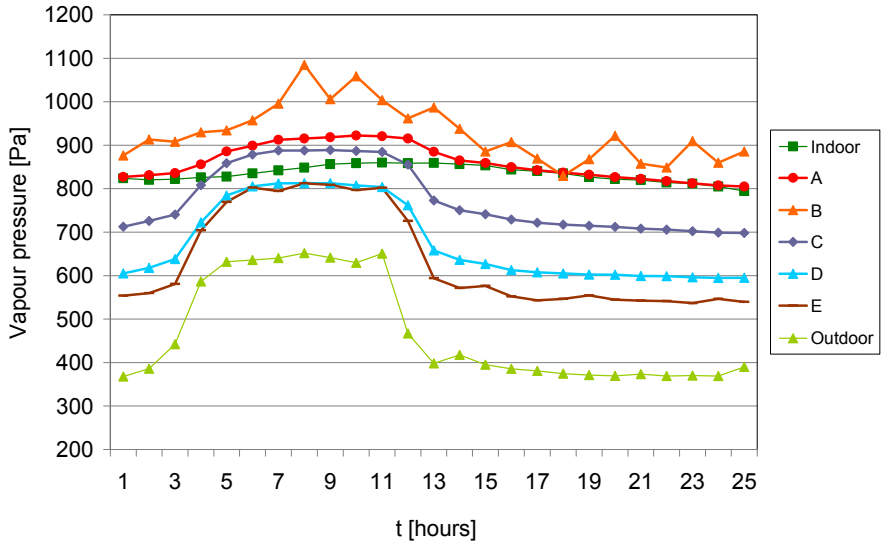

Figure 24. Vapour pressure, Element 2. April without cladding. Indoor, Depths A – E, and Outdoor. Example of a 24-hour cycle starting at 9 AM. For designations, see also Appendix D.

Figure 25 shows that the temperature was about the same in the whole element as in the middle of the thermal insulation (Depth C). The differences were larger behind the wind barrier (Depth E), but still no more than 1 ºC (Figure 26). In Element 4 the difference was about 3 ºC (Figure H15). In cases where it was possible to distinguish between the temperatures at different positions, the temperature was highest in the lower part of the element and lowest in the upper part. This was illustrated in Figure 26 where the upper three curves are from sensors located in the lower fifth of the element and the lower three curves from sensors located in the upper fifth of the element.

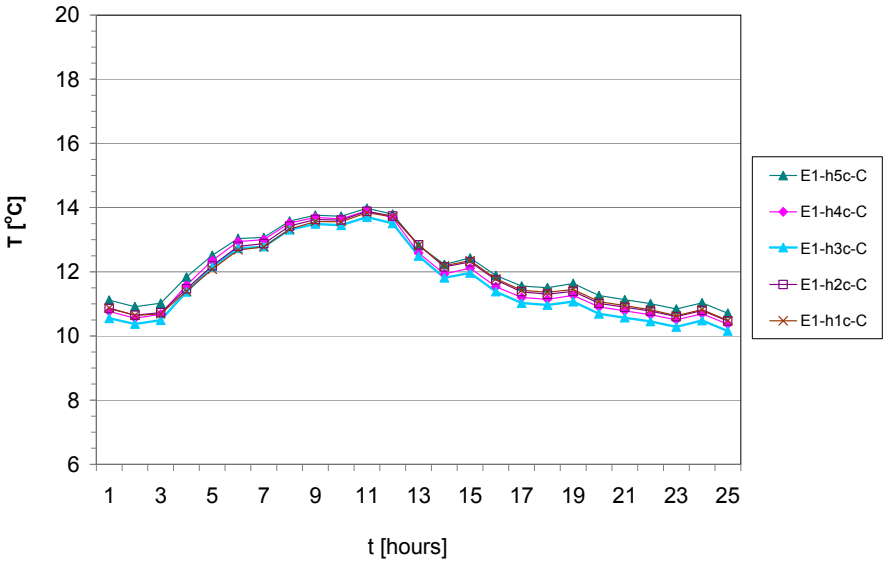

Figure 25. Temperature, Depth C (in the middle of the thermal insulation). Element 1. April without cladding. For designations, see also Appendix D.

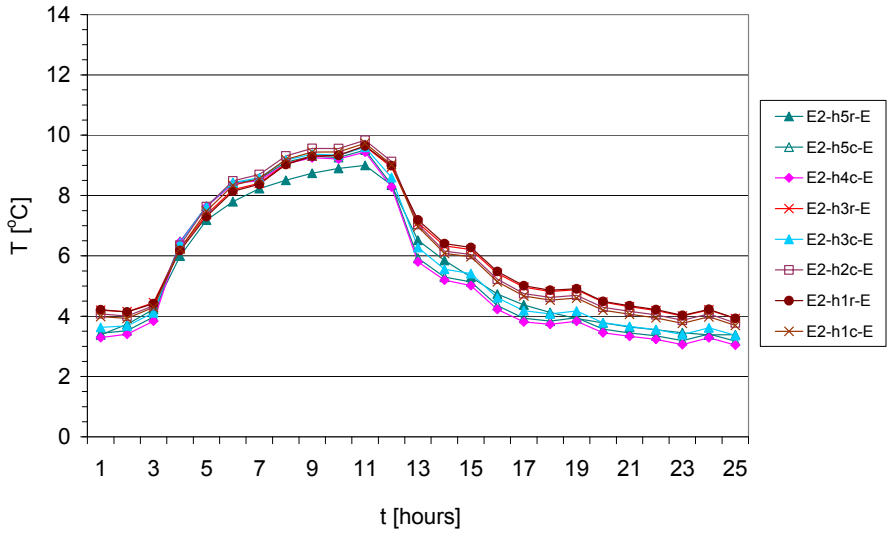

Figure 26. Temperature, Depth E (behind the wind barrier). Element 2. April without cladding. 2430 mm from the bottom of the element (h5r, h5c), 2130 mm from the bottom of the element (h4c), at the middle (h3r, h3c), 500 mm from the bottom of the element (h2c) and 200 mm from the bottom of the element (h1r, h1c). Sensors designated 'c' are placed in the centre, vertically, sensors designated 'r' are placed 100 mm from the right side of the element (cf. Figure 5). Size of element 2630 × 650 mm (excl. top rail and bottom rail).

Figure H14, Appendix H, shows that there was no dependency of height at Depth A, if the result at 'h1c' was disregarded. At Depth C (Figure H15) the result was somewhat confusing as discussed previously in the section 'General remarks'. At level E (Figure H16) the most interesting observation was

the dependency of the horizontal position, whether the sensor was placed in the centre of the element (designation 'c') or closer to the next element (designation 'r'). RH was about 5 % lower at the 'r' position indicating some kind of edge effect, especially at the bottom of the element ('h1').

Since there was almost no dependency of the height on the temperature, there are no figures showing the vapour pressure shown since these will give no additional information of the figures showing RH.

September without cladding (test M3S)

None of the temperature curves at Depths A, C and E (Figure 27) were smooth, which indicated that the elements did not reach steady-state completely before the September cycle was introduced. Comparing with the results in test M3A (April with cladding) RH was much higher at Depths A and C, but only a little higher at Depth E (Figure 28). This could only partly be explained by a higher RH_{indoor}.

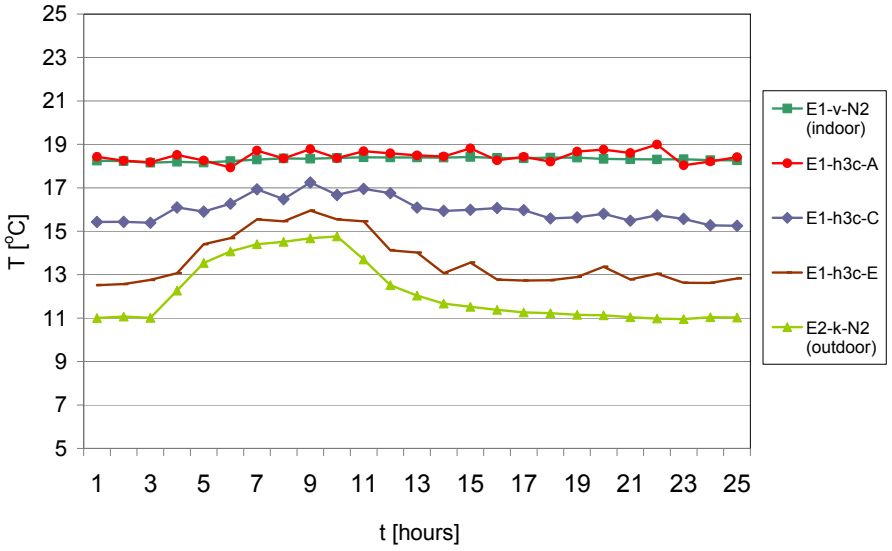

Figure 27. Temperature, Element 1. September without cladding. Indoor, Depths A, C and E, and Outdoor. Example of 24-hour cycle starting at 9 AM. For designations, see also Appendix D.

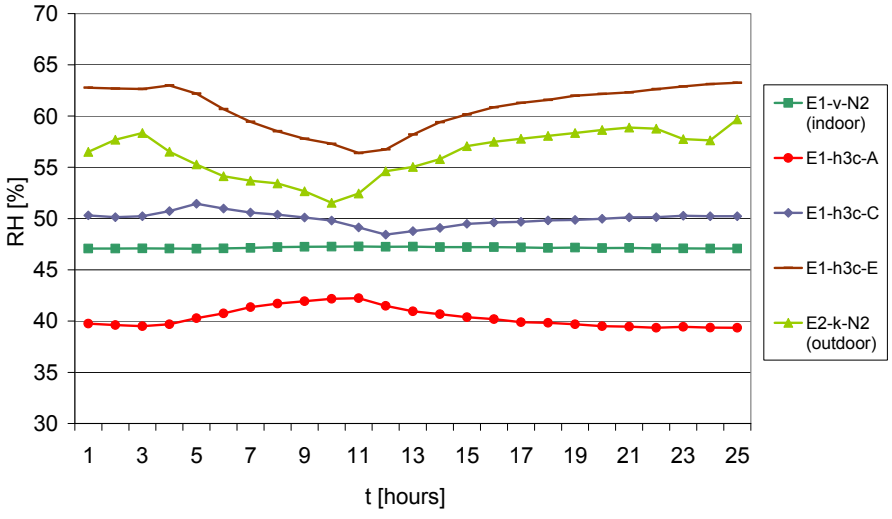

Figure 28. RH, Element 1. September without cladding. Indoor, Depths A, C and E, and Outdoor. Example of 24-hour cycle starting at 9 AM. For designations, see also Appendix D.

In Figure 29 showing the vapour pressure in Element 1 the curves are much more unstable and they do not coincide at the end of the 24-hour cycle as in the previous test (Figure 23). Both the temperature (Figure 27) and the vapour pressure indicate that the elements had not reached steady-state before introducing the September cycle. As in the previous test the effect of the change in the outdoor vapour pressure was most prominent at Depth E (behind the wind barrier).

The results from Element 2 (no vapour barrier), shown in Figure I6, Appendix I, gave an even more blurred picture, with a quite unstable level of vapour pressure in several layers of the element and in most cases also a higher vapour pressure than at the indoor side. This was probably caused by the absence of steady-state at the beginning of the test.

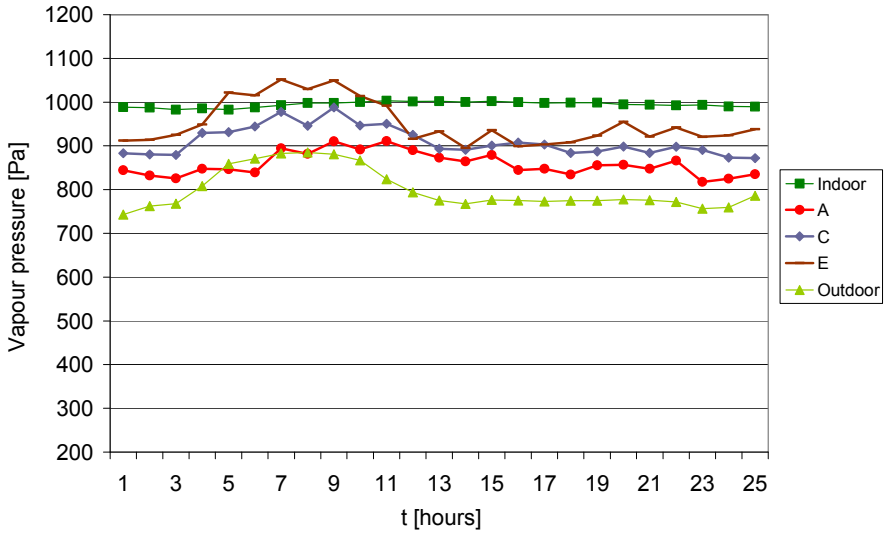

Figure 29. Vapour pressure, Element 1. September without cladding. Example of 24-hour cycle starting at 9 AM. For designations, see also Appendix D.

Figures 30 and 31 show the variation in temperature with height at Depths C and E. The irregular curves illustrate that the elements had not reached steady-state before the September cycle was started; there was no relation between the vertical position of a sensor and the temperature. Therefore it was not possible to conclude whether there was convection through the element.

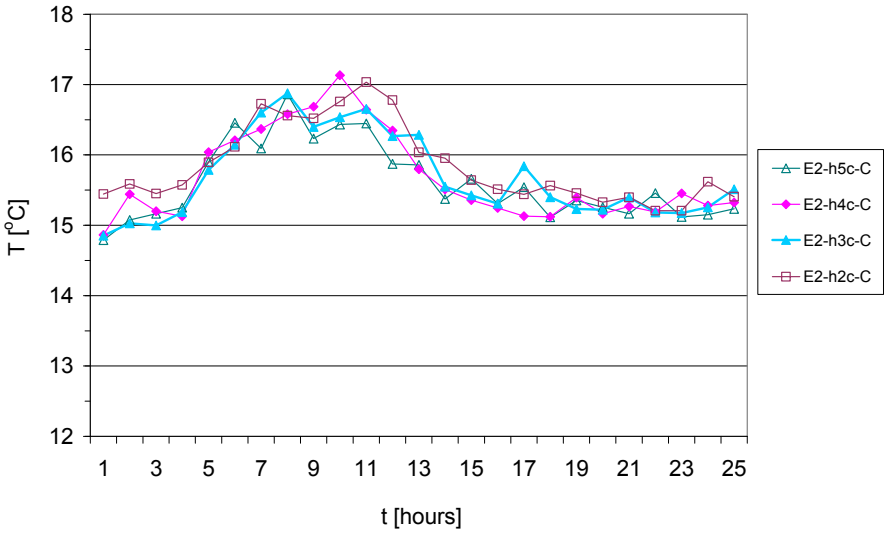

Figure 30. Temperature, Depth C (in the middle of the thermal insulation). Element 2. September without cladding. For designations, see also Appendix D.

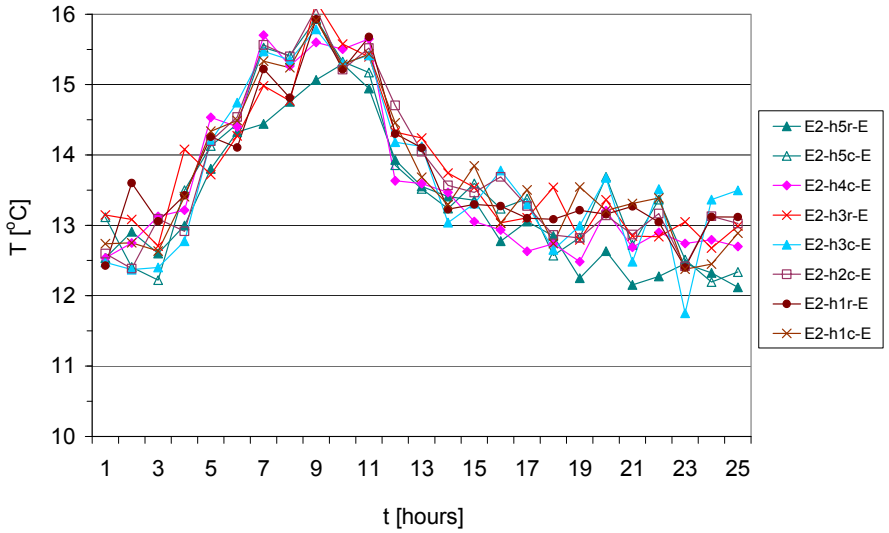

Figure 31. Temperature, Depth E (behind the wind barrier). Element 2. September without cladding. Example of 24-hour cycle. For designations, see also Appendix D.

April with cladding (test M4A)

Before test M4, a cladding was added to the outdoor side of all four elements, with a 25 mm vented cavity behind the cladding.

The difference between the temperature at Depth E (in the thermal insulation, at the wind barrier) and outdoor was 2 ºC in 'April without cladding' (Figure 21) and about 4 ºC in 'April with cladding' (Figure 32); less in Element 4. This indicated that the vented cavity has a positive effect on the insulation capacity of the wall, although the temperature gradient across the wind barrier (from Depth E to Depth F) was surprisingly high in the case with cladding.

Whether the cladding had other effects was difficult to conclude, because the April cycle was not the same before and after mounting the cladding, cf. chapter 'Experimental vs modelled cycles'. The lower set point of the cycle was higher in the 'April with cladding' test.

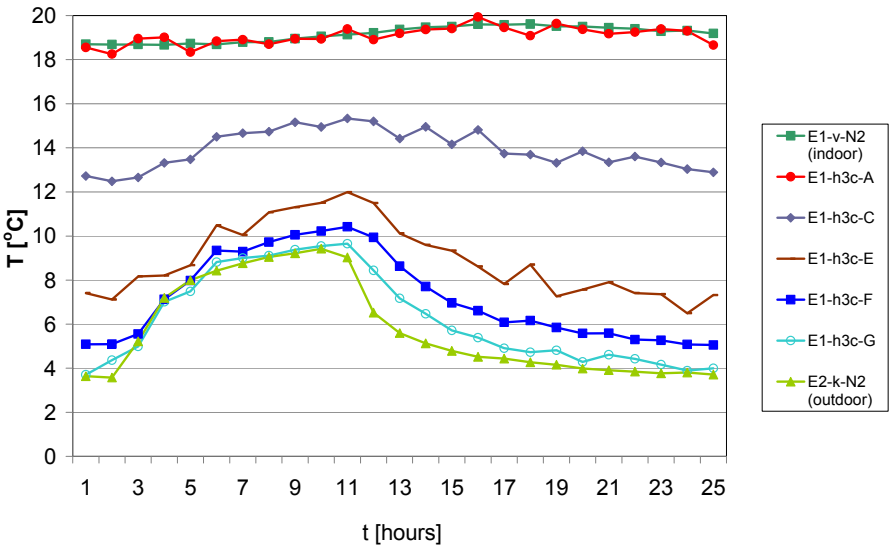

Figure 32. Temperature, Element 1. April with cladding. Indoor, Depths A - G, and Outdoor. Example of 24-hour cycle starting at 9 AM. For designations, see also Appendix D.

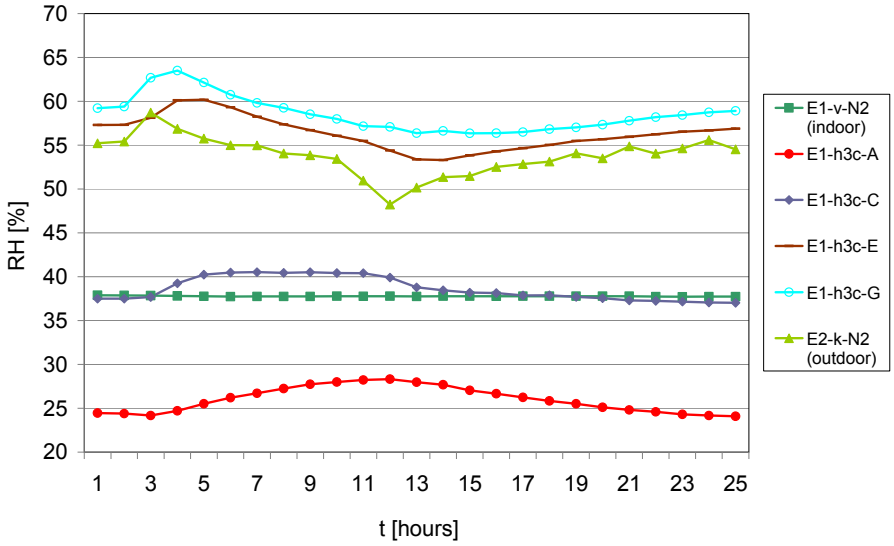

Figure 33. RH, Element 1. April with cladding. Indoor, Depths A - G, and Outdoor. Example of 24-hour cycle starting at 9 AM. For designations, see also Appendix D.

In Figure 34 showing the vapour pressure in Element 1, it was no surprise that the vapour pressure at Depth G (in the cavity, at the cladding) was higher than outdoors and lower than at Depth E. This showed that for instance the vapour pressure in the cavity was not affected by the presence of a vapour barrier.

Compared with test M3A (April without cladding) the curves representing the vapour pressure at Depths A, C and E were not as stable at the end of the 24-hour cycle, although they almost coincided. Compared with test M3S (September without cladding) this indicated that it was easier to reach conditions representing April than September, maybe due to the larger temperature difference between the indoor side and the outdoor side in the April cycle.

On the other hand the result for Element 2 (Figure J6, Appendix J) showed that the ability to control the test conditions also seemed to be dependent on the existence of a vapour barrier, since Figure J6 gave a blurred picture much like the one in Figure I6 ('September without cladding').

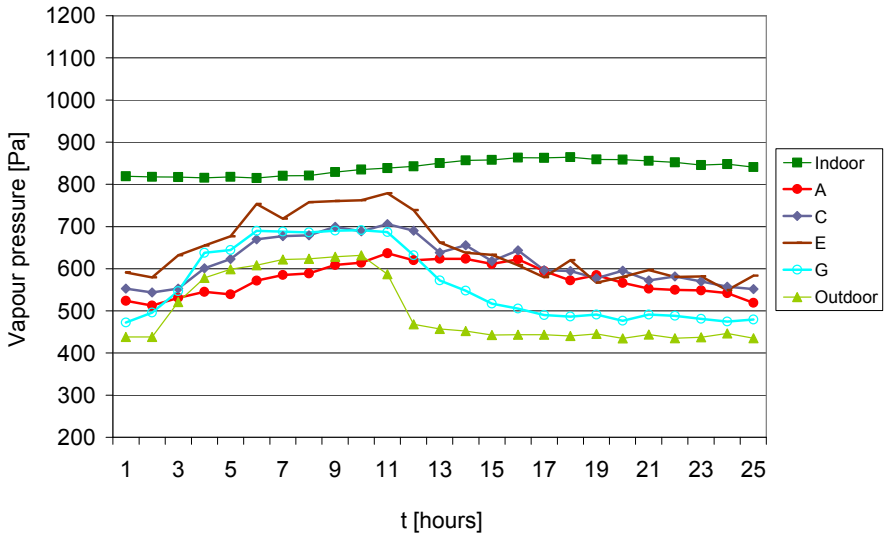

Figure 34. Vapour pressure, Element 1. April with cladding. Indoor, Depths A - G, and Outdoor. Example of 24-hour cycle starting at 9 AM. For designations, see also Appendix D.

After mounting the cladding it was difficult to see any pattern in the distribution of the temperature in a vertical direction, especially inside the thermal

insulation (e.g. Depth C). The elements probably did not reach steady-state before the tests with varying climate were carried out, as seen from the irregular shape of the curves in Figure 32. The only exception was the temperature in the vented cavity, at the cladding (Depth G), where a 0.5 - 1 ºC difference was seen between the upper and lower parts of the element when the outdoor temperature fell, as shown in Figure 35.

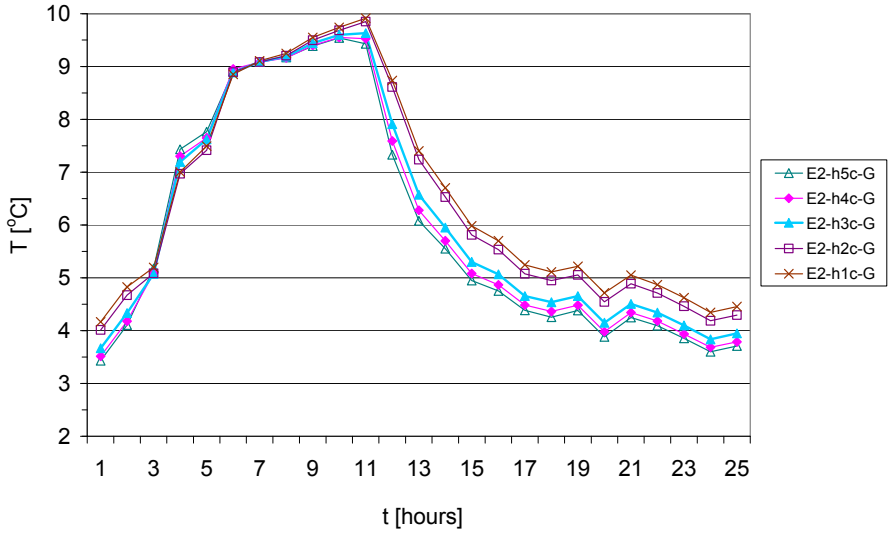

Figure 35. Temperature, Depth G. Element 2. April with cladding. Example of 24-hour cycle starting at 9 AM. For designations, see also Appendix D.

September with cladding (test M4S)

Figure 36 and the corresponding figures for the other elements (Figures K1 – K10, Appendix K) indicate that the elements did not reach steady-state before the September cycle was introduced, cf. the unstable cycles at Depths C and E. Apart from this both the temperature, Figure 36, and the RH, Figure 37, was distributed through the element as expected with the highest temperature and the lowest RH close to the indoor side etc.

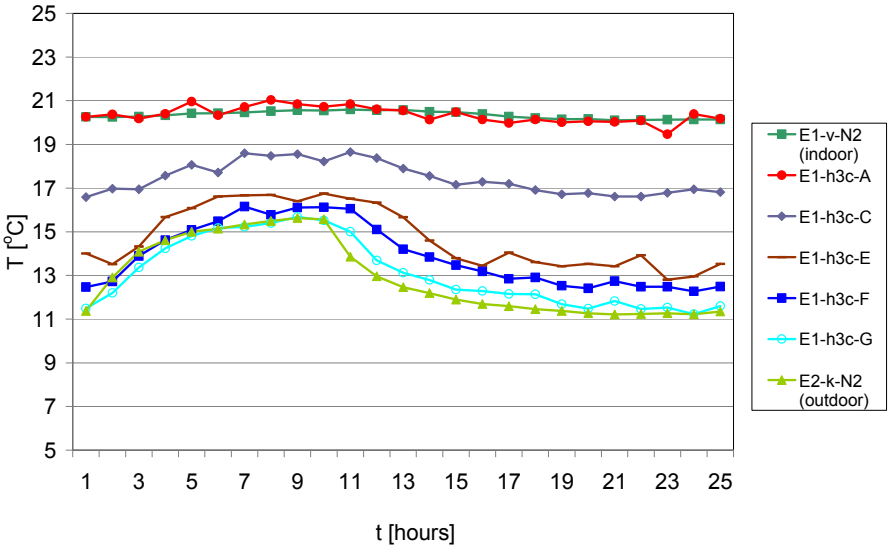

Figure 36. Temperature, Element 1. September with cladding. Indoor, Depths A - G, and Outdoor. Example of 24-hour cycle starting at 9 AM. For designations, see Appendix D.

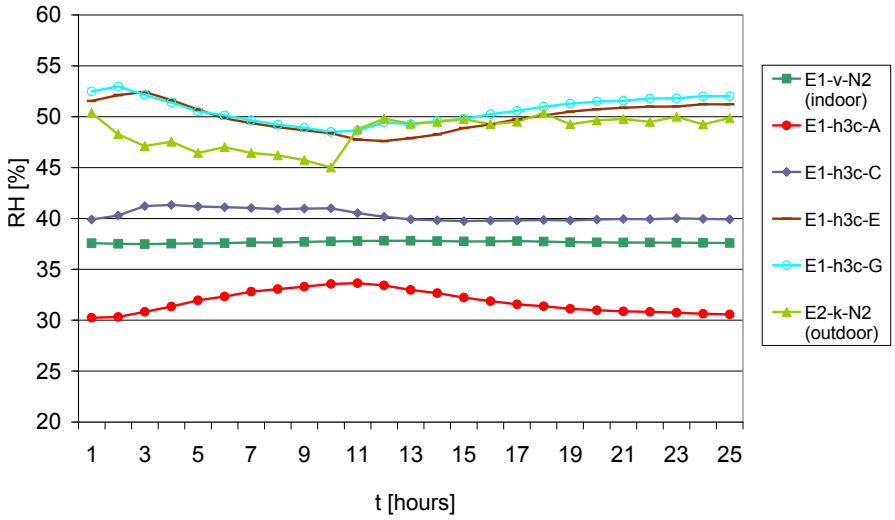

Figure 37. RH, Element 1. September with cladding. Indoor, Depths A, C, E and G, and Outdoor. Example of 24-hour cycle starting at 9 AM. For designations, see also Appendix D.

Compared with the test without cladding (M3S), the temperature cycles were maybe a bit more stable, but apart from that the cladding showed no effect on the temperatures at Depths A-E. The 'September with cladding' test was carried out with a 2 ºC higher temperature at the indoor side than the 'September without cladding' test due to a higher temperature in the laboratory hall (free floating temperature in the laboratory hall, cf. chapter 'Experimental results vs. modelled cycles').

When taking into account that the RH_{indoor} was 37 % at 'September with cladding' while it was 47 % at 'September without cladding', the RH pattern has not changed. The RH at Depth G (in the vented cavity, at the cladding) was about the same as the RH at Depth E (in thermal insulation, at the wind barrier), probably because this also equalled the RH level at the outdoor side. The shift in RH_{indoor} was related to changed conditions outside the climate simulator; changes that were too large to be compensated for by the vaporiser in the indoor climate chamber.

The vapour pressure in Element 1, Figure 38, was almost the same as in the ‘September without cladding’ test (M3S), Figure 29, and with the same pattern with curves that did not coincide at the end of the 24-hour cycle. As in the ‘April with cladding’ test (M4A), the vapour pressure at Depth G was lower than at Depth E and higher than the outdoor vapour pressure. The corresponding figure for Element 2 (Figure K6, Appendix K) was very close to Figure I6, before mounting the cladding. Again the absence of steady-state before introducing a temperature cycle made it difficult to conclude anything on this basis, although the vapour pressure at Depth G as expected was closer to the outdoor vapour pressure than the vapour pressure at Depth E.

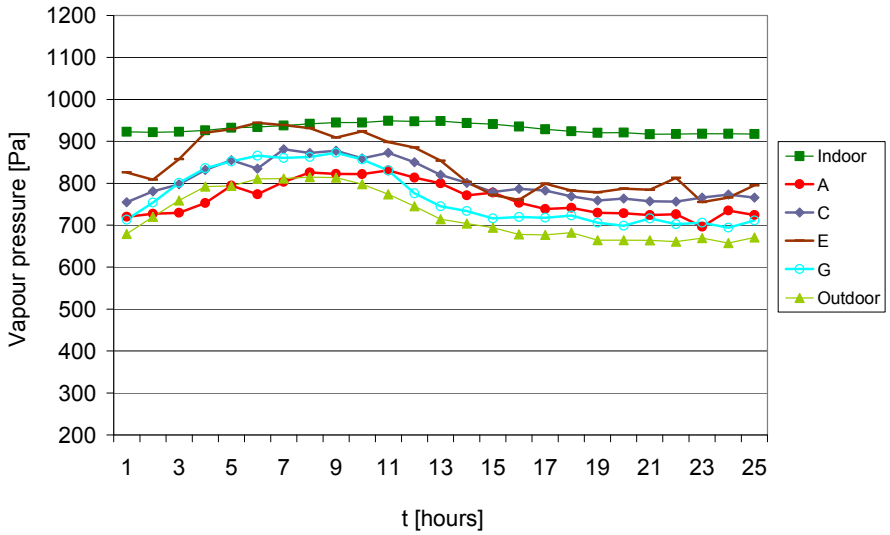

Figure 38. Vapour pressure, Element 1. September with cladding. Indoor, Depths A, C, E and G, and Outdoor. Example of 24-hour cycle starting at 9 AM. For designations, see also Appendix D.

At Depth C (Figure 39) and E (not shown) it was not possible to see any dependency of the measured temperatures on the height of the sensors. On the other hand the measured temperature was in practice the same at all heights. At Depths F and G (not shown) the temperature profiles were more stable, and at the end of a 24-hour cycle the temperature was about 0.5 ºC higher in the lower part of the element (h1c, h2c) than in the upper part (h4c, h5c), as in the 'April with cladding' test, see Figure 40.

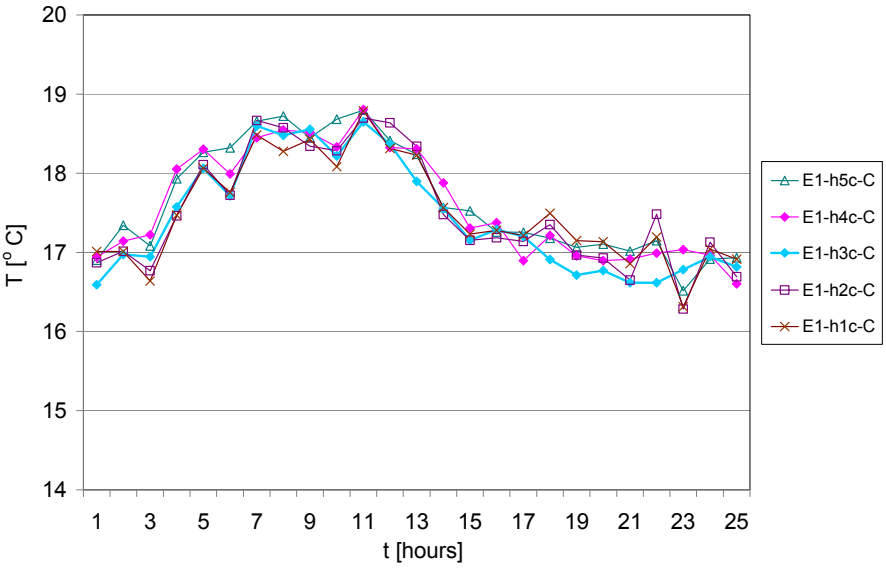

Figure 39. Temperature, Depth C. Element 1. September with cladding. Example of 24-hour cycle. For designations, see also Appendix D.

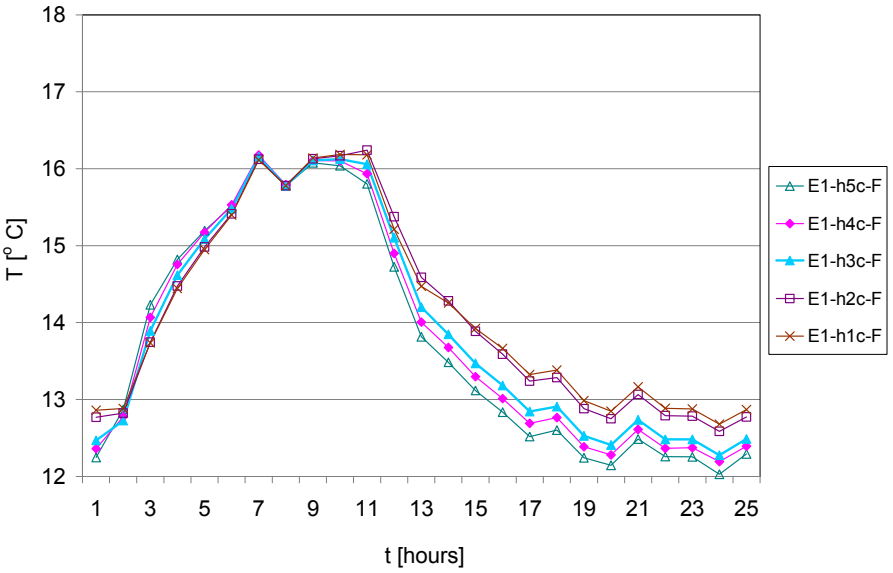

Figure 40. Temperature, Depth F. Element 1. September with cladding. Example of 24-hour cycle. For designations, see also Appendix D.

After these tests, a second test with the September cycle was carried out, seeking to improve the results that were going to be used in the computer model (Steskens, in press).

Although the test set-up was exposed to steady-state conditions for about a month before the September cycle was started, the irregular shape of the curves in Figure 41 shows that not even so the test elements had reached steady-state before the test. The steady-state exposure took place in a period characterised by clear skies, i.e. large differences in temperature between day and night. This made it impossible to keep a constant temperature in the indoor climate chamber with the present set-up.

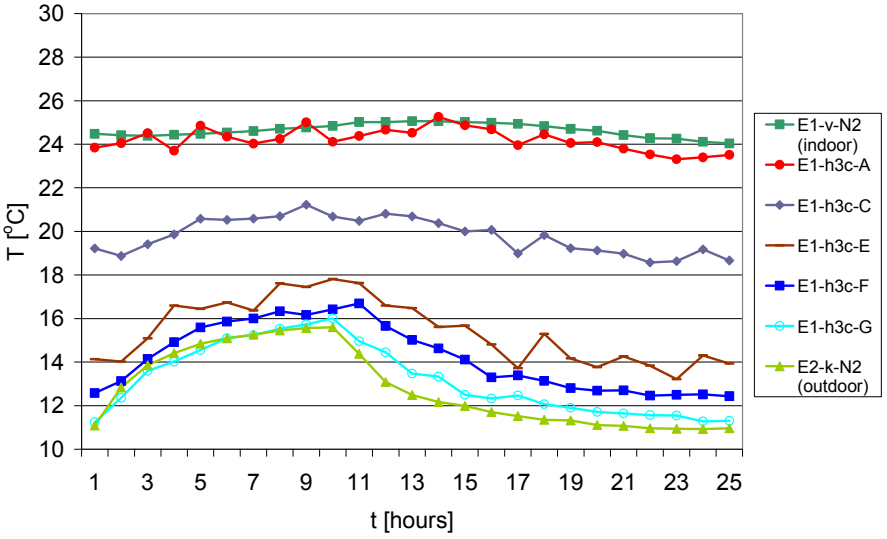

Figure 41. Temperature, Element 1. September with cladding. New test. Indoor, Depths A - G, and Outdoor. Example of 24-hour cycle. For designations, see also Appendix D.

Comparison of elements

As shown previously in the chapter 'Results and discussion', one should be careful when comparing results of the different tests. The conditions were not sufficiently comparable either because differences in the boundary con-

ditions, or the conditions in the elements were not close enough to steady-state before a temperature cycle was introduced.

Instead it was possible to compare the elements in each of the tests and discuss the differences. Results at Depth C (in the middle of the thermal insulation) and Depth E (in the thermal insulation, at the wind barrier) are compared and discussed in the following. Additional figures are included in Appendices F – K.

Comparison of elements – Depth C

In Figures 42 – 53 temperature and RH at Depth C (in the middle of the thermal insulation) in the four elements are compared. In some cases elements are represented both by sensors at 'h3c' and at 'h4c', referring to the previous parts of the chapter 'Results and discussion'.

As already presented, some of the tests were not performed at optimal conditions, illustrated by the scattered temperature curves in Figures 45 – 47, as opposed to the smooth curves in Figures 42 – 44.

In general, the temperature was 1 – 2 ºC higher in Element 4 than in the other elements; the difference was smallest in the tests with a September cycle due to the smaller temperature gradient across the elements, see Figures 42 – 47. This was not surprising since Element 4 had 50 mm cellular concrete instead of a gypsum board and 50 mm less thermal insulation, which meant that it had a different temperature profile through the element.

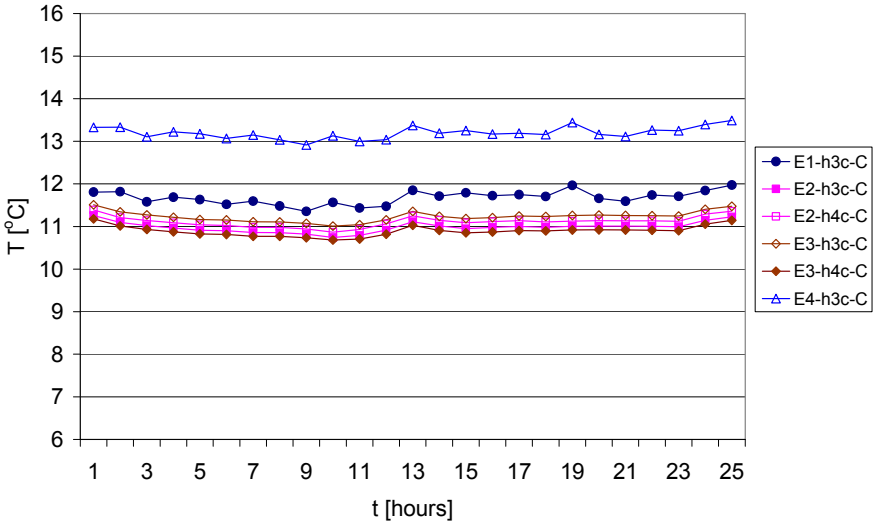

Figure 42. Temperature, Depth C. Steady-state without vapour barrier. Elements 1, 2, 3 and 4.

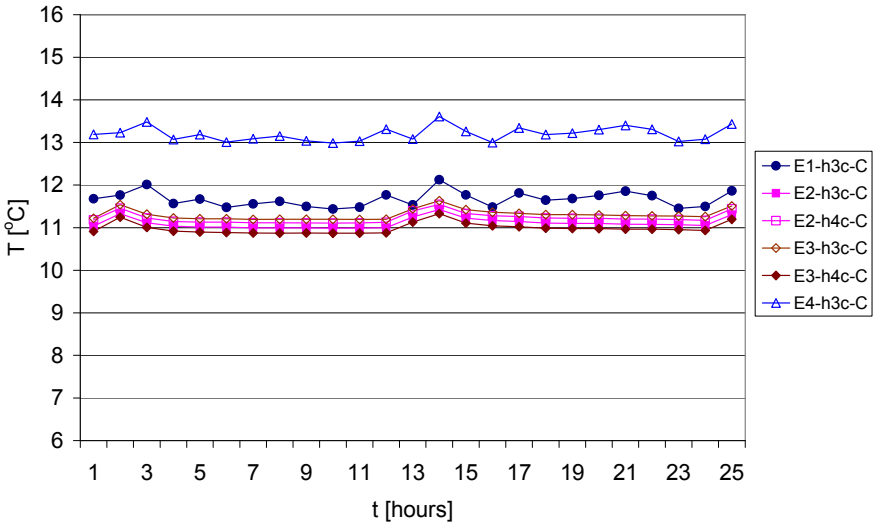

Figure 43. Temperature, Depth C. Steady-state with vapour barrier at Elements 1 and 3. Elements 1, 2, 3 and 4.

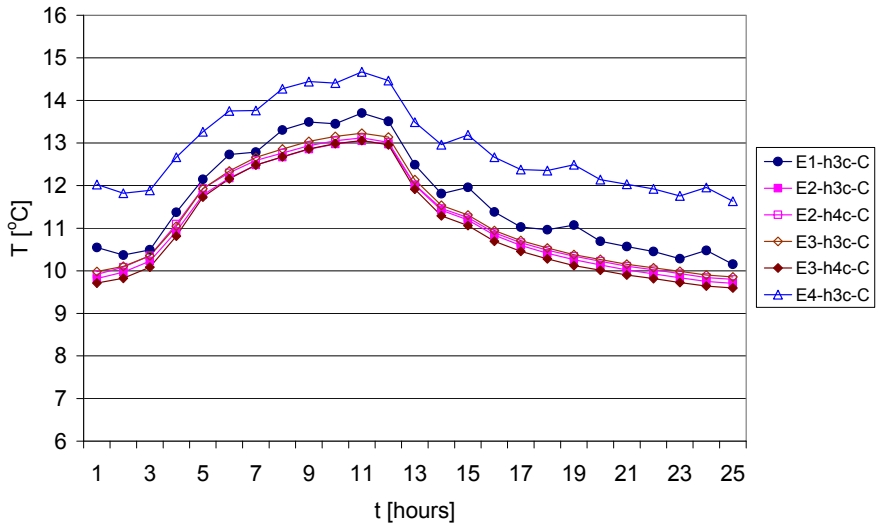

Figure 44. Temperature, Depth C. April without cladding. Elements 1, 2, 3 and 4.

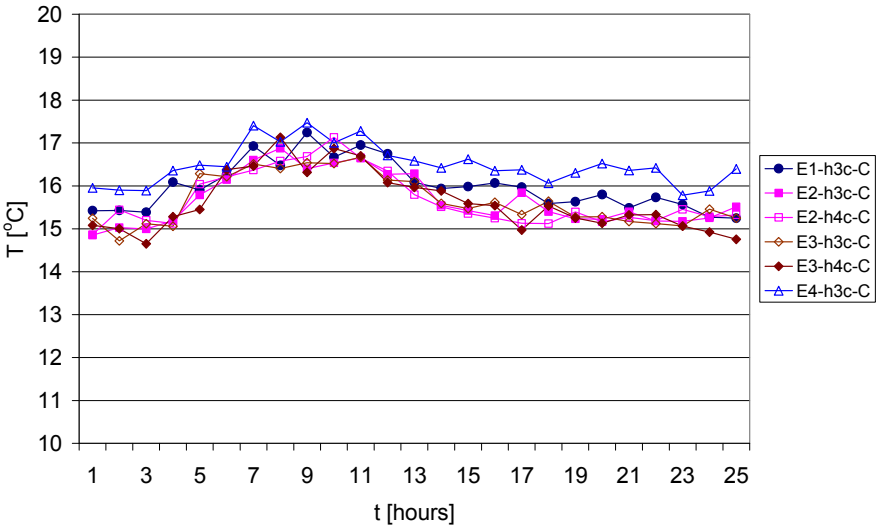

Figure 45. Temperature, Depth C. September without cladding. Elements 1, 2, 3 and 4.

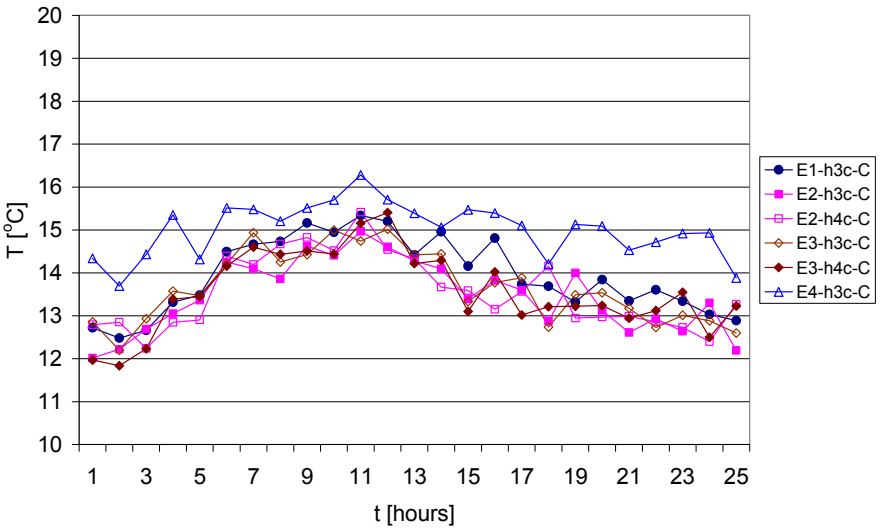

Figure 46. Temperature, Depth C. April with cladding. Elements 1, 2, 3 and 4.

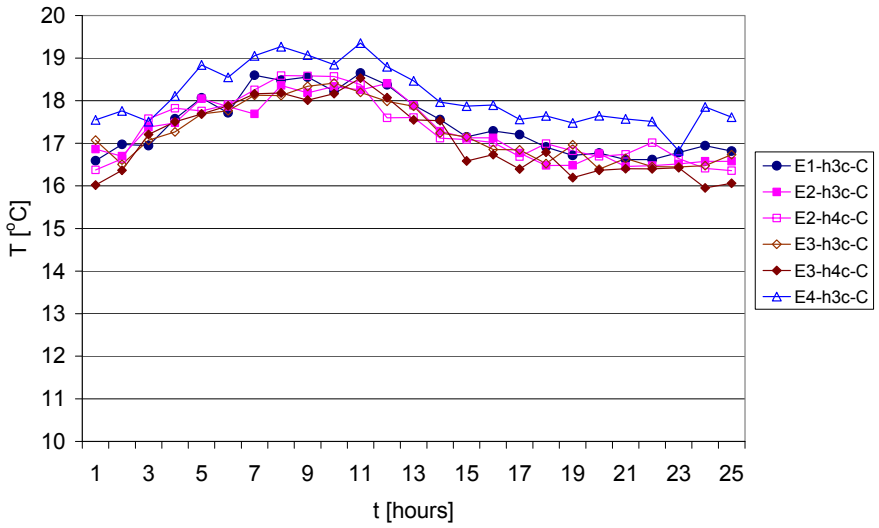

Figure 47. Temperature, Depth C. September with cladding. Elements 1, 2, 3 and 4.

Comparing the RH in the different elements, see Figures 48 – 53, it was first observed that Element 2 in general showed a very high RH. This was not surprising since Element 2 contained no vapour barrier, but one would have expected that RH in Elements 1, 2 and 3 were closer to each other before adding a vapour barrier on Elements 1 and 3 (Figure 48). As expected, these elements showed a sharp decrease in RH when adding a vapour barrier, cf. Figure 49.

It should also be noted that with September cycles RH was the same in Elements 2 and 3, cf. Figures 51 and 53 (remember to compare results based on 'h4c'). This was not the case in the other tests. Another, more surprising observation was the difference between RH in Elements 1 and 3 in the case without vapour barrier, even when replacing the misleading results at position 'h3c' with 'h4c' (Figure 48). After mounting the vapour barrier, the difference could be explained by the fact that Element 3 had a slit at the inner cladding and the wind barrier, thereby reducing the effect of the vapour barrier (Figure 49).

Element 4, with cellular concrete as inner cladding instead of a gypsum board and no vapour barrier, had a much lower RH than Element 2, which was also without a vapour barrier. In stead the tests indicated than 50 mm cellular concrete (Element 4) had almost the same effect on the RH conditions as a vapour barrier (Element 1), cf. the fact that RH in Element 4 was much closer to RH in Element 1 than in Element 2.

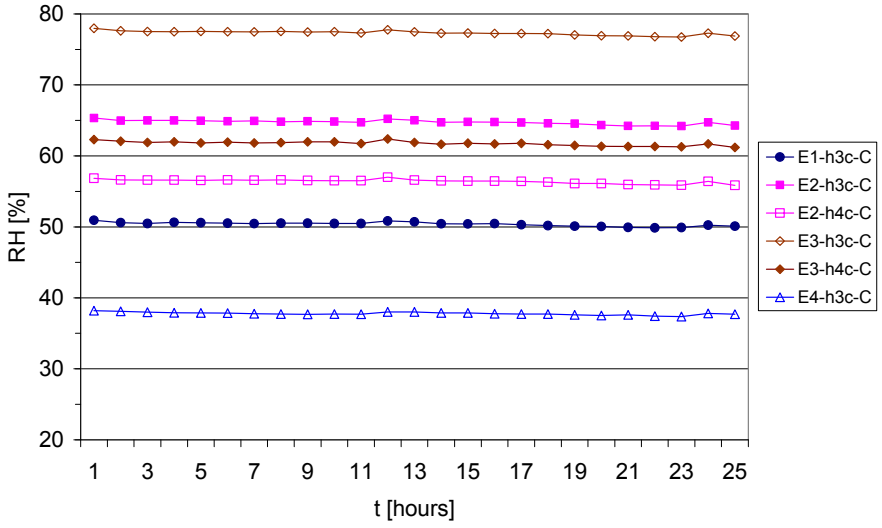

Figure 48. RH, Depth C. Steady-state without vapour barrier. Elements 1, 2, 3 and 4.

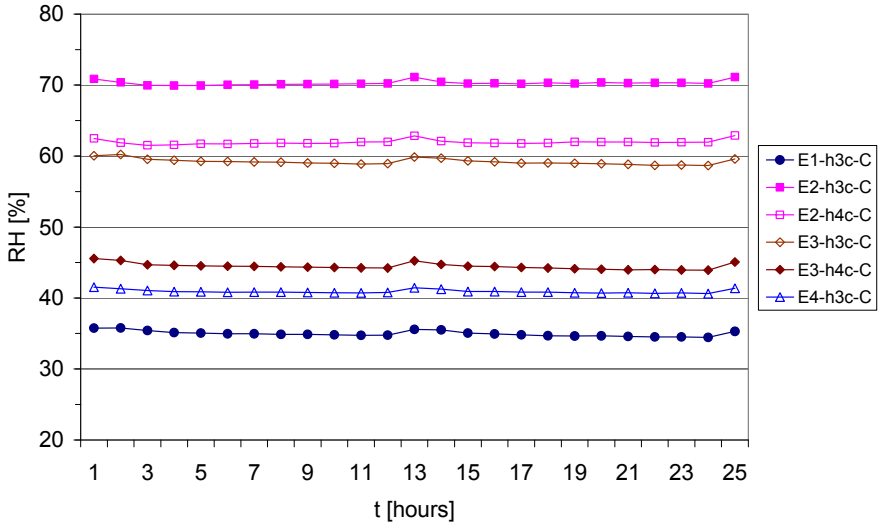

Figure 49. RH, Depth C. Steady-state with vapour barrier at Elements 1 and 3. Elements 1, 2, 3 and 4.

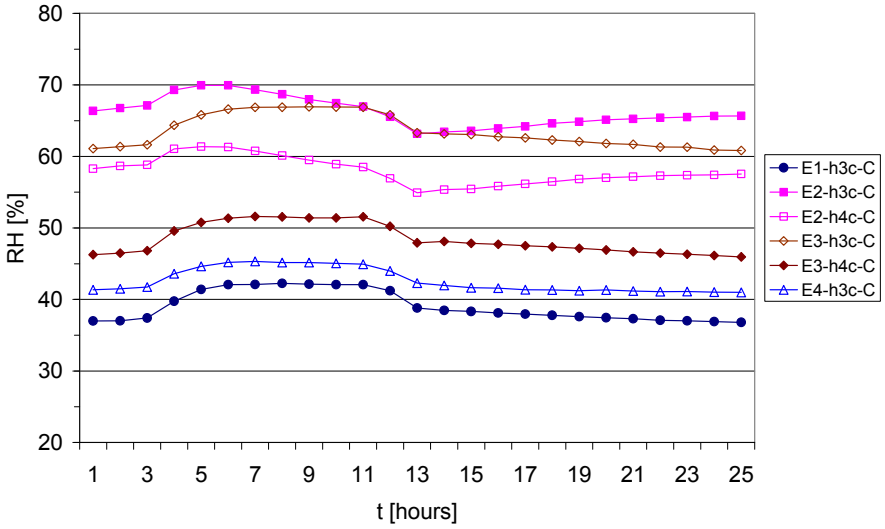

Figure 50. RH, Depth C. April without cladding. Elements 1, 2, 3 and 4.

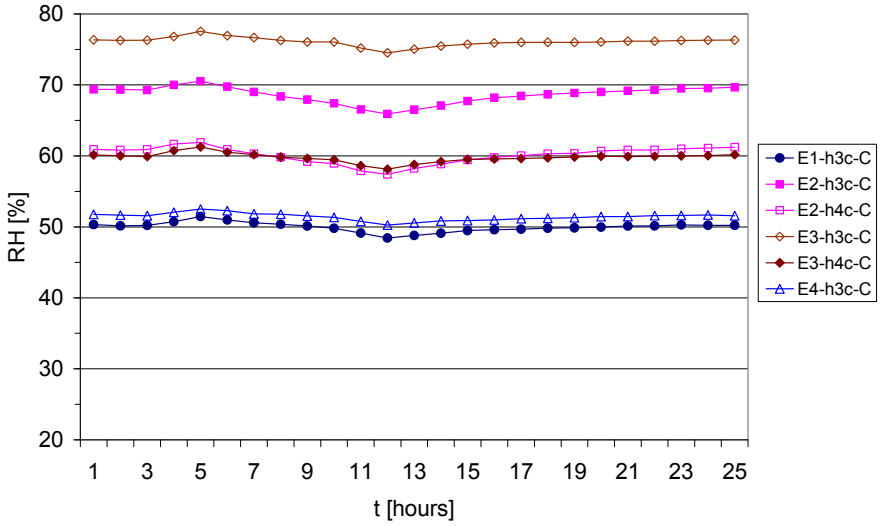

Figure 51. RH, Depth C. September without cladding. Elements 1, 2, 3 and 4.

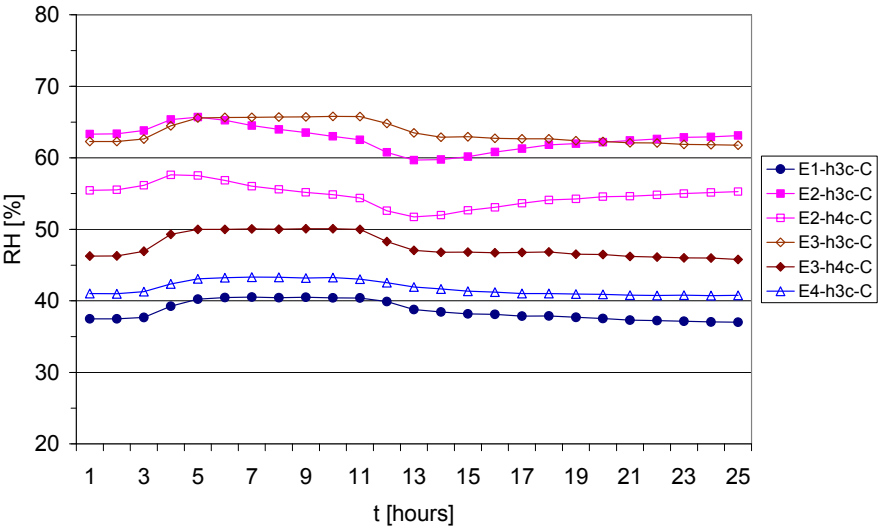

Figure 52. RH. Depth C. April with cladding. Elements 1, 2, 3 and 4.

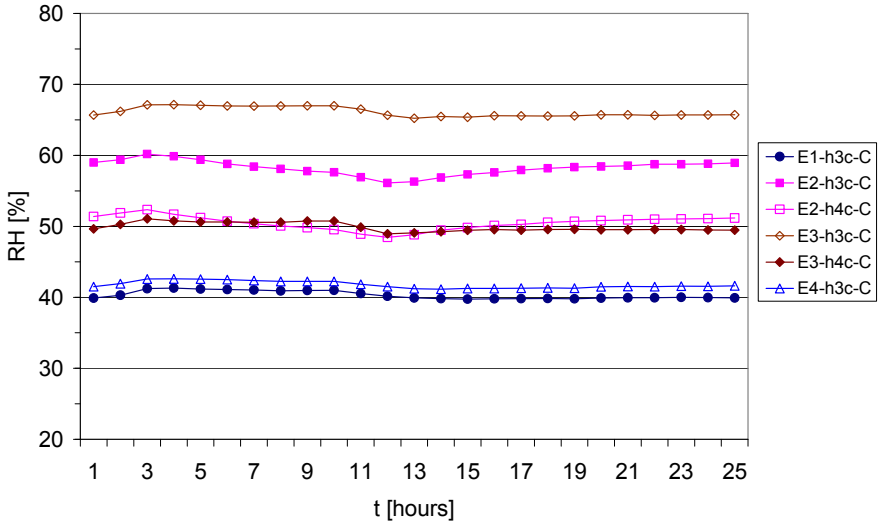

Figure 53. RH, Depth C. September with cladding. Elements 1, 2, 3 and 4.

Comparison of elements – Depth E

Temperature and RH at Depth E (in the thermal insulation, at the wind barrier) in the four elements were compared, see Figures 54 – 65. In some cases both 'h3c' and 'h4c' is included, referring to the previous chapters.

When replacing 'h3c' with 'h4c' in Element 4, the temperature was more or less the same in all four elements, with the lowest temperature in Element 4, as opposed to the situation at Depth C, see Figures 54 – 59. Still, the temperature curves were much smoother in the first tests, see Figures 54 – 56, than in the last, see Figures 57 – 59.

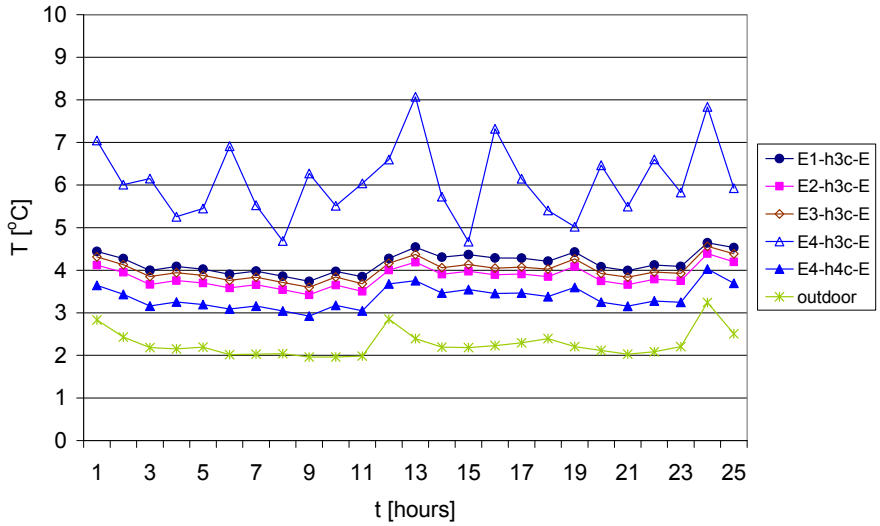

Figure 54. Temperature, Depth E. Steady-state without vapour barrier. Elements 1, 2, 3 and 4, and outdoor.

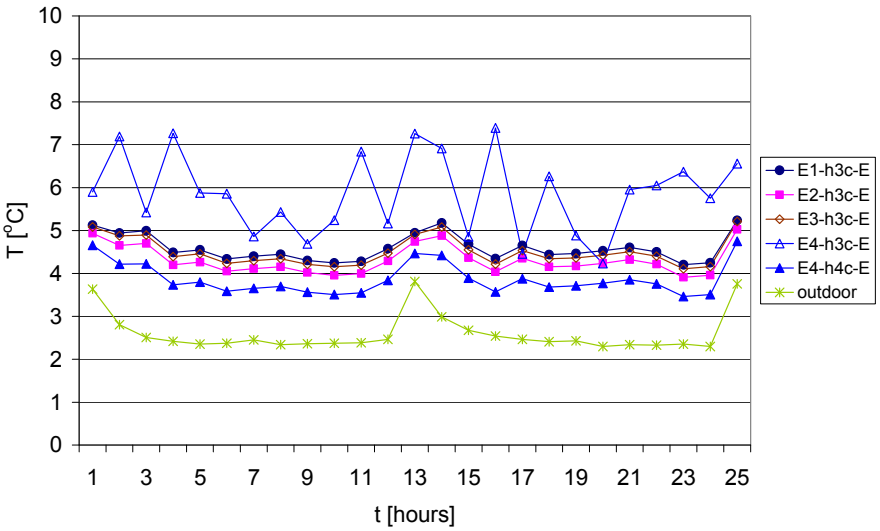

Figure 55. Temperature, Depth E. Steady-state with vapour barrier at Elements 1 and 3. Elements 1, 2, 3 and 4, and outdoor.

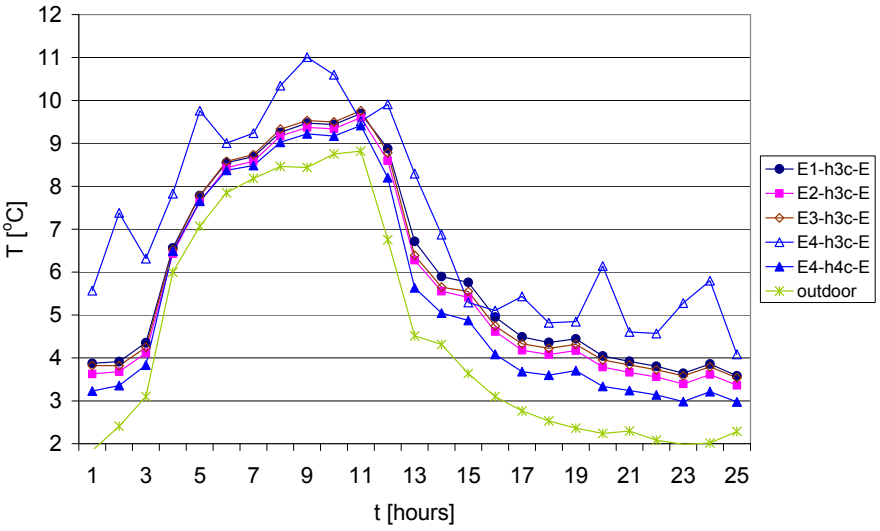

Figure 56. Temperature, Depth E. April without cladding. Elements 1, 2, 3 and 4, and outdoor.

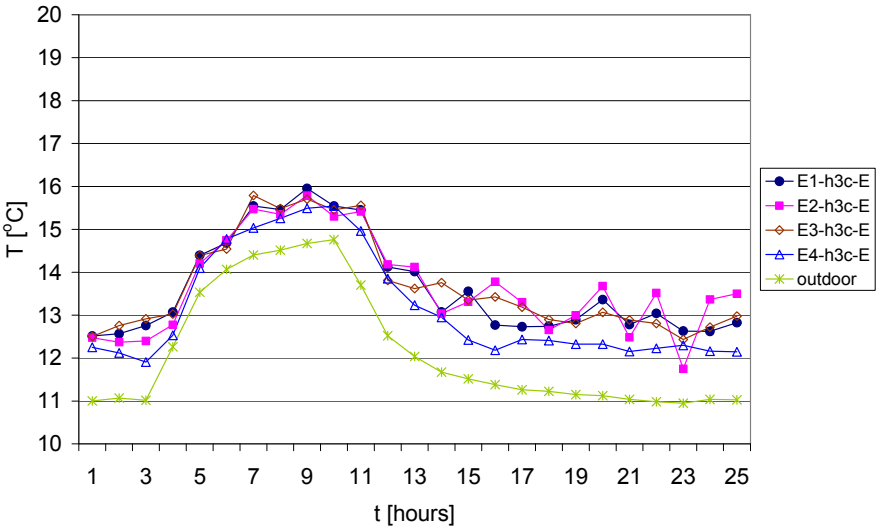

Figure 57. Temperature, Depth E. September without cladding. Elements 1, 2, 3 and 4, and outdoor.

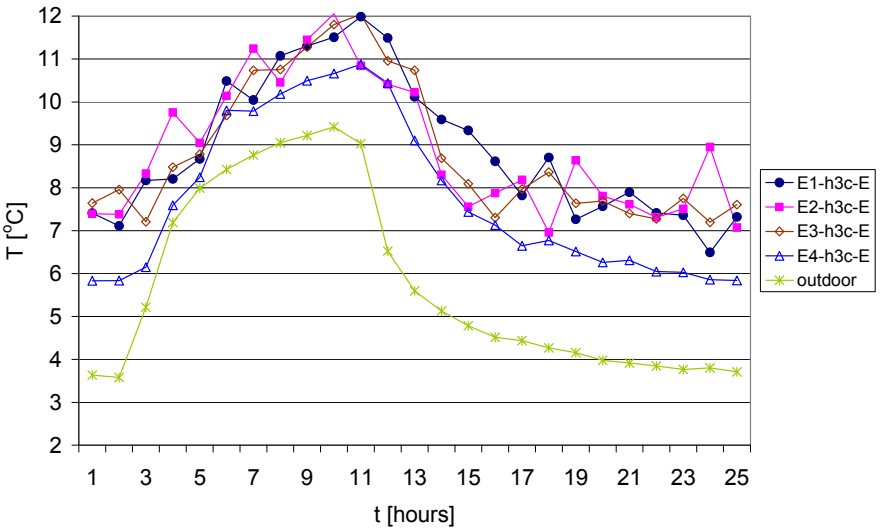

Figure 58. Temperature, Depth E. April with cladding. Elements 1, 2, 3 and 4, and outdoor.

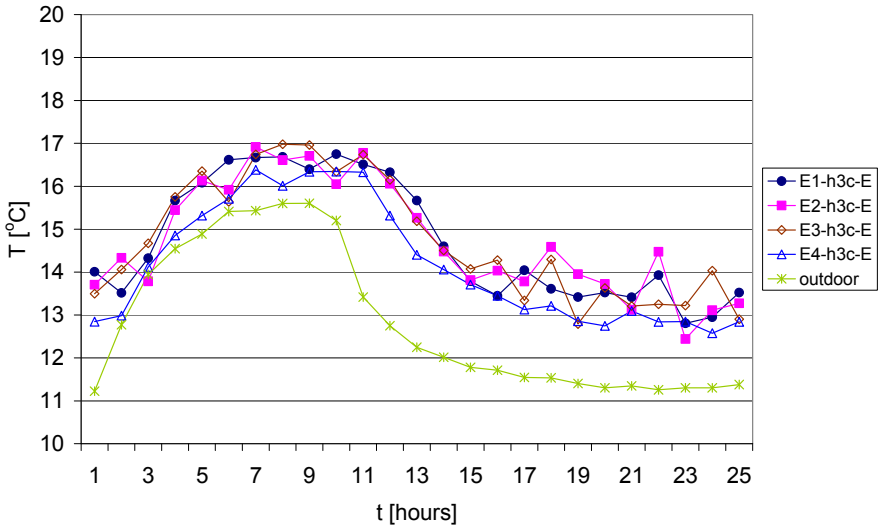

Figure 59. Temperature, Depth E. September with cladding. Elements 1, 2, 3 and 4, and outdoor.

Before Elements 1 and 3 were equipped with a vapour barrier, RH was the same in Elements 1, 2, and 3, and somewhat lower in Element 4, cf. Figure 60. After adding the vapour barrier, RH was still the same in Elements 1 and 3, cf. Figure 61, showing a sharp decrease compared with Element 2 as expected. The difference between RH in Element 2 and RH in Elements 1 and 3 was reduced when introducing a temperature cycle, cf. Figures 62 – 65. Especially with the September cycle the difference was reduced probably due to the smaller temperature gradients and the related RH gradients.

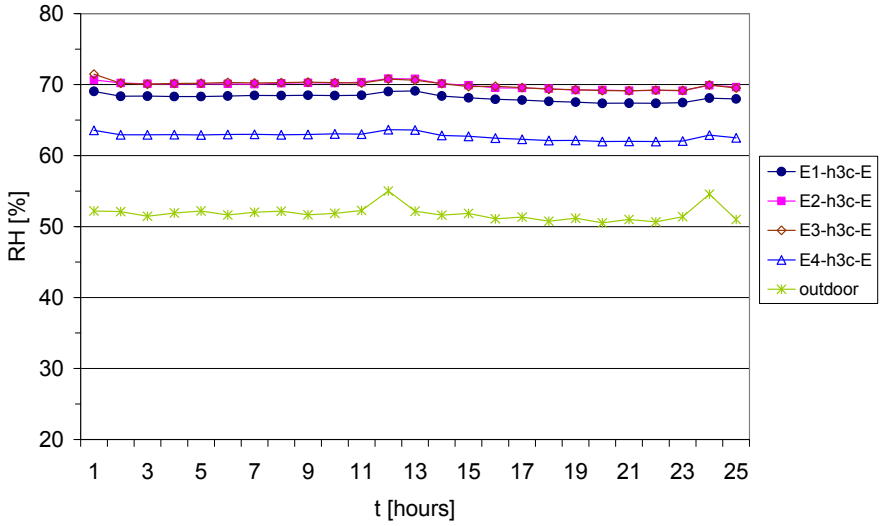

Figure 60. RH, Depth E. Steady-state without vapour barrier. Elements 1, 2, 3 and 4.

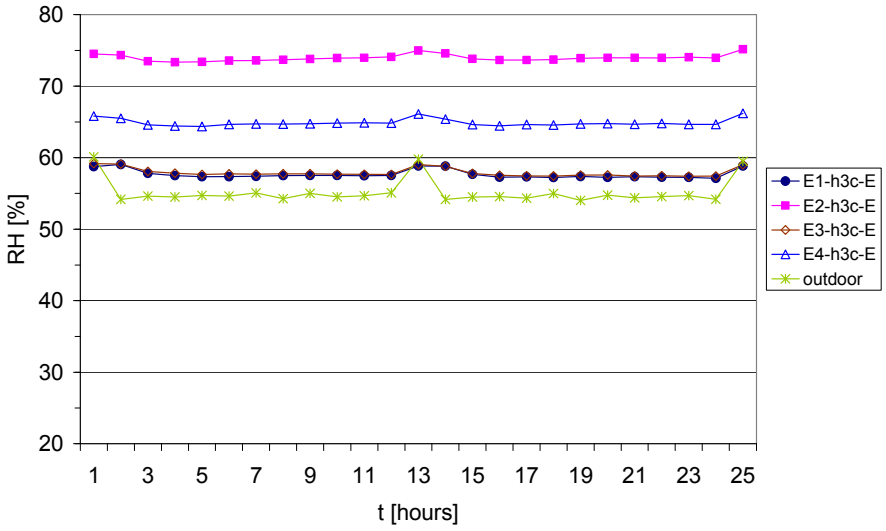

Figure 61. RH, Depth E. Steady-state with vapour barrier at Elements 1 and 3. Elements 1, 2, 3 and 4, and outdoor.

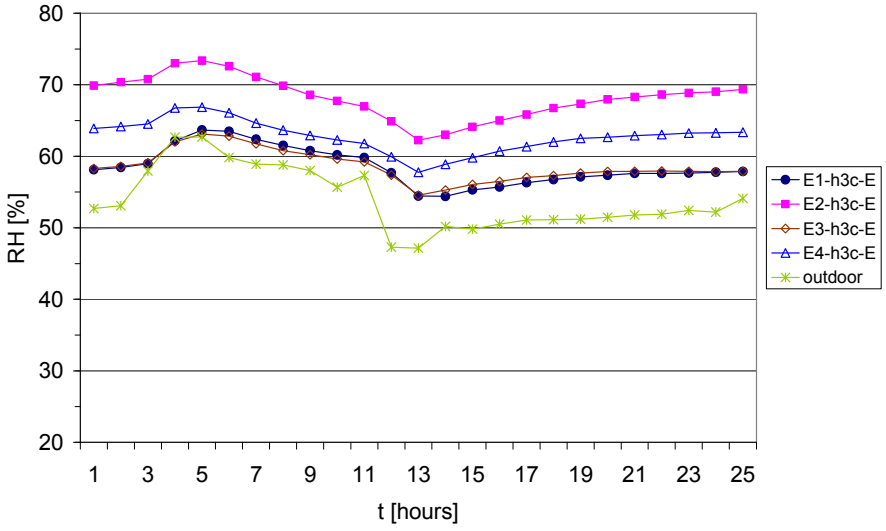

Figure 62. RH, Depth E. April without cladding. Elements 1, 2, 3 and 4, and outdoor.

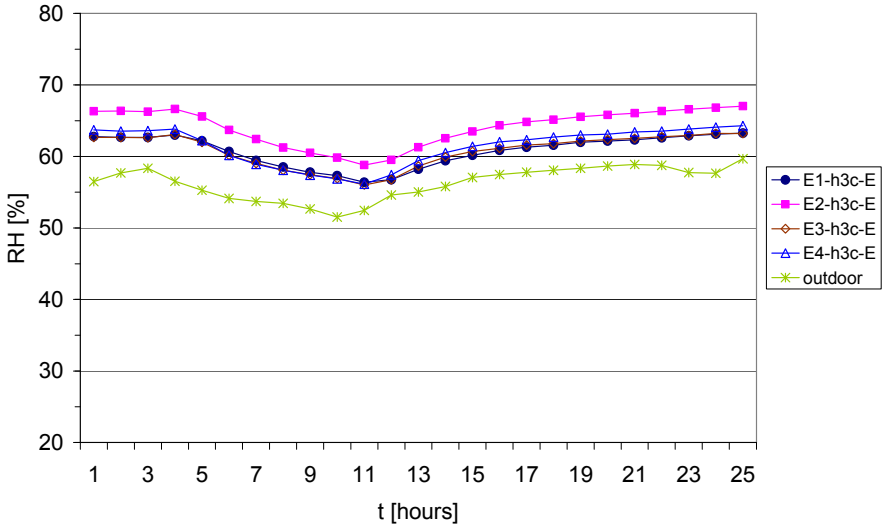

Figure 63. RH, Depth E. September without cladding. Elements 1, 2, 3 and 4, and outdoor.

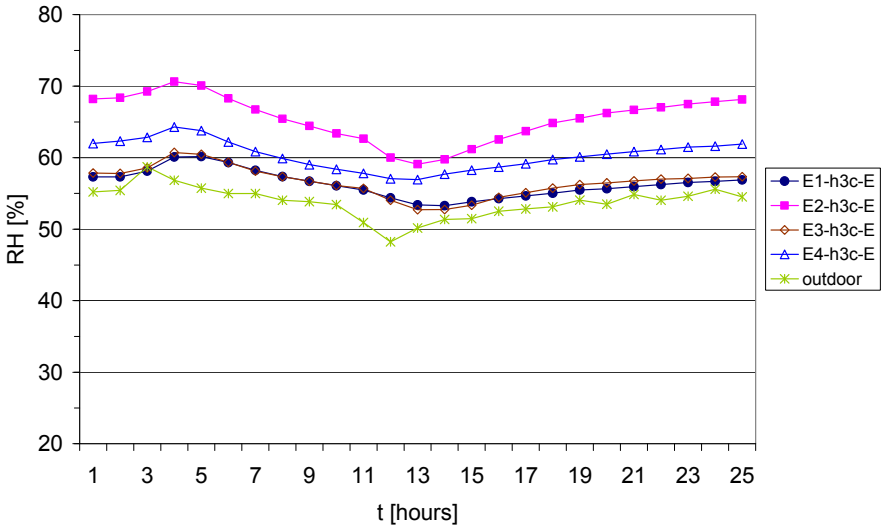

Figure 64. RH, Depth E. April with cladding. Elements 1, 2, 3 and 4, and outdoor.

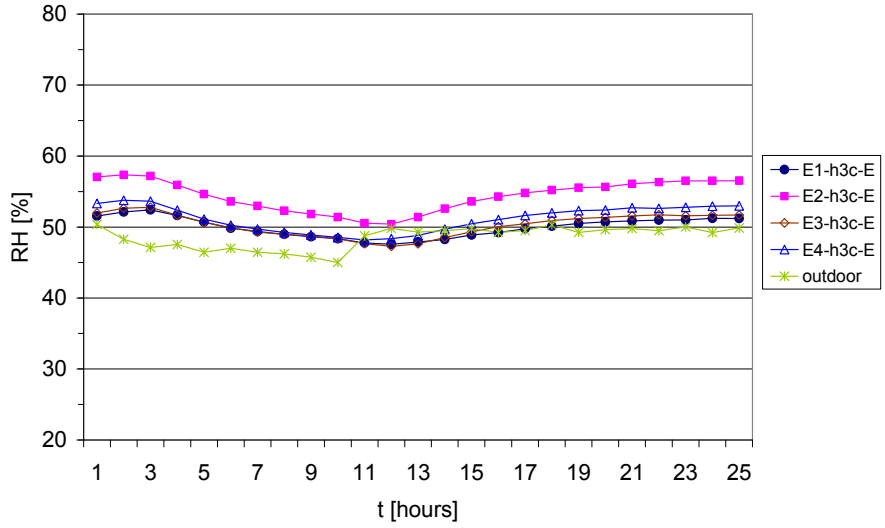

Figure 65. RH, Depth E. September with cladding. Elements 1, 2, 3 and 4, and outdoor.

Comparison of elements – other depths

As at Depth C, the temperature in Element 4 was higher than in the other elements at Depth B (at the indoor side of the thermal insulation), cf. Figures F23, G13, etc. In accordance with this, the RH was lower, especially compared with Element 2, cf. Figures F27, G17, etc. As in the case with Depth C, it was expected that the temperature was higher in Element 4 than in the other elements because cellular concrete has a higher thermal conductivity than mineral wool. On the other hand, the temperature difference at Depth B between Element 2 and 3 and the scatter in the temperature in Element 2 could not be explained.

As expected, there was no temperature difference between the elements at Depth G (at the cladding), cf. Figures J20 and K16. Also the RH showed no difference; cf. Figures J25 and K21, which showed that the cavity had worked.

It was not analysed in the present study whether these differences and the differences at Depths C and E in temperature and RH matched each other or whether other factors must be present; only qualitative analyses were made.

Experimental results vs modelled cycles

In order to perform temperature cycles according to the model cycles for April and September, set points had to be chosen for the temperature of the air at the outlet of the cooling machine. Since the cooling machine was quite new, no previous experience was yet available as reference. Pre-tests were made to get data concerning the time constant of the system, taking into consideration the thermal mass of the climate chamber.

The set points for the cooling machine used in the four tests are given in Appendix E. Please note that especially the April cycle was changed before test M4 (with cladding), because the lower set point was too low in test M3 (without cladding). This is illustrated in Figure 66.

The modelled and actual cycles were compared for each the four tests: 'April without cladding', 'September without cladding', 'April with cladding', and 'September with cladding' cf. Figures 66 – 69. In each case two consecutive cycles were chosen to illustrate the repeatability. This was considered to be very good.

Figure 66 shows that the lower set point for the April cycle was chosen too low. Unfortunately the wrong sensors were used as basis for finding relevant set points for the cooling machine. This was not discovered until later. For 'April with cladding' (M4) the set points were adjusted resulting in a much better correspondence (Figure 68).

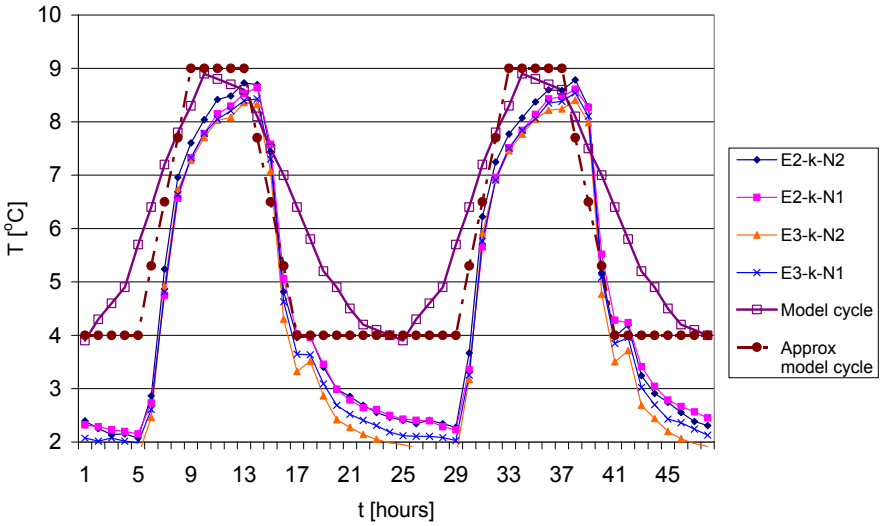

Figure 66. Temperature, outdoor side. April without cladding (M3A) compared with model cycle and approximated model cycle. Two consecutive 24-hour cycles starting at 3:00 AM.

'September with cladding' (Figure 67): In this case there was good correspondence between model and measurements although a small increase in the upper set point for the cooling machine would have made the correspondence even better. The second of the two 24-hour cycles shown in Figure 67 was started one hour too late, showing the disadvantage of using manual changes of set points.

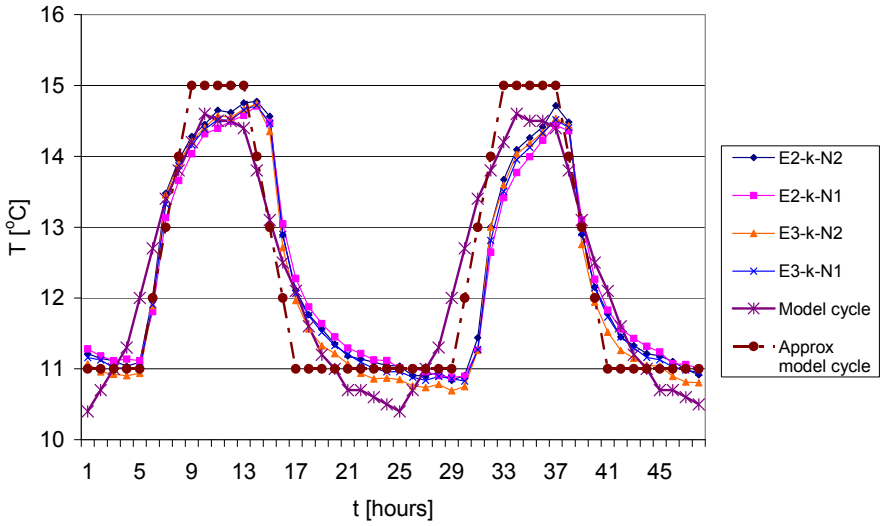

Figure 67. Temperature, outdoor side. September without cladding (M3S) compared with model cycle and approximated model cycle. Two consecutive 24-hour cycles starting at 3:00 AM.

Compared to 'April without cladding', Figure 66, the correspondence between the model and the measurements of the outdoor side temperature was much better during the 'April with cladding' test, Figure 68. Also in this case the second cycle was started one hour too late.

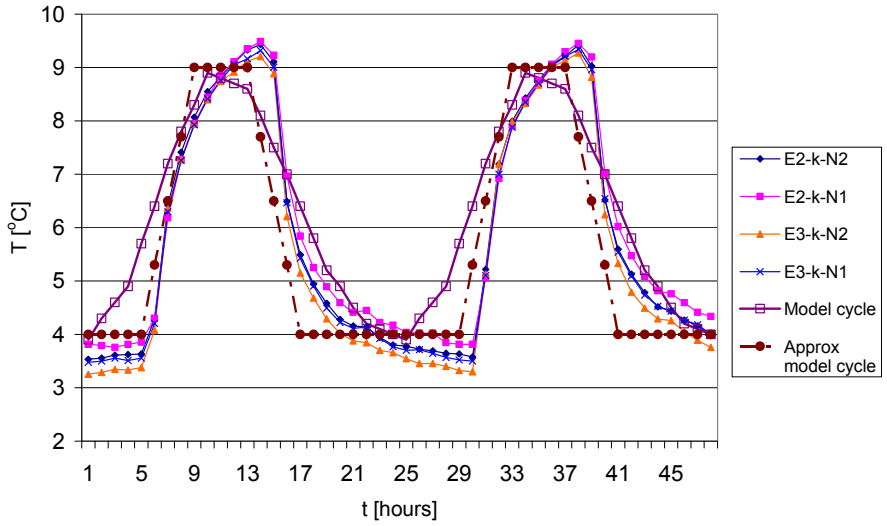

Figure 68. Temperature, outdoor side. April with cladding (M4) compared with model cycle and approximated model cycle. Two consecutive 24-hour cycles starting at 3:00 AM.

Finally, Figure 69 shows that the correspondence between model and measurements was very good in the 'September with cladding' test, although a lowering of the upper set point for the cooling machine would have made the correspondence even better. In this case both cycles were started at the correct time.

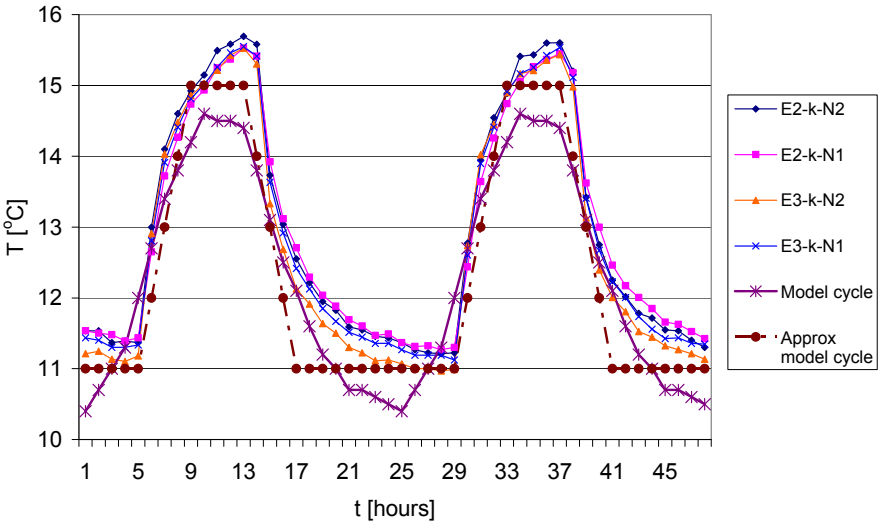

Figure 69. Temperature, outdoor side. September with cladding (M4) compared with model cycle and approximated model cycle. Two consecutive 24-hour cycles starting at 3:00 AM.

In general, it was demonstrated that it was possible to follow the stipulated cycles where the time constant of the system was taken into account, although a time span that was one hour shorter between the shift from the lower to the upper set point and back would have improved the correspondence even further.

Repeatability of cycles

In each of the four cases, tests were carried through for about two weeks, in most cases with a break during the weekend because the set point had to be changed manually. With this in mind and the fact that it was not always possible to change the set point at a fixed time, the repeatability of the cycles seemed pretty good, cf. Figures 70 – 73.

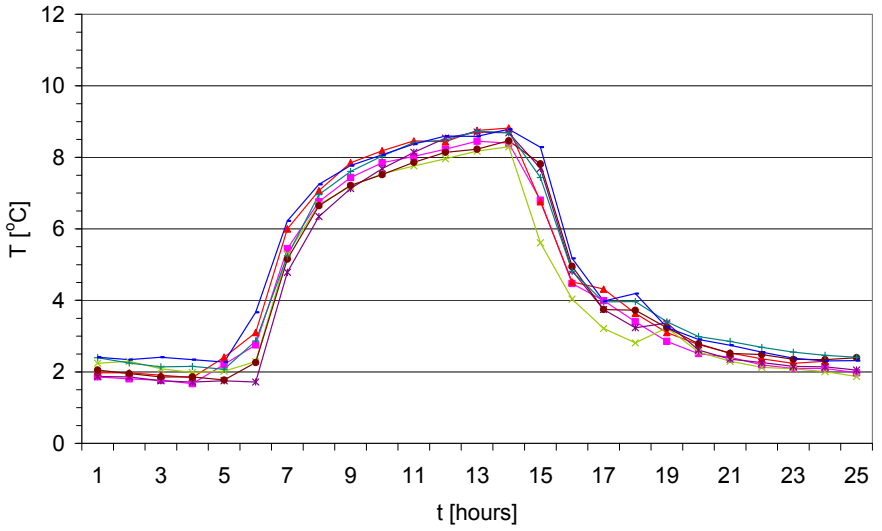

Figure 70. Temperature, outdoor side. Repeatability (7 cycles). April without cladding.

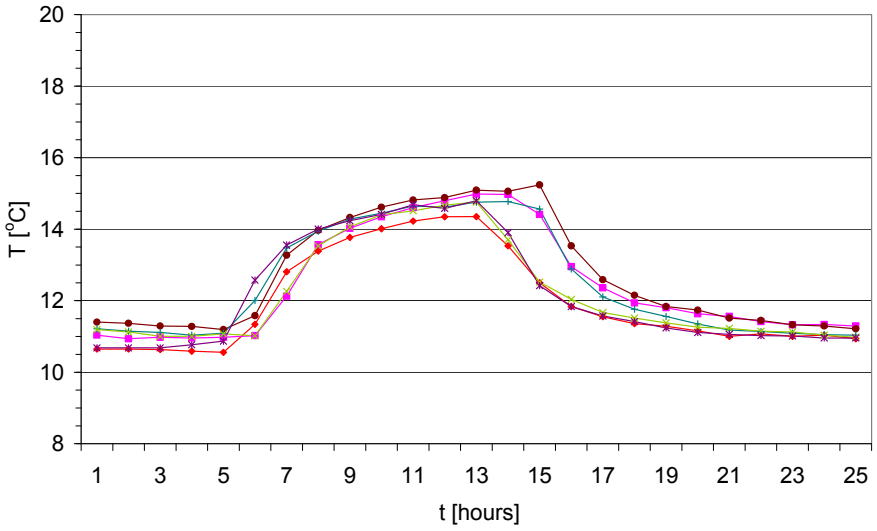

Figure 71. Temperature, outdoor side. Repeatability (6 cycles). September without cladding.

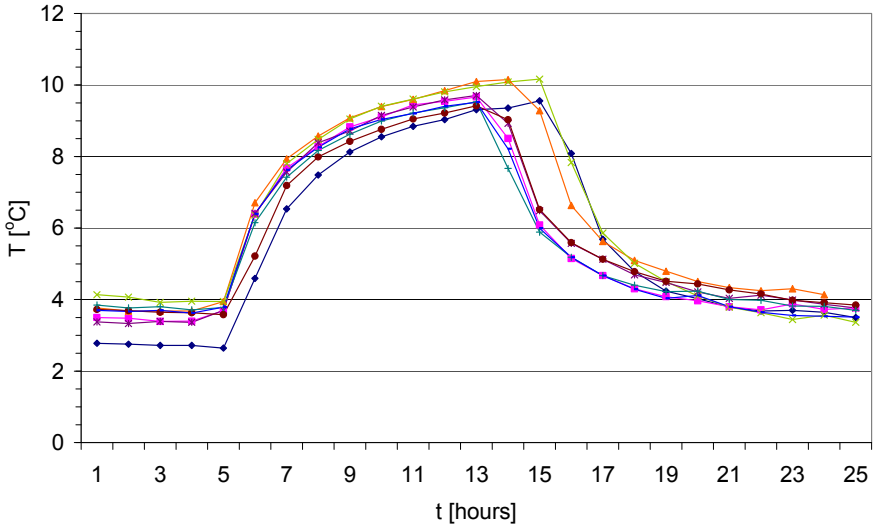

Figure 72. Temperature, outdoor side. Repeatability (8 cycles). April with cladding.

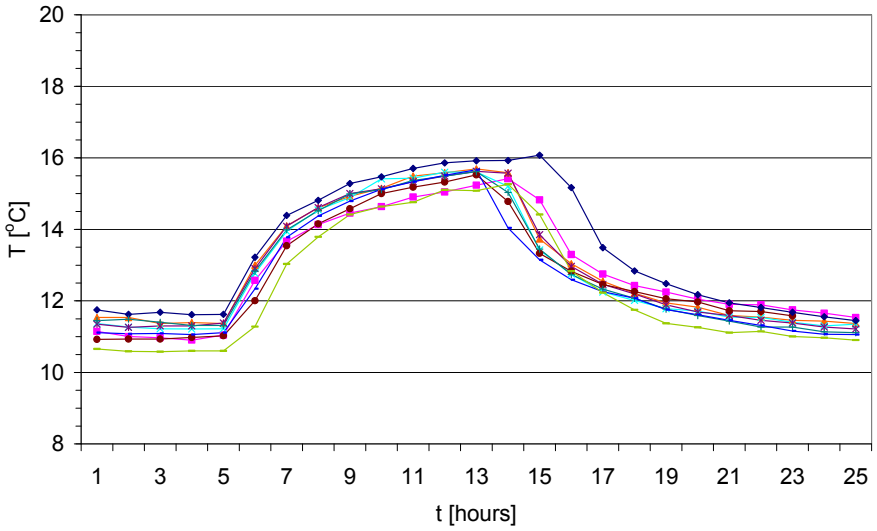

Figure 73. Temperature, outdoor side. Repeatability (9 cycles). September with cladding.

Of course, automatic change of set points would improve the repeatability, but in this case the main problem was the limited time for the tests, limiting the number of cycles that could be performed. In each of the four cases a 24 hour period in the middle of the curves was chosen to represent the specific test in the figures included in this report.

Experimental results vs computer model

Experimental results are compared with simulation using the computer model studied in (Steskens, in press), cf. Figure 74.

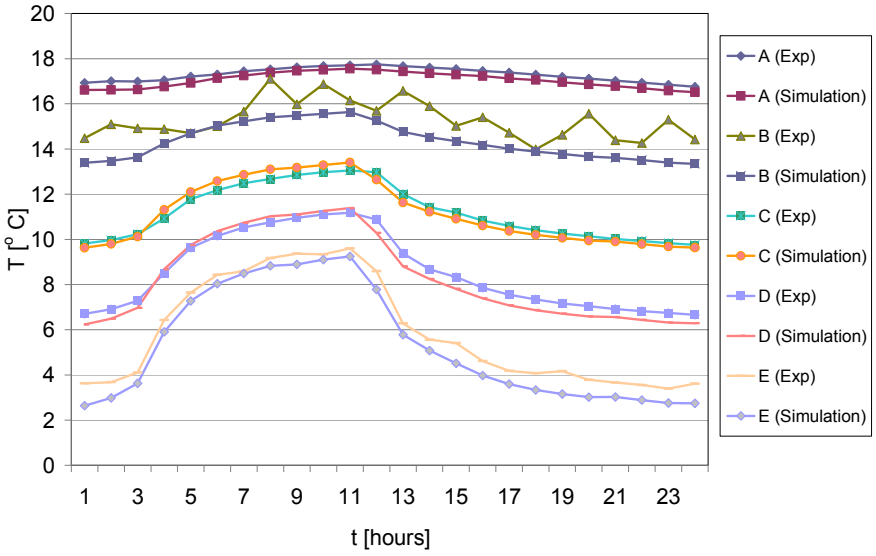

Figure 74. April without cladding, Element 2. Comparison of experimental results and simulations by computer model. Depths A, B, C, D and E. Simulations made by Paul Steskens, DTU BYG.

In this case, 'April without cladding', there was good correspondence between the experimental results and the computer simulation. This was not the case when comparing experimental results and computer simulations based on 'September without cladding', 'April with cladding' and 'September with cladding' (not shown), probably because the temperature, RH and vapour pressure gradients in the elements were not close enough to steady-state before these tests were started, cf. Figures 27-29, 32-34 and 36-38.

Further tests with a set-up with less influence from the climate in the laboratory hall on the conditions at the indoor (and outdoor) side are needed in order to conclude on the correspondence between the specific computer model and experimental results.

Conclusion

Based on the analysis of the results of the different tests and the experience by performing them, the following conclusions are made:

- The test set-up proved to be sensitive to changes in temperature and RH conditions at the indoor side. Therefore, it was necessary to ensure that the conditions at the indoor side could be kept more stable, and independent of the conditions in the laboratory hall, e.g. by increasing the thermal insulation of the indoor climate chamber, or by stabilising the temperature and RH conditions in the laboratory where the test set-up was placed.
- With the present test set-up it was possible to follow stipulated temperature cycles where the time constant of the system was taken into account, although a time span one hour shorter between the shift from the lower to the upper set point and back would have improved the correspondence even further.
- The present test set-up contained many features which should be followed up by additional tests given enough time for the elements to reach steady-state before climatic cycles like the ones used in the project or other cycles were carried out. The installation of a new cooling machine with a larger cooling capacity improved the situation a lot, because it proved to be much more stable and precise than the old one.
- In the tests with stipulated temperature cycles at the outdoor side the tests showed that it took more than a month to get full-scale elements like the ones tested in steady-state before exposure to temperature cycles.
- The study did not include RH cycles at the outdoor side. Instead the RH was free floating. Therefore the results could not be used to conclude on the behaviour in real April or September climate.
- Not all the possible combinations of results were studied in detail in this report, e.g. the conditions at the centre of an element vs. the conditions closer to the edge of an element.
- Since the boundary conditions changed more than intended between the different tests, including not having reached steady-state in some cases, the results could be used as an indicator only for the differences between the different types of elements involved. No comparisons were made with other tests based on similar conditions. Maybe such comparisons could help explain some of the more surprising results, e.g. the seemingly strong dependency of the height in the middle of the thermal insulation.
- Comparing the different elements tested, it was possible to see
  - the effect on the RH and the vapour pressure across an element of including a vapour barrier; in some cases a vapour barrier with a slit was just as bad as no vapour barrier.
  - the effect on the RH of having 50 mm cellular concrete and 145 mm thermal insulation or a gypsum board and 195 mm thermal insulation; RH was much lower in the first case, both inside the thermal insulation and behind the wind barrier.
- Additional tests including a shelf and a radiator mounted at the indoor side should be carried out in order to conclude on local conditions around such elements.
- At the present state it is not possible to conclude about the ability of the computer model (Steskens, in press) to simulate experimental results. This presupposes additional tests where the elements have enough time to reach steady-state conditions before a specified temperature (and RH) cycle is introduced.

References

de Place Hansen, E. J. & Brandt, E. (2009). The influence of ventilation on moisture conditions in facades with wooden cladding. In *Proceedings of the Fourth International Building Physics Conference: Energy efficiency and new approaches* (pp. 347-354). Istanbul: Beysan Matbaacilik ve Reklamcilik, Istanbul.

de Place Hansen, E. J. & Hansen, K. K. (1999a). *Sorptionsisotermer* (Report R-58). Lyngby: Technical University of Denmark, Dept of Structural Engineering and Materials, BYG-DTU. [in Danish]

de Place Hansen, E.J. & Hansen, K.K. (1999b). *Vanddamppermeabilitet (kopforsøg)* (Report R-59). Lyngby: Technical University of Denmark, Dept of Structural Engineering and Materials, BYG-DTU. [in Danish]

H+H Danmark A/S. (2009). *Multipladen 535: Teknisk information*. Højbjerg. Located 20091016 at: http://www.hplush.dk/multipladen

ISOVER. (2009a). *Diffusruller: Produktspecifikation*. Vamdrup. Located 20091016 at: http://www.isover.dk/sw2350.asp

ISOVER. (2009b). *Diffusruller: Produktdata*. Vamdrup. Located 20091016 at: http://www.isover.dk/sw3956.asp

Kaaris, H. (2003). *Klimasimulatorer: Teknisk dokumentation for accelereret ældning, perioden 1994-2002* (By og Byg Dokumentation 048). Hørsholm: Statens Byggeforskningsinstitut. [in Danish]

Knauf Danogips. (2009a). *9 EH-3 Vindtæt plade: Produktdatablad*. Hobro. Located 20091016 at: http://byggesystemer.knaufdanogips.dk/xpdf/produktdatablad_9-eh3.pdf

Knauf Danogips (2009b). *13 A-1 Standardplade: Produktdatablad*. Hobro. Located 20091016 at http://byggesystemer.knaufdanogips.dk/xpdf/produktdatablad_a-1-13-mm.pdf

Orbita-Film GmbH. (2008). *Dampfsperrbahnen: Art.Nr. 510376 / 510397* (EN 13984). Weisand-Gölzau.

Steskens, P. (in press). *Modelling of the hygrothermal interactions in between the indoor environment and the building envelope* (Ph.D.-thesis). Lyngby: Technical University of Denmark.

U.S. Department of Energy. (2009). *EnergyPlus simulation software: Weather data. All Regions: Europe WMO Region 6: Denmark.* Washington. Located 20091218 at: http://apps1.eere.energy.gov/buildings/energyplus/cfm/weather_data3.cfm/region=6_europe_wmo_region_6/country=DNK/cname=Denmark

Appendix A. Test set-up

Cross sections of the test set-up are shown in Figures A1 – A7.

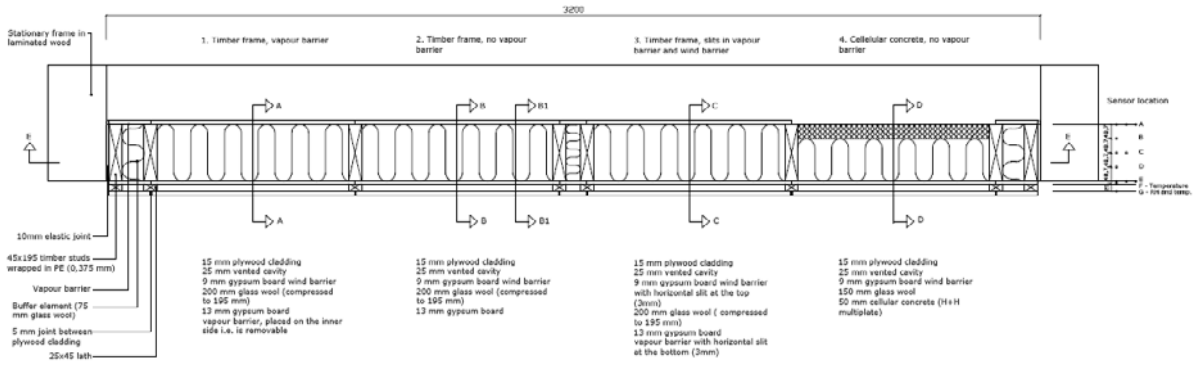

Figure A1. Horizontal cross section F-F with a description of the layers in each of the four elements.

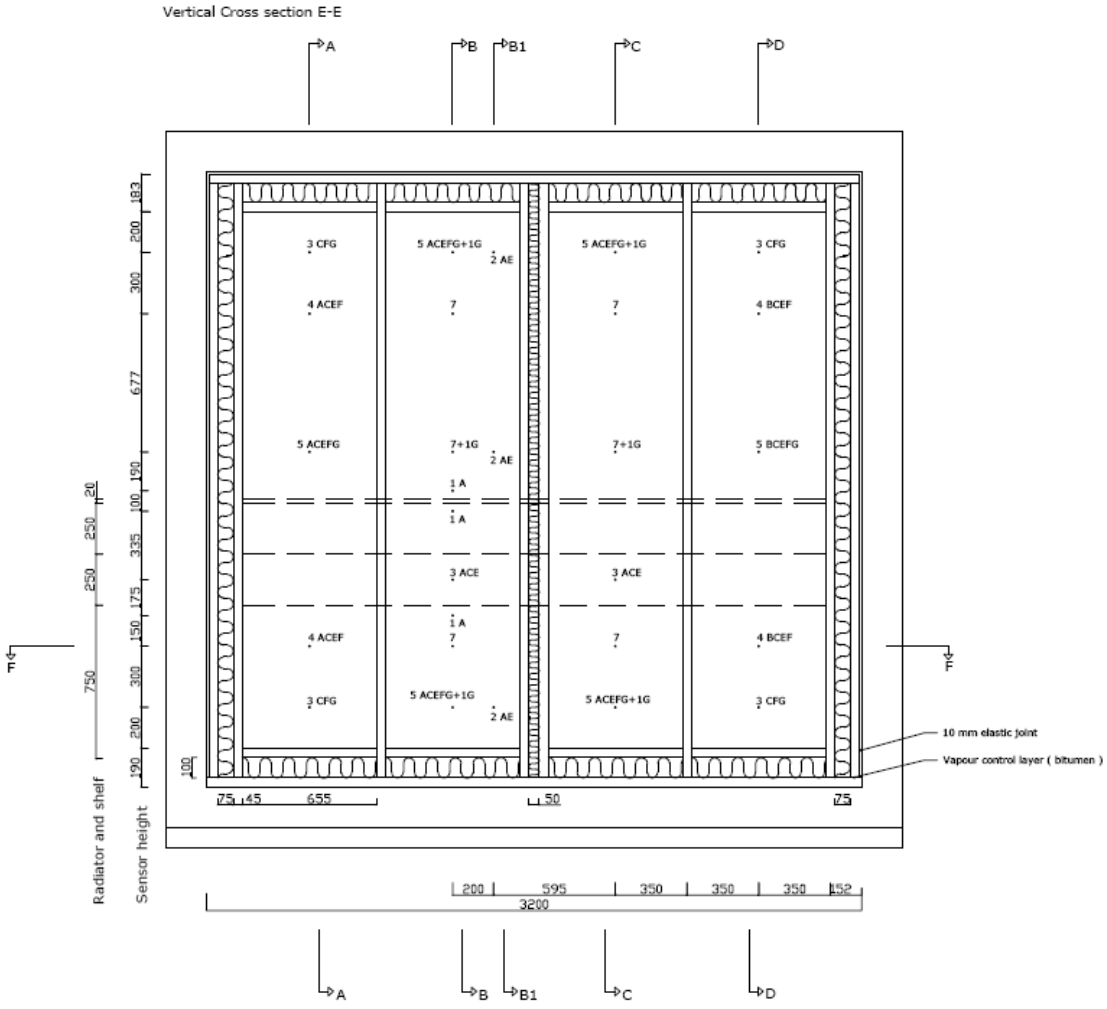

Figure A2. Vertical cross section E-E with position of the sensors. A, B, C, D, E, F and G refer to different positions in the horizontal direction, as shown in Figure A1. Seen from the outdoor side, with Element 1 at left.

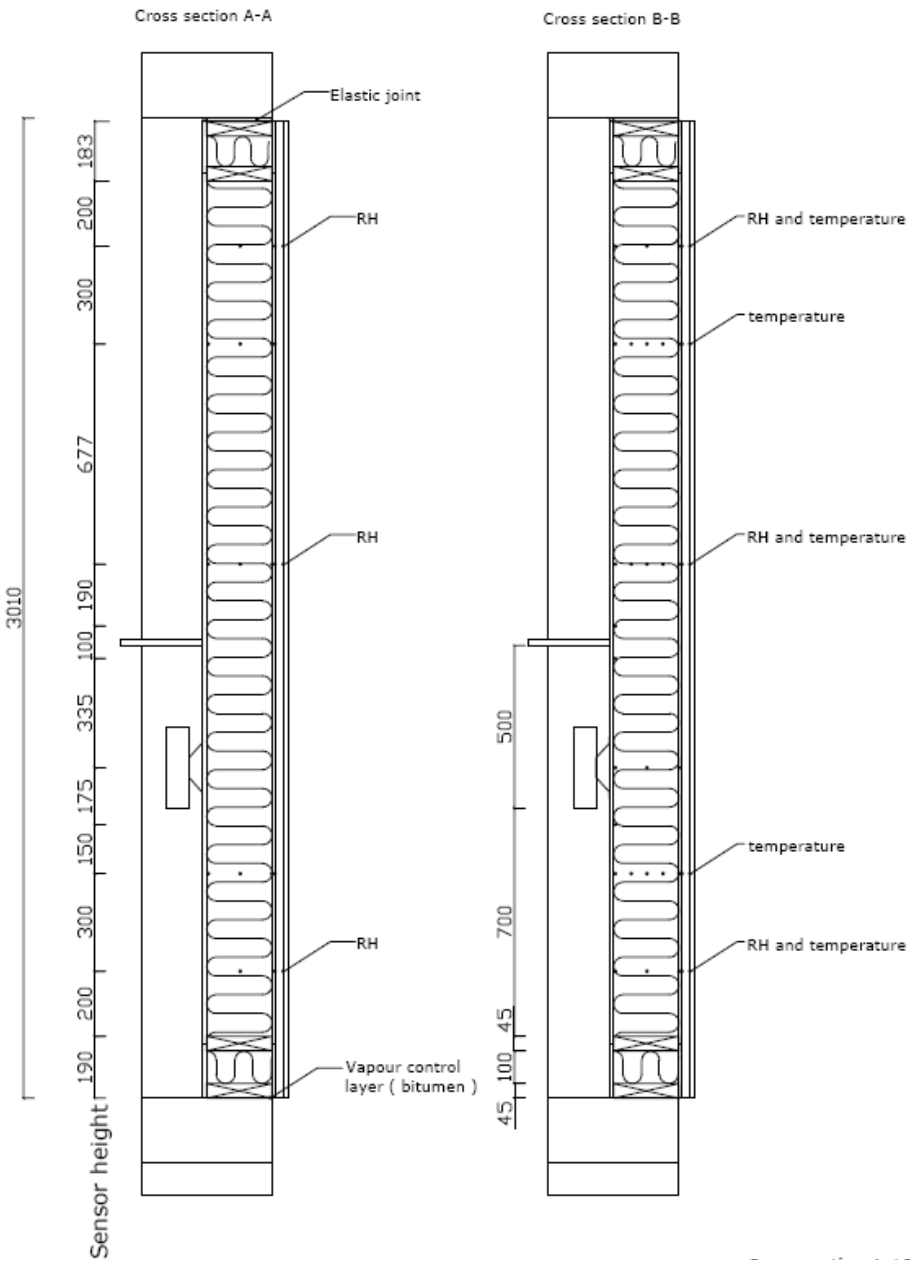

Figure A3. Vertical cross sections A-A and B-B. Indoor side at left. A radiator and a shelf are shown at the indoor side of the test elements, i.e. in the indoor climate chamber. These should simulate 2D-conditions along the wall. Because of limited time such tests were not made and therefore the radiator and the shelf were not mounted.

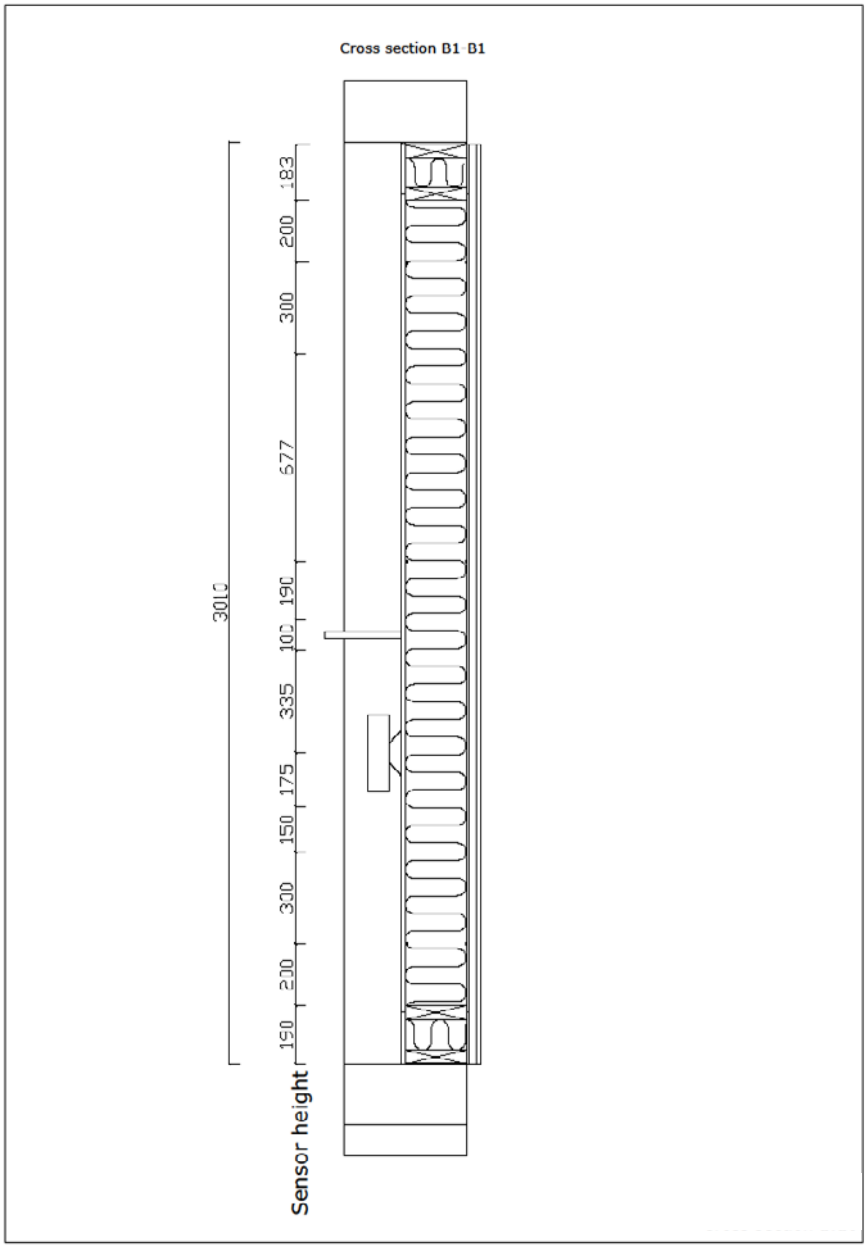

Figure A4. Vertical cross section B1-B1. Indoor side at left. A radiator and a shelf are shown at the indoor side of the test elements, i.e. in the indoor climate chamber. These should simulate 2D-conditions along the wall. Because of limited time such tests were not made and therefore the radiator and the shelf were not mounted.

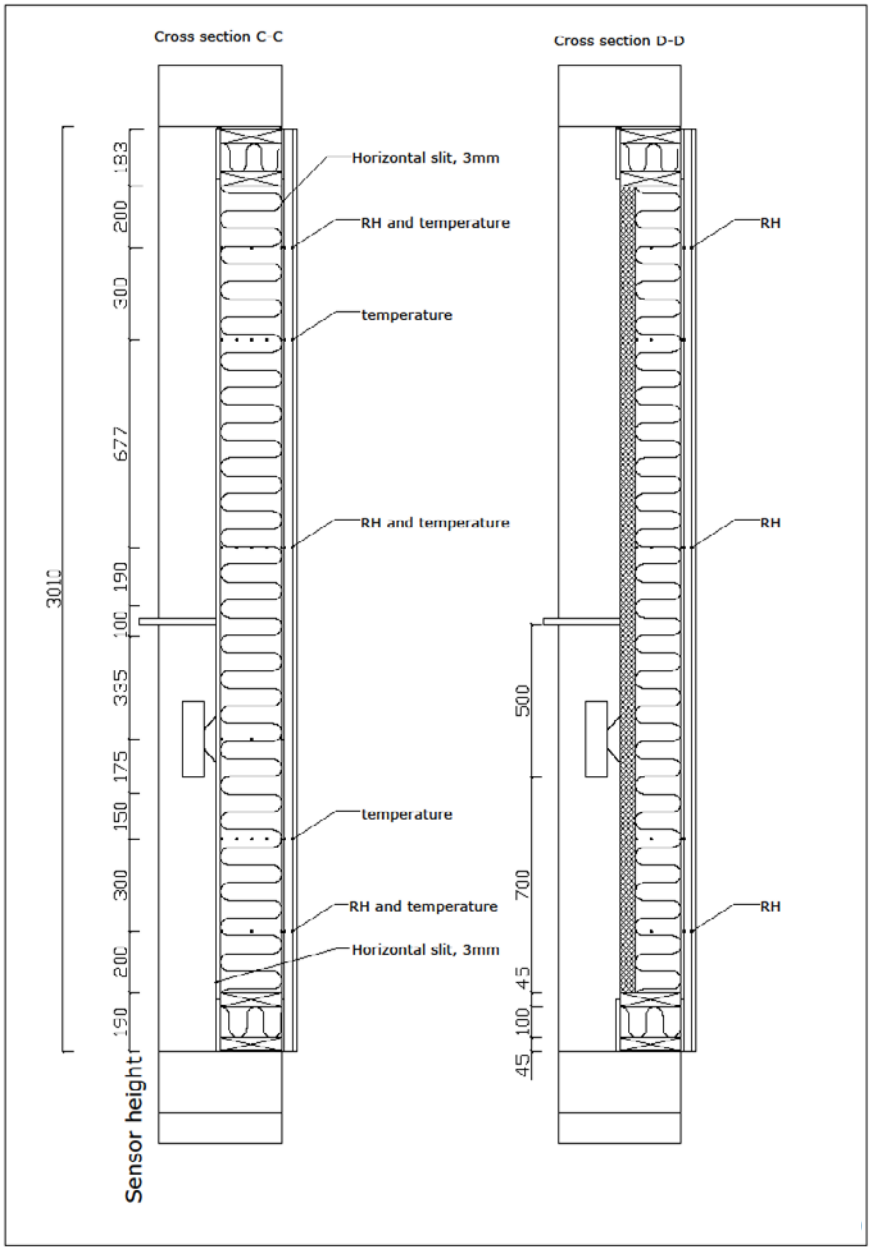

Figure A5. Vertical cross sections C-C and D-D. Indoor side at left. A radiator and a shelf are shown at the indoor side of the test elements, i.e. in the indoor climate chamber. These should simulate 2D-conditions along the wall. Because of limited time such tests were not made and therefore the radiator and the shelf were not mounted.

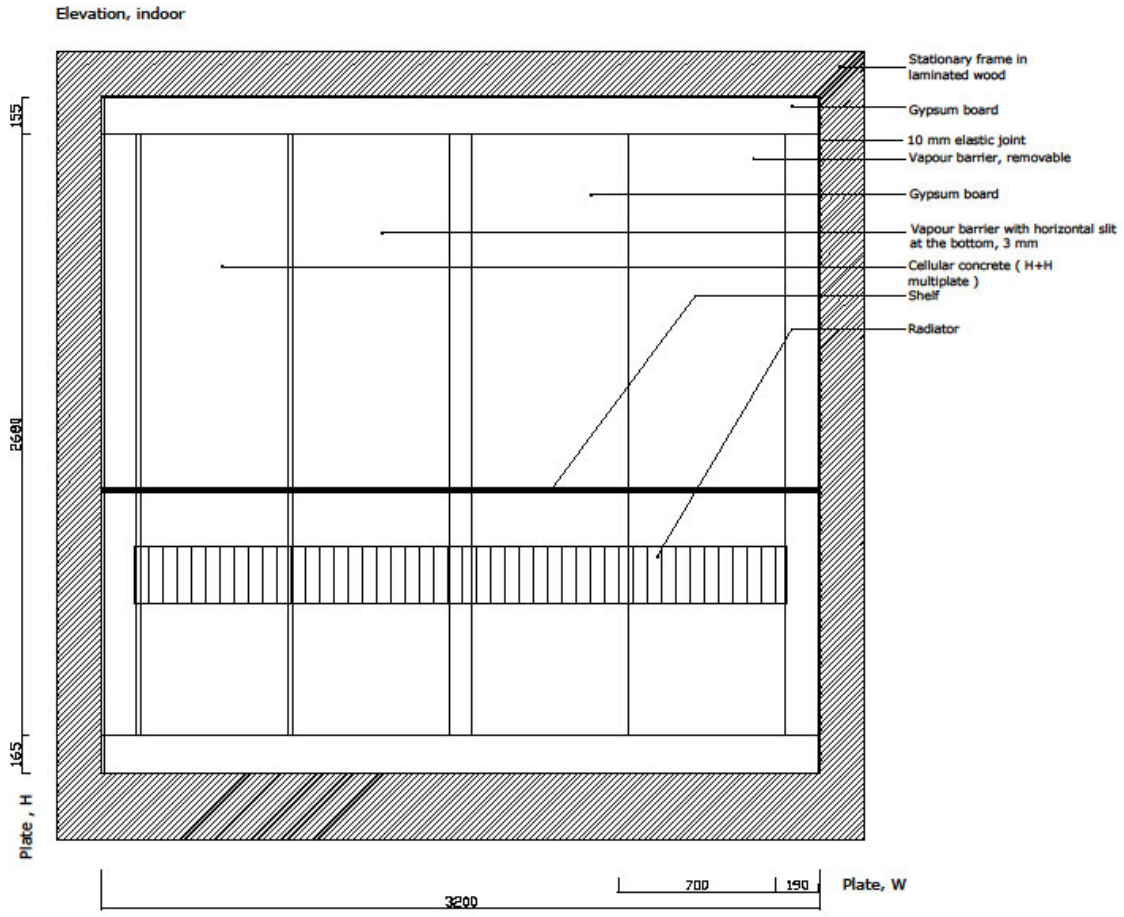

Figure A6. Elevation indoor. The shelf and the radiator were to mounted in order to simulate 2D-conditions along the wall. Because of limited time such tests were not made and therefore the radiator and the shelf were not mounted.

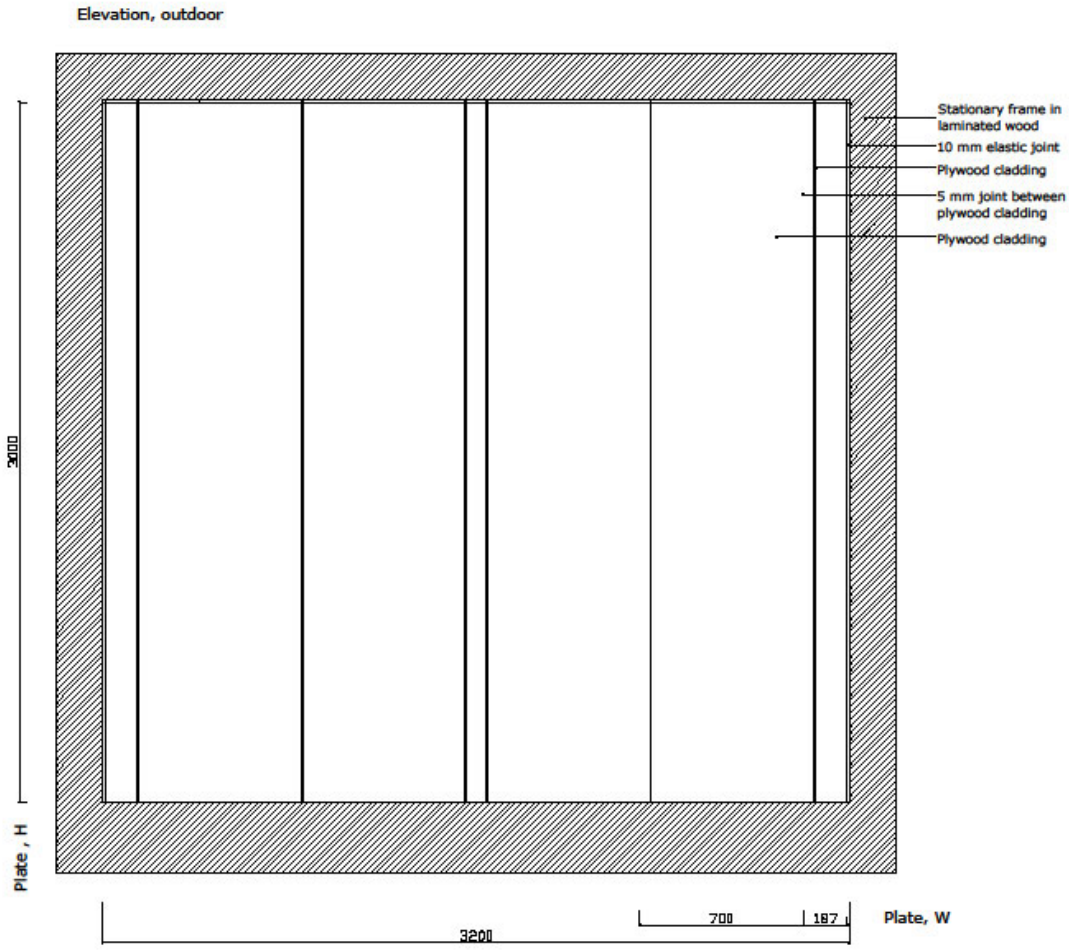

Figure A7. Elevation outdoor.

Photos of the test set-up are shown in Figures A8 – A14.

Figure A8. Climate simulator at SBi. Indoor side at left, outdoor side at right.

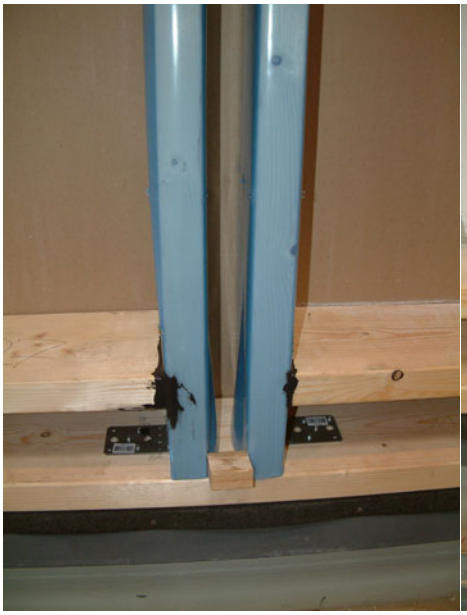

Figure A9. Duct for cables between the two vertical studs.

Figure A10. Reducing 3D effects.

Figure A11. Placement of bricks at the outdoor side to increase the thermal mass for stabilising the temperature. Fans are added in order to ensure that the bricks are activated as thermal mass.

Figure A12. After mounting a vapour barrier on the indoor side of Element 3. At the left Element 4 (cellular concrete), at the right Element 2 where no vapour barrier was mounted. Suspended RH sensors (Rotronic) are seen in front of the elements.

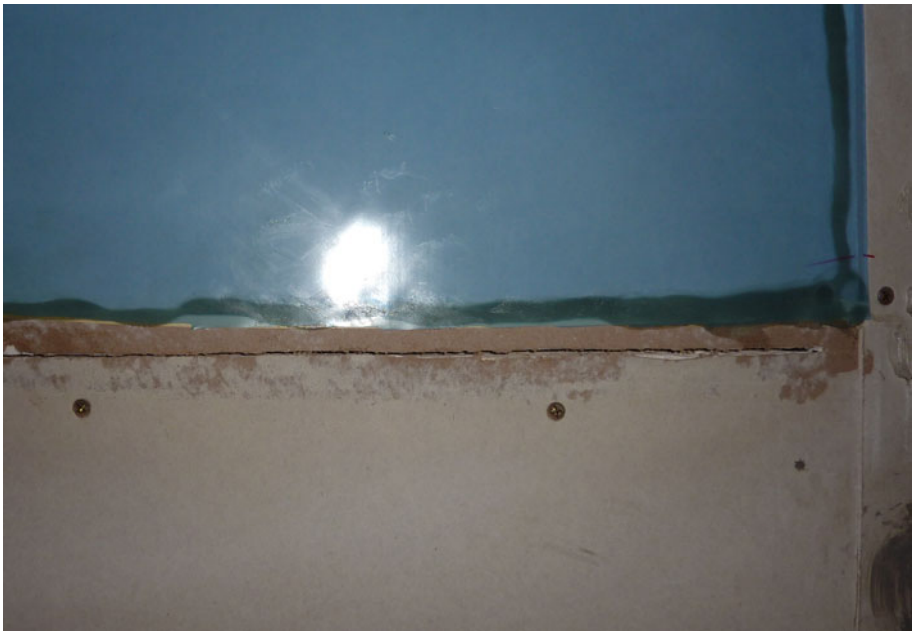

Figure A13. Element 3 with a slit (see arrow) below the vapour barrier.

Figure A14. Element 4 seen from the outdoor side after mounting the cladding. The sensors are fixed at the back (indoor) side of the cladding while the wires are led on the outdoor side in order to disturb the conditions in the cavity as little as possible.

Data-logging

Data-logger: Campbell Scientific CR 10 with Multiplexers
Sampling rate: 60 s
Data-logging: 10 min average

Three data-loggers were used to collect data from the different sensors, named CR10_1, CR10_2 and CR10X1. Each of these could contain data from about three days of measurements. Two or three times a week the content of the data-loggers were transferred to a computer.

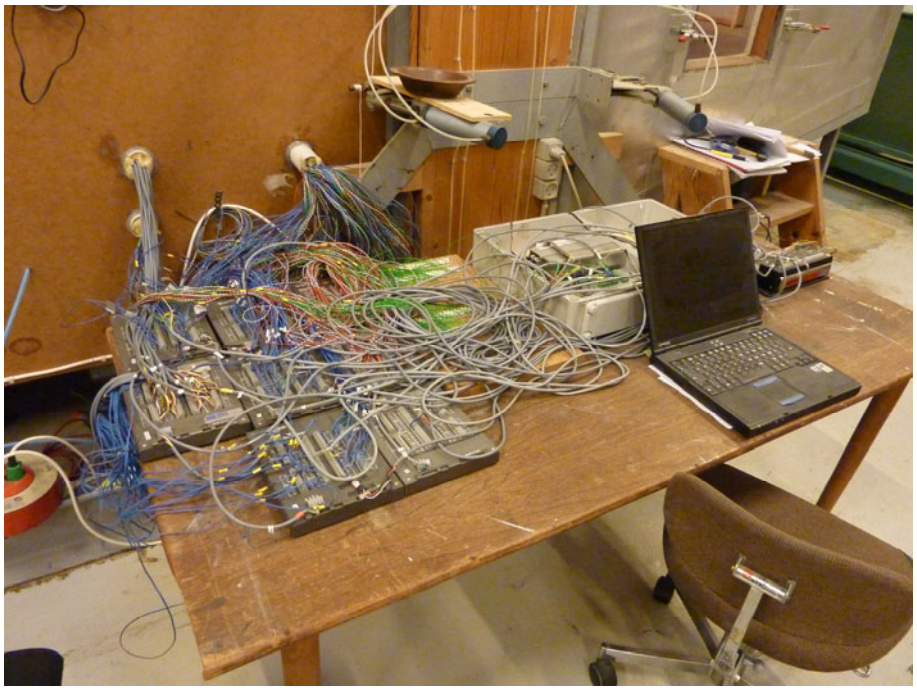

Figure A15. Table with data-loggers, wires, computer, etc.

Sensors

Table A1. Information and specifications of sensors.

Sensor	Position	Characteristics	Picture
Thermocouple	At different depths in the elements, cf. Appendix D	Standard copper-constantan thermocouple Range: -250 ºC - + 350 ºC Accuracy: +/- 0,1 ºC at 100 ºC	See Figure A16
RH sensor	Same	Manufacturer: Honeywell Model: HIH-4000-004 Humidity Sensor Range: 0 – 100 % RH Accuracy: +/- 3,5 % RH	See Figure A17
RH sensor	In front of the elements at the indoor (500 mm) and outdoor sides (750 mm)	Manufacturer: Rotronic Model: HygroClip Range: 0- 100 % RH Accuracy: +/- 1,5 % RH at 23 ºC	See Figure A18

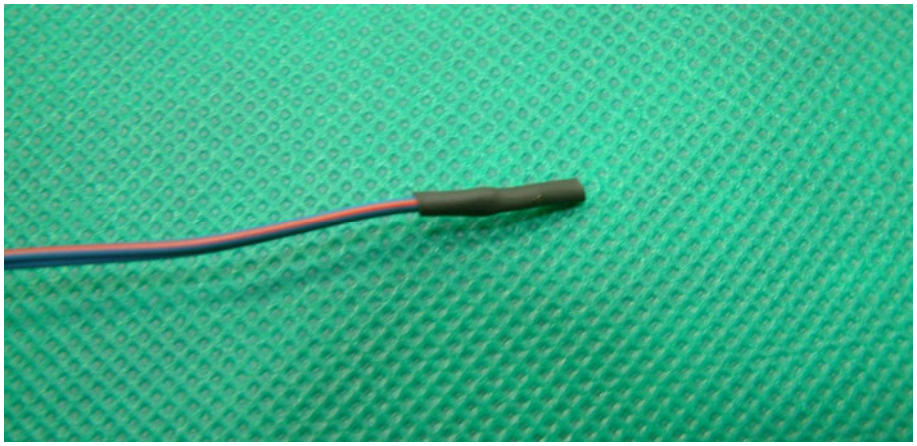

Figure A16. Thermocouple. Specifications: see Table A1.

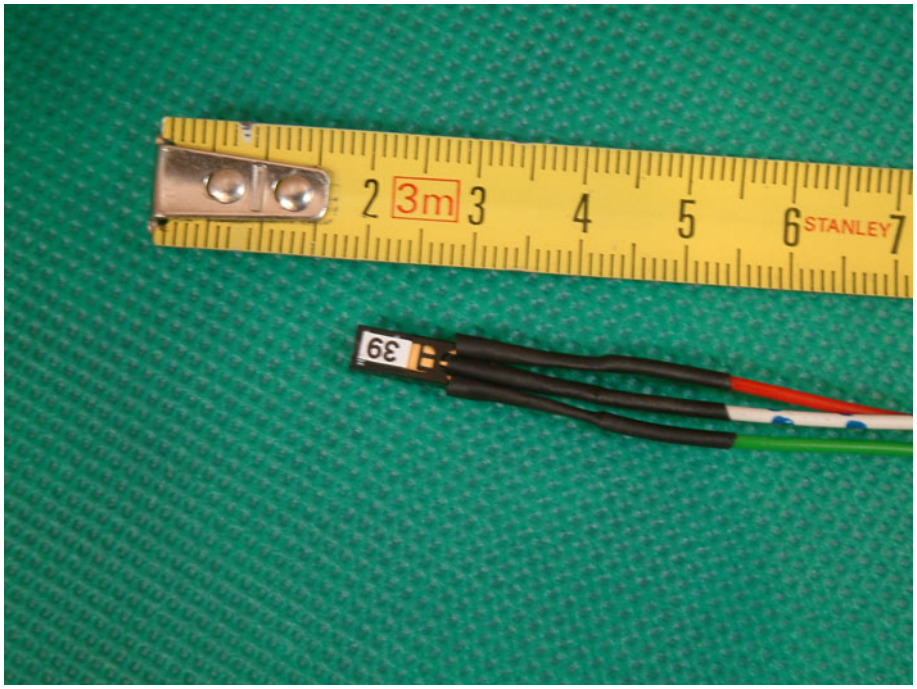

Figure A17. RH sensor. Specifications: see Table A1.

Figure A18. RH sensor (Rotronic). Specifications: see Table A1.

Cooling machine

Manufacturer: Johnson Controls Denmark ApS
Compressor type: Bitzer LH84/4EC-6,2Y-40P
Compressor performance at -30 ºC/+27 ºC: 5220 kW
Evaporator type: SEARLE KME 80-8L
Ventilator type: Øland GTHB-031-B
Ventilator max performance: 2100 m^3/h

Figure A19. Cooling machine and compressor.

Figure A20. Climate simulator with inlet (top) and outlet (bottom) at the outdoor climate chamber for air from and to the cooling machine.

Appendix B. Test series

Before the main tests (M1 – M4) a pre-test (P1) was made to measure air velocity at the indoor side in order to get data for calculation of surface transfer coefficients that were to be used in the model studied by Steskens (in press). Table B1 describes the pre-test.

Table B1. Pre-test (P1).

Series	Layers in elements	Purpose/activity	Duration of test
before P1		Thermocouples and RH sensors are mounted on the gypsum board [1]	
P1	No vapour barriers No cladding	Measurement of the air velocity at different distances from a fan placed at the indoor side by means of a hand-held anemometer. The fans were placed at different positions at the floor in the indoor climate chamber. The air velocity was measured at 50, 100, 200 and 400 mm from the surface, in the same grid as used for the Rotronic sensors (placed 500 mm from the surface). The anemometer was oriented in such way that it measures the air velocity of vertical air movements.	4 hours

Note 1: Since the RH sensors in position I were reused outdoor in test M4, they were mounted in such a way that they could be removed undamaged. Therefore they were mounted with glue about 2 cm from the end of the cable, where the sensor was placed. The sensor was slightly bended against the surface to let it touch the surface without fixing it to the surface.

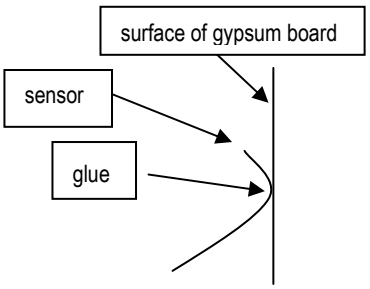

Table B2 describes the main tests that were carried out in order to measure temperature and humidity profiles in facade elements. The measurements should be compared with simulations based on a computer model (Steskens, in press).

Table B2. Main tests.

Series	Layers in elements	Purpose/activity	Duration of test
M1	No vapour barriers No cladding	Steady-state without vapour barriers. RH sensors are kept on the surface of the gypsum board at the indoor side.	2 weeks - 1 month *
after M1		Mounting of vapour barriers at indoor side of Elements 1 and 3 (slit in vapour barrier on Element 3). Tape in front of the slit at Element 3 is removed, at indoor side (at the bottom of the element) and at outdoor side (at the top). The vapour barriers are mounted with special joint glue to ensure air-tightness. Silicone is used to seal the wire outtakes. RH sensors used at the surface of the gypsum board at the indoor side are moved to the outdoor side.	1 day
M2	Vapour barriers at Elements 1 and 3. No cladding	Steady-state with vapour barriers.	2 weeks – 1 month *
after M2		Changing to varying climate on the outdoor side.	1 week **
M3	Vapour barriers at Elements 1 and 3. No cladding	Varying climate without cladding. Daily cycles simulating temperatures in April and September. Each test was preceded by a period of steady-state corresponding to the lower set point of the specific month.	> 1 month ***
after M3		Sensors are mounted at cladding and cladding is added at all elements	3 weeks
M4	Vapour barriers at Elements 1 and 3. Cladding at all elements	Varying climate with cladding and a 25 mm vented cavity. Same variation of the climate as in test M3. The cladding consists of plates of plywood mounted side-by-side on laths. Each test was preceded by a period of steady-state corresponding to the lower set point of the specific month.	> 1 month ***

*: Data were evaluated after 2 weeks to analyse whether it was necessary to proceed.
**: Including time to identify relevant set points
***: It was planned to let each of these tests last 1 month, but due to limited amount of time, they were closed after 2 weeks.

Appendix C. Materials

Data for the materials used in the test elements.

Table C1. Materials.

Material	Brand	TUN-NR	Characteristics
glass wool	Isover Diffus 320	5019646	Thermal conductivity[2]: λ = 40 mW/m K Density[2]: 13 kg/m^3 Air permeability[2]: 2,17·10^{-4} m^2/s m Pa Water vapour permeability[3]: 155·10^{-12} kg/s m Pa Sorption isotherm: see [4]
cellular concrete	H+H Multipladen 535		Thermal conductivity[5]: λ_{design} = 140 mW/m K Specific heat capacity: 1kJ/kg K Density[5]: 535 ± 15 kg/m^3 Size of block[5]: 600 x 400 mm
vapour barrier	CE folie 0.20		Water vapour resistance[6]: 550 GPa m^2 s /kg
gypsum board, inner cladding	13 A-1 standard plate		Thermal conductivity[7]: λ = 250 mW/m K Density[7]: 736 kg/m3 Water vapour permeability[7]: 20·10^{-12} kg/s m Pa
gypsum board, wind barrier	9 EH-3 windproof plate		Thermal conductivity[8]: λ = 210 mW/m K Density[7]: 789 kg/m3 Water vapour permeability[7]: 15·10^{-12} kg/s m Pa
plywood			Density 600 kg/m^3 Water vapour diffusion resistance[9]: 4 GPa s m^2/kg

Sources:
[1] (ISOVER, 2009a)
[2] (ISOVER, 2009b)
[3] (de Place Hansen & Hansen, 1999b)
[4] (de Place Hansen & Hansen, 1999a)
[5] (H+H Danmark A/S, 2009)
[6] (Orbita-Film, 2008)
[7] (Knauf Danogips, 2009b)
[8] (Knauf Danogips, 2009a)
[9] (de Place Hansen & Brandt, 2009)

Appendix D. Sensor mapping

This appendix describes how the different positions of sensors in the elements were designated. The designations are used in the figures showing the results of the main tests, see chapter 'Results and Discussion' and Appendices F to K. Not all combinations of vertical and horizontal positions are used.

Table D1. Designation of sensors, horizontal position.

Designation = depth	Distance from the indoor side	
v (I, indoor side)	0 mm	Indoor conditions – in front of the element
A	13 mm	In the insulation, at the indoor gypsum cladding
B	61.5 mm	In the insulation, 48.75 mm insulation on the indoor side
C	110.5 mm	In the insulation, 97.5 mm insulation on the indoor side
D	159.25 mm	In the insulation, 146.25 mm insulation on the indoor side
E	208 mm	In the insulation, at the wind barrier, 195 mm insulation on the indoor side
F	217 mm	In the vented cavity, at the wind barrier (i.e. at the outdoor side before the cladding is mounted, which takes place between test M3 and M4)
G	242 mm	In the vented cavity, at the cladding (only test M4)
k (O, outdoor side)		Outdoor conditions – in front of the element

Table D2. Horizontal position of sensors in the different elements

Element	Depth
1	A, C, E, F, G
2	A – G
3	A – G
4	B, C, E, F, G

Table D3. Designation of sensors, vertical position.

Designation	Position from bottom of element	
h5c	2430 mm	
h5r	2430 mm	only Element 2, at Depths A and E
h4c	2130 mm	
h3c	1450 mm	
h3r	1450 mm	only Element 2, at Depths A and E
hx9	1260 mm	only Element 2, at Depth A
hx8	1160 mm	only Element 2, at Depth A
hx7	825 mm	Elements 2 and 3, at Depths A, C and E
hx6	650 mm	only Element 2, at Depth A
h2c	500 mm	
h1c	200 mm	
h1r	200 mm	only Element 2, at Depths A and E

Index c means centre line, 325 mm from left side of element.
Index r means right side, 555 mm from left side of element (only Element 2).

Example: E2-h3c-A. ‘E2’ refers to element 2, ‘h3c’ to the vertical position (table D3), and ‘A’ to the horizontal position (table D1)

See also Figures D1 and A2. At minimum sensors were placed at three heights, typically 'h1c', 'h3c' and 'h5c' or 'h2c', 'h3c' and 'h4c'.

Figure D1 also shows the joints in the cellular concrete layer. Sensors at 'h5c' are only placed at Depth C (in the middle of the thermal insulation layer), at Depth F (on the outer, cold side of the wind barrier) and at Depth G (at the inner side of the cladding). At these depths the joint close to the height 'h5c' is of no importance.

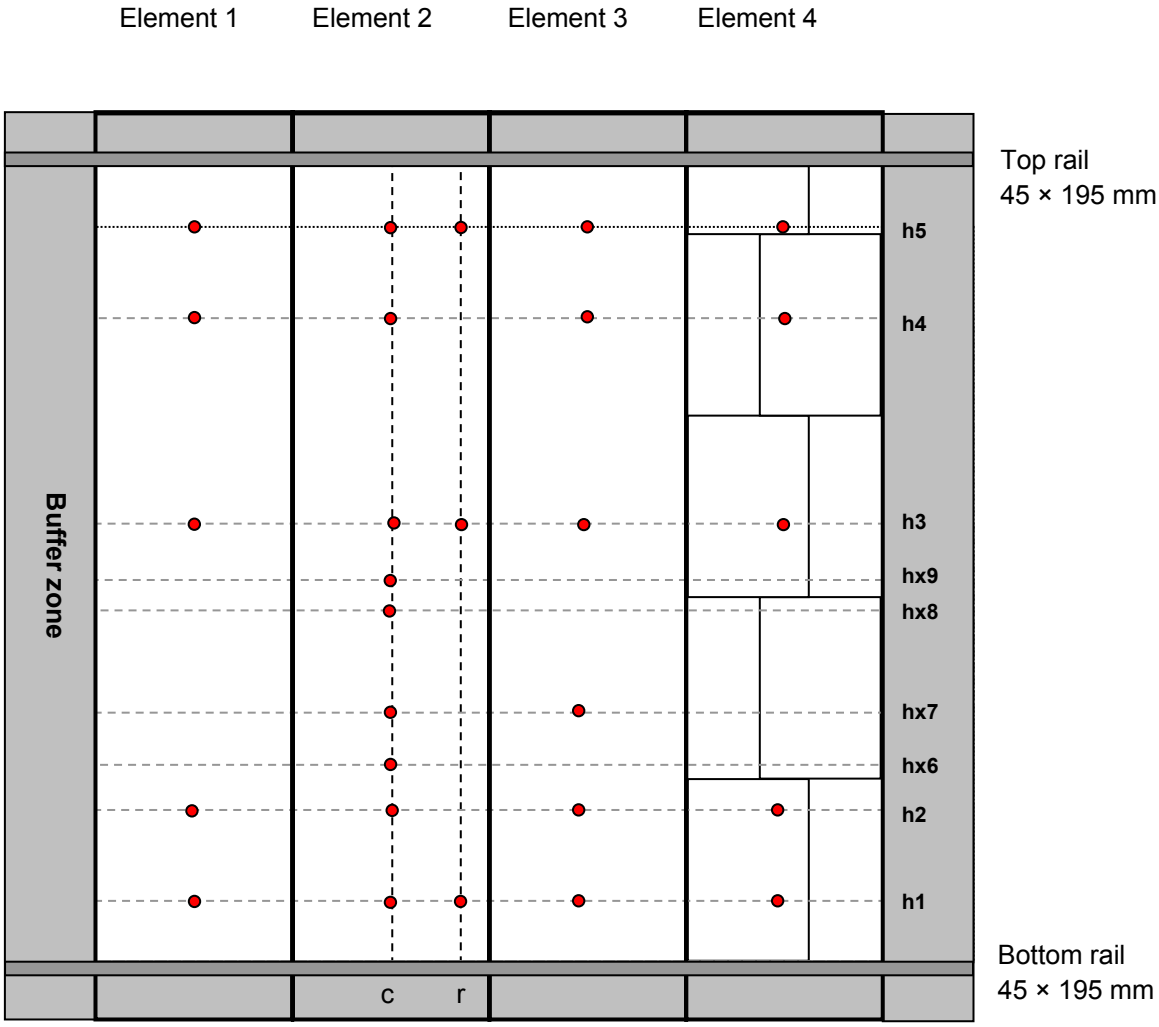

Figure D1. Position and numbering of sensors in the four elements seen from the outdoor side. At element 4 the joints between the concrete blocks are shown.

At the outdoor side four pairs of RH and temperature sensors were fixed in a 2×2 grid of 900 × 1000 mm 800 mm in front of the elements. Upper sensors were fixed at 300 mm above level 'h3c', and lower sensors were fixed at 500 mm above level 'h1c'.

At the indoor side nine pairs of RH and temperature sensors were fixed in a 3×3 grid of 700 × 750 mm 500 mm in front of the elements. Upper sensors were fixed at 650 mm from the top of the element, and lower sensors were fixed at 550 mm from the bottom of the element.

Appendix E. Temperature cycles

For the tests at varying climate, two climatic cycles representing April and September were selected based on the average hourly air temperature and relative humidity per month presented as part of weather data by the U.S. Department of Energy (U.S. Department of Energy, 2009). Originally, also July was to be simulated, but due to delays in the experiments, July had to be left out.

Statistics for DNK_Copenhagen_IWEC

– Location -- COPENHAGEN - DNK {N 55° 37'} {E 12° 40'} {GMT +1.0 hours}
– Elevation – 5 m above sea level
– Standard Pressure at Elevation -- 101265Pa
– Data Source -- IWEC Data
– WMO Station 061800

Approximated temperature cycles

The climatic cycles which were executed should fulfill the following requirements:

– The climatic cycle was prescribed by fixed set points for the temperature of the air which was supplied by the cooling machine to the outdoor side of the climate chamber.
– A cycle should have a maximum of three different set points for the supply air temperature. The set points were programmed using three different programs. During the climatic cycle (which lasted 24 hours), the programs were switched manually. Therefore, the entire cycle should be executable during office hours.

For each of the two simulated months (April and September) Tables E1 and E2 list

– Column 1: time [hours]
– Column 2: desired temperature at the outdoor side of the climate chamber, i.e. average hourly temperature (U.S. Department of Energy, 2009).
– Column 3: approximated temperature at the outdoor side of the climate chamber.
– Column 4: set point for the temperature at the outdoor side where the time-constant of the system was taken into account, including the restrictions for the maximum cooling load that could be supplied by the cooling machine.
– Column 5: the corresponding set point for the cooling machine in order to ensure an air temperature according to the set points in Column 4.

The cycles are also shown in Figures E1 and E2.

Table E1. Simulation of April climate (temperature). Desired and approximated temperature at the outdoor side, and corresponding set point for the cooling machine.

	Outdoor (cold) side of climate chamber			Cooling machine
Time [hh:mm]	Model cycle T [°C]	Approximated cycle T [°C]	$T_{set\ point}$ [°C]	$T_{set\ point}$ [°C]
00:00	4.2	4.0	4.0	- 3.5
01:00	4.1	4.0	4.0	- 3.5
02:00	4.0	4.0	4.0	- 3.5
03:00	3.9	4.0	4.0	- 3.5
04:00	4.3	4.0	4.0	- 3.5
05:00	4.6	4.0	4.0	- 3.5
06:00	4.9	4.0	4.0	- 3.5
07:00	5.7	4.0	9.0	3.5
08:00	6.4	5.3	9.0	3.5
09:00	7.2	6.5	9.0	3.5
10:00	7.8	7.7	9.0	3.5
11:00	8.3	9.0	9.0	3.5
12:00	8.9	9.0	9.0	3.5
13:00	8.8	9.0	9.0	3.5
14:00	8.7	9.0	9.0	3.5
15:00	8.6	9.0	4.0	- 3.5
16:00	8.1	7.7	4.0	- 3.5
17:00	7.5	6.5	4.0	- 3.5
18:00	7.0	5.3	4.0	- 3.5
19:00	6.4	4.0	4.0	- 3.5
20:00	5.8	4.0	4.0	- 3.5
21:00	5.2	4.0	4.0	- 3.5
22:00	4.9	4.0	4.0	- 3.5
23:00	4.5	4.0	4.0	- 3.5

Note: the approximated temperature was based on the time-constant of the system (taking into account the thermal mass of the climate chamber).
The set point for the cooling machine was somewhat dependent on the temperature in the laboratory surrounding the climate simulator, because this influenced the temperature at the indoor side of the test elements and further on through these to the outdoor side.

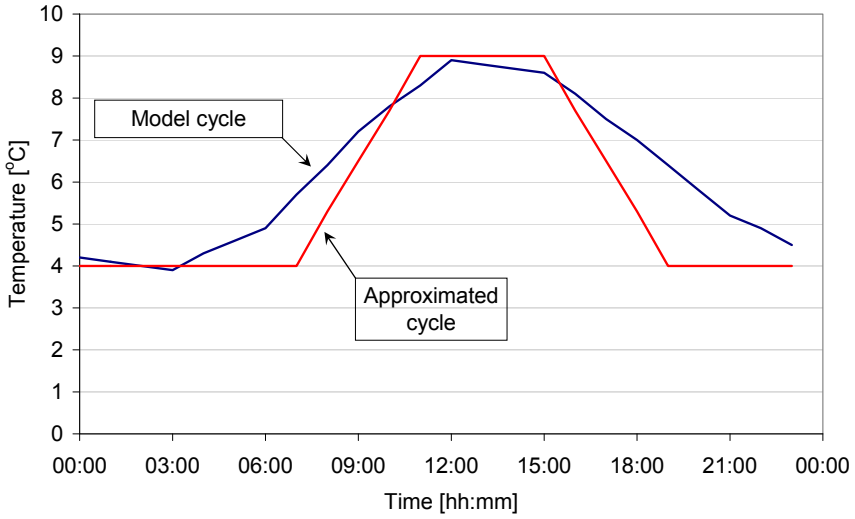

Figure E1. Temperature cycle, April. Model cycle based average hourly temperature and approximated, simplified cycle.

Table E2. Simulation of September climate (temperature). Desired and approximated temperature at the outdoor side, and corresponding set point for the cooling machine.

	Outdoor (cold) side of climate chamber			Cooling machine
Time [hh:mm]	Model cycle T [°C]	Approximated cycle T [°C]	$T_{set\ point}$ [°C]	$T_{set\ point}$ [°C]
00:00	10.7	11.0	11.0	5.5
01:00	10.6	11.0	11.0	5.5
02:00	10.5	11.0	11.0	5.5
03:00	10.4	11.0	11.0	5.5
04:00	10.7	11.0	11.0	5.5
05:00	11.0	11.0	11.0	5.5
06:00	11.3	11.0	11.0	5.5
07:00	12.0	11.0	15.0	12.0
08:00	12.7	12.0	15.0	12.0
09:00	13.4	13.0	15.0	12.0
10:00	13.8	14.0	15.0	12.0
11:00	14.2	15.0	15.0	12.0
12:00	14.6	15.0	15.0	12.0
13:00	14.5	15.0	15.0	12.0
14:00	14.5	15.0	15.0	12.0
15:00	14.4	15.0	11.0	5.5
16:00	13.8	14.0	11.0	5.5
17:00	13.1	13.0	11.0	5.5
18:00	12.5	12.0	11.0	5.5
19:00	12.1	11.0	11.0	5.5
20:00	11.6	11.0	11.0	5.5
21:00	11.2	11.0	11.0	5.5
22:00	11.0	11.0	11.0	5.5
23:00	10.7	11.0	11.0	5.5

Note: The approximated temperature was based on the time-constant of the system (taking into account the thermal mass of the climate chamber).
The set point for the cooling machine was somewhat dependent on the temperature in the laboratory surrounding the climate simulator, because this influenced the temperature in at the indoor side of the test elements and further on through these to the outdoor side.

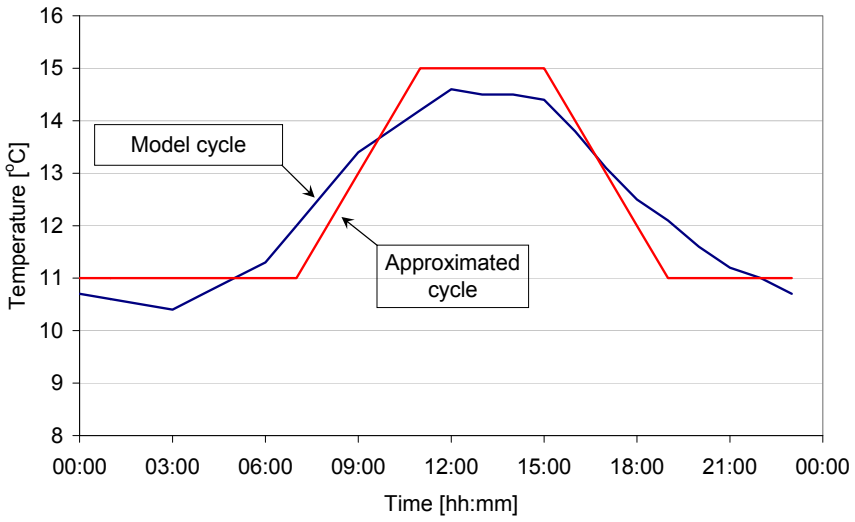

Figure E2. Temperature cycle, September. Model cycle based average hourly temperature and approximated, simplified cycle.

Cooling machine – set points

Table E3 shows the set points used in the test with April and September cycles before and after mounting the cladding. Please note that especially the April cycle was changed when testing with cladding because the lower set point was too low in the first case (without cladding). This is illustrated in Figure 66.

Table E3. Set points for the cooling machine.

	Lower set point	Upper set point
April without cladding	- 6.0 ºC	+ 3.5 ºC
September without cladding	+ 5.5 ºC	+ 12.0 ºC
April with cladding	- 3.5 ºC	+ 3.5 ºC
September with cladding	+ 5.0 ºC	+ 12.0 ºC
Sep with cladding. 2nd test [1]	+ 4.0 ºC	+ 11.0 ºC

Note: A second test with September cycles with cladding were performed about a month after the first test. The results of the first test showed that it was made before the test set-up had reached steady-state. In the meantime the temperature in the laboratory hall surrounding the test set-up had increased. Therefore the set points for the cooling machine had to be lower in the second test.

Appendix F. Steady-state without vapour barrier (M1)

This appendix contains figures showing how the temperature and RH distributed from the indoor side to the outdoor side in all four elements, in addition to the results of Element 1 shown in the part of the chapter 'Results and discussion' that presents results from test M1. For Element 1 and 2 also the vapour pressure is shown. Appendix F also contains some figures illustrating how the temperature and RH distributed from the top to the bottom of an element. Finally comparisons are made between the different elements at specific levels (heights), in addition to the figures in the section 'Comparison of elements' of the chapter 'Results and discussion'.

In all cases results are shown as a 24-hour cycle representing the specific test. All 24-hour cycles are shown from midnight to midnight with defrosting periods at noon and midnight.

If nothing else is indicated the results were based on sensors in height 'h3c', about halfway between the top and the bottom of the element. For position of sensors refer to Appendix D.

In figures where the temperature and RH at the different depths from the indoor side to the outdoor side are shown for one specific element, e.g. Figure F4, 'h4c' replaces 'h3c' at Depth C in Elements 2 and 3, since the results showed that 'h3c' was not representative of the RH level. Also, h4c' replaces 'h3c' at Depth E in Element 4, where 'h3c' was not representative for the temperature.

Temperature, RH and vapour pressure from indoor to outdoor sides

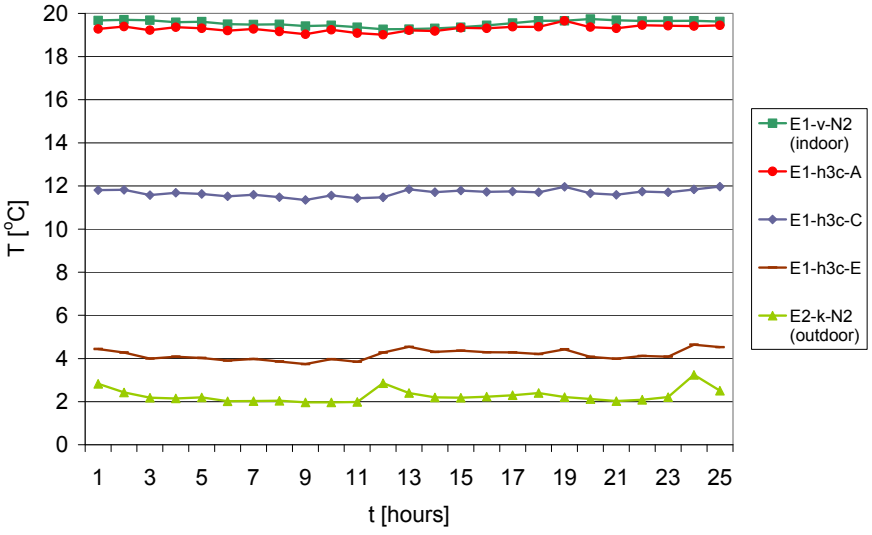

Figure F1. Temperature, Element 1. Steady-state without vapour barrier. Temperature at the indoor side, behind the indoor gypsum cladding (A), in the centre of the thermal insulation (C), in the thermal insulation, at the wind barrier (E) and at the outdoor side. 24-hour cycle starting at midnight with defrosting periods at noon and midnight. 'E2-k-N2' placed in front of Element 2 represents the temperature at the outdoor side, cf. 'Results and discussion', 'General remarks'.

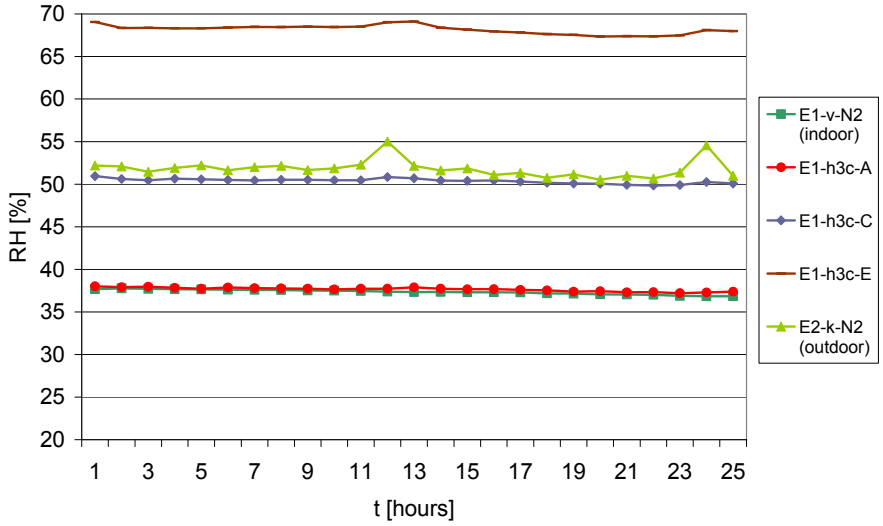

Figure F2. RH, Element 1. Steady-state without vapour barrier.

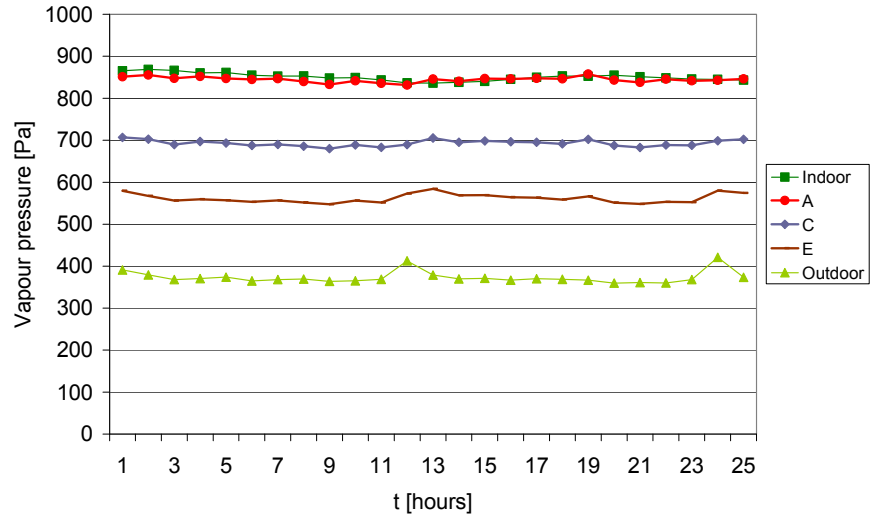

Figure F3. Vapour pressure, Element 1. Steady-state without vapour barrier.

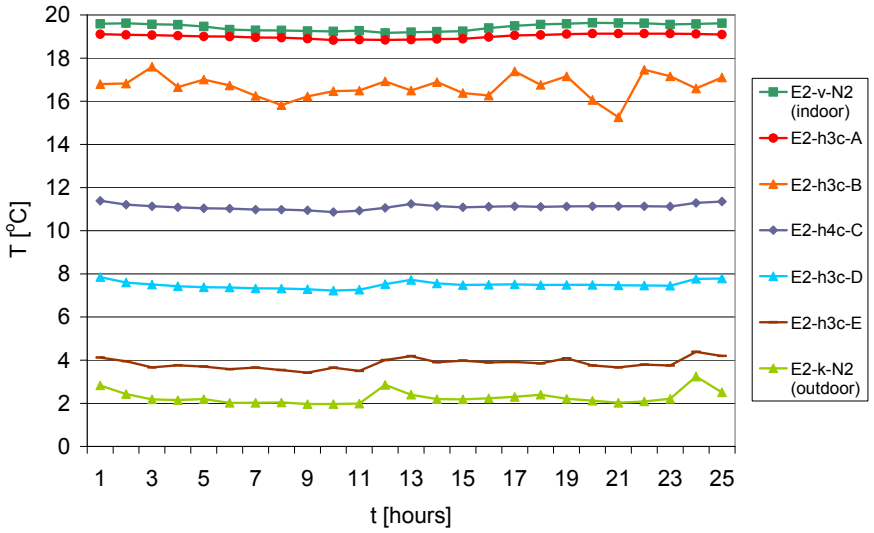

Figure F4. Temperature, Element 2. Steady-state without vapour barrier. 'h4c' replaces 'h3c' at Depth C.

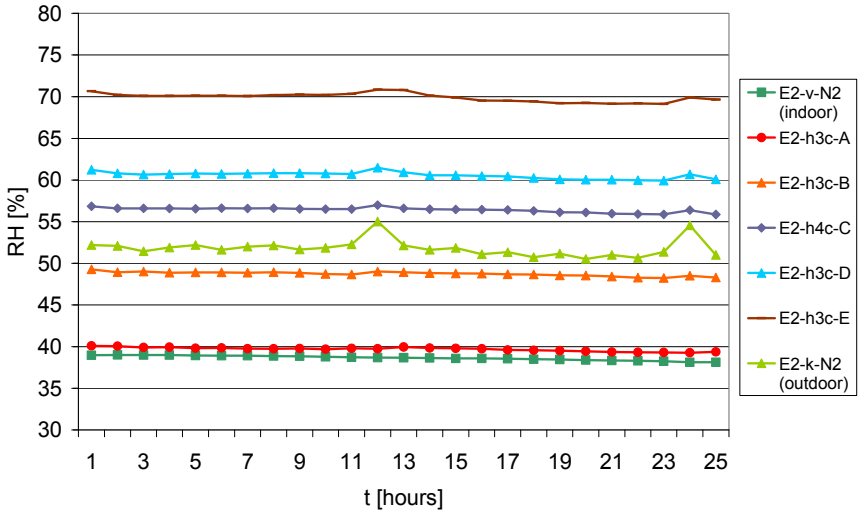

Figure F5. RH, Element 2. Steady-state without vapour barrier. 'h4c' replaces 'h3c' at Depth C.

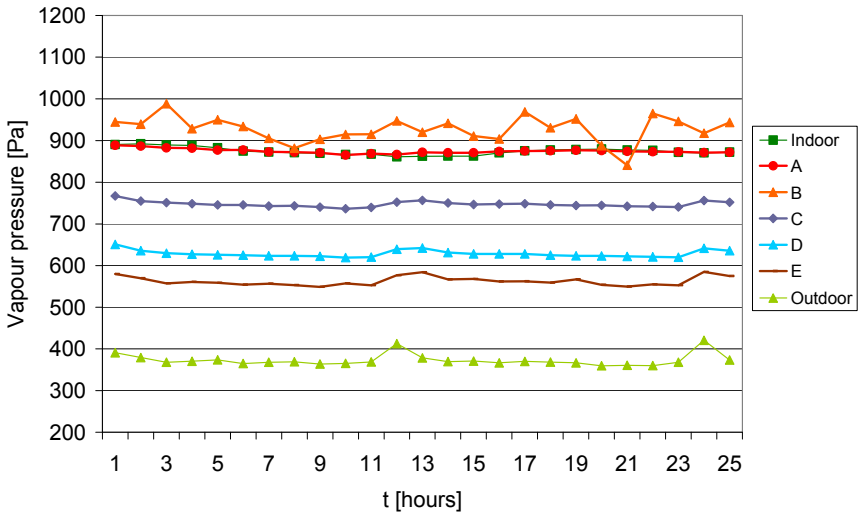

Figure F6. Vapour pressure, Element 2. Steady state without vapour barrier. 'h4c' replaces 'h3c' at Depth C.

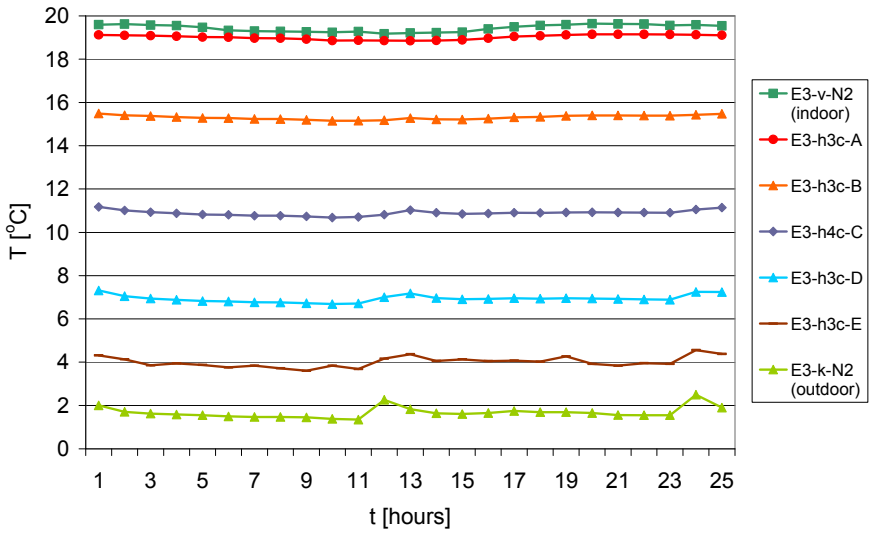

Figure F7. Temperature, Element 3. Steady-state without vapour barrier.'h4c' replaces 'h3c' at Depth C.

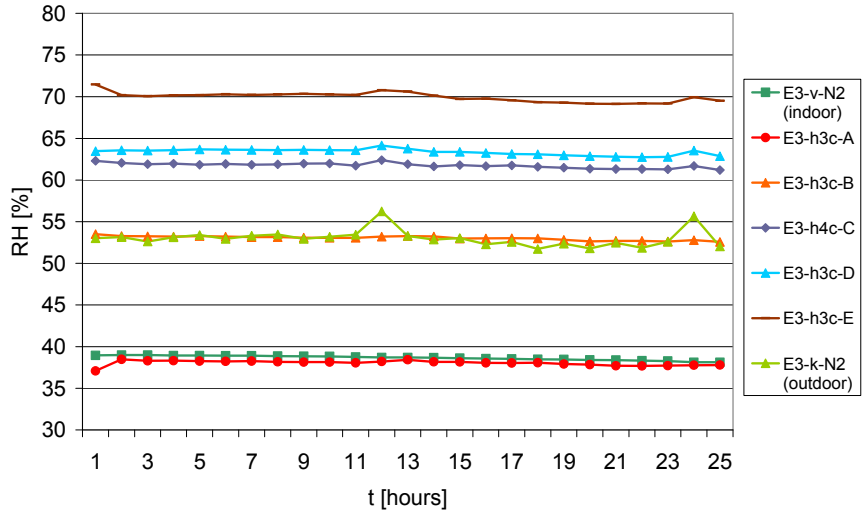

Figure F8. RH, Element 3. Steady-state without vapour barrier. 'h4c' replaces 'h3c' at Depth C.

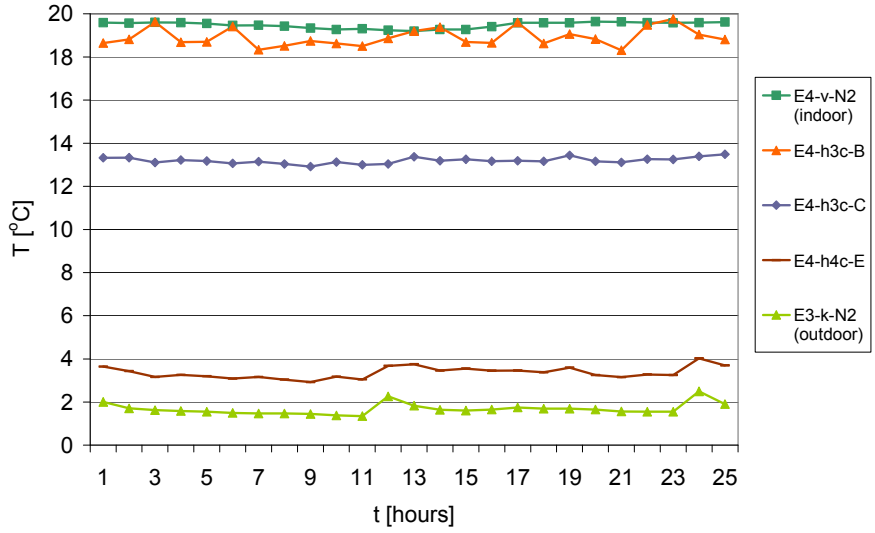

Figure F9. Temperature, Element 4. Steady-state without vapour barrier. 'h4c' replaces 'h3c' at Depth E.

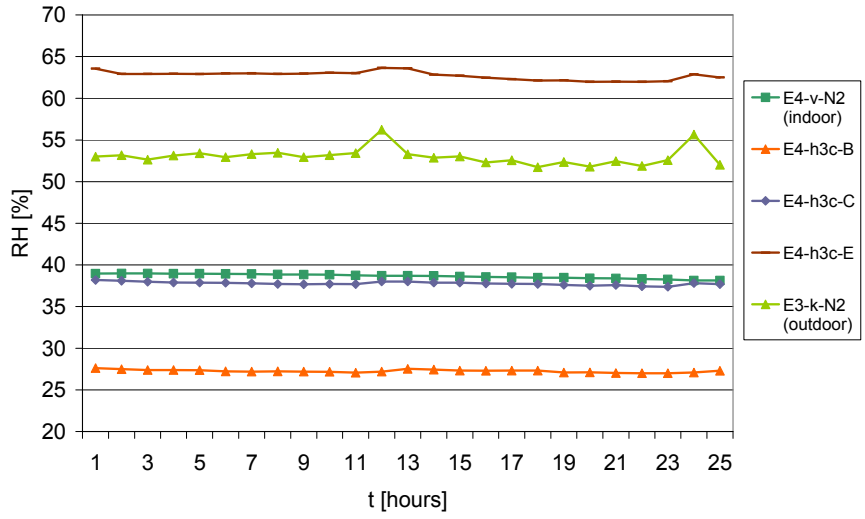

Figure F10. RH, Element 4. Steady-state without vapour barrier.

Temperature at different heights – Element 2

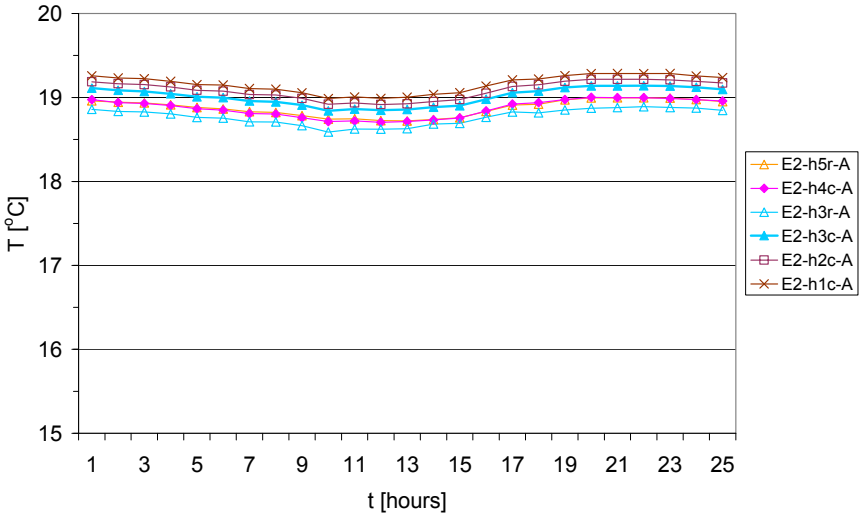

Figure F11. Temperature, Depth A. Element 2. Steady-state without vapour barrier.

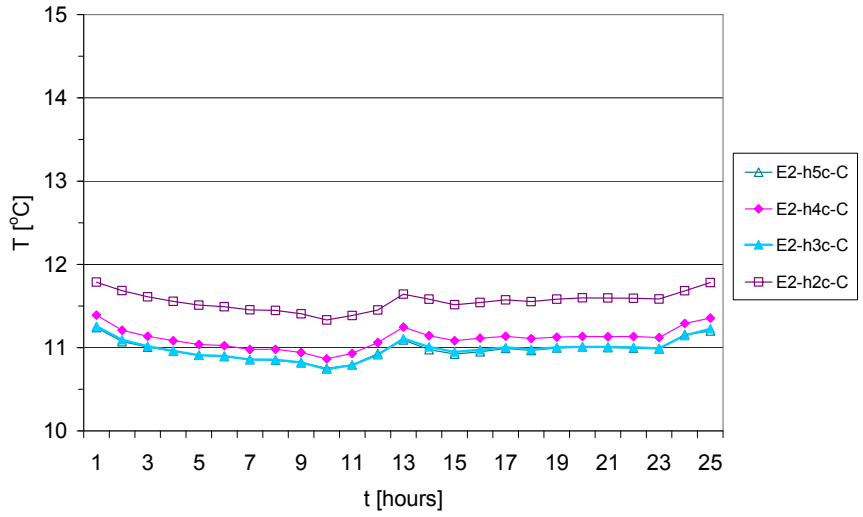

Figure F12. Temperature, Depth C. Element 2. Steady-state without vapour barrier.

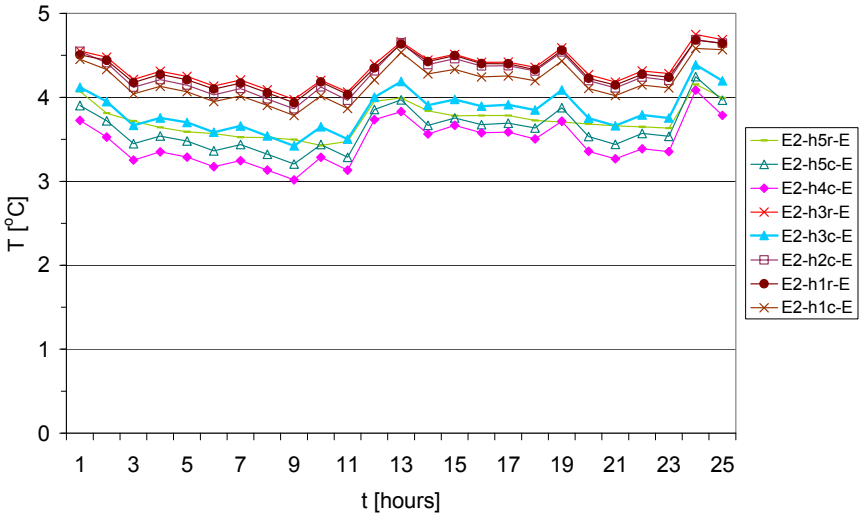

Figure F13. Temperature, Depth E. Element 2. Steady-state without vapour barrier.

RH at different heights – Element 3

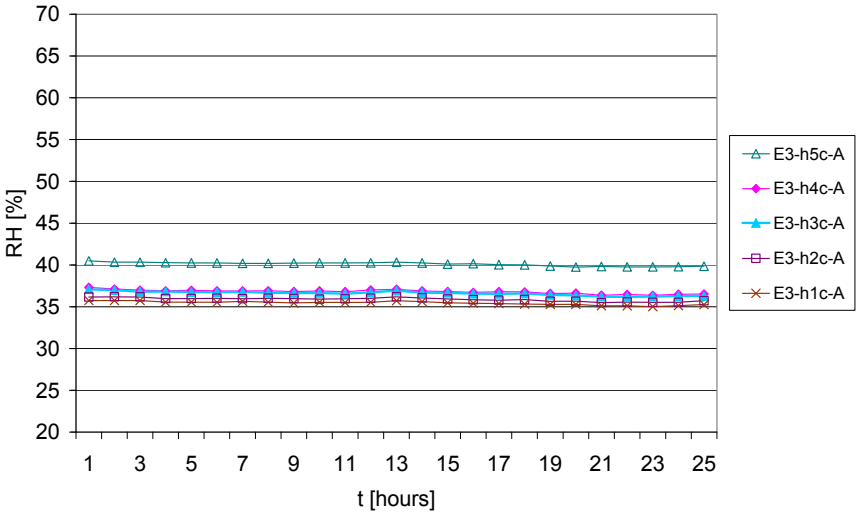

Figure F14. RH, Depth A. Element 3. Steady-state without vapour barrier.

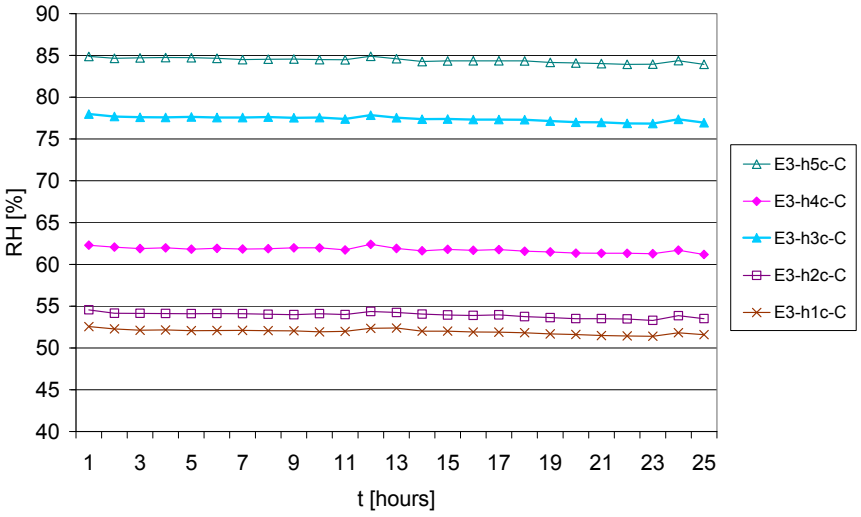

Figure F15. RH, Depth C. Element 3. Steady-state without vapour barrier.

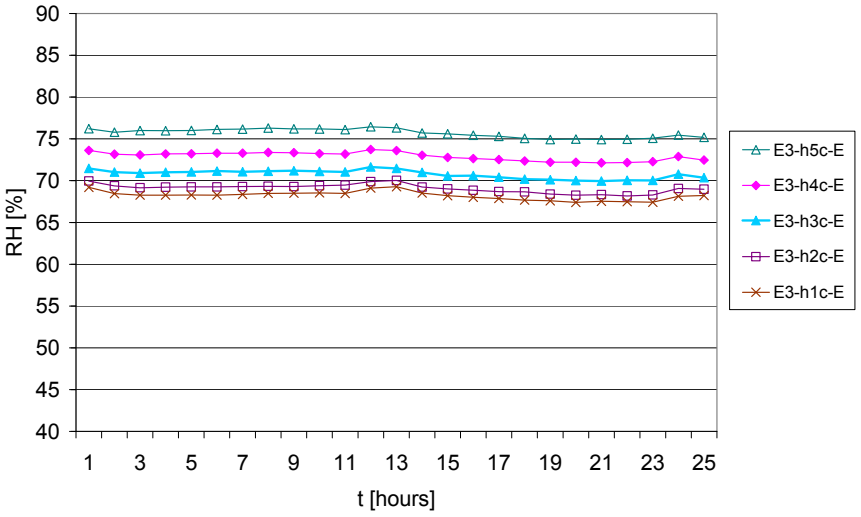

Figure F16. RH, Depth E. Element 3. Steady-state without vapour barrier.

Temperature and RH at different heights – Element 4

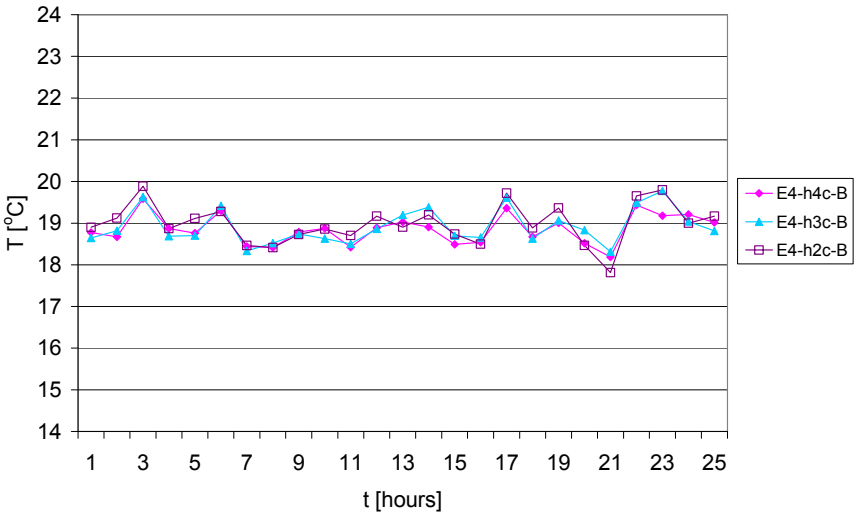

Figure F17. Temperature, Depth B. Element 4. Steady-state without vapour barrier.

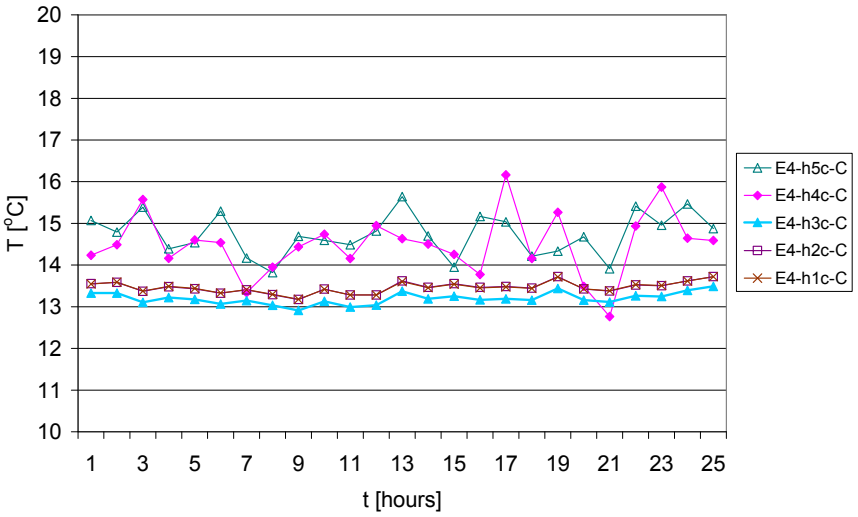

Figure F18. Temperature, Depth C. Element 4. Steady-state without vapour barrier.

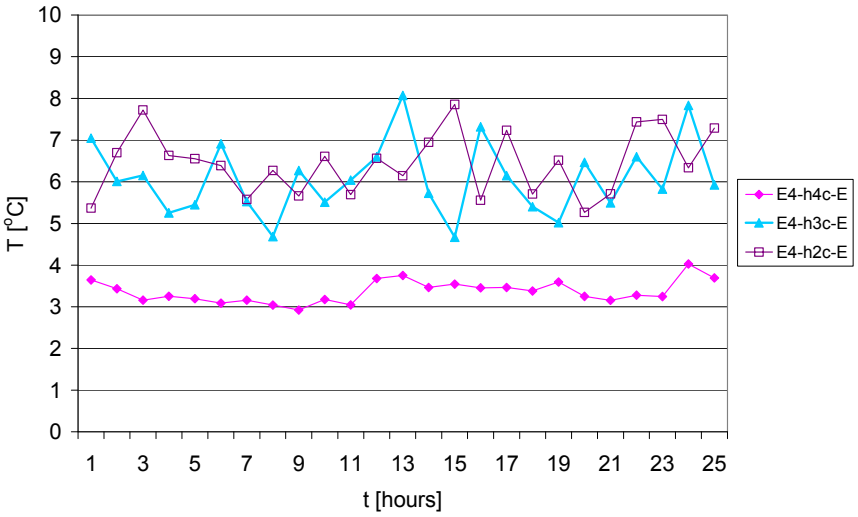

Figure F19. Temperature, Depth E. Element 4. Steady-state without vapour barrier.

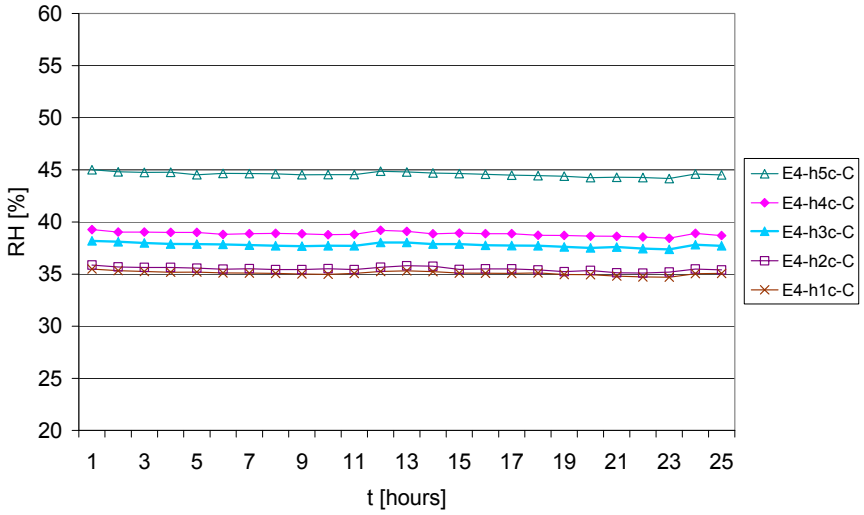

Figure F20. RH, Depth C. Element 4. Steady-state without vapour barrier.

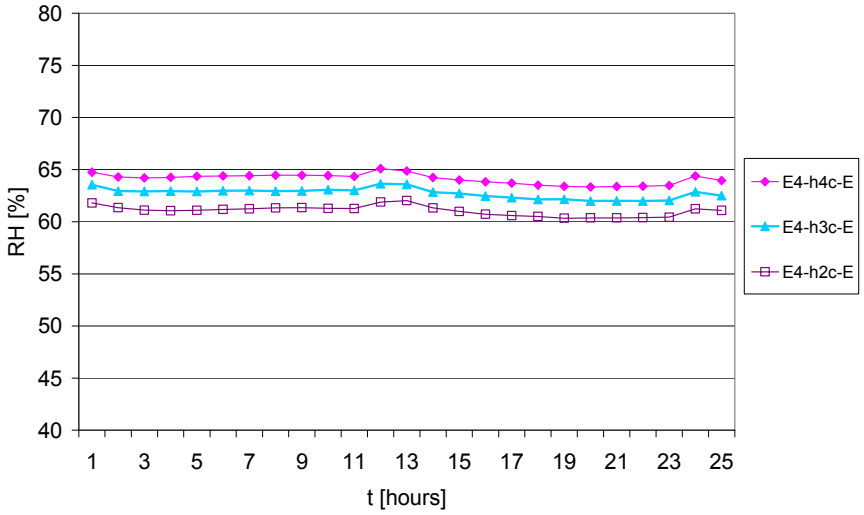

Figure F21. RH, Depth E. Element 4. Steady-state without vapour barrier.

Comparison of elements

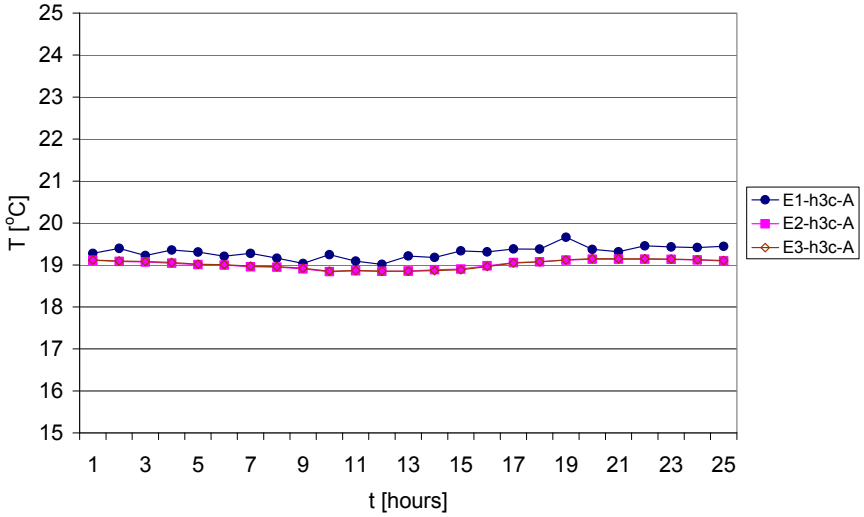

Figure F22. Temperature, Depth A. Elements 1, 2 and 3. Steady-state without vapour barrier.

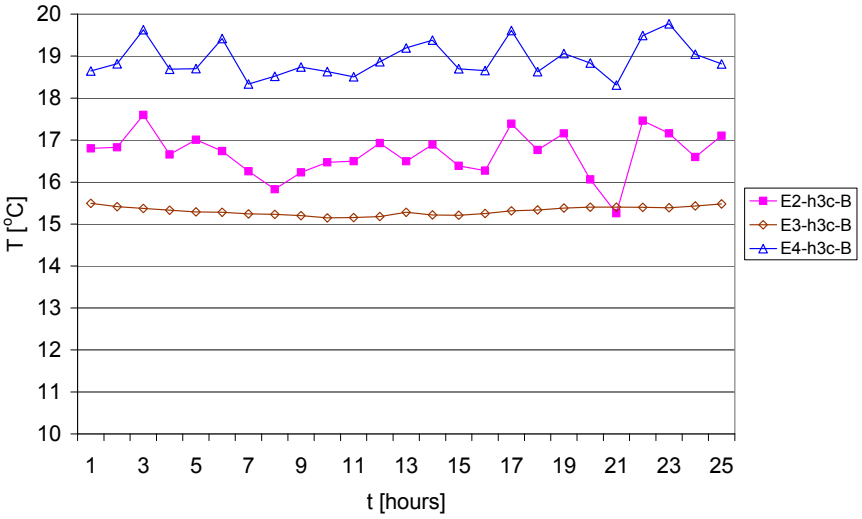

Figure F23. Temperature, Depth B. Elements 2, 3 and 4. Steady-state without vapour barrier.

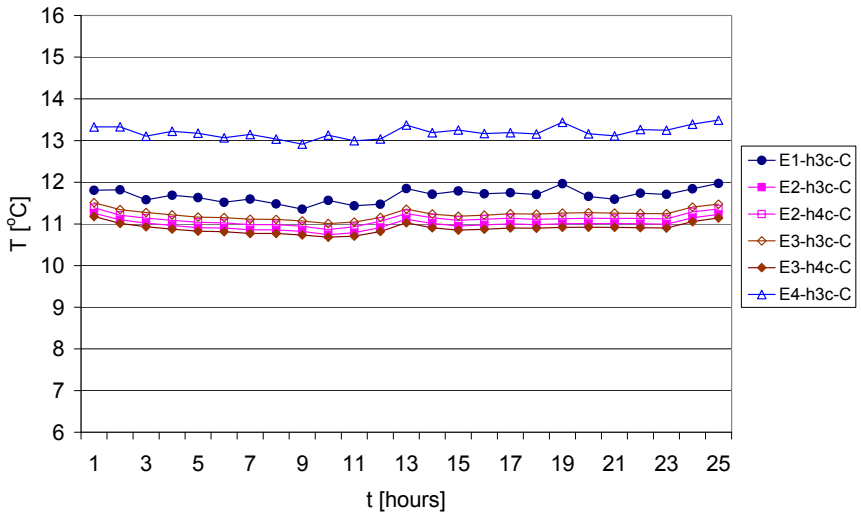

Figure F24. Temperature, Depth C. Elements 1, 2, 3 and 4. Steady-state without vapour barrier. Both 'h3c' and 'h4c' are included for Elements 2 and 3, cf. Figure F28.

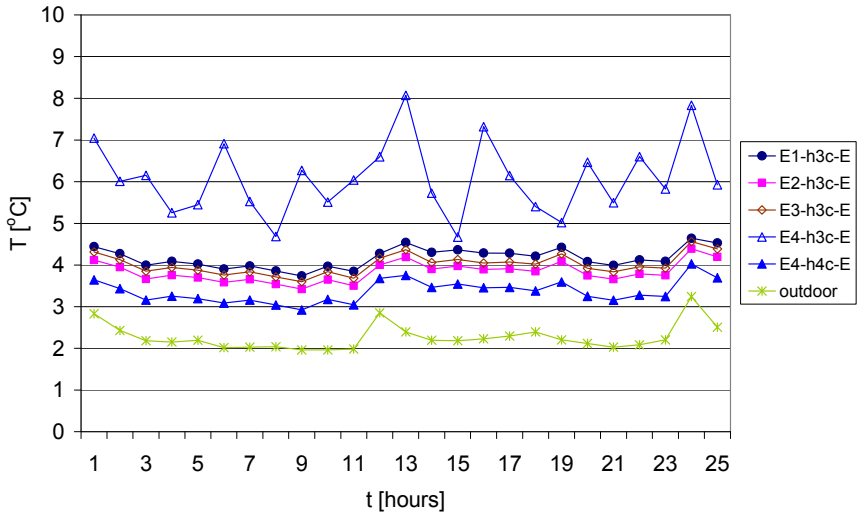

Figure F25. Temperature, Depth E. Elements 1, 2, 3 and 4, and outdoor. Steady-state without vapour barrier. Both 'h3c' and 'h4c' are included for Element 4, cf. Figure 13 or Figure F19.

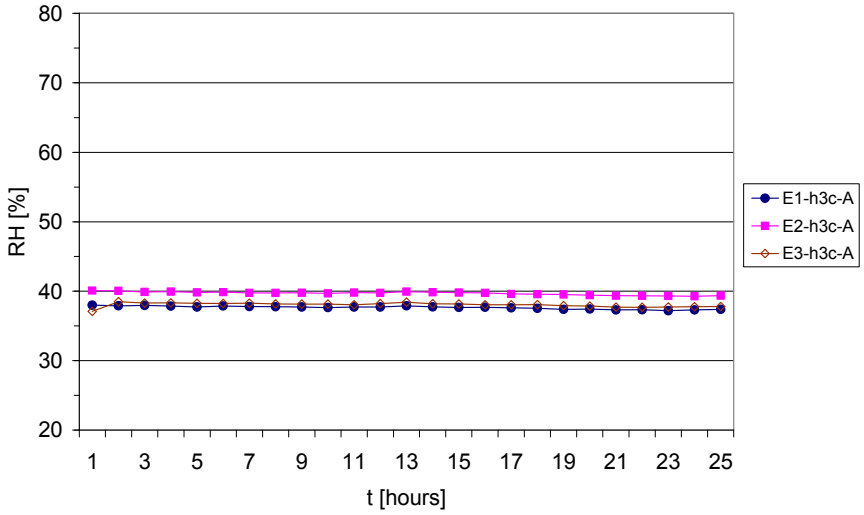

Figure F26. RH, Depth A. Elements 1, 2 and 3. Steady-state without vapour barrier.

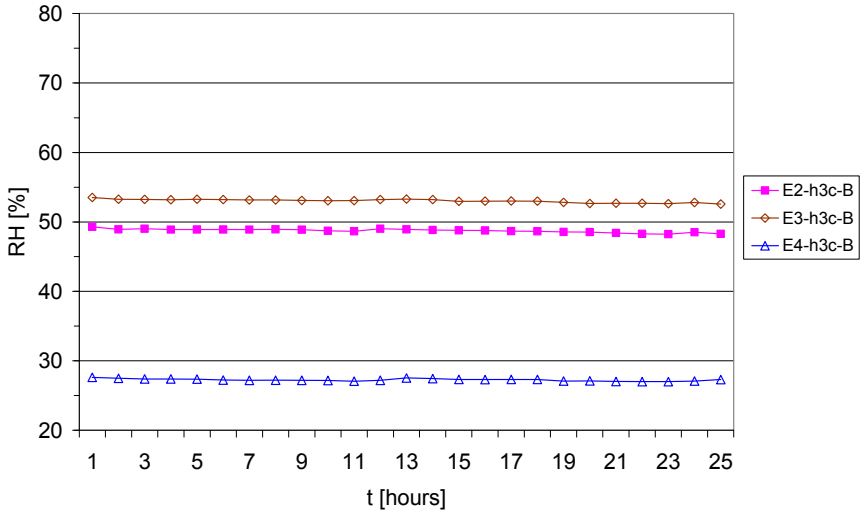

Figure F27. RH, Depth B. Elements 2, 3 and 4. Steady-state without vapour barrier.

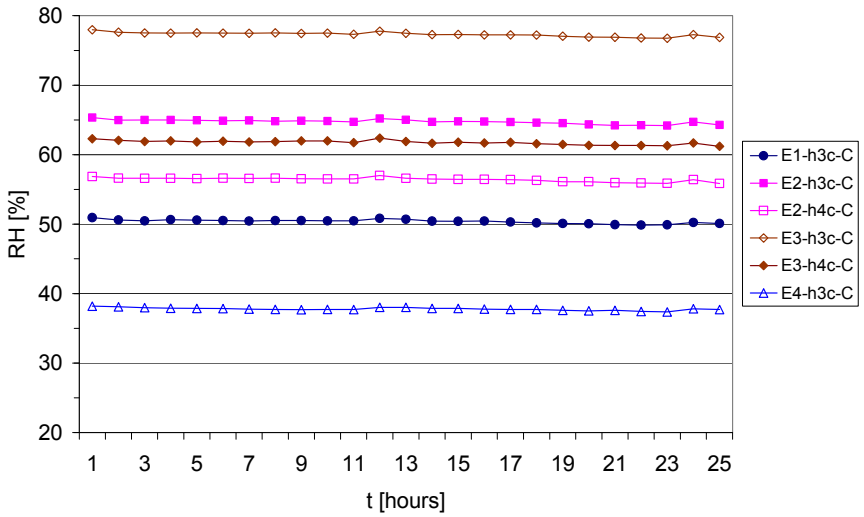

Figure F28. RH, Depth C. Elements 1, 2, 3 and 4. Steady-state without vapour barrier. 'h4c' is included for Elements 2 and 3. 'h3c' is not representative for RH in these elements.

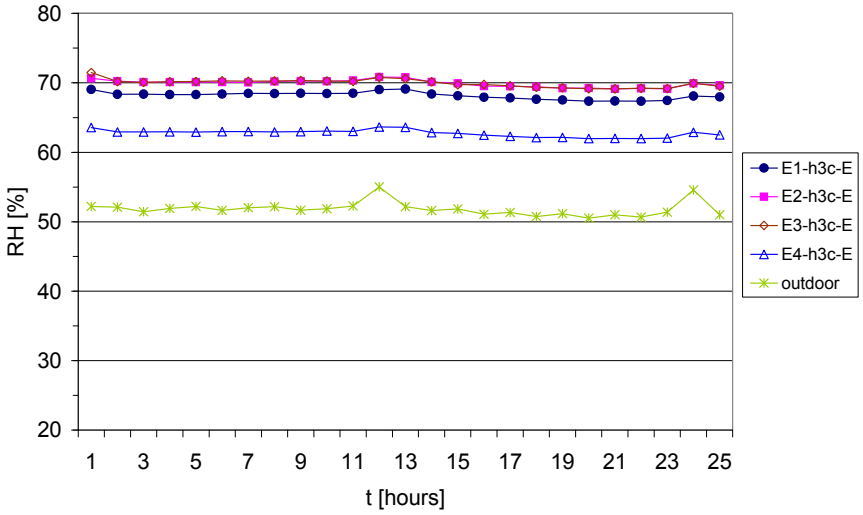

Figure F29. RH, Depth E. Elements 1, 2, 3 and 4. Steady-state without vapour barrier.

Appendix G. Steady-state with vapour barrier (M2)

This appendix contains figures showing how the temperature and RH distributed from the indoor side to the outdoor side in all four elements, in addition to the results of Element 1 shown in the part of the chapter 'Results and discussion' that presents results of test M2. For Elements 1 and 2 also the vapour pressure is shown.

'h4c' replaced 'h3c' at Depth C in Elements 2 and 3 (e.g. Figures G4 – G8), since the results showed that 'h3c' was not representative of the RH level. Also, h4c' replaced 'h3c' at Depth E in Element 4, where 'h3c' was not representative of the temperature.

For the position of sensors refer to Appendix D. See also the introduction to Appendix F. Please note that only Elements 1 and 3 had a vapour barrier. Elements 2 and 4 remained unchanged compared with test M1.

Temperature, RH and vapour pressure from indoor to outdoor sides

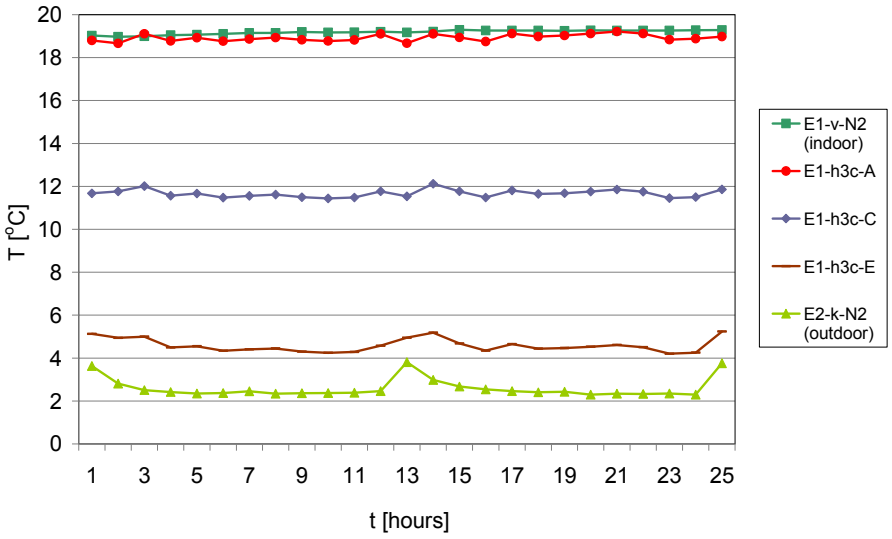

Figure G1. Temperature, Element 1. Steady-state with vapour barrier. Temperature at the indoor side, behind the indoor gypsum cladding (A), in the centre of the thermal insulation (C), in the thermal insulation, at the wind barrier (E) and at the outdoor side. 24-hour cycle starting at midnight with defrosting periods at noon and midnight. 'E2-k-N2' placed in front of Element 2 represents the temperature at the outdoor side, cf. 'Results and discussion', 'General remarks'.

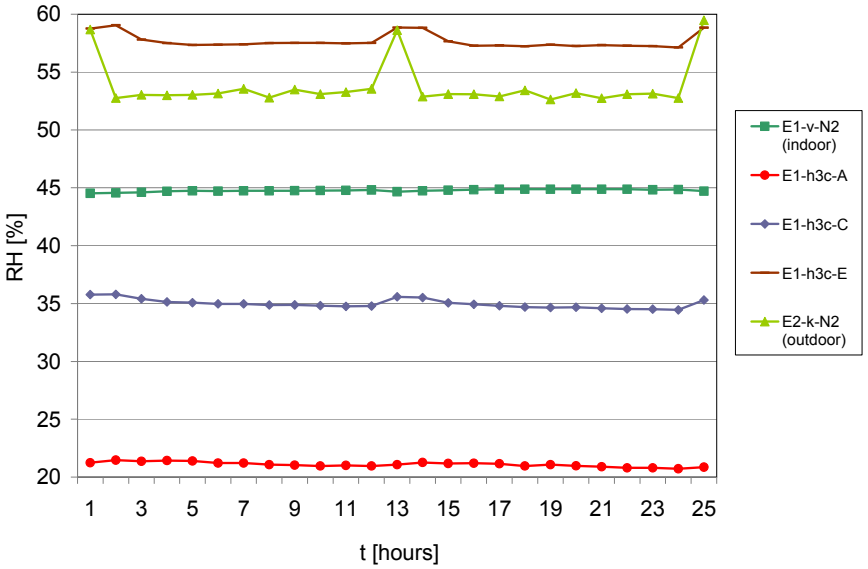

Figure G2. RH, Element 1. Steady-state with vapour barrier.

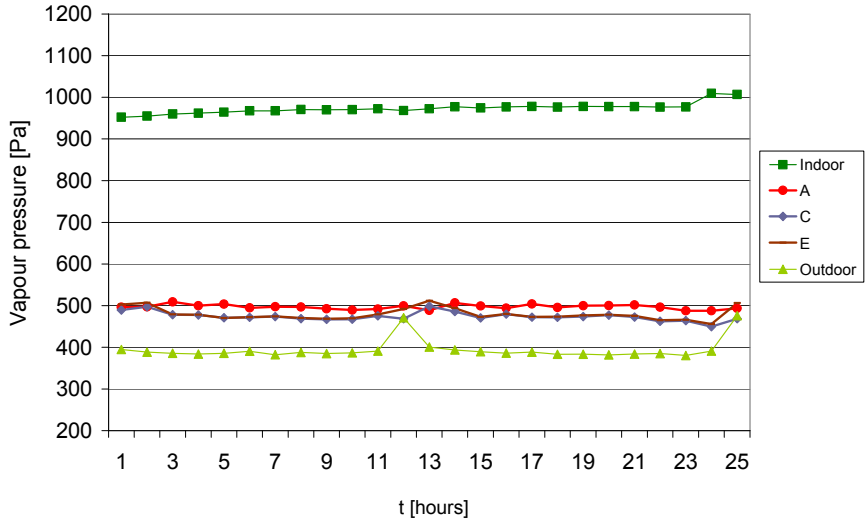

Figure G3. Vapour pressure, Element 1. Steady state with vapour barrier.

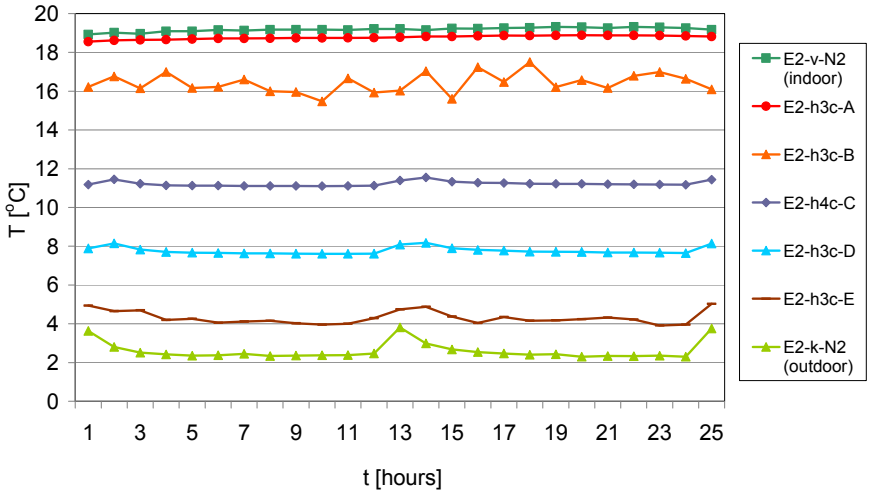

Figure G4. Temperature, Element 2. Steady-state with vapour barrier at Elements 1 and 3. 'h4c' replaces 'h3c' at Depth C.

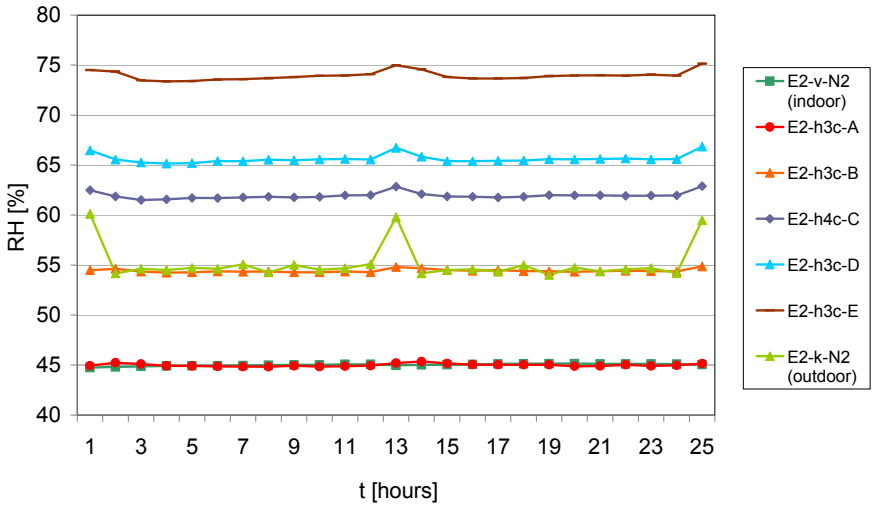

Figure G5. RH, Element 2. Steady-state with vapour barrier at Elements 1 and 3. 'h4c' replaces 'h3c' at Depth C.

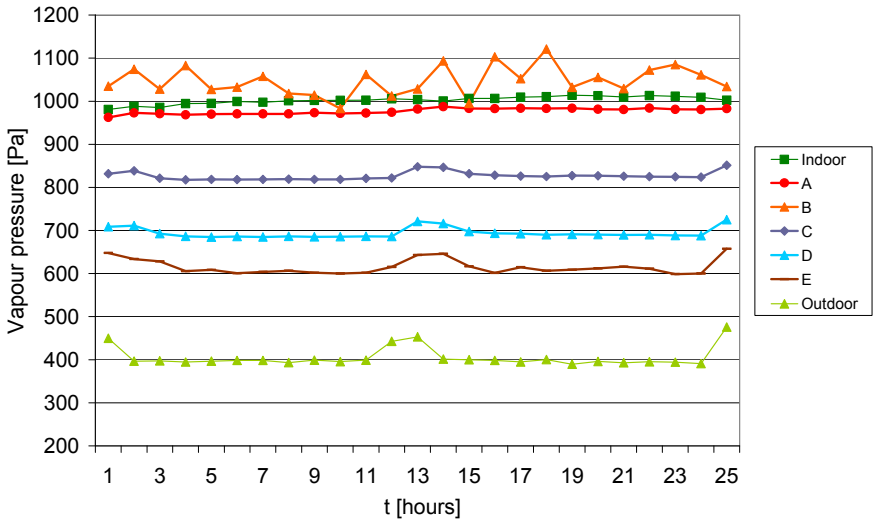

Figure G6. Vapour pressure, Element 2. Steady-state with vapour barrier at Elements 1 and 3. 'h4c' replaces 'h3c' at Depth C.

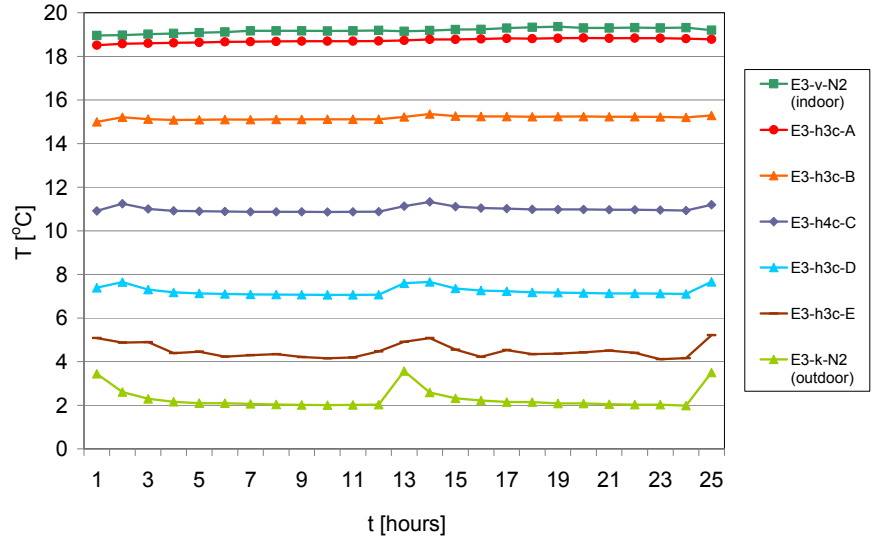

Figure G7. Temperature, Element 3. Steady-state with vapour barrier at Elements 1 and 3. 'h4c' replaces 'h3c' at Depth C.

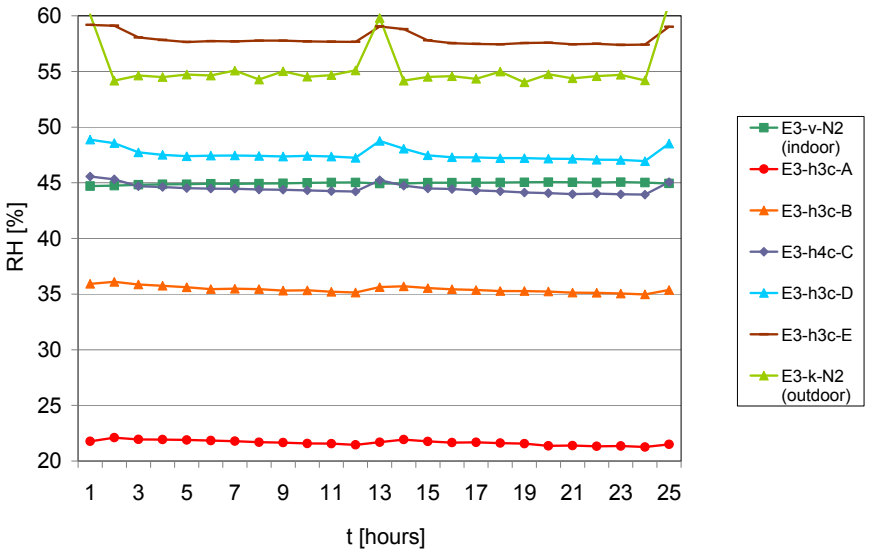

Figure G8. RH, Element 3. Steady-state with vapour barrier at Elements 1 and 3. 'h4c' replaces 'h3c' at Depth C.

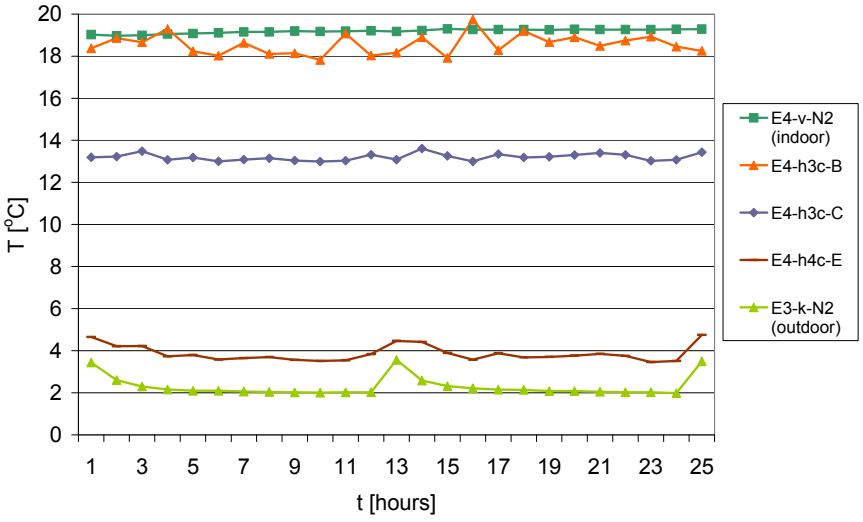

Figure G9. Temperature, Element 4. Steady-state with vapour barrier at Elements 1 and 3. 'h4c' replaces 'h3c' at Depth E.

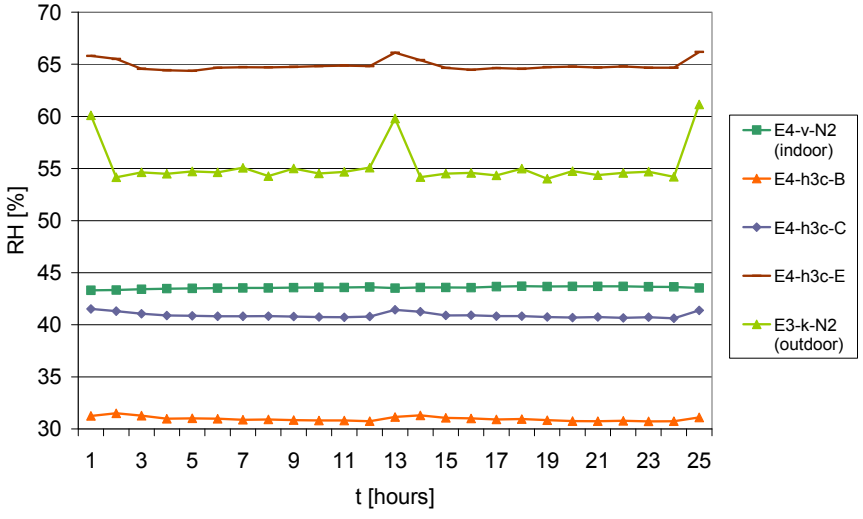

Figure G10. RH, Element 4. Steady-state with vapour barrier at Elements 1 and 3.

RH at different heights – Element 3

Only one figure is shown to illustrate the effect on RH of adding a vapour barrier to Elements 1 and 3. The temperature conditions were not changed from test M1 to test M2.

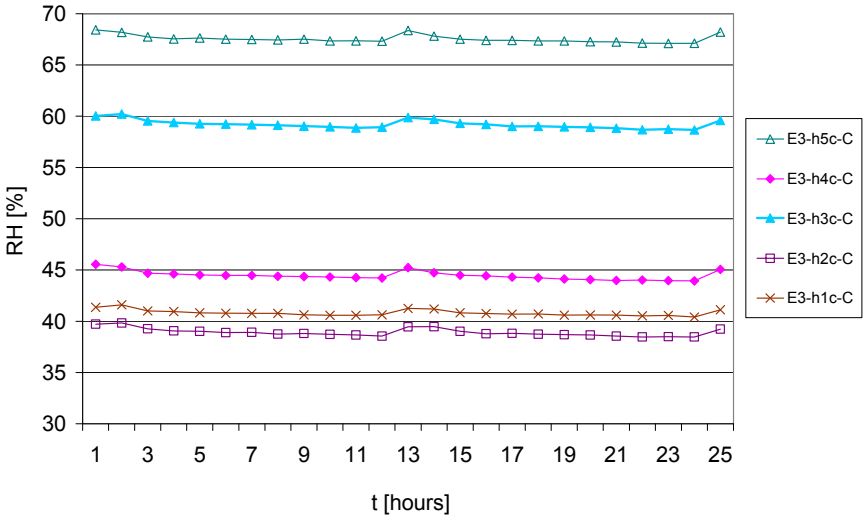

Figure G11. RH, Depth C. Element 3. Steady-state with vapour barrier.

Comparison of elements

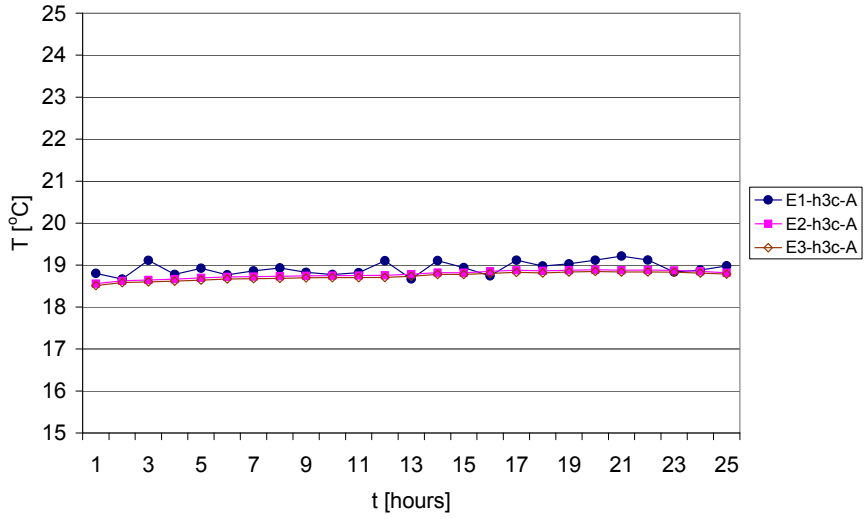

Figure G12. Temperature, Depth A. Elements 1, 2 and 3. Steady-state with vapour barrier at Elements 1 and 3.

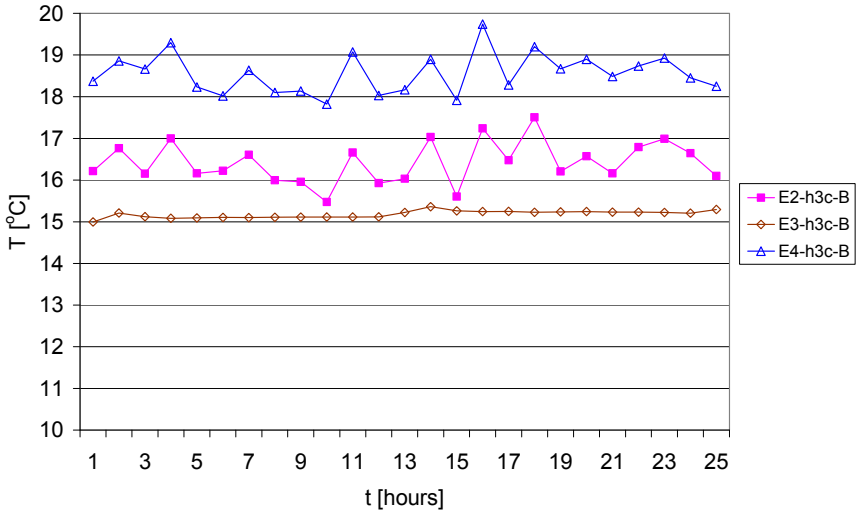

Figure G13. Temperature, Depth B. Elements 2, 3 and 4. Steady-state with vapour barrier at Elements 1 and 3.

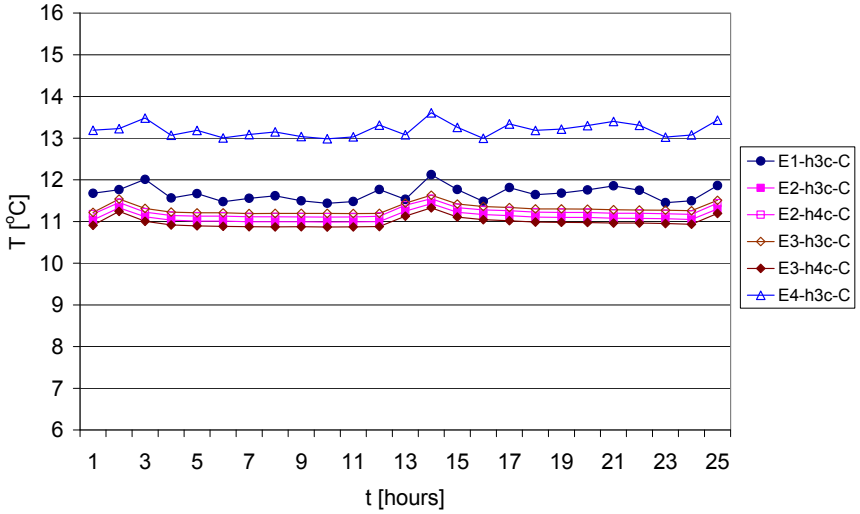

Figure G14. Temperature, Depth C. Elements 1, 2, 3 and 4. Steady-state with vapour barrier at Elements 1 and 3. Both 'h3c' and 'h4c' are included for Elements 2 and 3, cf. Figure G18.

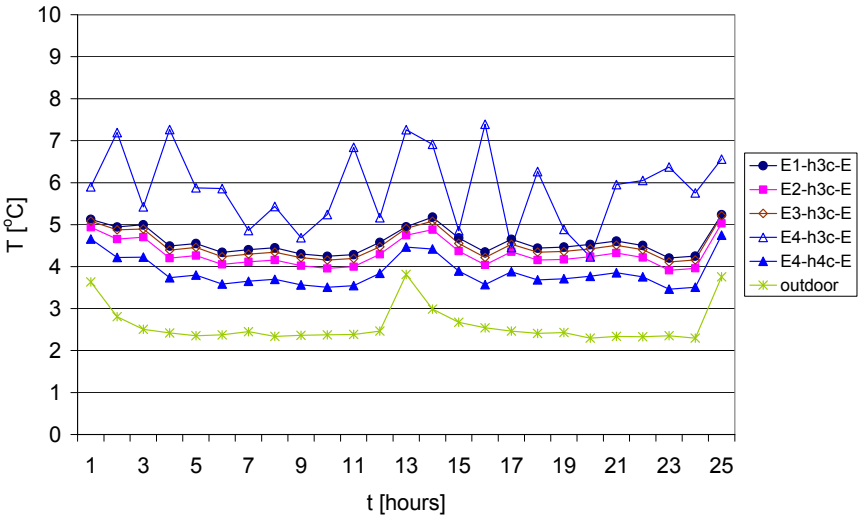

Figure G15. Temperature, Depth E. Elements 1, 2, 3 and 4, and outdoor. Steady-state with vapour barrier at Elements 1 and 3. Both 'h3c' and 'h4c' are included for Element 4, cf. Figure 13.

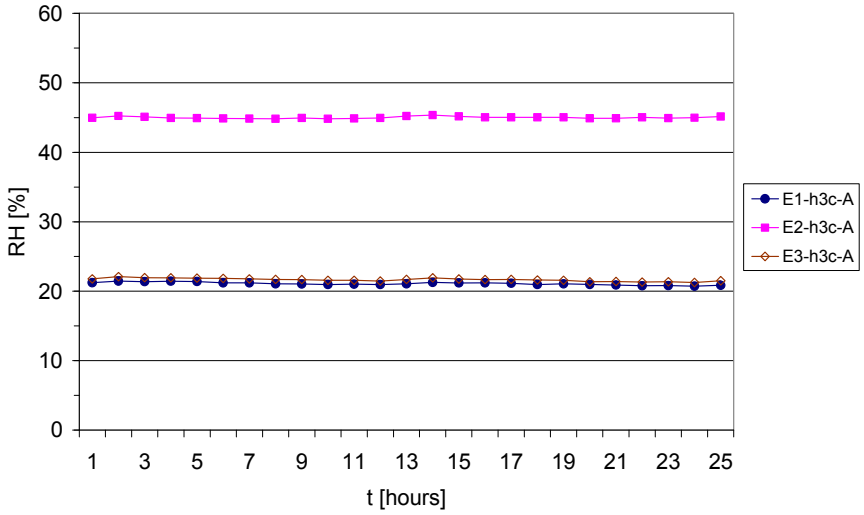

Figure G16. RH, Depth A. Elements 1, 2 and 3. Steady-state with vapour barrier at Elements 1 and 3.

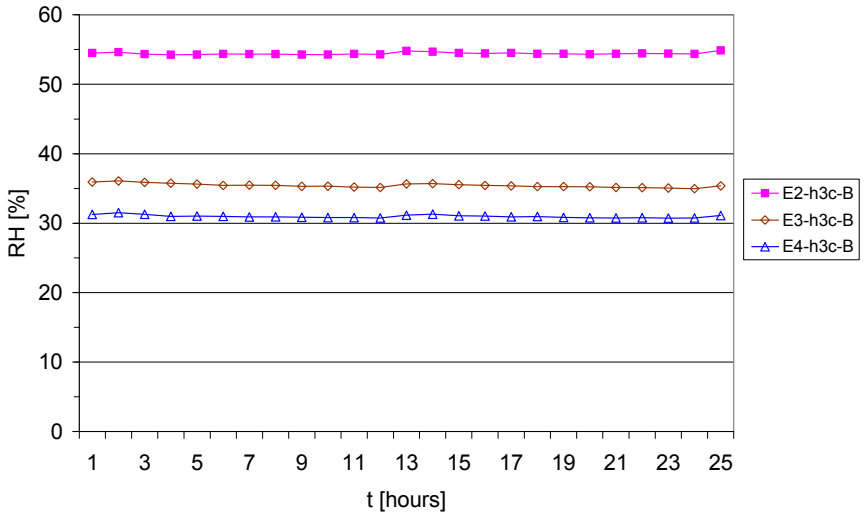

Figure G17. RH, Depth B. Elements 2, 3 and 4. Steady-state with vapour barrier at Elements 1 and 3.

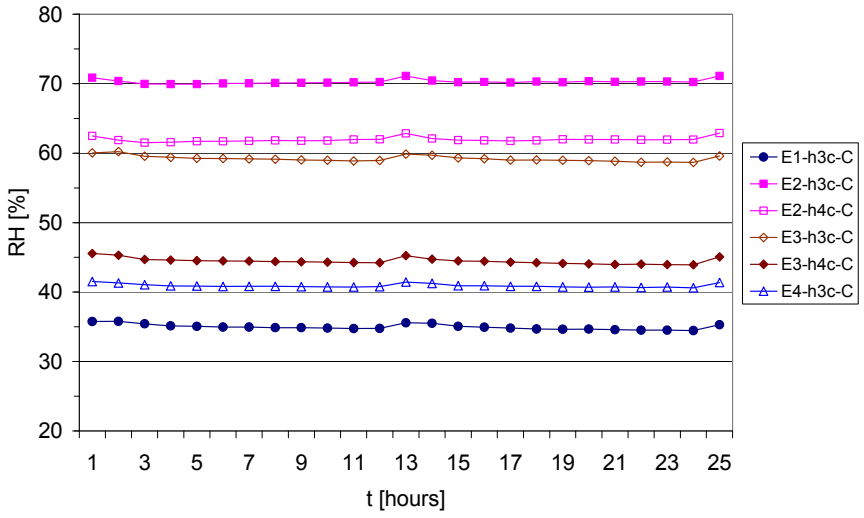

Figure G18. RH, Depth C. Elements 1, 2, 3 and 4. Steady-state with vapour barrier at Elements 1 and 3. 'h4c' are included for Elements 2 and 3. 'h3c' is not representative of RH in these elements.

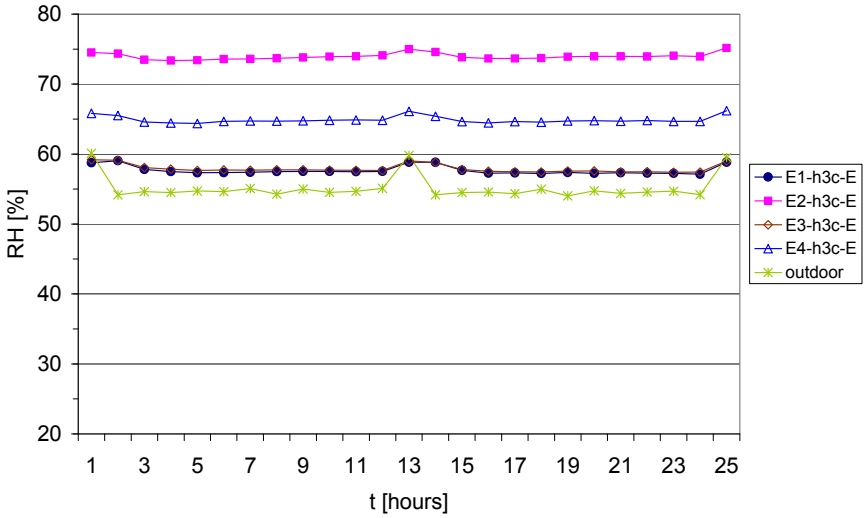

Figure G19. RH, Depth E. Elements 1, 2, 3 and 4, and outdoor. Steady-state with vapour barrier at Elements 1 and 3.

Appendix H. April without cladding (M3A)

This appendix contains figures showing how the temperature and RH distributed from the indoor side to the outdoor side in all four elements, in addition to the results of Element 1 shown in the part of the chapter 'Results and discussion' that presents results of test M3A. For Elements 1 and 2 also the vapour pressure is shown. Appendix H also contains some figures illustrating how the temperature and RH distributed from the top to the bottom of an element. Finally comparisons are made between the different elements at specific levels (heights), in addition to the figures in the section 'Comparison of elements' of the chapter 'Results and discussion'.

In all cases results are shown as a 24-hour cycle representing the specific test. All 24-hour cycles are shown from 9 AM to 9 AM with defrosting periods at noon and midnight, most notably seen in figures with RH results.

If not otherwise indicated, the results were based on sensors in height h3c, about halfway between the top and the bottom of the element. For the position of sensors refer to Appendix D.

In figures where the temperature and RH at the different depths from the indoor side to the outdoor side are shown for one specific element, e.g. Figure H4, 'h4c' replaced 'h3c' at Depth C in Elements 2 and 3, since the results showed that 'h3c' was not representative of the RH level. Also, h4c' replaced 'h3c' at Depth E in Element 4, where 'h3c' was not representative of the temperature.

Temperature, RH and vapour pressure from indoor to outdoor sides

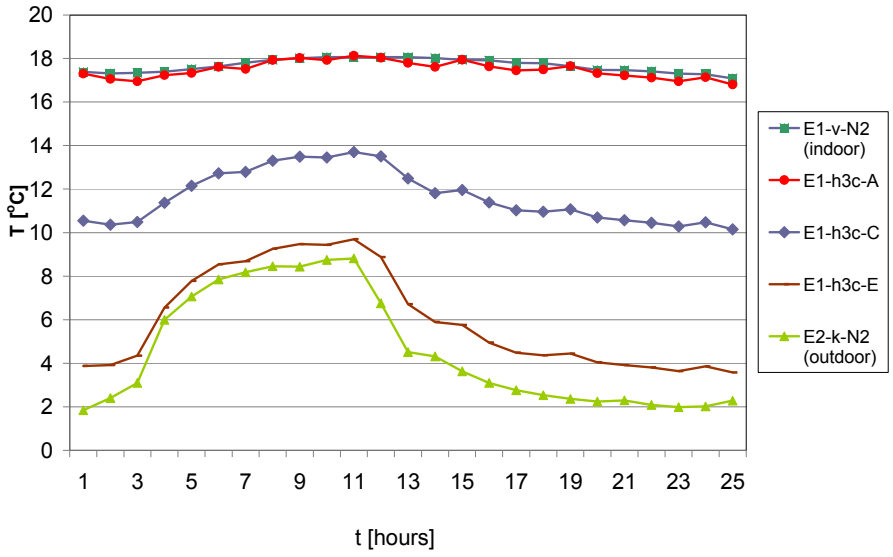

Figure H1. Temperature, Element 1. April without cladding. Temperature at the indoor side, behind the indoor gypsum cladding (A), in the centre of the thermal insulation (C), in the thermal insulation, at the wind barrier (E) and at the outdoor side. Example of 24-hour cycle starting at 9 AM. 'E2-k-N2' placed in front of Element 2 represents the temperature at the outdoor side, cf. 'Results and discussion', 'General remarks'.

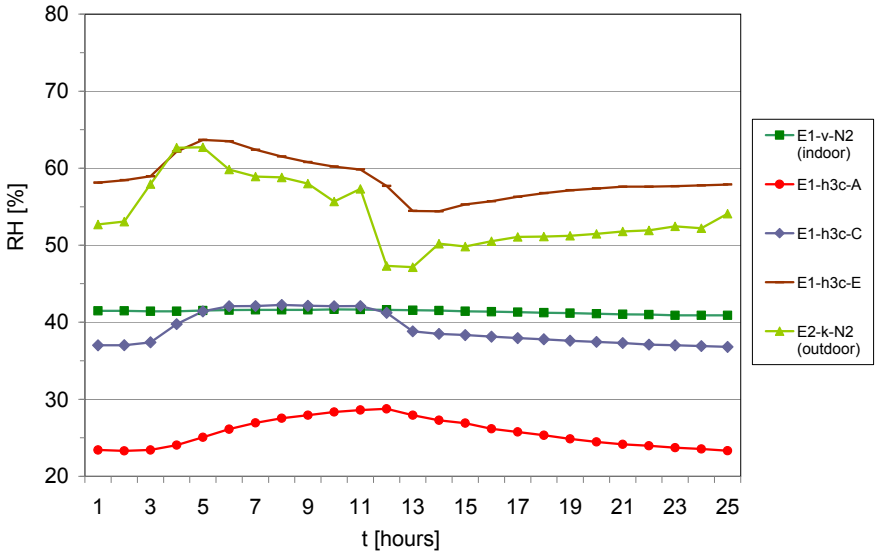

Figure H2. RH, Element 1. April without cladding.

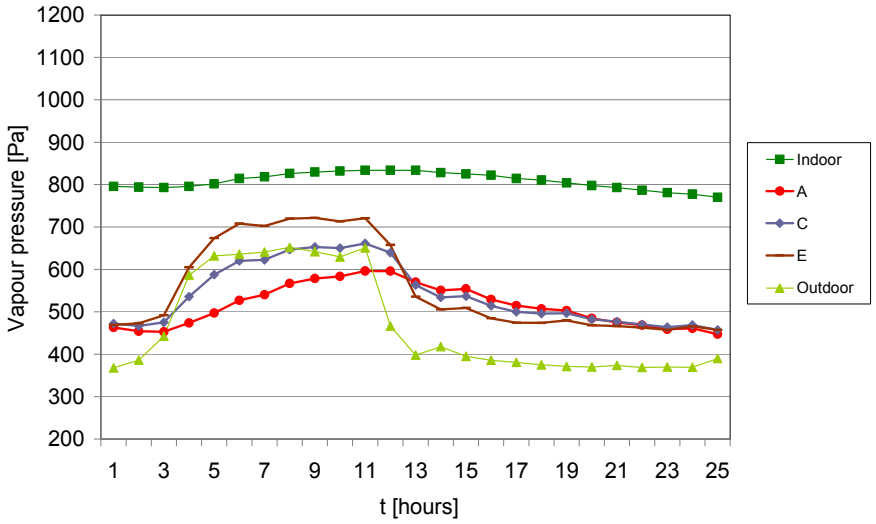

Figure H3. Vapour pressure, Element 1. April without cladding.

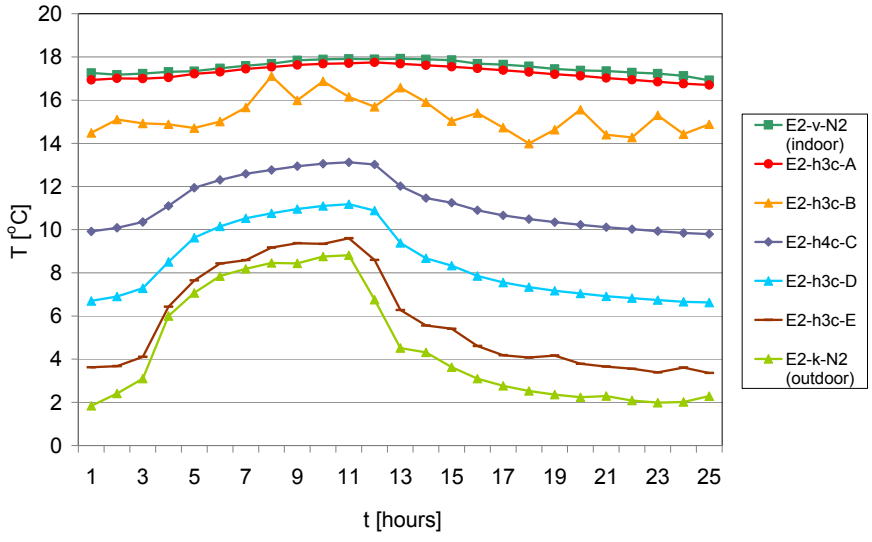

Figure H4. Temperature, Element 2. April without cladding. 'h4c' replaces 'h3c' at Depth C.

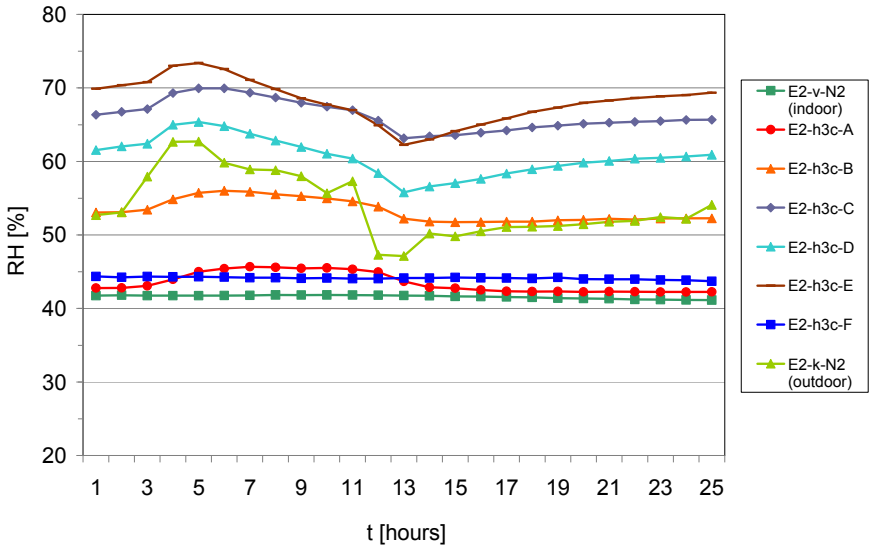

Figure H5. RH, Element 2. April without cladding. 'h4c' replaces 'h3c' at Depth C.

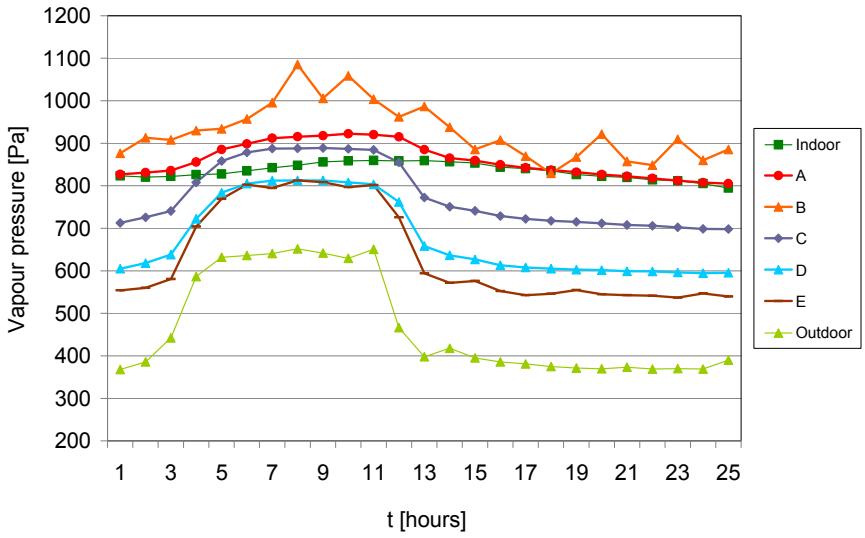

Figure H6. Vapour pressure, Element 2. April without cladding. 'h4c' replaces 'h3c' at Depth C.

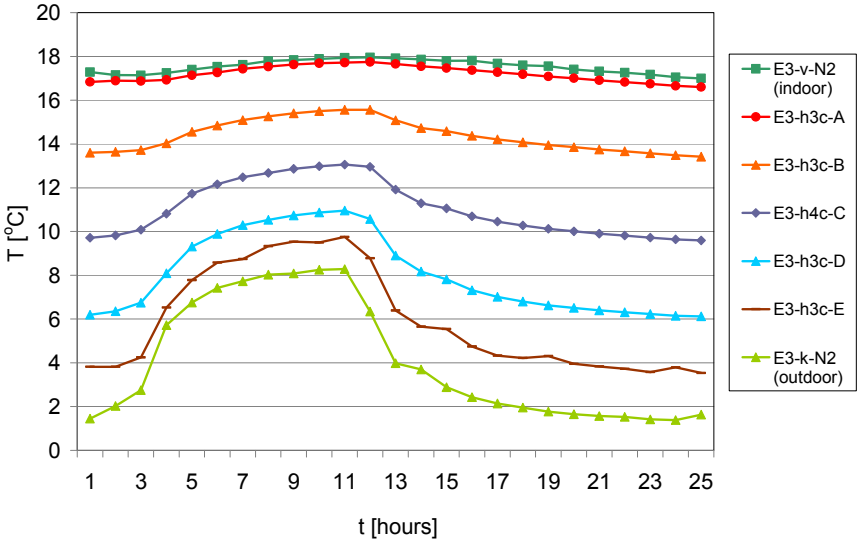

Figure H7. Temperature, Element 3. April without cladding. 'h4c' replaces 'h3c' at Depth C.

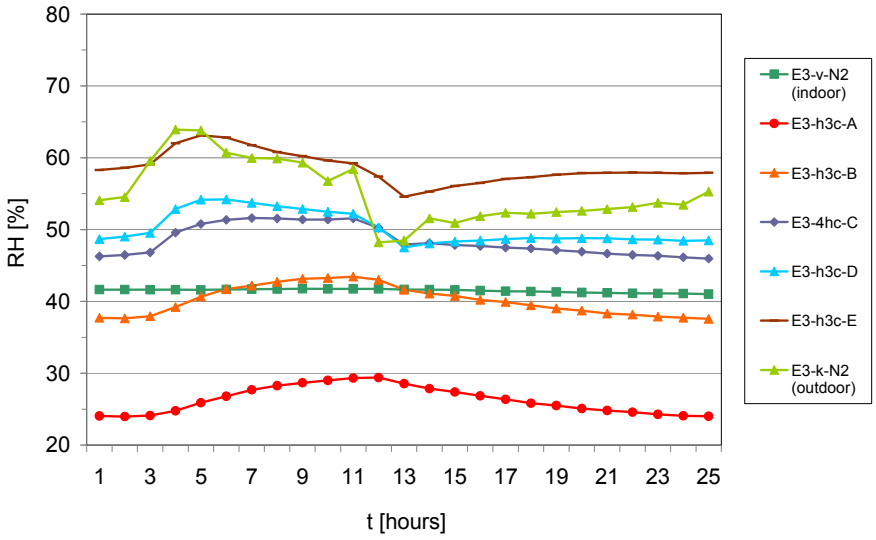

Figure H8. RH, Element 3. April without cladding. 'h4c' replaces 'h3c' at Depth C.

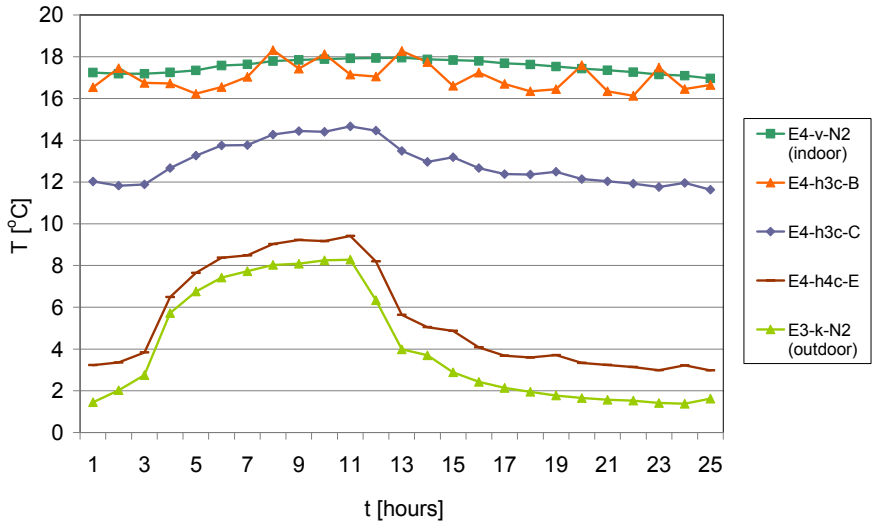

Figure H9. Temperature, Element 4. April without cladding. 'h4c' replaces 'h3c' at Depth E.

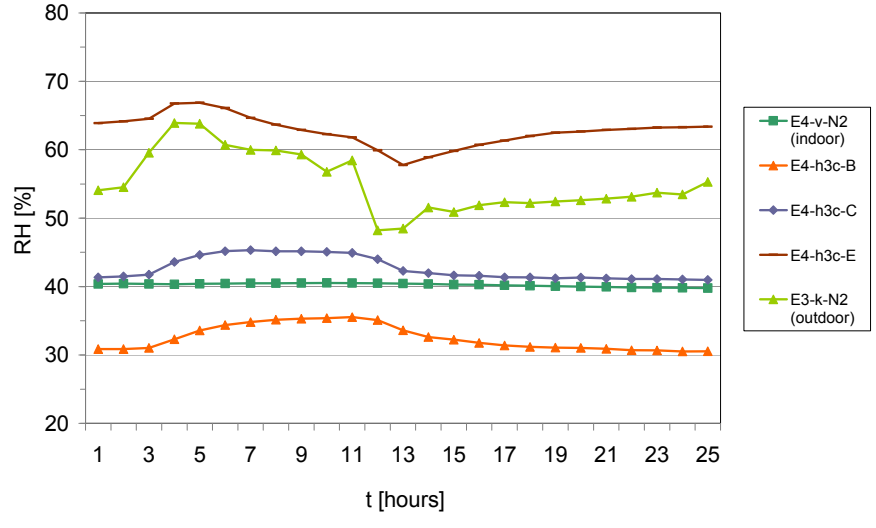

Figure H10. RH, Element 4. April without cladding.

Temperature and RH at different heights – Element 2

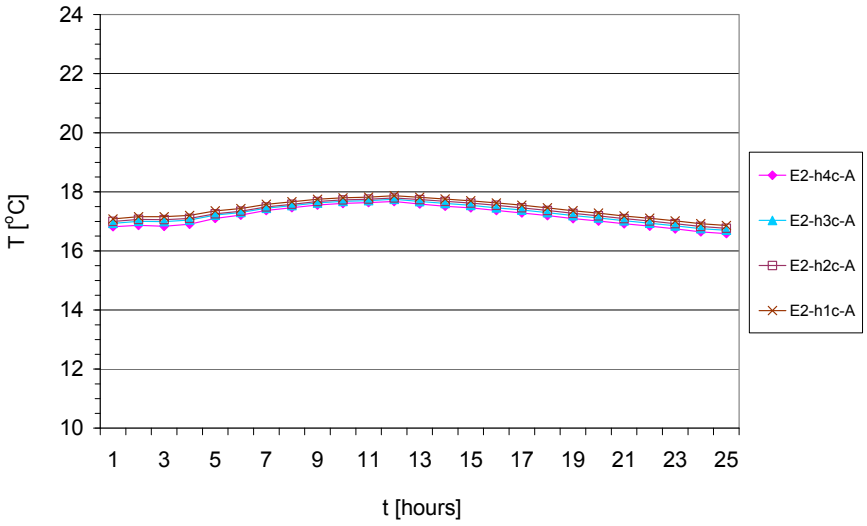

Figure H11. Temperature, Depth A. Element 2. April without cladding.

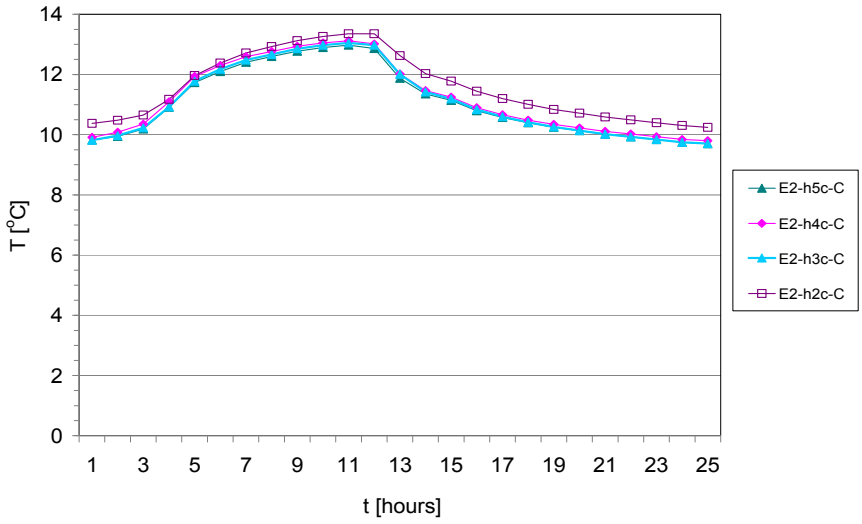

Figure H12. Temperature, Depth C. Element 2. April without cladding.

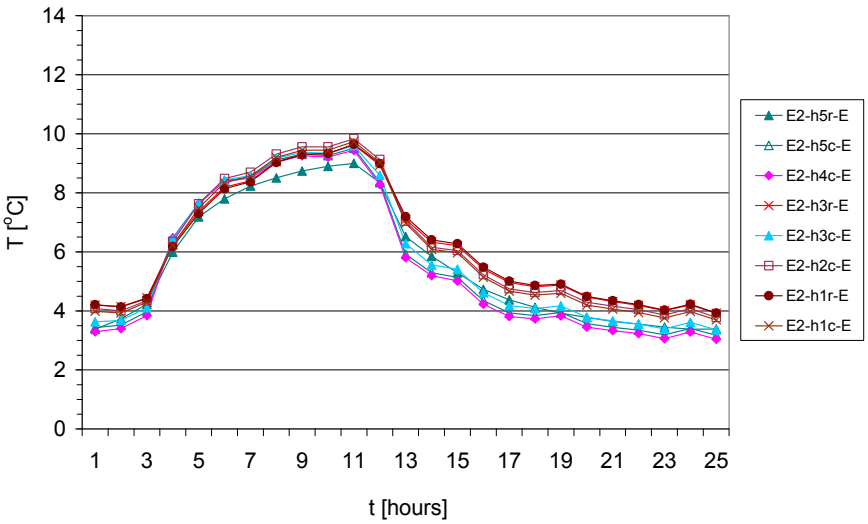

Figure H13. Temperature, Depth E. Element 2. April without cladding.

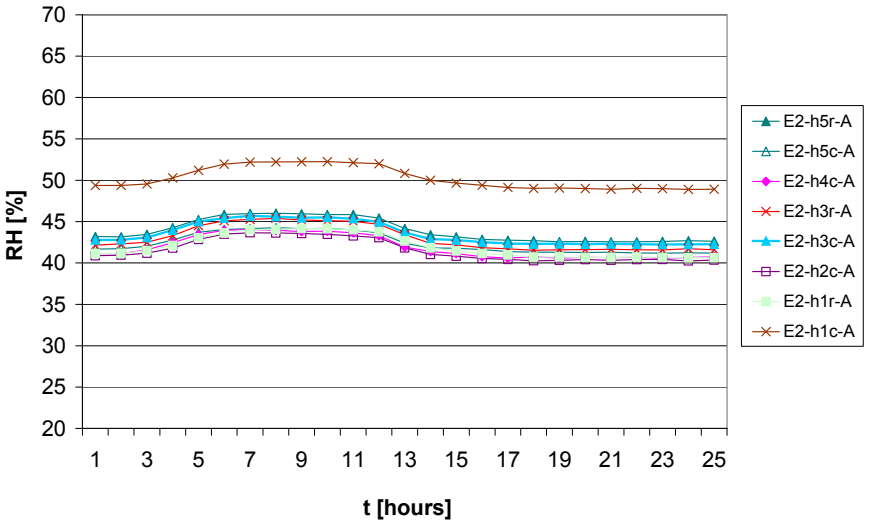

Figure H14. RH, Depth A. Element 2. April without cladding.

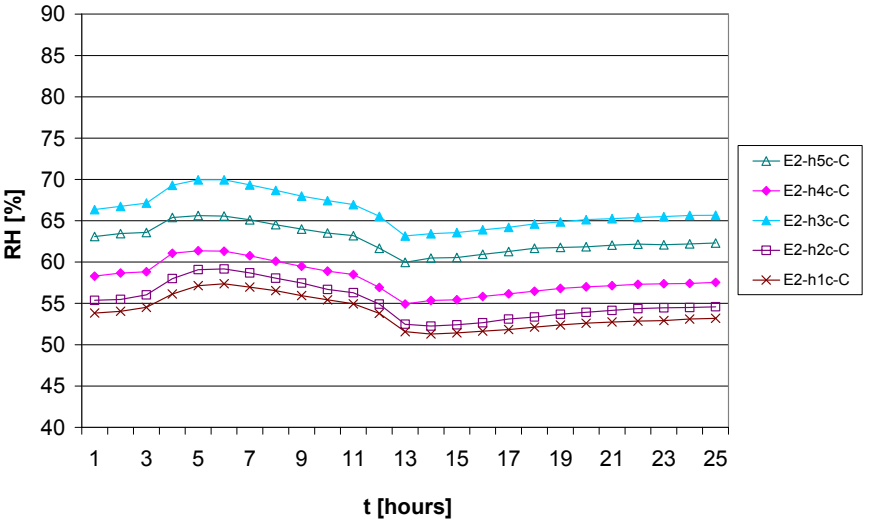

Figure H15. RH, Depth C. Element 2. April without cladding.

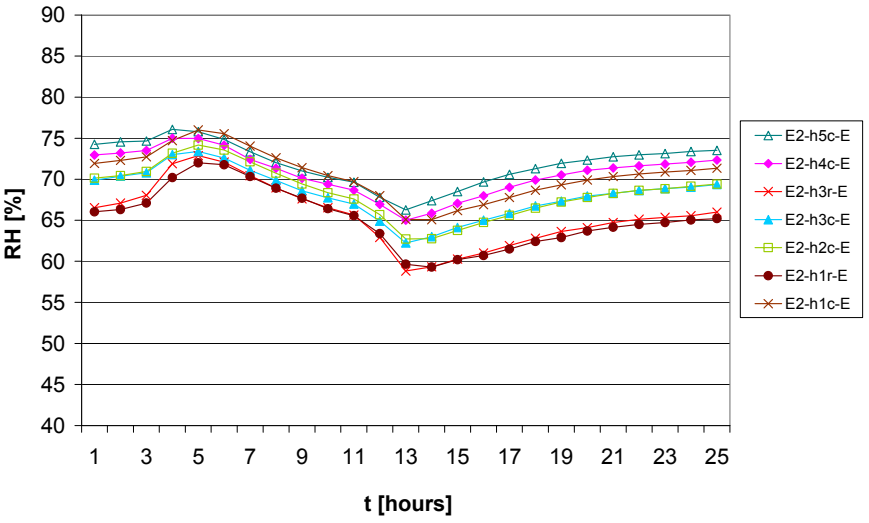

Figure H16. RH, Depth E. Element 2. April without cladding.

Temperature at different heights – Element 4

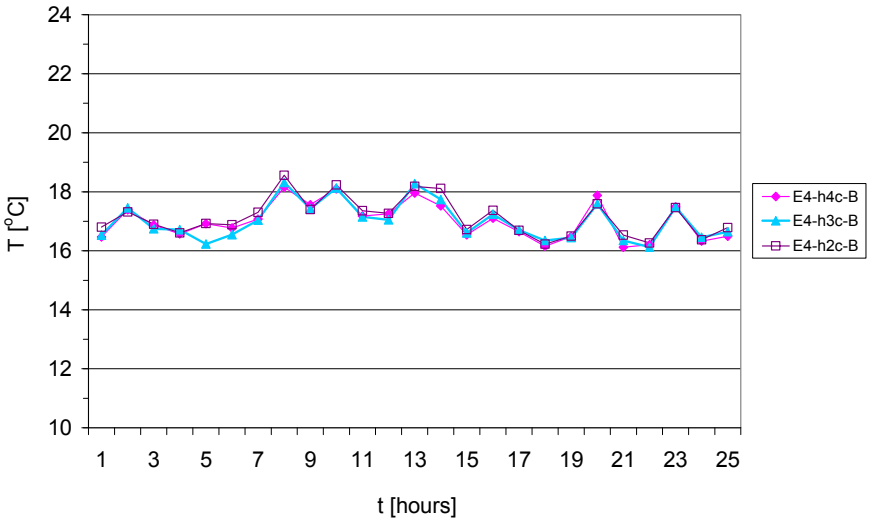

Figure H17. Temperature, Depth B. Element 4. April without cladding.

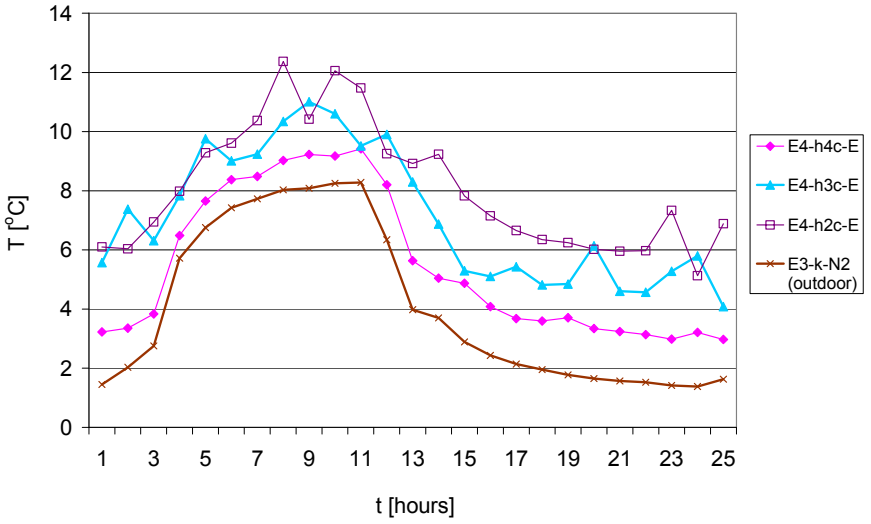

Figure H18. Temperature, Depth E. Element 4. April without cladding.

Comparison of elements

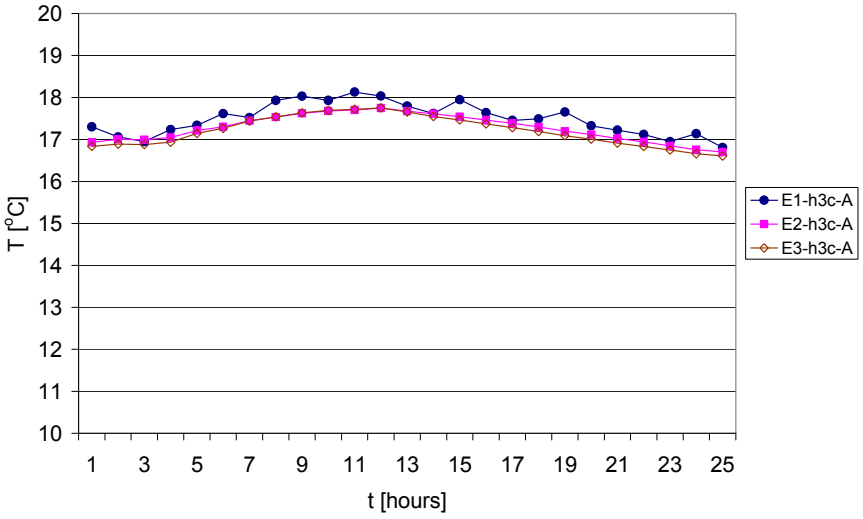

Figure H19. Temperature, Depth A. April without cladding. Elements 1, 2 and 3.

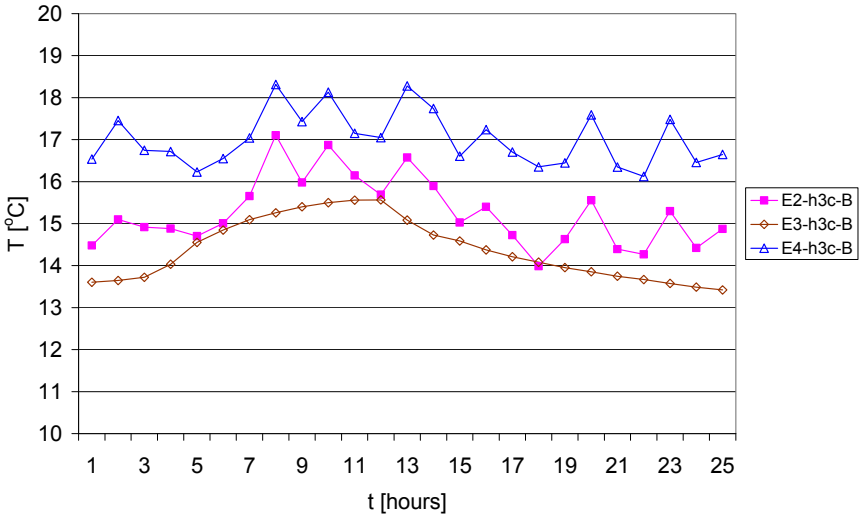

Figure H20. Temperature, Depth B. April without cladding. Elements 2, 3 and 4.

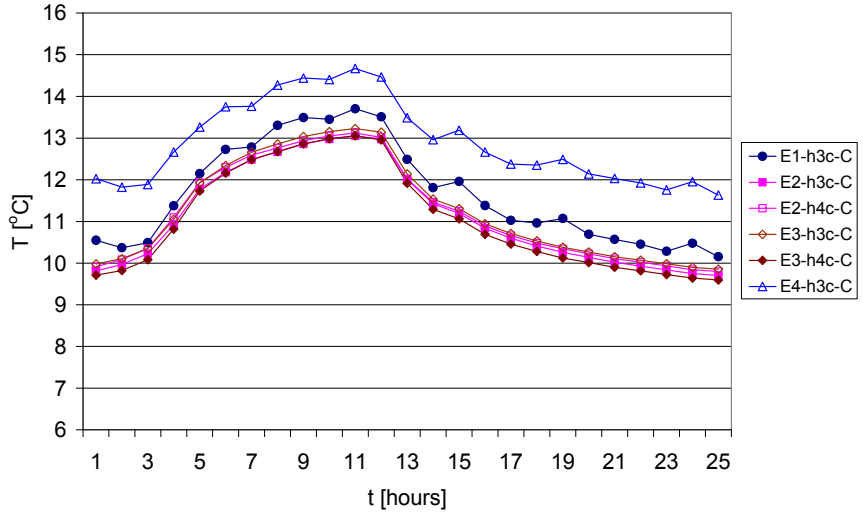

Figure H21. Temperature, Depth C. April without cladding. Elements 1, 2, 3 and 4. Both 'h3c' and 'h4c' are included for Elements 2 and 3, cf. Figure H22.

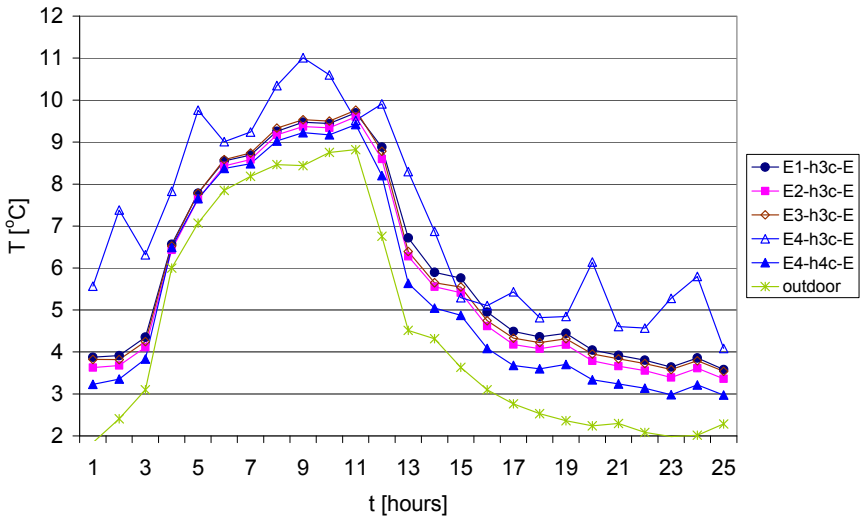

Figure H22. Temperature, Depth E. April without cladding. Elements 1, 2, 3 and 4, and outdoor. Both 'h3c' and 'h4c' are included for Element 4, cf. Figure 13.

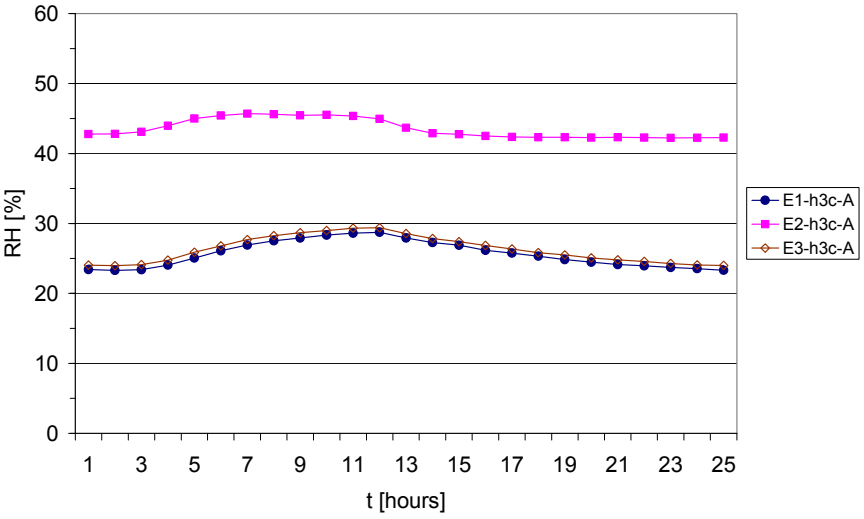

Figure H23. RH, Depth A. April without cladding. Elements 1, 2 and 3.

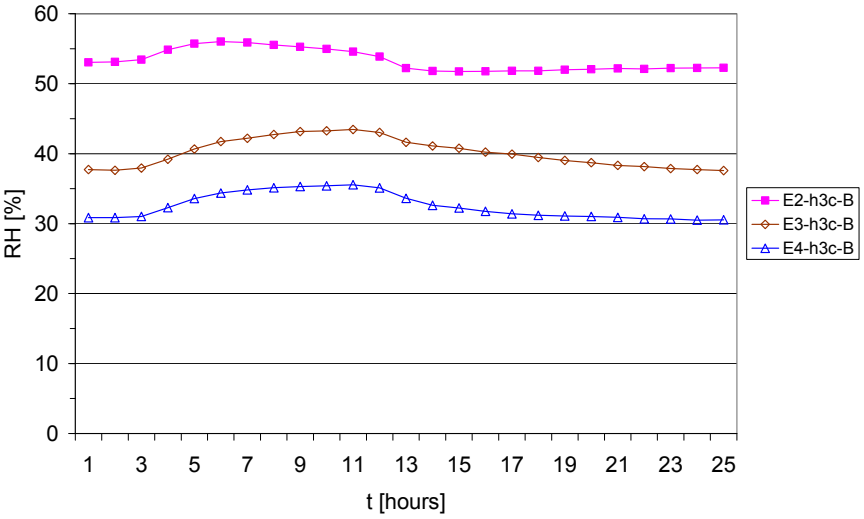

Figure H24. RH, Depth B. April without cladding. Elements 2, 3 and 4.

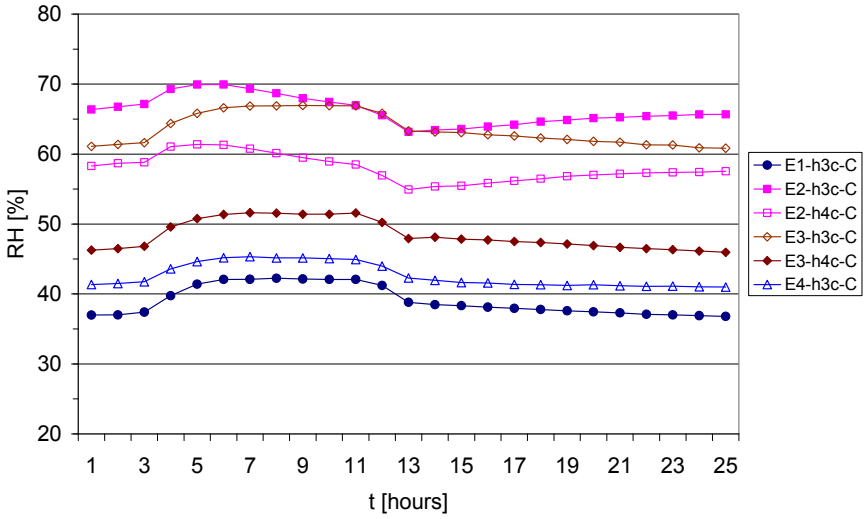

Figure H25. RH, Depth C. April without cladding. Elements 1, 2, 3 and 4. 'h4c' is included for Elements 2 and 3. 'h3c' is not representative of RH in these elements.

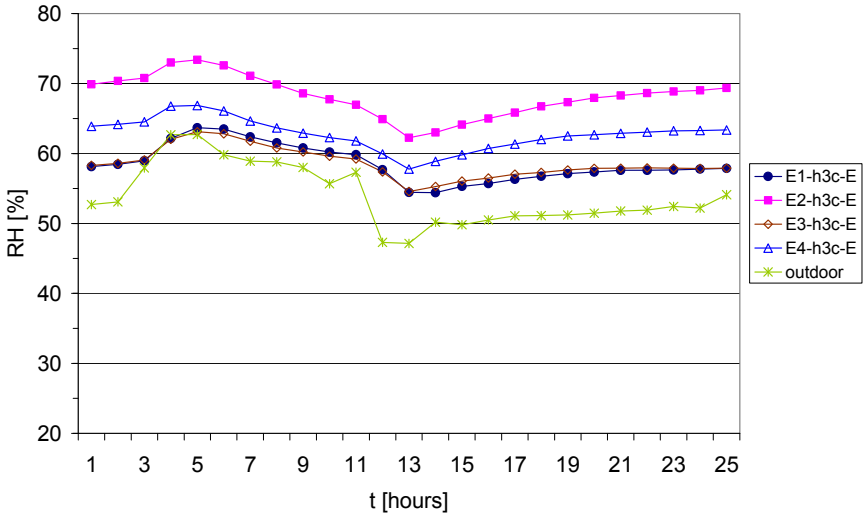

Figure H26. RH, Depth E. April without cladding. Elements 1, 2, 3 and 4, and outdoor.

Appendix I. September without cladding (M3S)

This appendix contains figures showing how the temperature and RH distributed from the indoor side to the outdoor side in all four elements, in addition to the results from Element 1 shown in the part of the chapter 'Results and discussion' that presents results of test M3S. For Elements 1 and 2 also the vapour pressure is shown. 'h4c' replaced 'h3c' at Depth C in Elements 2 and 3 (e.g. Figures I4 – I8), since the results showed that 'h3c' was not representative of the RH level. For the position of sensors refer to Appendix D. See also introduction to Appendix H.

Temperature, RH and vapour pressure from indoor to outdoor sides

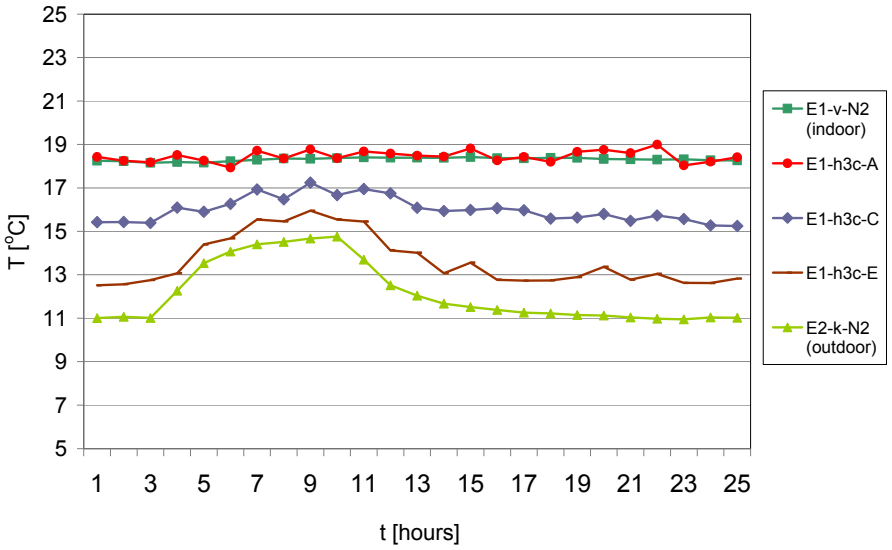

Figure I1. Temperature, Element 1. September without cladding. Temperature at the indoor side, behind the indoor gypsum cladding (A), in the centre of the thermal insulation (C), in the thermal insulation, at the wind barrier (E), and at the outdoor side. Example of 24-hour cycle starting at 9 AM. 'E2-k-N2' placed in front of Element 2 represents the temperature at the outdoor side, cf. 'Results and discussion', 'General remarks'.

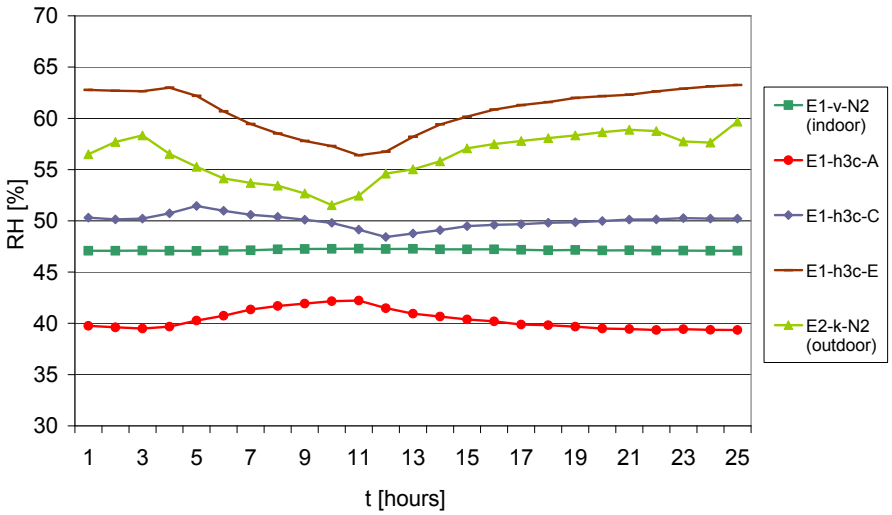

Figure I2. RH, Element 1. September without cladding.

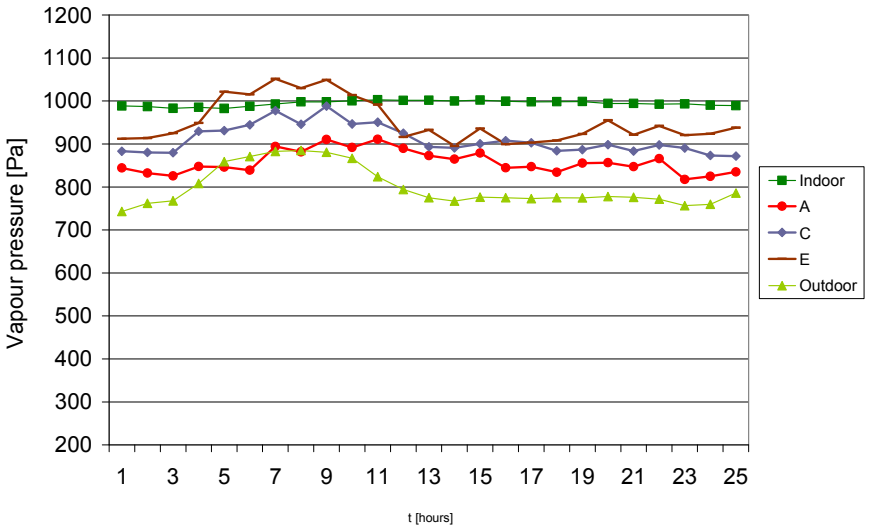

Figure I3. Vapour pressure, Element 1. September without cladding.

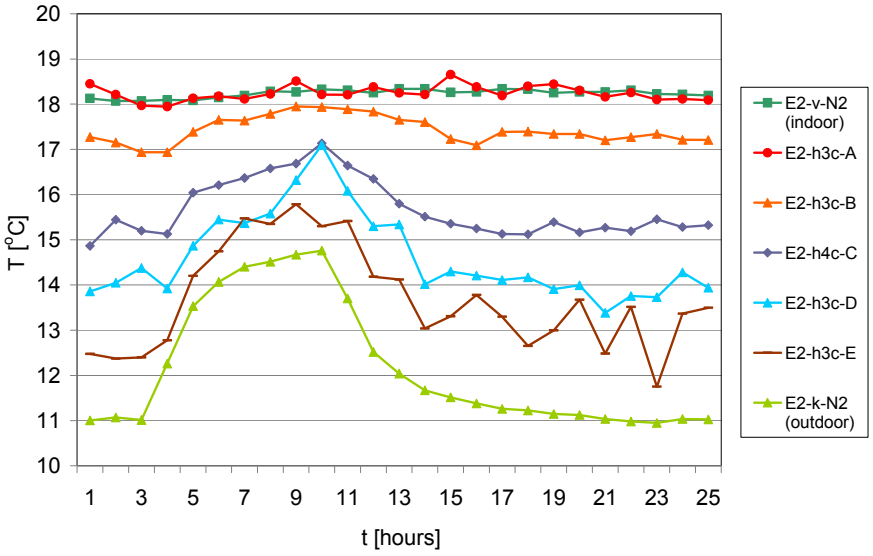

Figure I4. Temperature, Element 2. September without cladding. 'h4c' replaces 'h3c' at Depth C.

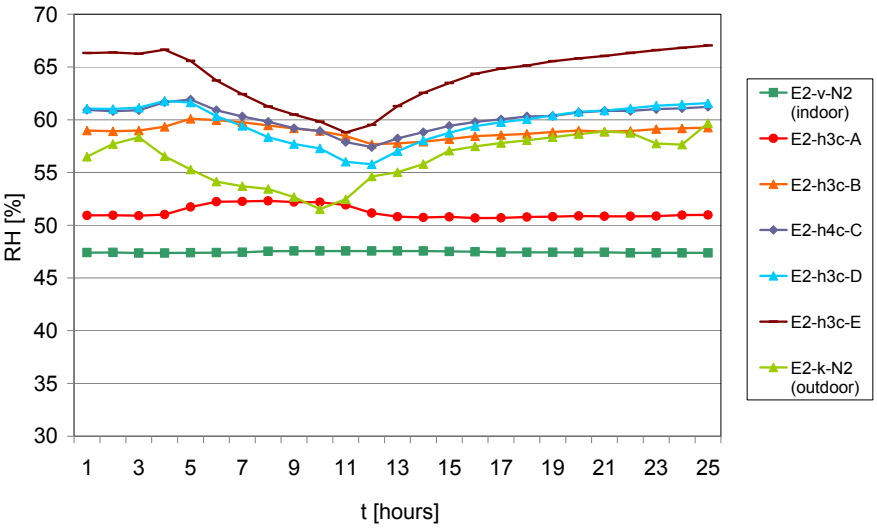

Figure I5. RH, Element 2. September without cladding. 'h4c' replaces 'h3c' at Depth C.

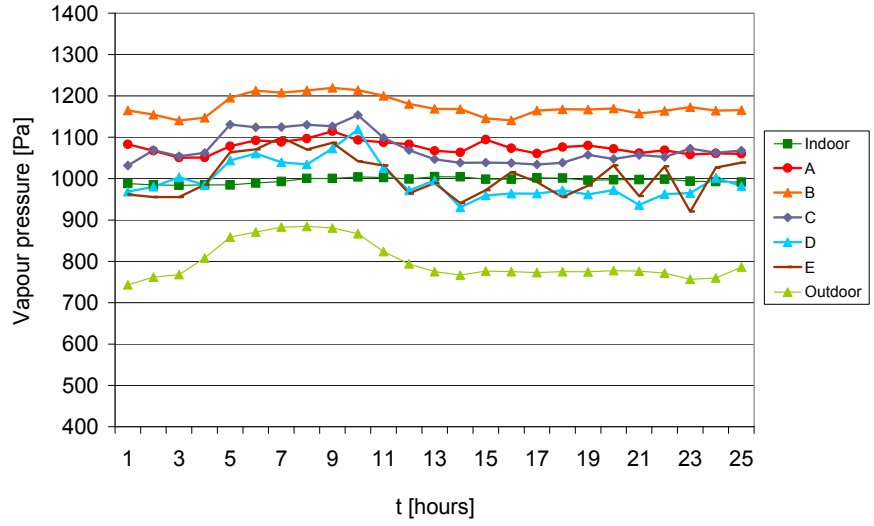

Figure I6. Vapour pressure, Element 2. September without cladding. 'h4c' replaces 'h3c' at Depth C.

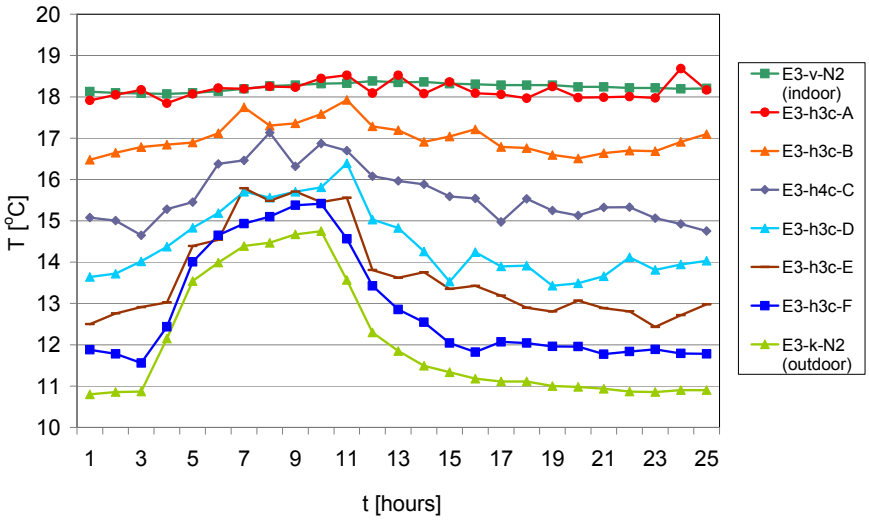

Figure I7. Temperature, Element 3. September without cladding. 'h4c' replaces 'h3c' at Depth C.

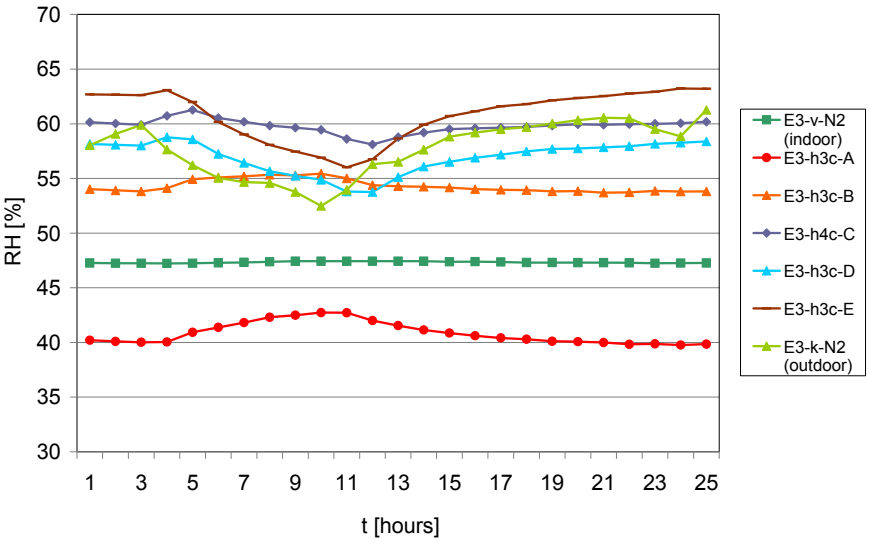

Figure I8. RH, Element 3. September without cladding.'h4c' replaces 'h3c' at Depth C.

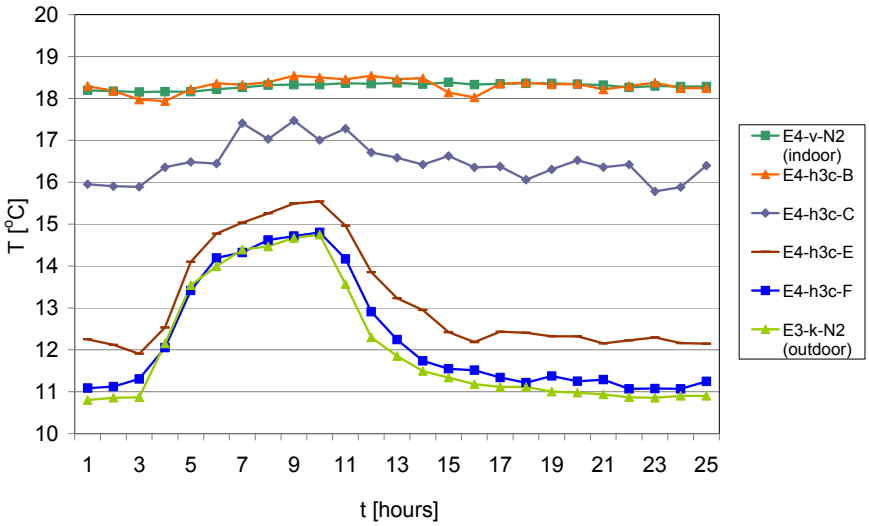

Figure I9. Temperature, Element 4. September without cladding.

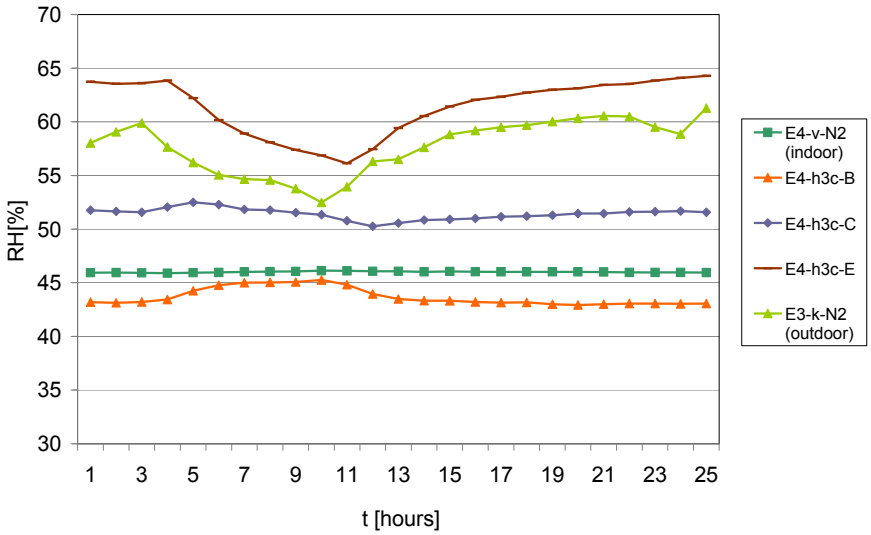

Figure I10. RH, Element 4. September without cladding.

Temperature at different heights – Element 2

The elements had not reached steady-state before the September cycle was introduced. Therefore, no RH or vapour pressure profiles are shown.

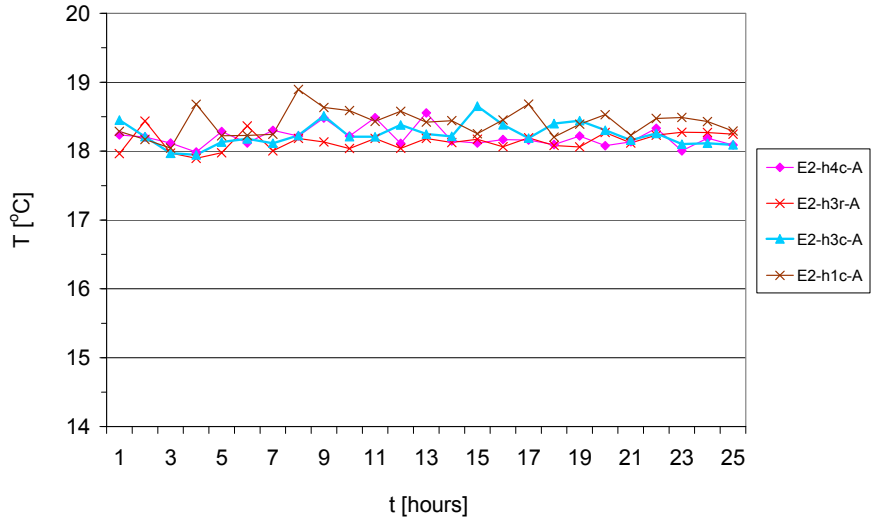

Figure I11. Temperature, Depth A. Element 2. September without cladding.

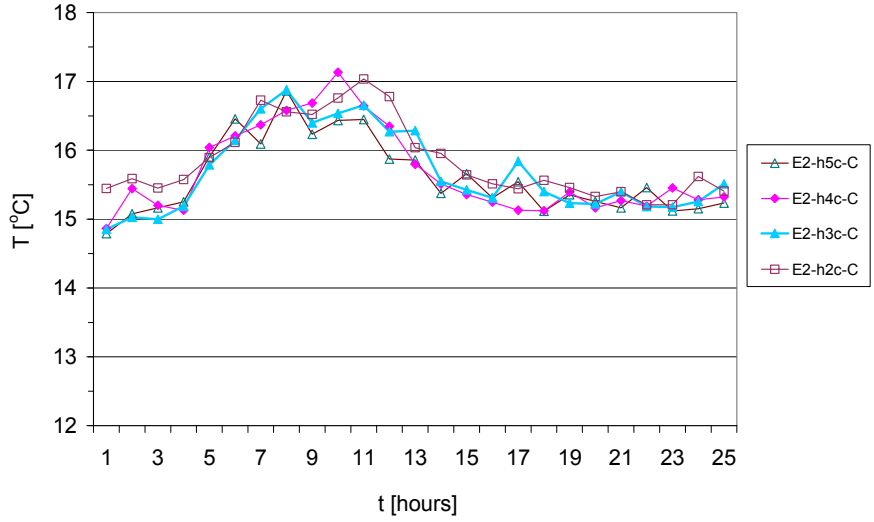

Figure I12. Temperature, Depth C. Element 2. September without cladding.

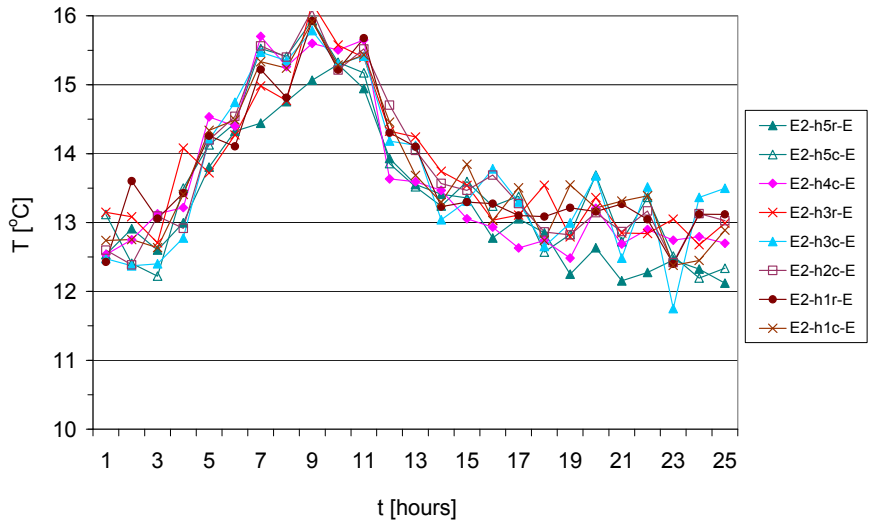

Figure I13. Temperature, Depth E. Element 2. September without cladding.

Comparison of elements

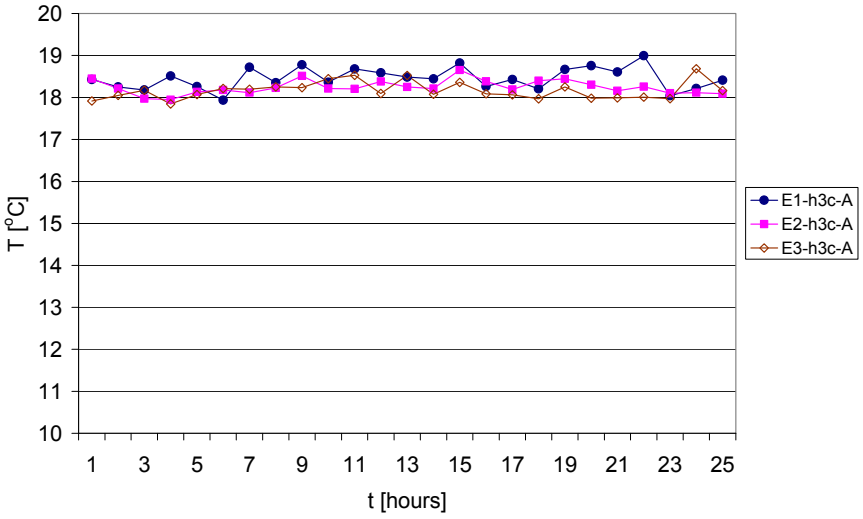

Figure I14. Temperature, Depth A. September without cladding. Elements 1, 2 and 3.

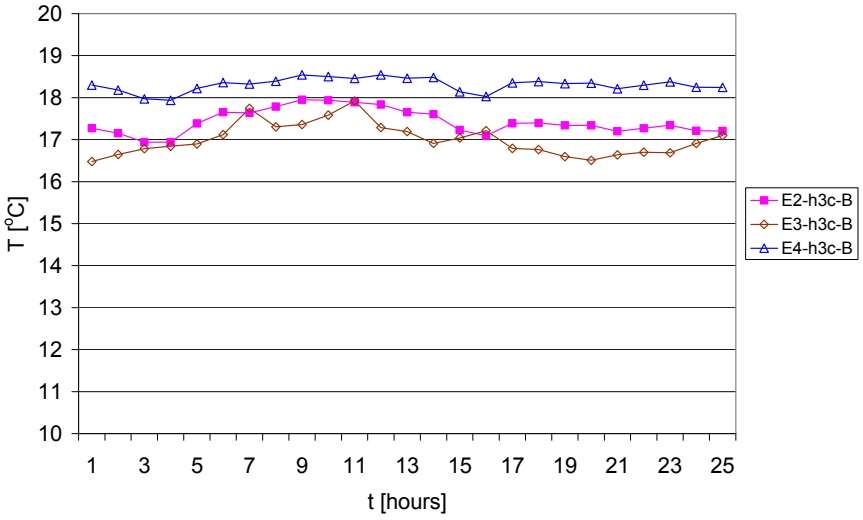

Figure I15. Temperature, Depth B. September without cladding. Elements 2, 3 and 4.

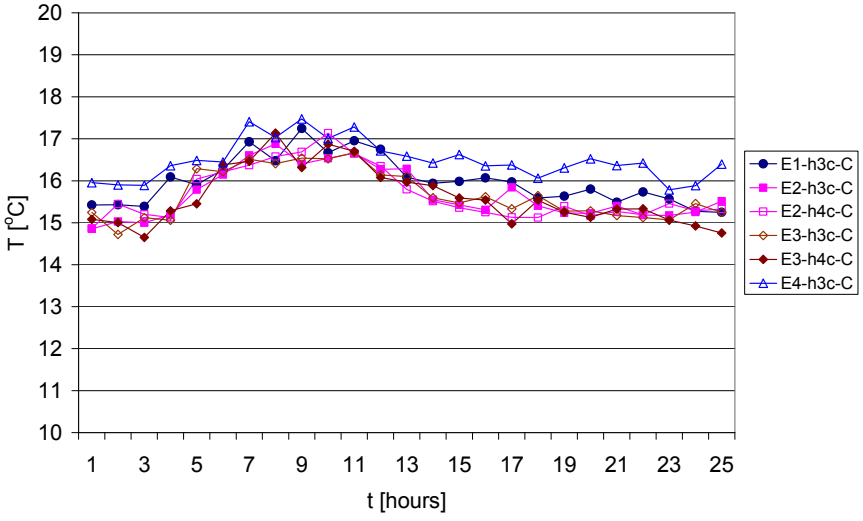

Figure I16. Temperature, Depth C. September without cladding. Elements 1, 2, 3 and 4. Both 'h3c' and 'h4c' are included for Elements 2 and 3, cf. Figure I21.

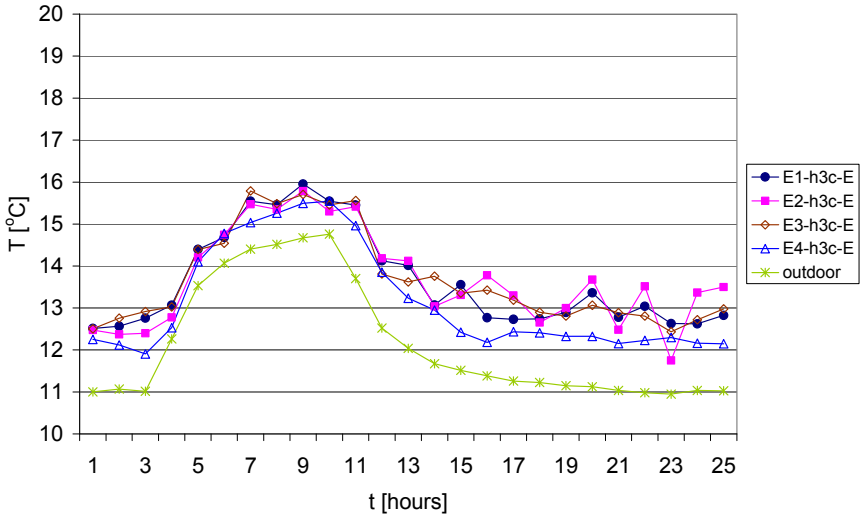

Figure I17. Temperature, Depth E. September without cladding. Elements 1, 2, 3 and 4, and outdoor.

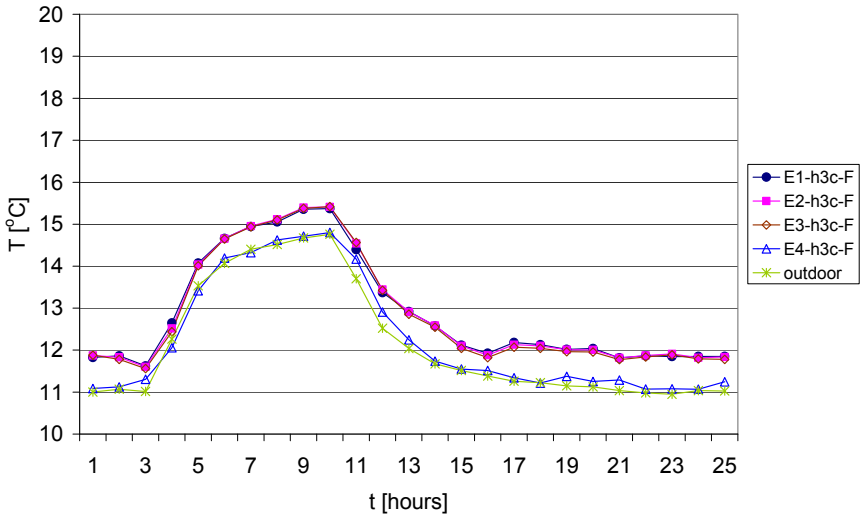

Figure I18. Temperature, Depth F. September without cladding. Elements 1, 2, 3 and 4, and outdoor.

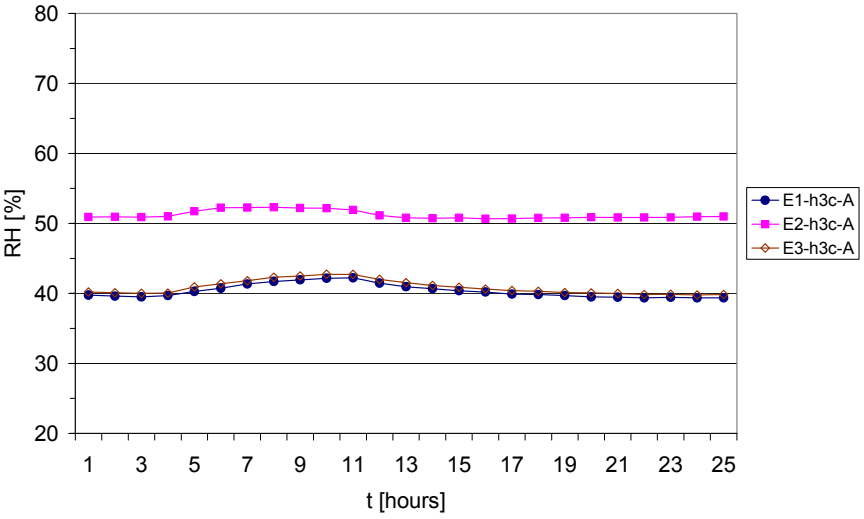

Figure I19. RH, Depth A. September without cladding. Elements 1, 2 and 3.

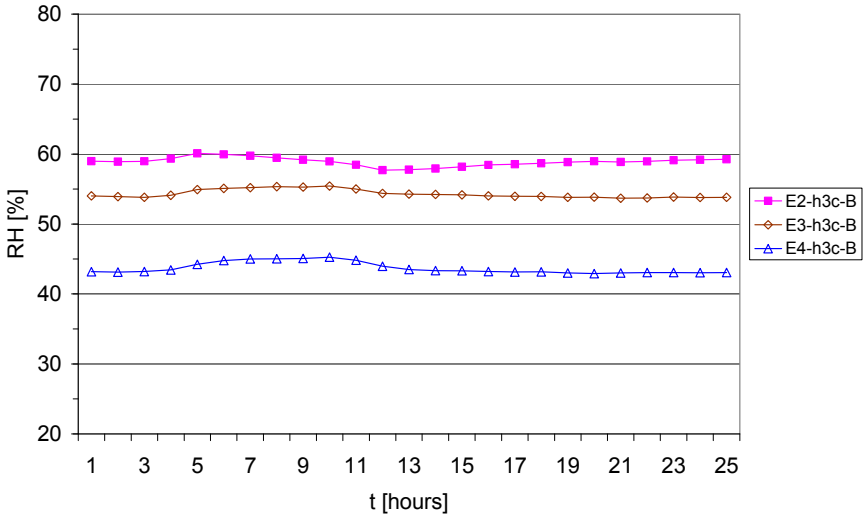

Figure I20. RH, Depth B. September without cladding. Elements 2, 3 and 4.

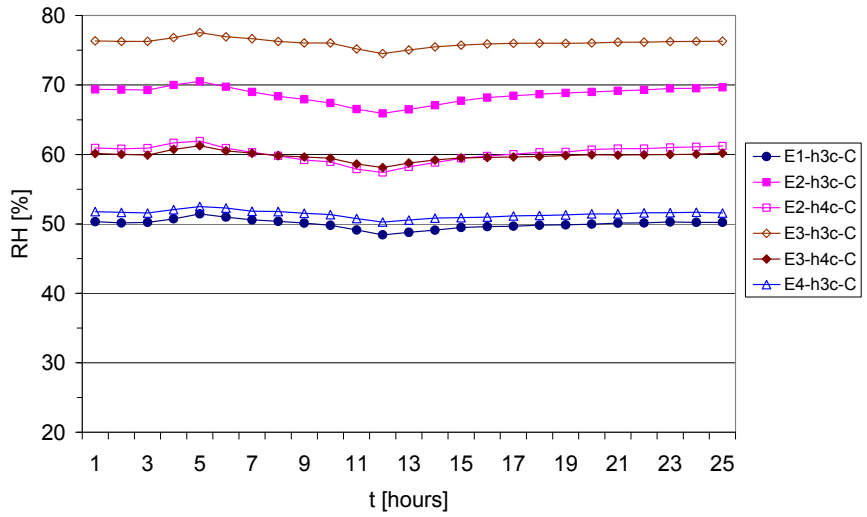

Figure I21. RH, Depth C. September without cladding. Elements 1, 2, 3 and 4. 'h4c' is included for Elements 2 and 3. 'h3c' is not representative of RH in these elements.

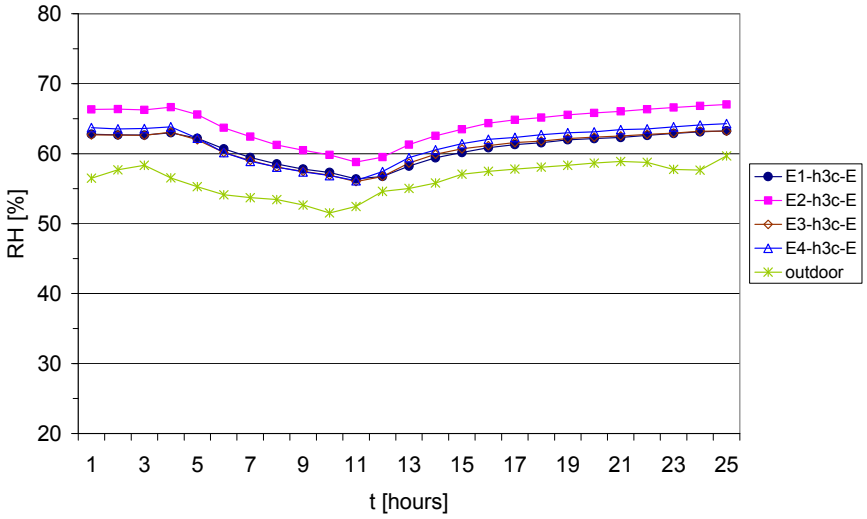

Figure I22. RH, Depth E. September without cladding. Elements 1, 2, 3 and 4, and outdoor.

Appendix J. April with cladding (M4A)

This appendix contains figures showing how the temperature and RH distributed from the indoor side to the outdoor side in all four elements, in addition to the results from Element 1 shown in the part of the chapter 'Results and discussion' that presents results of test M4A. For Elements 1 and 2 also the vapour pressure is shown. 'h4c' replaced 'h3c' at Depth C in Elements 2 and 3 (e.g. Figures J4 – J8), since the results showed that 'h3c' was not representative of the RH level. For the position of sensors refer to Appendix D. See also introduction to Appendix H.

Temperature, RH and vapour pressure from indoor to outdoor sides

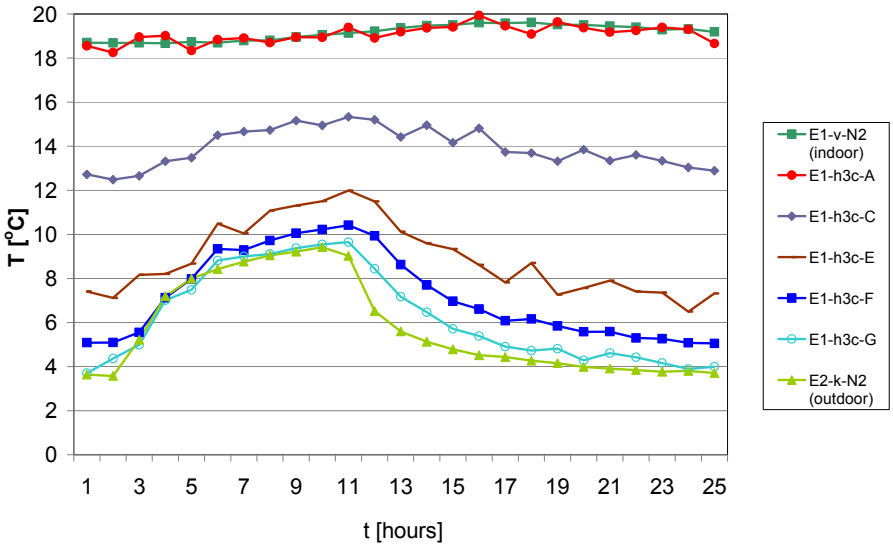

Figure J1. Temperature, Element 1. April with cladding. Temperature at the indoor side, behind the indoor gypsum cladding (A), in the centre of the thermal insulation (C), in the thermal insulation, at the wind barrier (E), in the cavity at the wind barrier (F), in the cavity, at the cladding (G), and at the outdoor side. Example of 24-hour cycle starting at 9 AM. 'E2-k-N2' placed in front of Element 2 represents the temperature at the outdoor side, cf. 'Results and discussion', 'General remarks'.

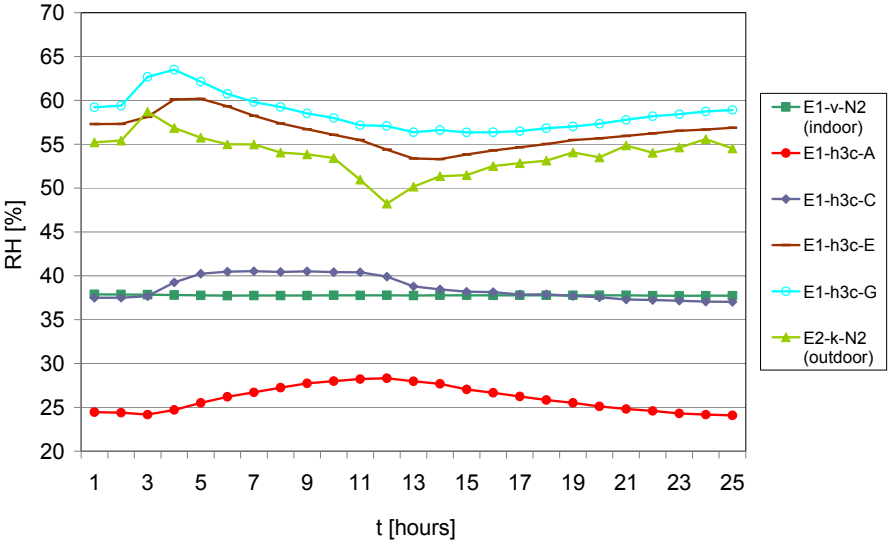

Figure J2. RH, Element 1. April with cladding.

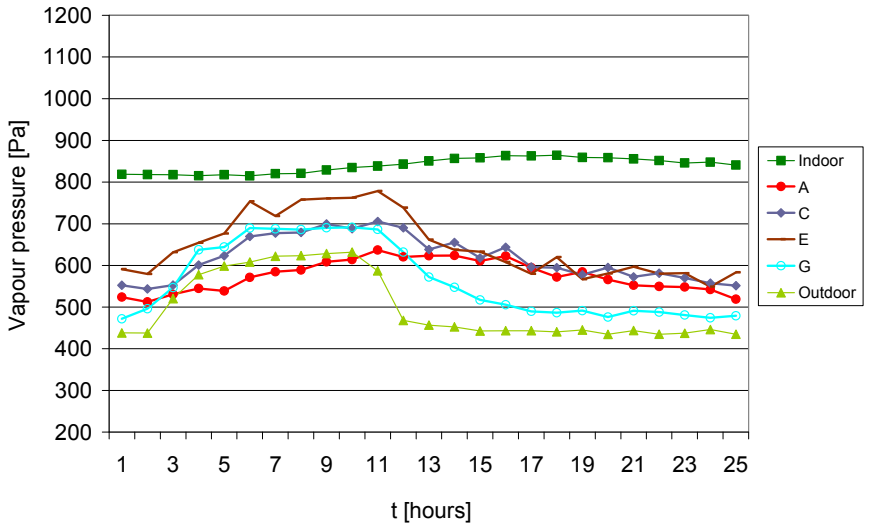

Figure J3. Vapour pressure, Element 1. April with cladding.

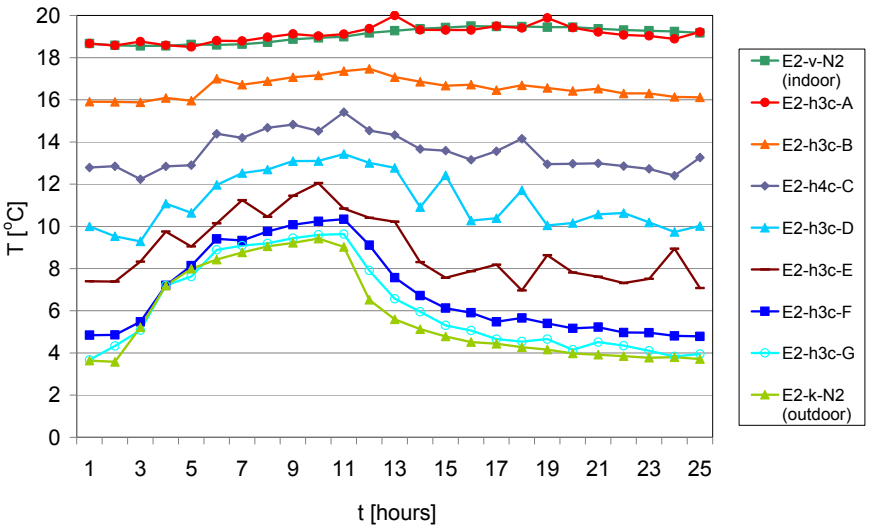

Figure J4. Temperature, Element 2. April with cladding. 'h4c' replaces 'h3c' at Depth C.

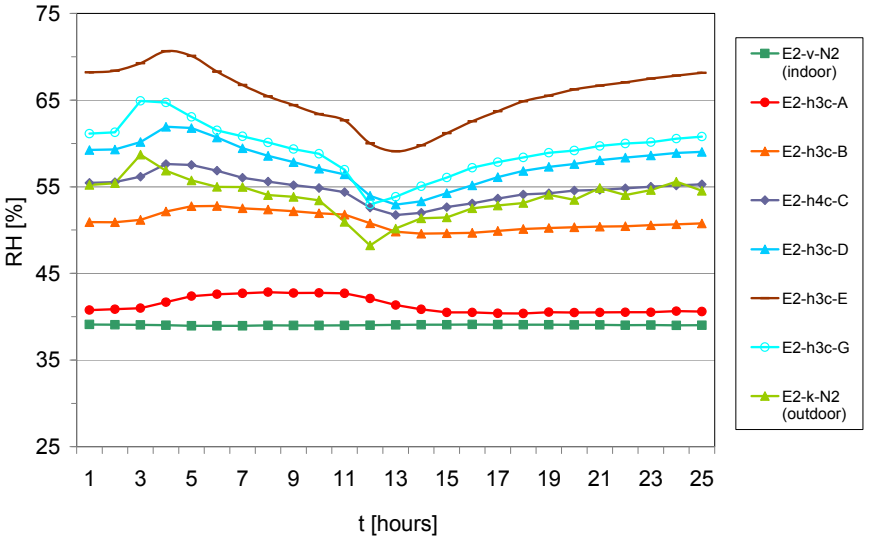

Figure J5. RH, Element 2. April with cladding. 'h4c' replaces 'h3c' in Depth C.

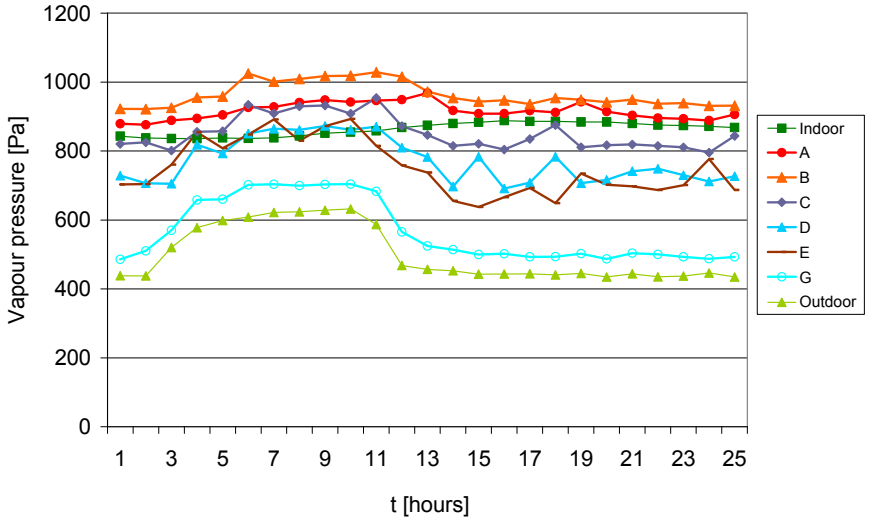

Figure J6. Vapour pressure, Element 2. April with cladding. 'h4c' replaces 'h3c' at Depth C.

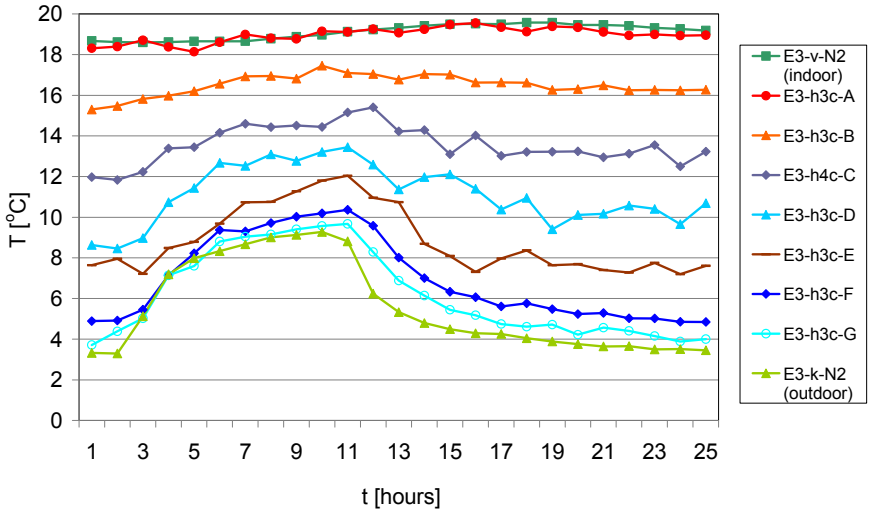

Figure J7. Temperature, Element 3. April with cladding. 'h4c' replaces 'h3c' at Depth C.

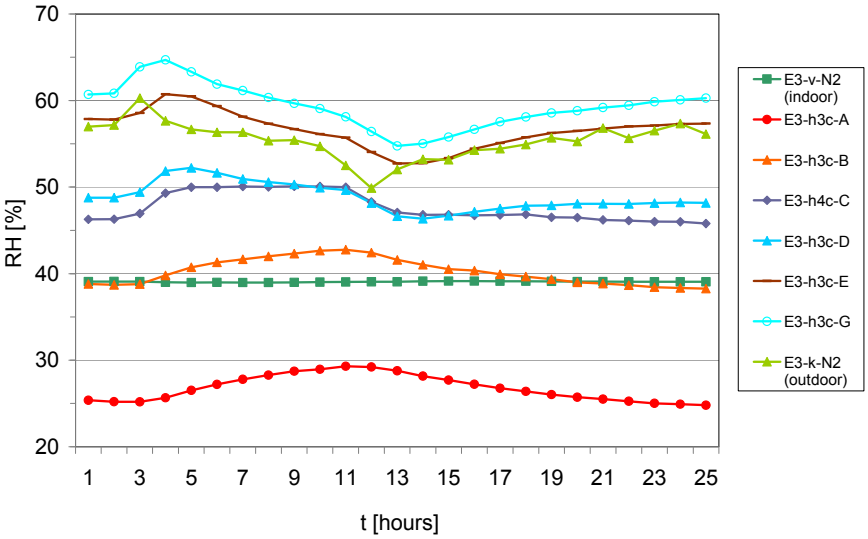

Figure J8. RH, Element 3. April with cladding. 'h4c' replaces 'h3c' at Depth C.

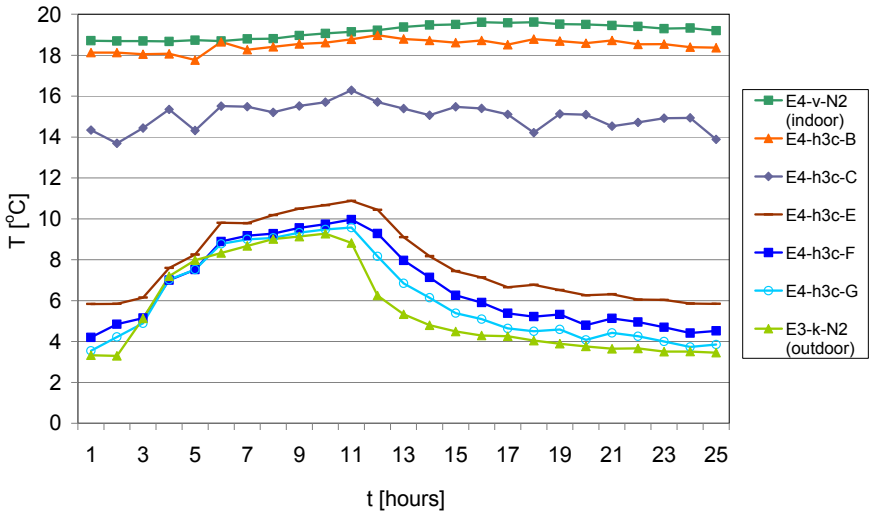

Figure J9. Temperature, Element 4. April with cladding.

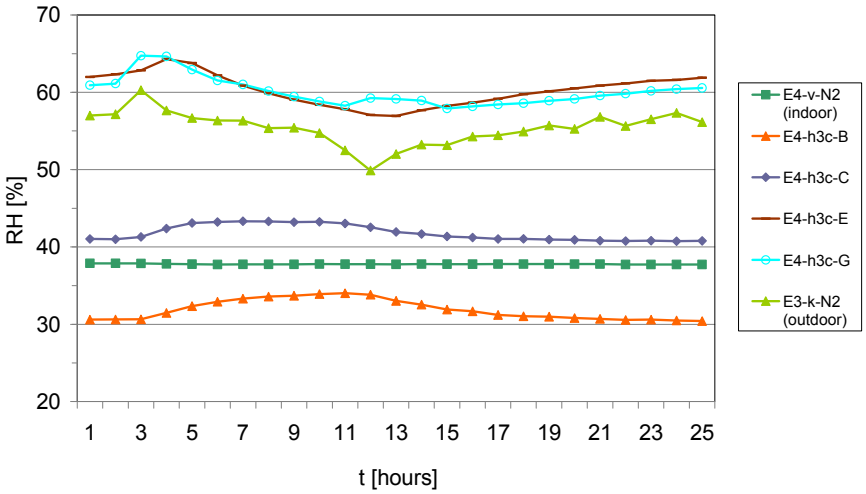

Figure J10. RH, Element 4. April with cladding.

Temperature at different heights – Element 2

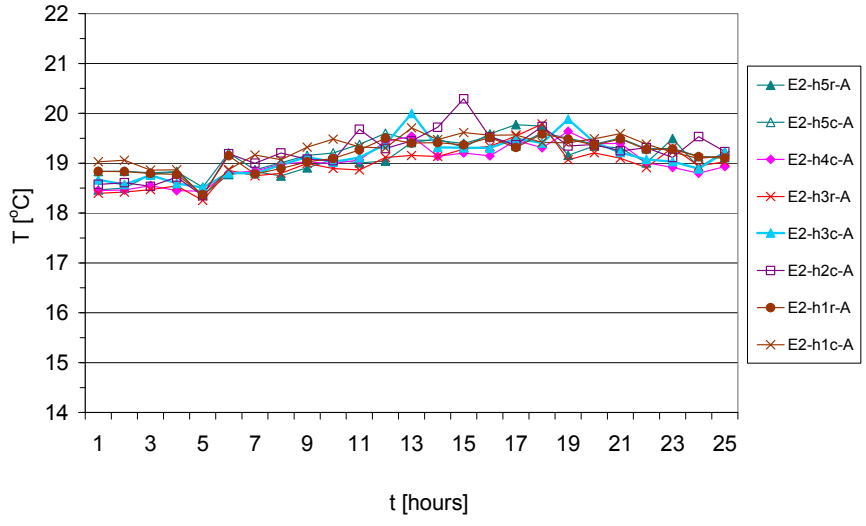

Figure J11. Temperature, Depth A. Element 2. April with cladding.

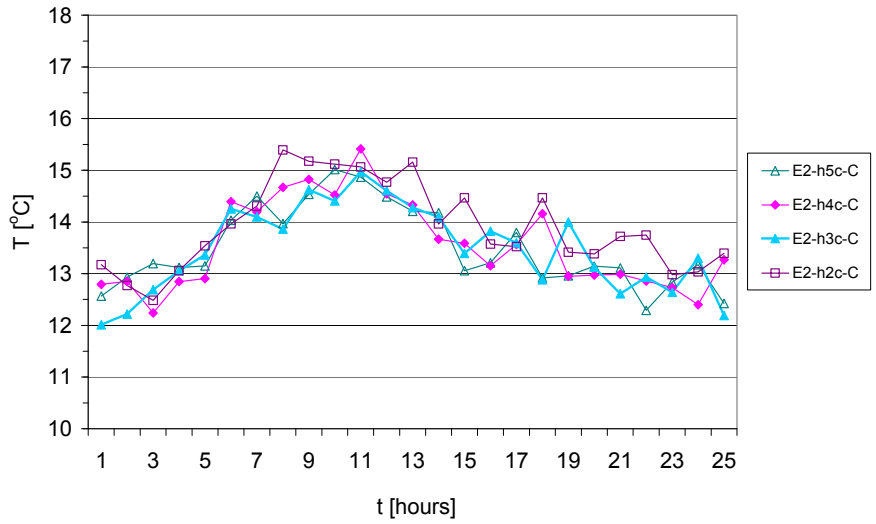

Figure J12. Temperature, Depth C. Element 2. April with cladding.

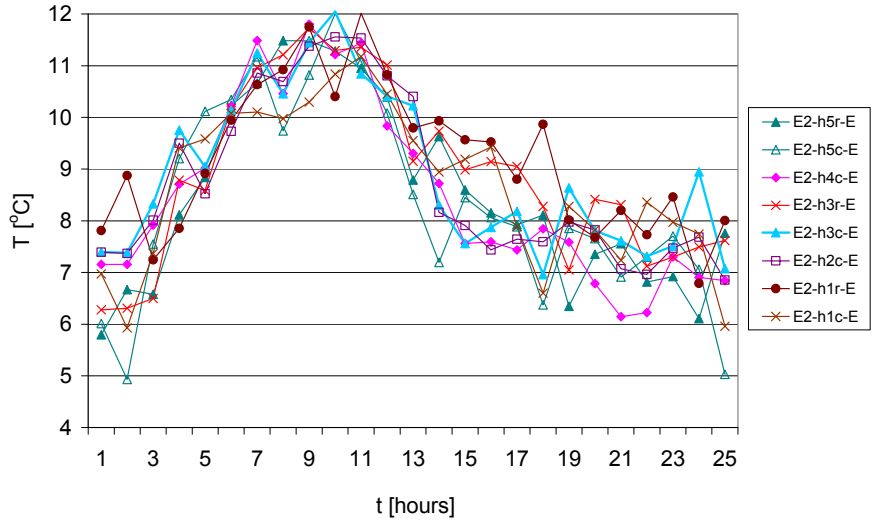

Figure J13. Temperature, Depth E. Element 2. April with cladding.

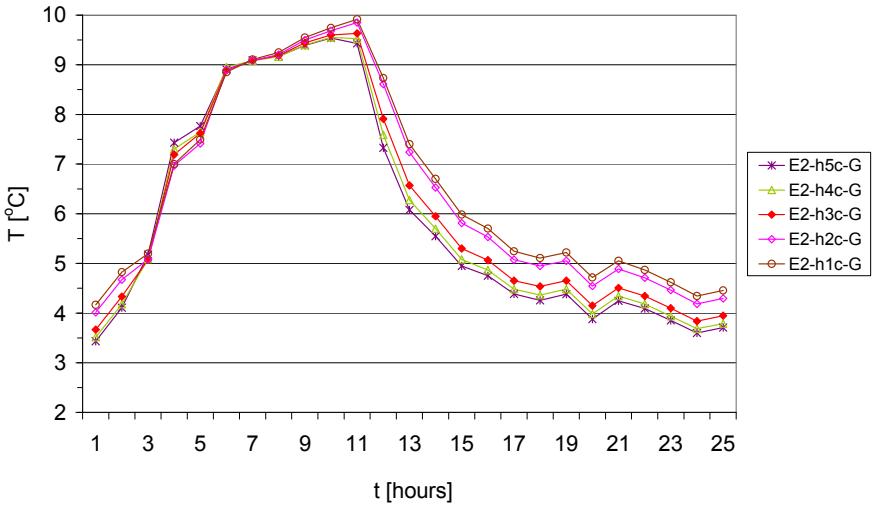

Figure J14. Temperature, Depth G. Element 2. April with cladding.

The pattern was about the same for the other elements. As in Appendix I, only temperature profiles are shown.

Comparison of elements

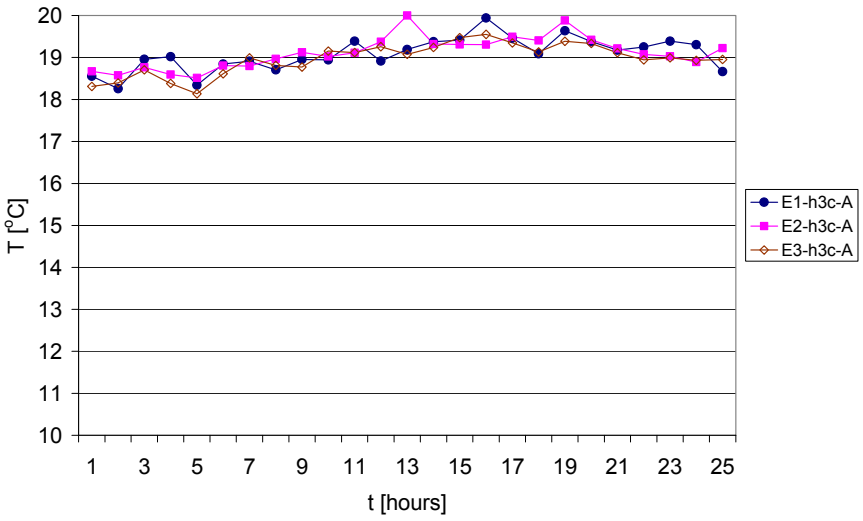

Figure J15. Temperature, Depth A. April with cladding. Elements 1, 2 and 3.

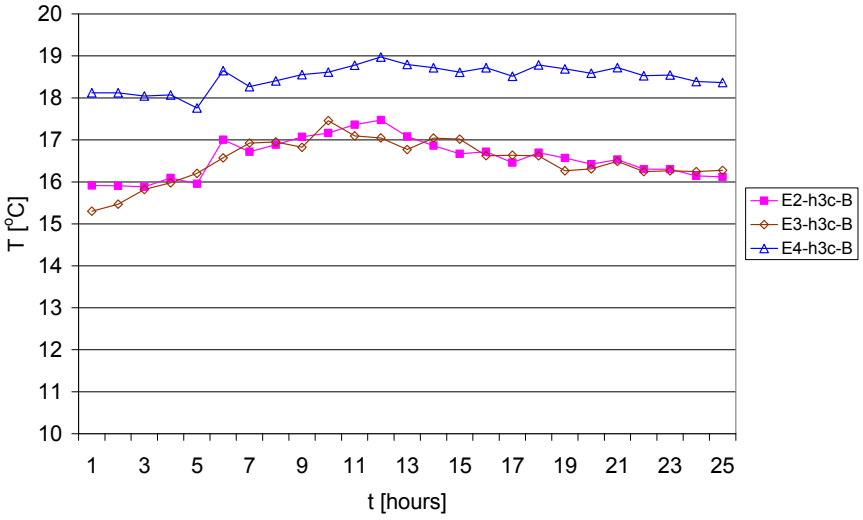

Figure J16. Temperature, Depth B. April with cladding. Elements 1, 2 and 3.

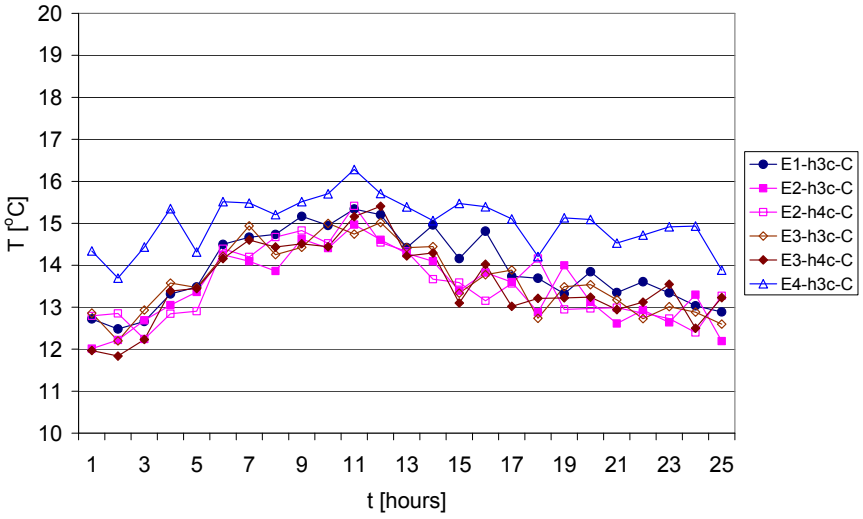

Figure J17. Temperature, Depth C. April with cladding. Elements 1, 2, 3 and 4. Both 'h3c' and 'h4c' are included for Elements 2 and 3, cf. Figure J23.

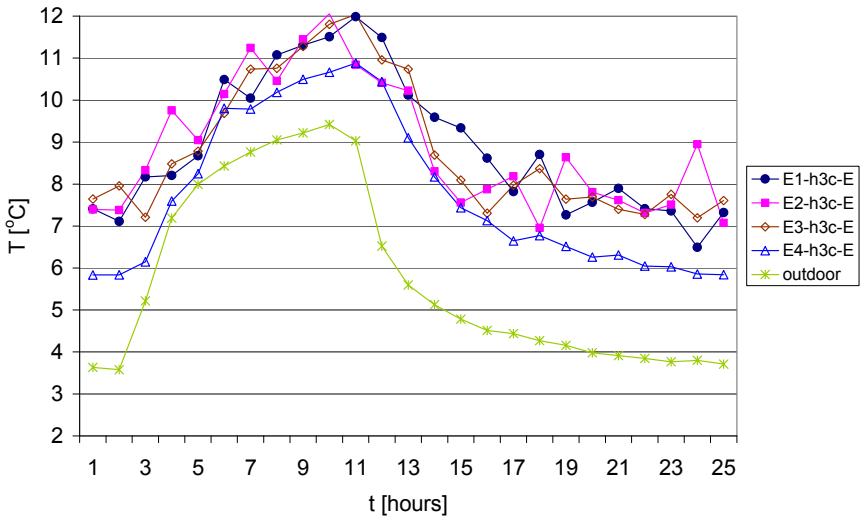

Figure J18. Temperature, Depth E. April with cladding. Elements 1, 2, 3 and 4, and outdoor.

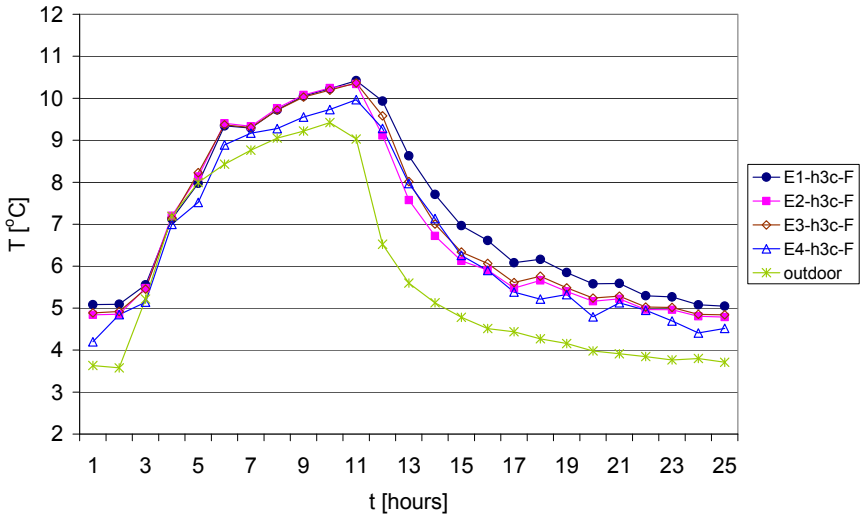

Figure J19. Temperature, Depth F. April with cladding. Elements 1, 2, 3 and 4, and outdoor.

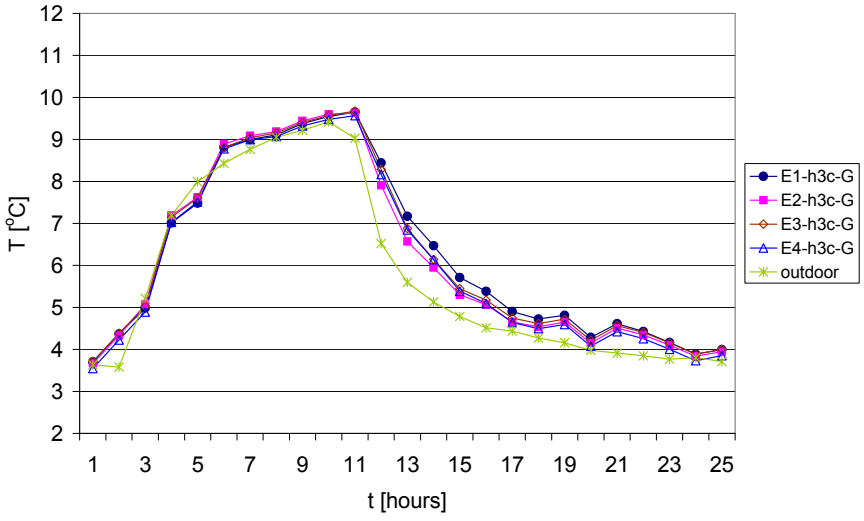

Figure J20. Temperature, Depth G. April with cladding. Elements 1, 2, 3 and 4, and outdoor.

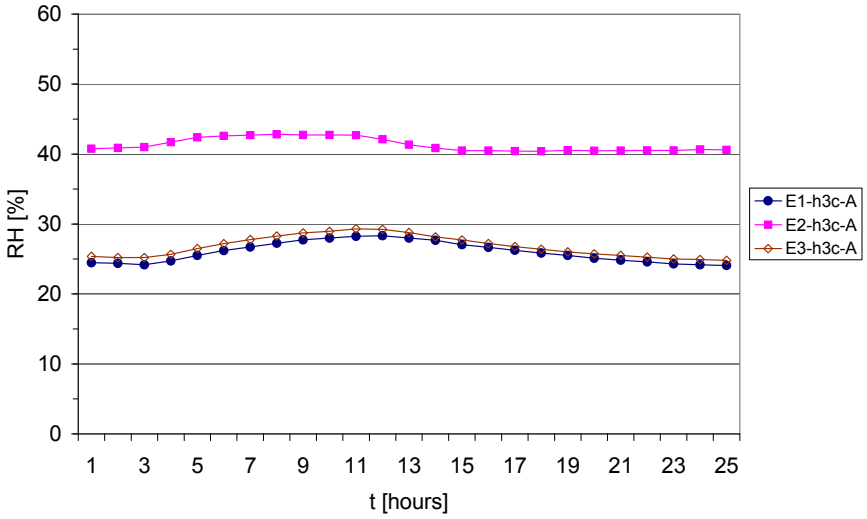

Figure J21. RH, Depth A. April with cladding. Elements 1, 2 and 3.

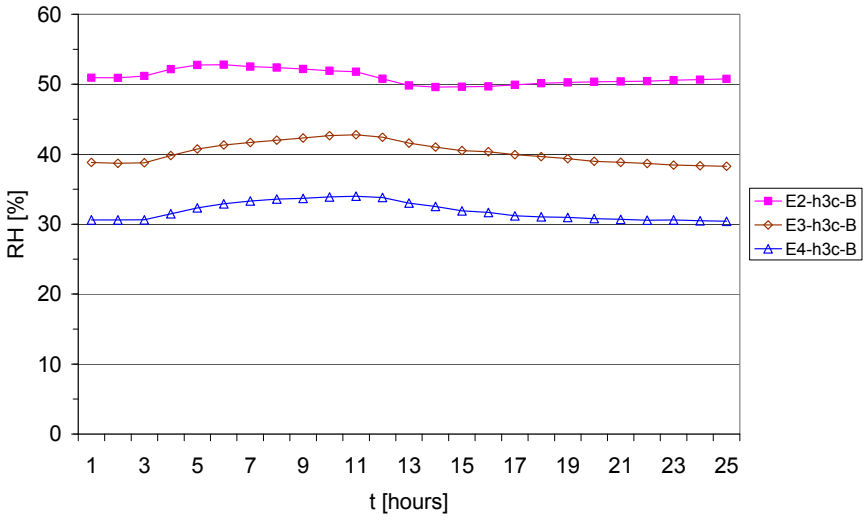

Figure J22. RH, Depth B. April with cladding. Elements 2, 3 and 4.

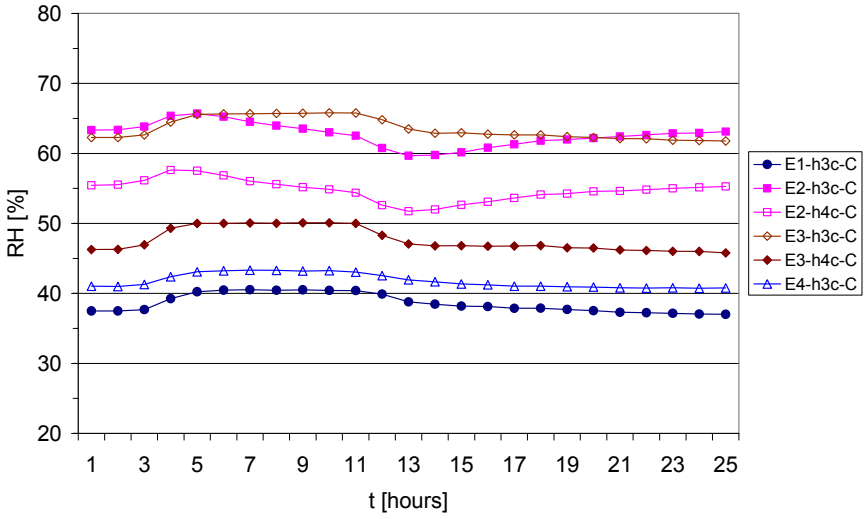

Figure J23. RH. Depth C. April with cladding. Elements 1, 2, 3 and 4. 'h4c' is included for Elements 2 and 3. 'h3c' is not representative of RH in these elements.

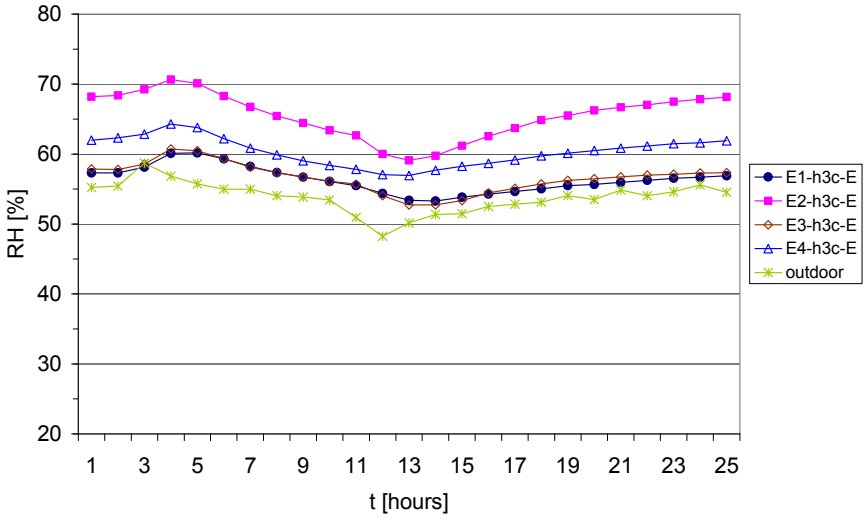

Figure J24. RH, Depth E. April with cladding. Elements 1, 2, 3 and 4, and outdoor.

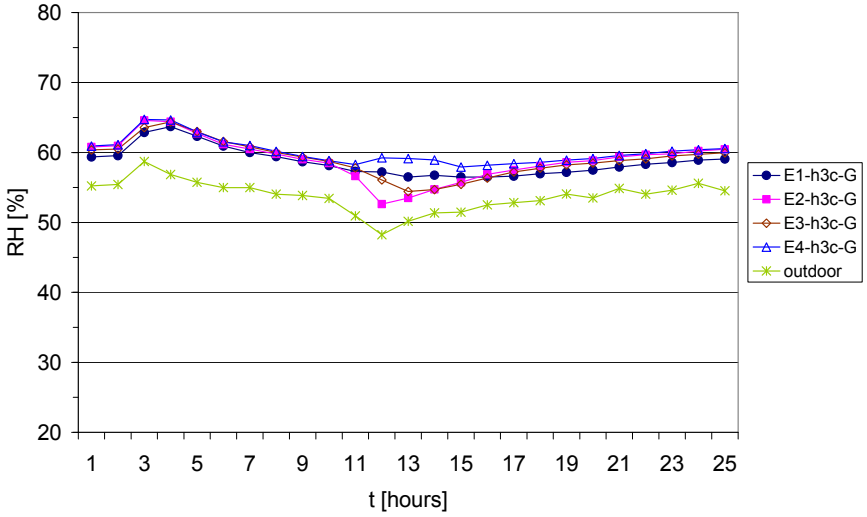

Figure J25. RH, Depth G. April with cladding. Elements 1, 2, 3 and 4, and outdoor.

Appendix K. September with cladding (M4S)

This appendix contains figures showing how the temperature and RH distributed from the indoor side to the outdoor side in all four elements, in addition to the results of Element 1 shown in the part of the chapter 'Results and discussion' that presents results of test M4S. For Elements 1 and 2 also the vapour pressure is shown. 'h4c' replaced 'h3c' at Depth C in Elements 2 and 3 (e.g. Figures K4 – K8), since the results showed that 'h3c' was not representative of the RH level. For the position of sensors refer to Appendix D. See also introduction to Appendix H.

Temperature, RH and vapour pressure from indoor to outdoor sides

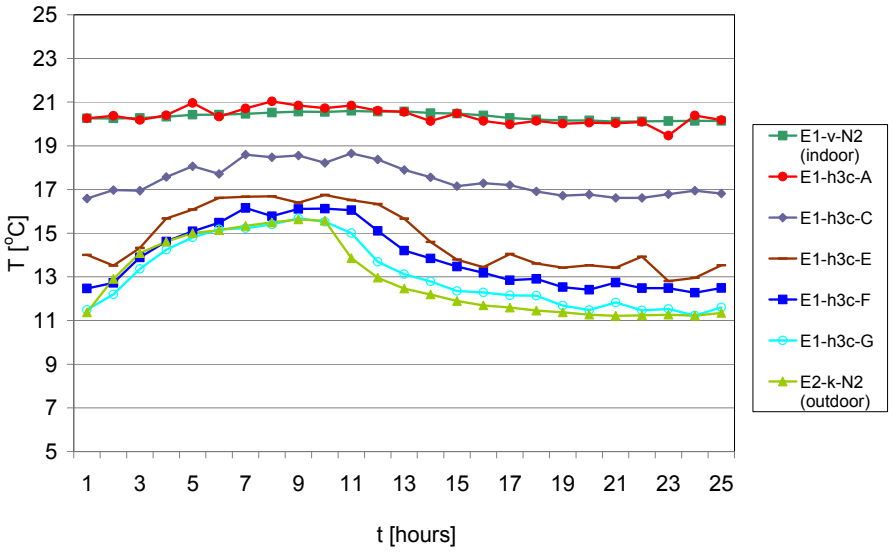

Figure K1. Temperature, Element 1. September with cladding. Temperature at the indoor side, behind the indoor gypsum cladding (A), in the centre of the thermal insulation (C), in the thermal insulation, at the wind barrier (E), in the cavity, at the wind barrier (F), in the cavity, at the cladding (G), and at the outdoor side. Example of 24-hour cycle starting at 9 AM. 'E2-k-N2' placed in front of Element 2 represents the temperature at the outdoor side, cf. 'Results and discussion', 'General remarks'.

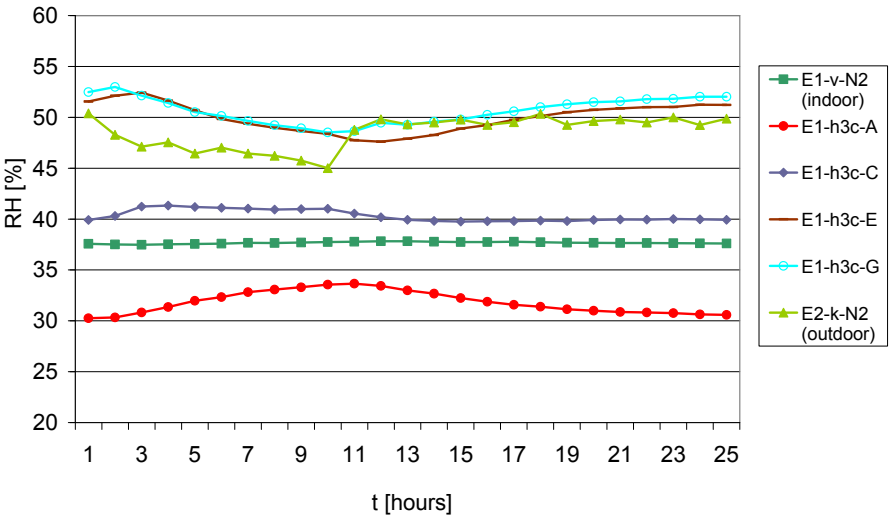

Figure K2. RH, Element 1. September with cladding.

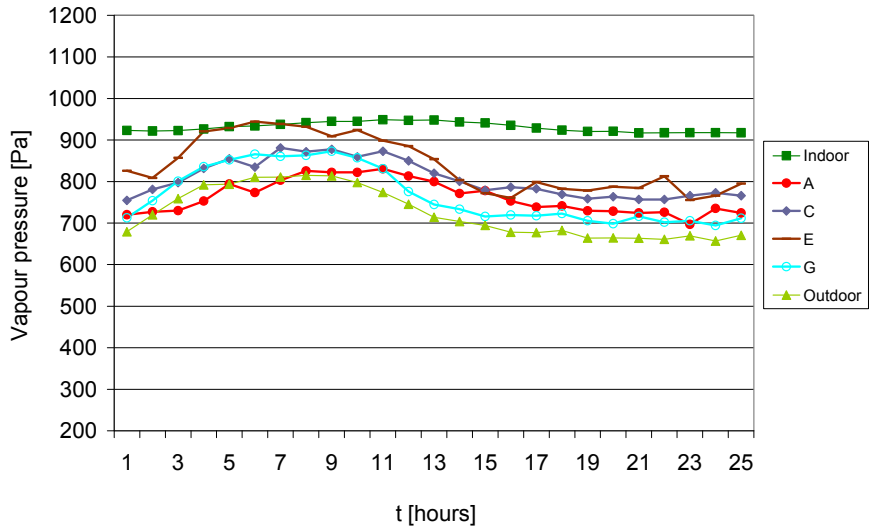

Figure K3. Vapour pressure, Element 1. September with cladding.

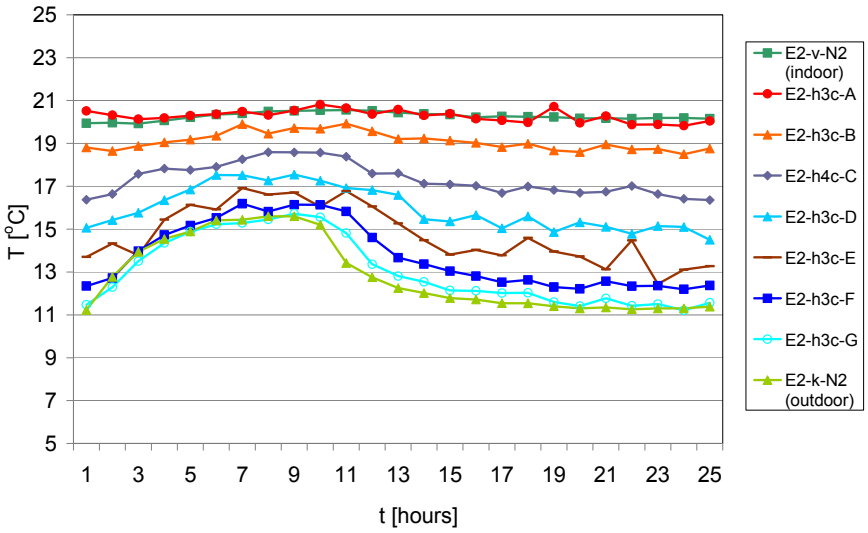

Figure K4. Temperature, Element 2. September with cladding. 'h4c' replaces 'h3c' at Depth C.

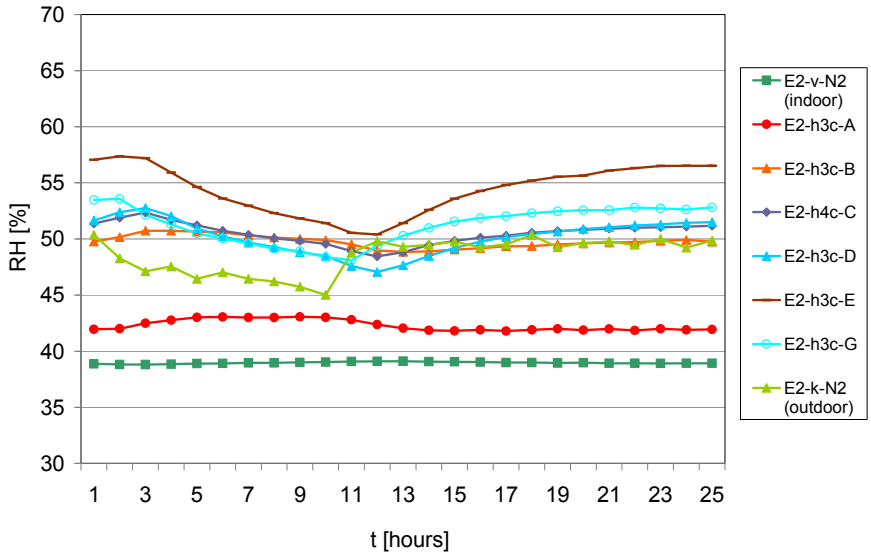

Figure K5. RH, Element 2. September with cladding. 'h4c' replaces 'h3c' at Depth C.

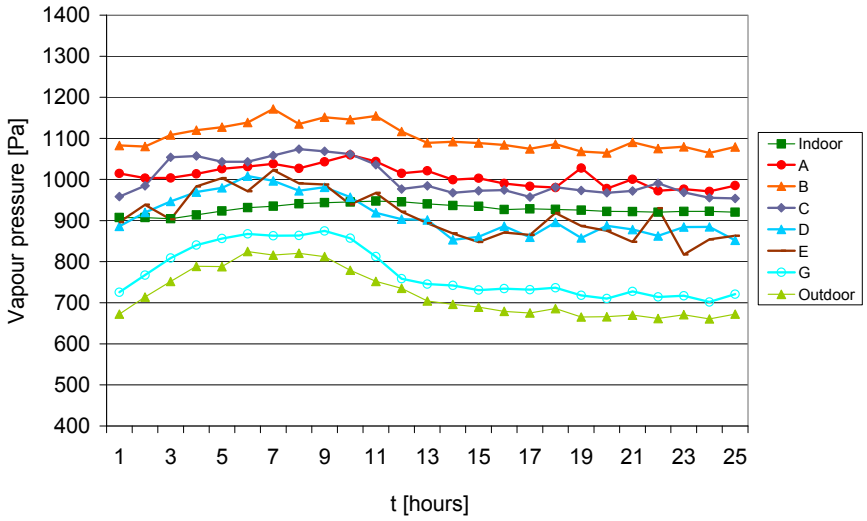

Figure K6. Vapour pressure, Element 2. September with cladding. 'h4c' replaces 'h3c' at Depth C.

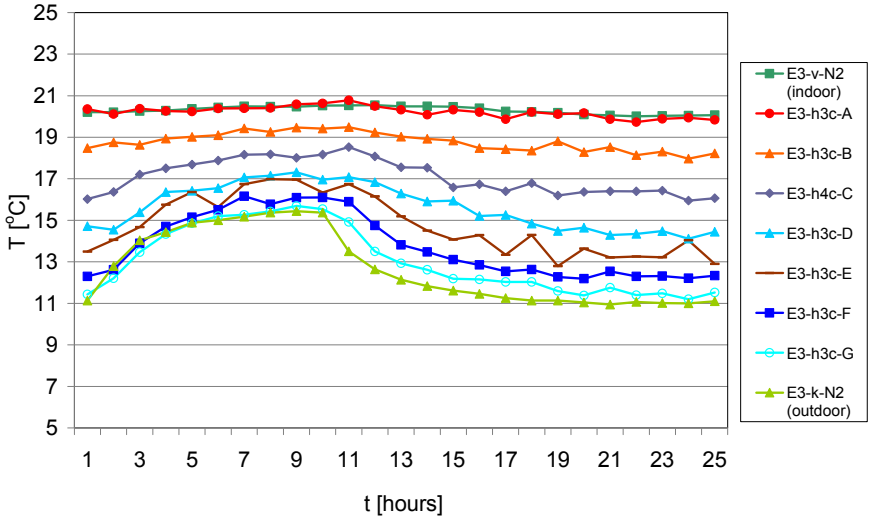

Figure K7. Temperature, Element 3. September with cladding. 'h4c' replaces 'h3c' at Depth C.

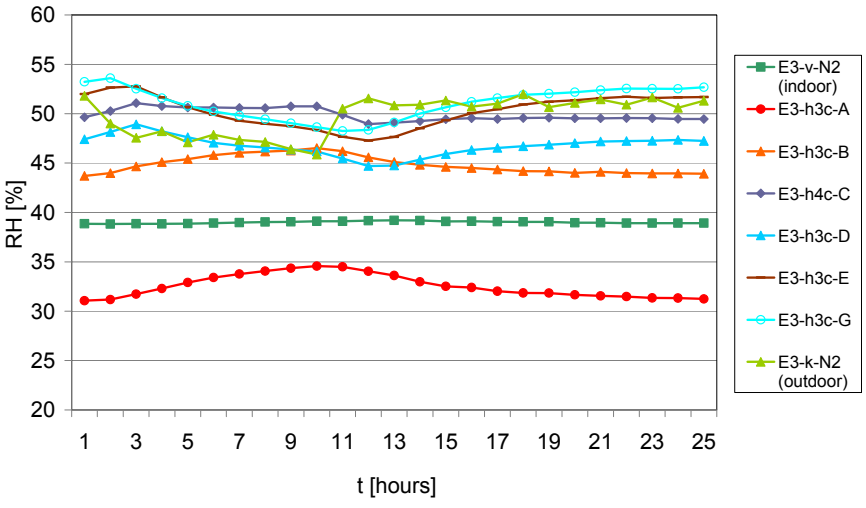

Figure K8. RH, Element 3. September with cladding. 'h4c' replaces 'h3c' at Depth C.

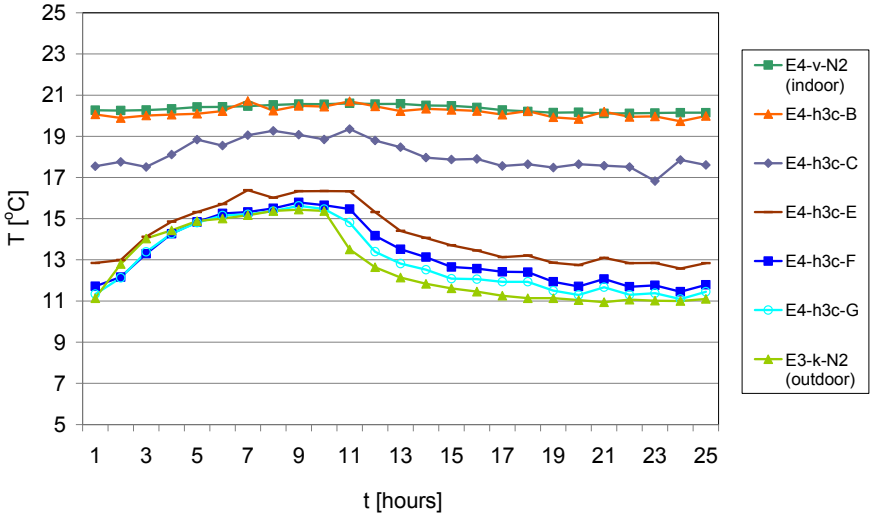

Figure K9. Temperature, Element 4. September with cladding.

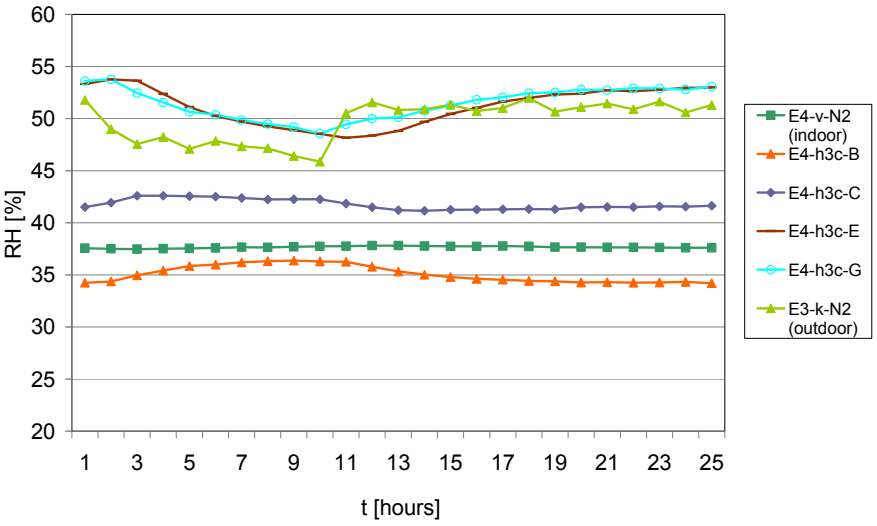

Figure K10. RH, Element 4. September with cladding.

Comparison of elements

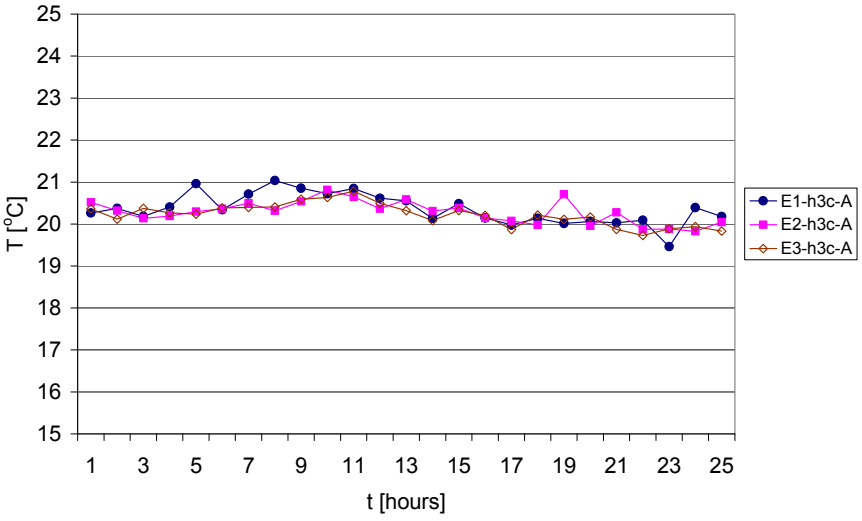

Figure K11. Temperature, Depth A. September with cladding. Elements 1, 2 and 3.

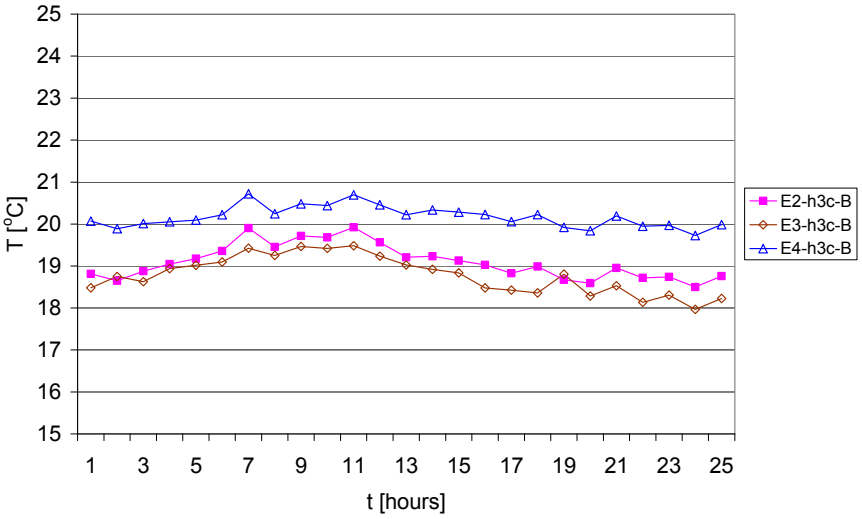

Figure K12. Temperature, Depth B. September with cladding. Elements 2, 3 and 4.

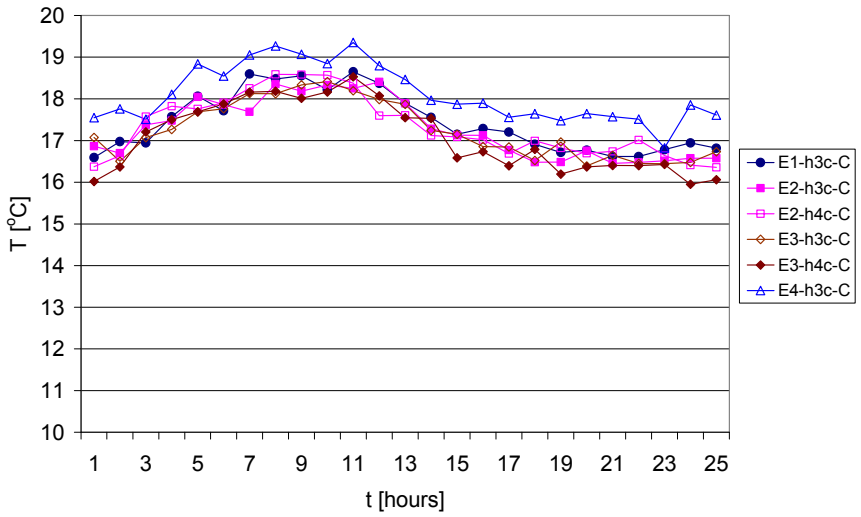

Figure K13. Temperature, Depth C. September with cladding. Elements 1, 2, 3 and 4. Both 'h3c' and 'h4c' are included for Elements 2 and 3, cf. Figure K19.

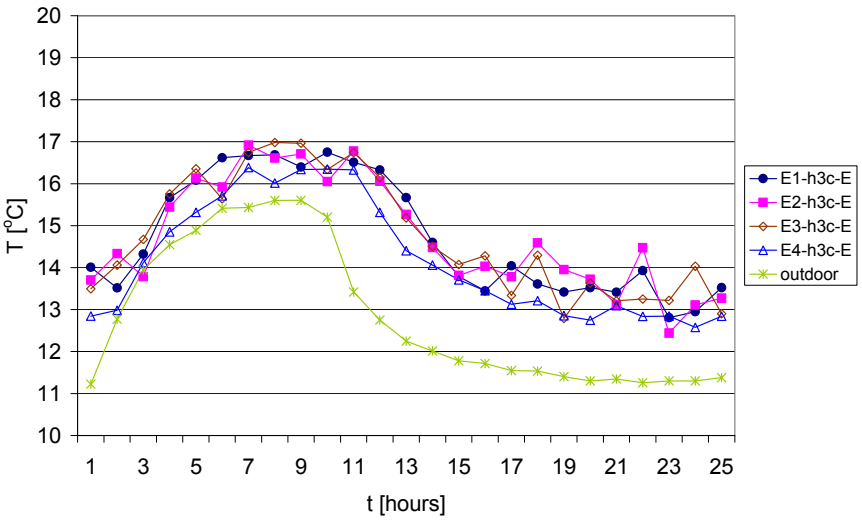

Figure K14. Temperature, Depth E. September with cladding. Elements 1, 2, 3 and 4, and outdoor.

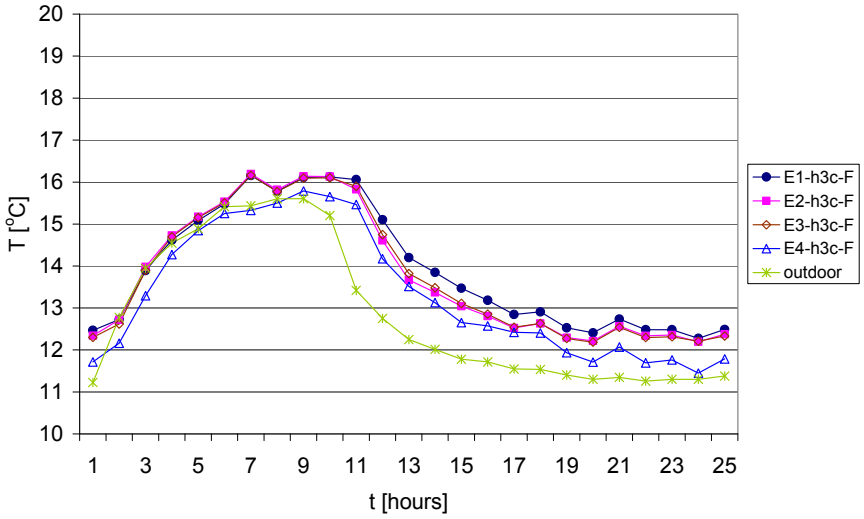

Figure K15. Temperature, Depth F. September with cladding. Elements 1, 2, 3 and 4, and outdoor.

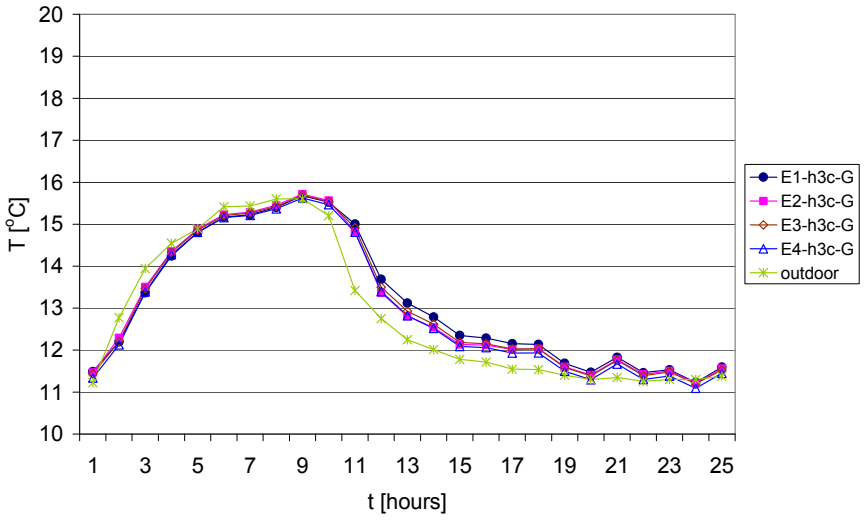

Figure K16. Temperature, Depth G. September with cladding. Elements 1, 2, 3 and 4, and outdoor.

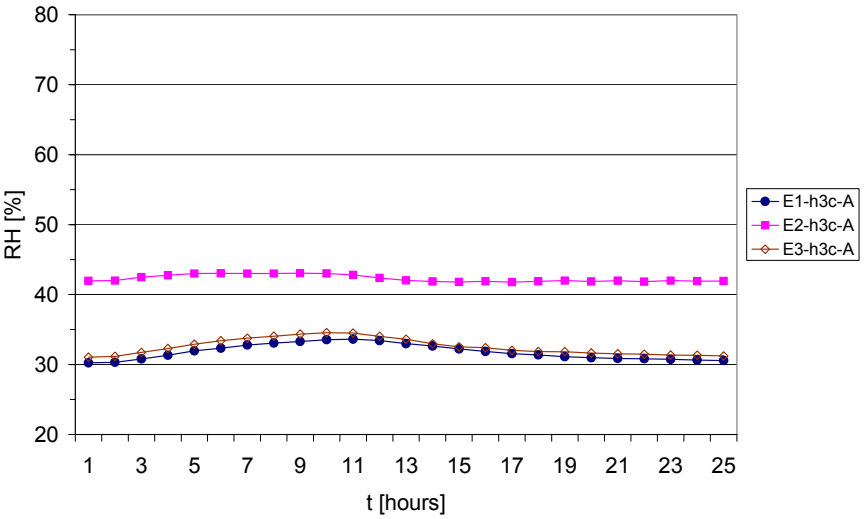

Figure K17. RH, Depth A. September with cladding. Elements 1, 2 and 3.

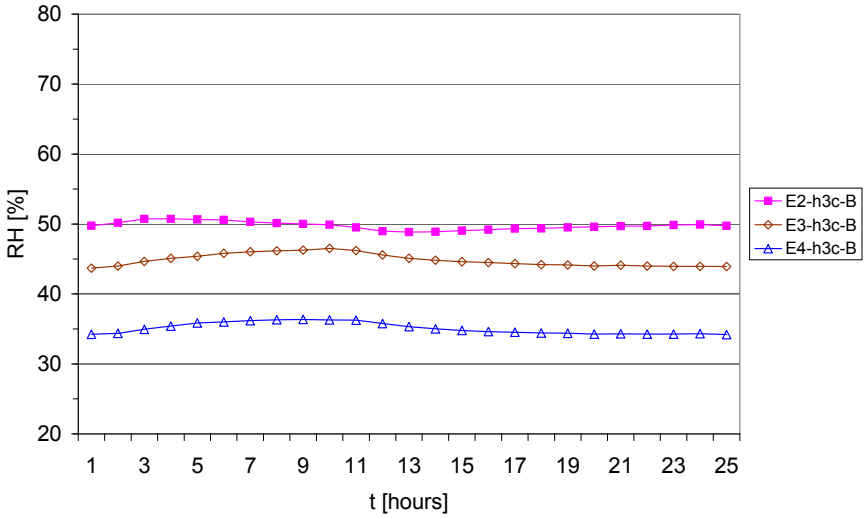

Figure K18. RH, Depth B. September with cladding. Elements 2, 3 and 4.

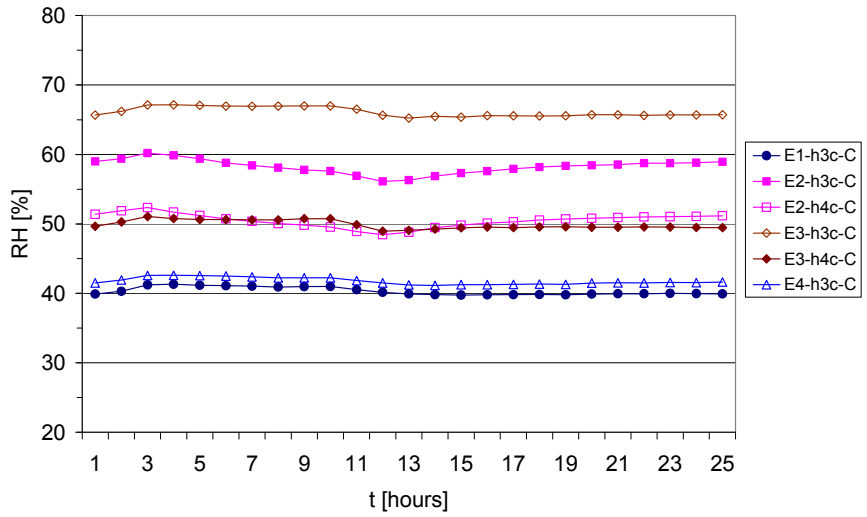

Figure K19. RH, Depth C. September with cladding. Elements 1, 2, 3 and 4. 'h4c' is included for Elements 2 and 3. 'h3c' is not representative of RH in these elements.

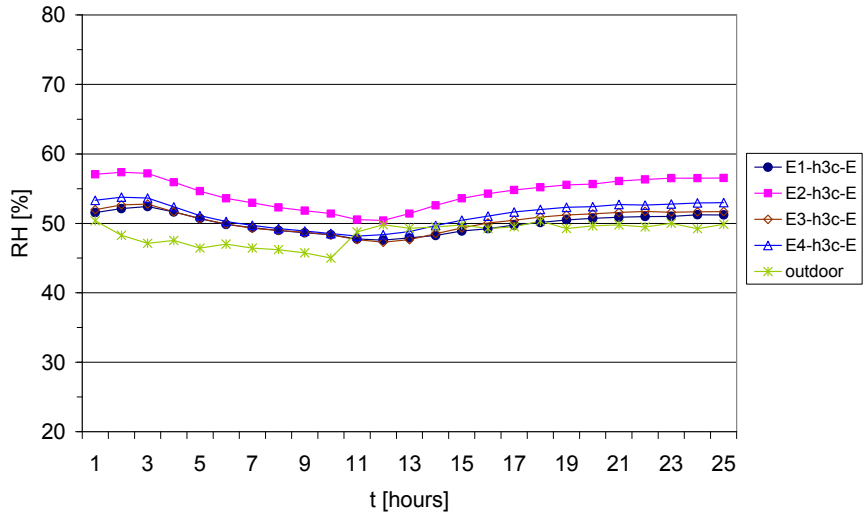

Figure K20. RH, Depth E. September with cladding. Elements 1, 2, 3 and 4, and outdoor.

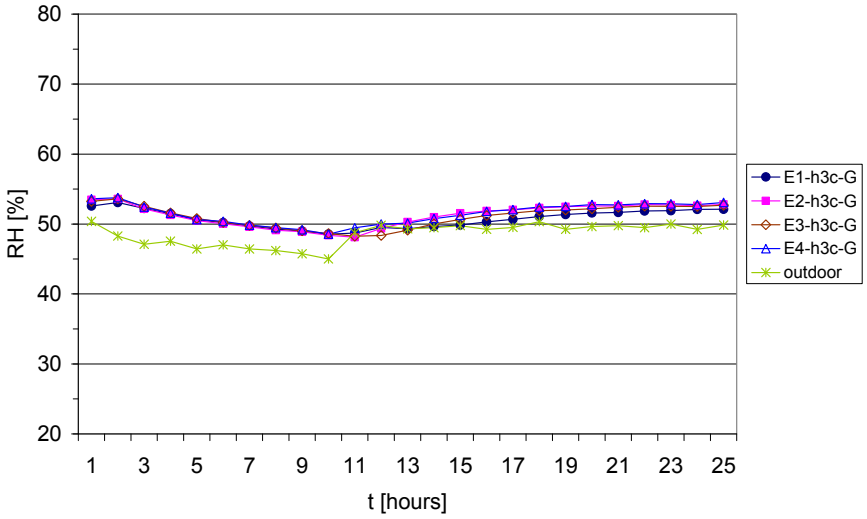

Figure K21. RH, Depth G. September with cladding. Elements 1, 2, 3 and 4, and outdoor.

Moisture and temperature levels and variations in time and space play a crucial role in the degradation processes of building materials. In order get a better prediction of the interaction between the indoor environment and the building component used in computational models for multidimensional Heat, Air and Moisture (HAM) conditions, experimental data are needed. Tests were performed in the large climate simulator at SBi involving full-scale wall elements. The elements were exposed for steady-state condi-tions, and temperature cycles simulating April and September climate in Denmark. The effect on the moisture and temperature conditions of the addi-tion of a vapour barrier and an outer cladding on timber frame walls was studied. The report contains comprehensive appendices documenting the full-scale tests. The tests were performed as a part of the project 'Model for Multidimensional Heat, Air and Moisture Conditions in Building Envelope Components' carried out as a co-project between DTU Byg and SBi.

1. udgave, 2010
ISBN 978-87-563-1413-8